REM/FIB & SIMS School

June/July 2020

Universität Siegen

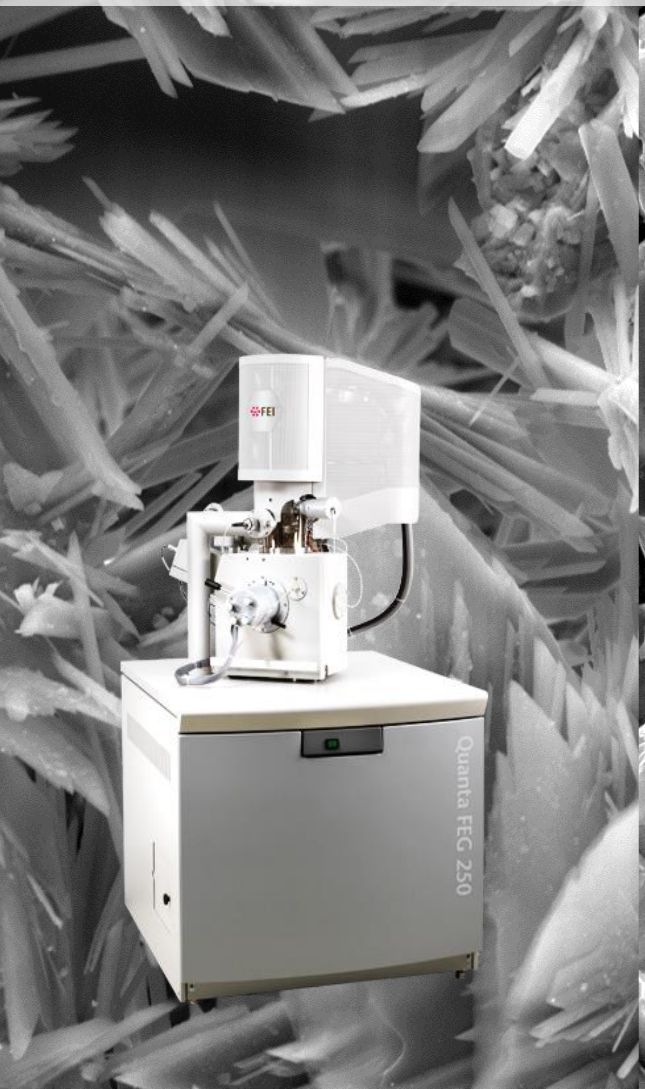

Lecturers & Trainers

Prof. Dr. **B. Butz**
PB-A 218, -3175
benjamin.butz@...

Prof. Dr. **M. Killian**
PB-A 415, -2984
manuella.killian@...

Dr.-Ing. **J. Müller**
PB-A 232, -2415
julian.mueller@...

Dr. **C. Pritzel**
PB-A 415, -2968
pritzel@...

Dr. **S. Afflerbach**
PB-C 007, -2968
afflerbach@...

Dr. **Y. Sakalli**
PB-A 232, -4750
sakalli@...

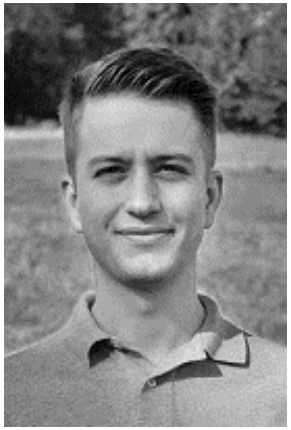

M. Hepp, MSc
PB-A 217, -3121
marco.hepp@...

P. auf dem Brinke
PB-H 001, -4646
petra.aufdembrinke@...

S. Leith, MSc
PB-A 426, -4646
Stewart.Leith@...

S. Weitz, BSc
PB-A 409/1, -2760
sebastian.weitz@...

Schedule and Lab Groups

	TUE 16/06/2020	WED 17/06/2020	THU 18/06/2020
09:00 – 10:30+	Lecture I **Basic Instrumentation**	Lecture III **SEM Imaging**	Lecture V **SIMS Basics & Application**
13:00 – 14:30+	Lecture II **Electron-Matter Interaction**	Lecture IV **EDX / FIB**	

Group 1	Group 2	Group 3	Group 4	Group 5	Group 6	Group 7	Group 8

Weekly lab Courses starting 23/06/2020

- TUE 09:00 – 12:00
- TUE 13:00 – 16:00
- THU 09:00 – 12:00

Participants List

Lab Course Time Schedule

Bring your own samples!
Please clarify with Dr. Sakalli

	Schedule for Lab Courses		
	Quanta ESEM PB-A 0127 09:00 - 12:00	**Helios NanoLab FIB PB-A 0126/1 13:00 - 16:00**	**Zeiss Ultra 55 PB-H 041 09:00 - 12:00**
Group 1	TUE, 23/06	TUE, 23/06	THU, 25/06
Group 2	TUE, 30/06	TUE, 30/06	THU, 02/07
Group 3	TUE, 07/07	TUE, 07/07	THU, 09/07
Group 4	TUE, 14/07	TUE, 14/07	THU, 16/07
Group 5	TUE, 21/07	TUE, 21/07	THU, 23/07
Group 6	TUE, 28/07	TUE, 28/07	THU, 30/07
Group 7	TUE, 04/08	TUE, 04/08	THU, 06/08
Group 8	TUE, 11/08	TUE, 11/08	THU, 13/08

Locations of Instruments

★ Zeiss Ultra 55 FESEM

Chair of Surface and material technology / Prof. Jiang
Paul-Bonatz-Str. 9-11, PB-H 041
Tel: 0271 740-2497

✦ ESEM Quanta FEG 250

Chemistry and Structure of novel Materials / Prof. Killian
Paul-Bonatz-Str 9-11, PB-A 0217
Tel.: 0271 740-2250

✹ Helios NanoLab 600 DualBeam

Micro- and Nanoanalytics / Prof. Butz
Paul-Bonatz-Str. 9-11, PB-H 0126/1
Tel: 0271 740-2551

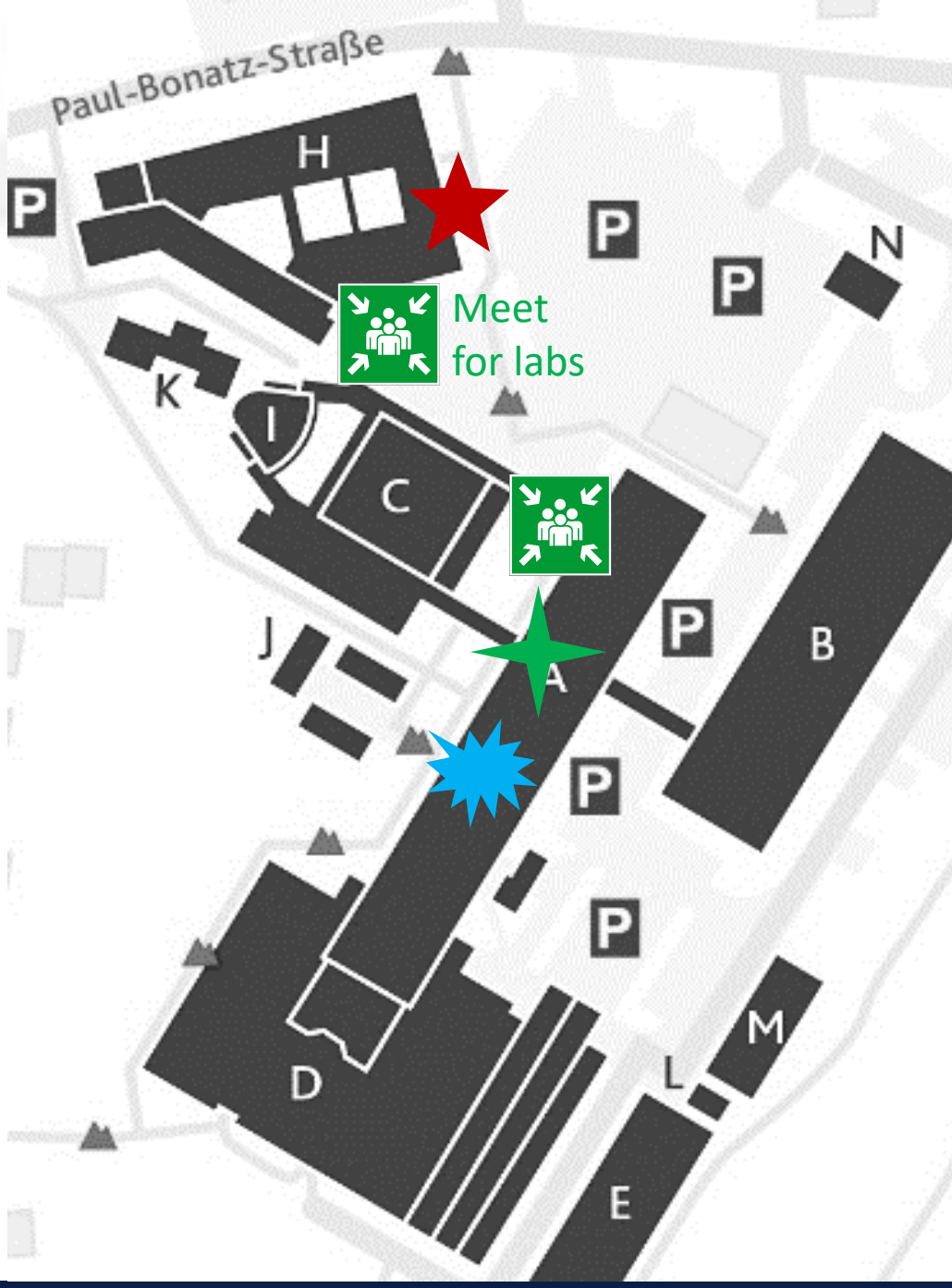

Fire Response

→Assembly point

- In case of fire (emergency) immediately leave the building and assemble at the assemply point

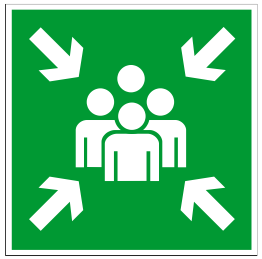

- Check for your colleagues
- Wait until further notice
- The buidling may earliest be entered after clearance by the responsible fire fighters

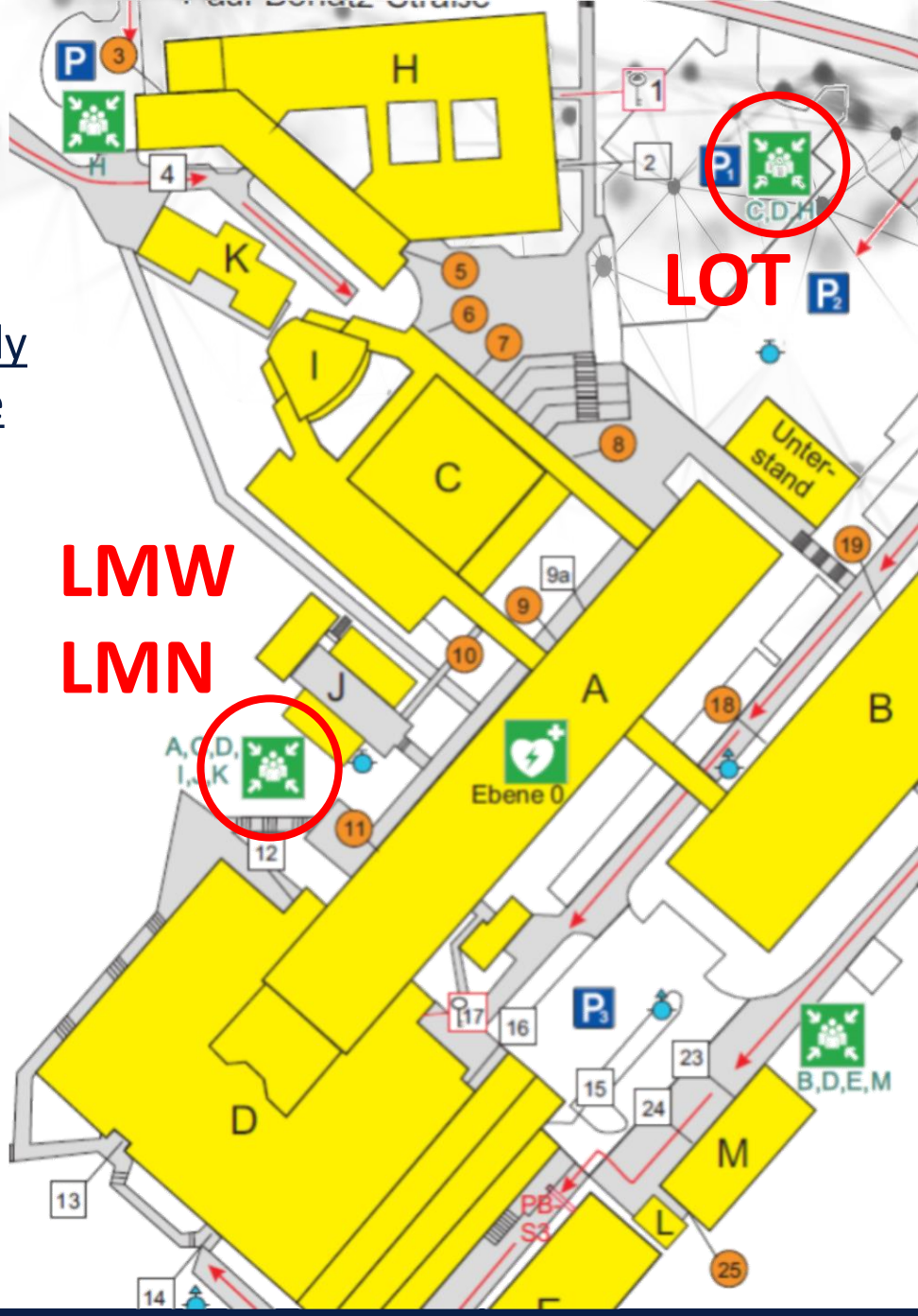

Corona Measures

- All participants and trainers must comply with the hygiene concept of the MNaF as well as and the general regulations by the university administration (*Regulations for Research, Teaching and Administration in Transitional Operation*, May 8, 2020), in particular

→ *Protective measures for distance and mouth-nose coverage:* **to enter the building please bring your own face mask; for the labs we will provide shields**

→ Protective measures for diseases and risk groups: **inform us in advance of any lab**

→ Research-specific supplements to the letter of May 8

- **Access to buildings restricted** → Pickup 10 minutes before the start of each lab (**be in time!**):
  - Zeiss Ultra: Entrance to the Zess building (PB-H)
  - Helios FIB & Quanta ESEM: Main entrance PB-A

Zeiss Ultra 55 FESEM

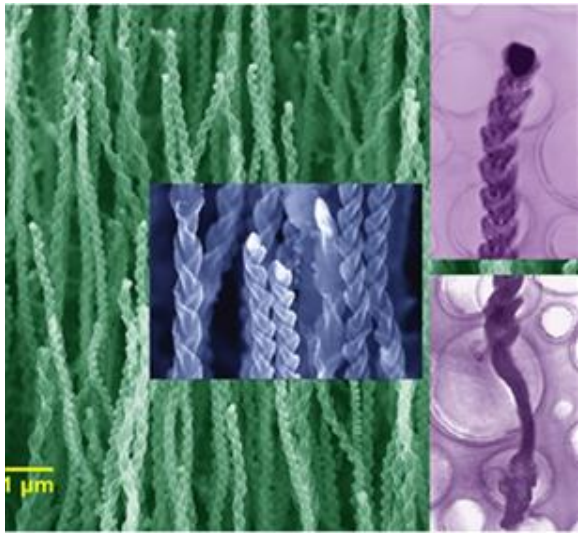

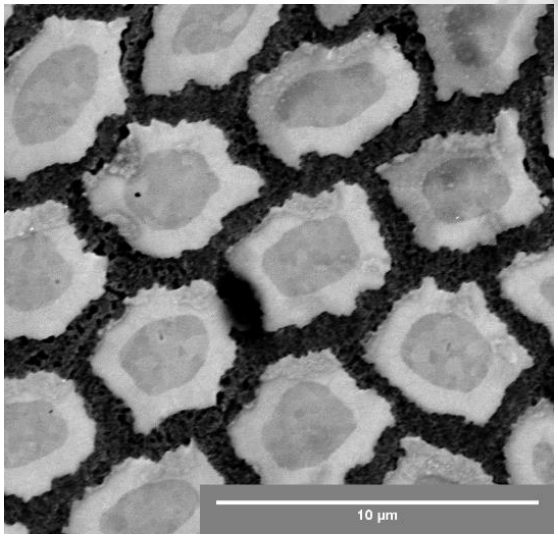

- Ultra-high resolution SEM for nanoscale analyses
- **Topographic & chemical imaging**
  (+ In-Lens & EsB detectors)
- **Chemical analyses by** EDXS

Helios NanoLab™ 600 DualBeam™

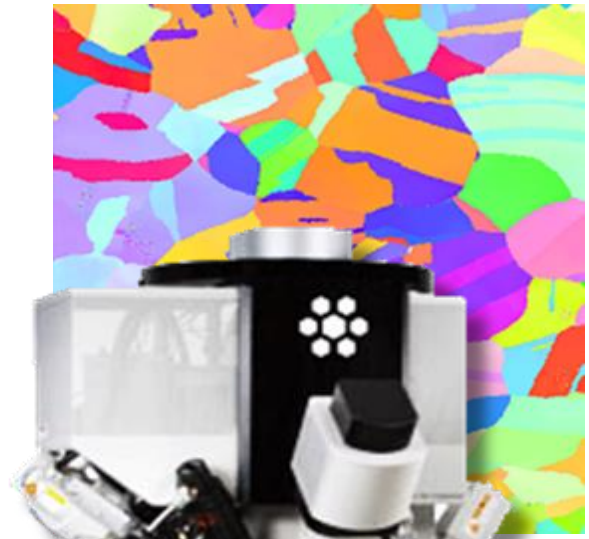

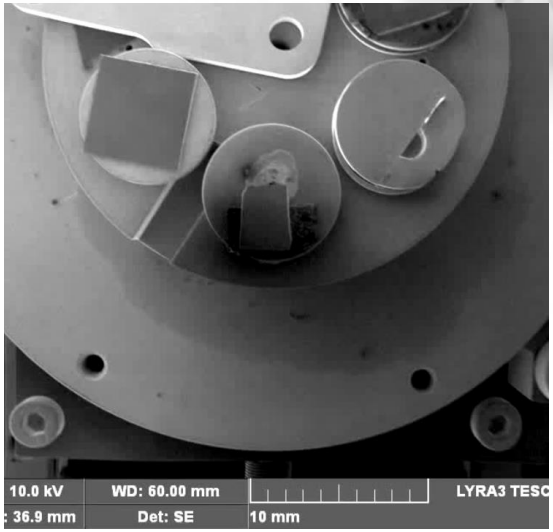

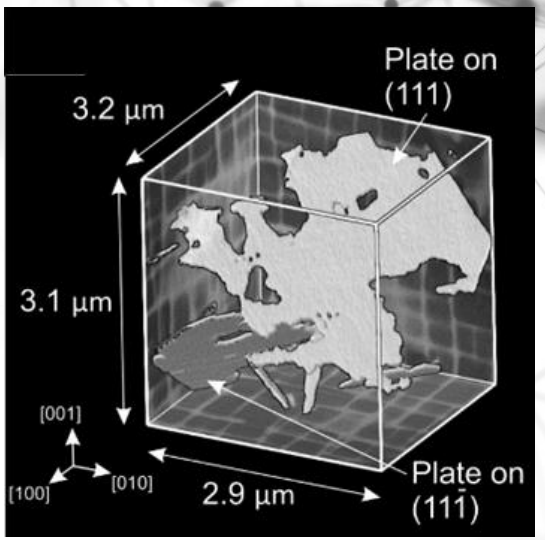

- Ultra-high resolution SEM
- **Topographic & chemical imaging**
  (+ InColumn & ion detectors)
- **Chemical analyses by** EDXS
- **Crystal structure & strain analyses** by EBSD
- High-resolution Ga ion column for sample manipulation, TEM sample preparation, 3D tomography

ESEM Quanta™ FEG 250

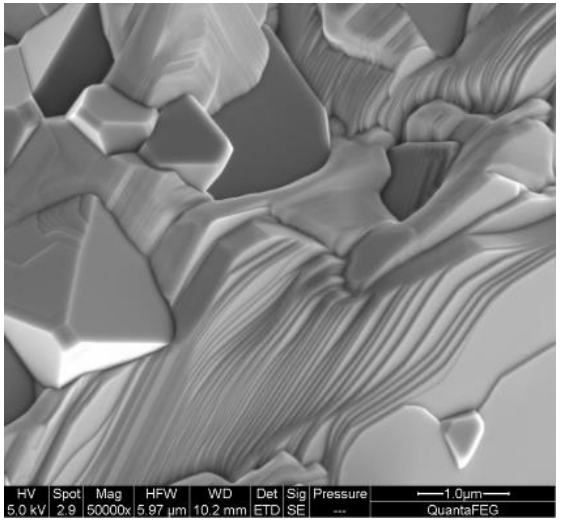

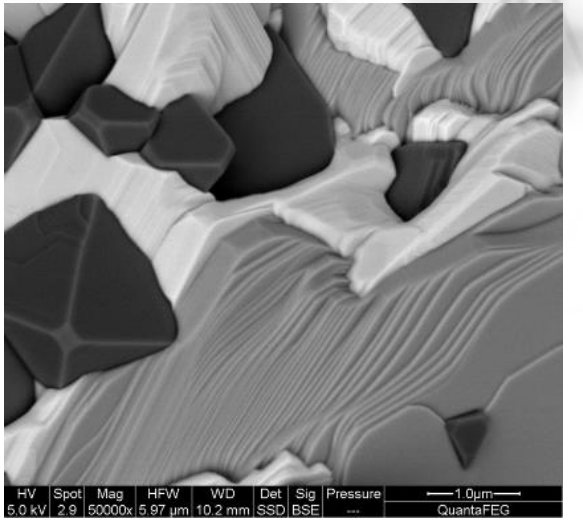

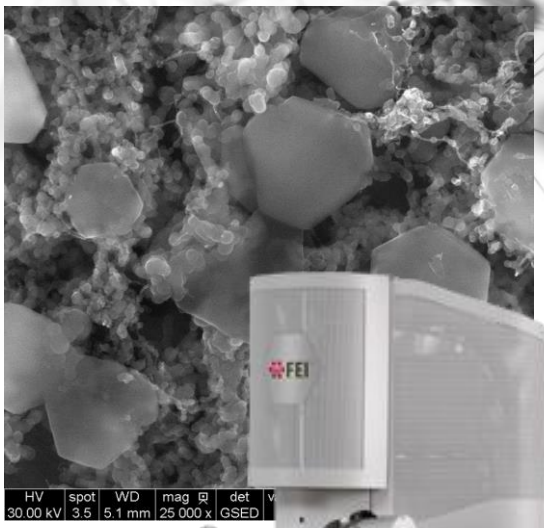

- **Low vacuum and ESEM** capability
  → Analyses (without charging), e.g., of **non-conductive or wet/hydrated specimens**

- **Topographic & chemical imaging**
- **Chemical analyses by** EDXS
- In situ capabilities (cooling, heating)

Scanning Electron & Ion Microscopy

UNIVERSITÄT SIEGEN

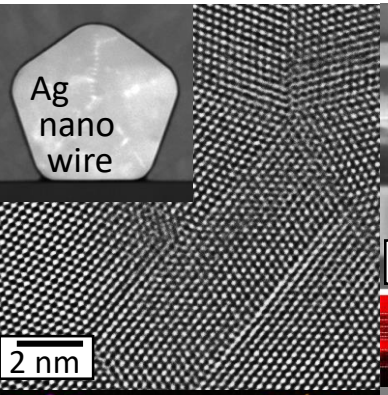

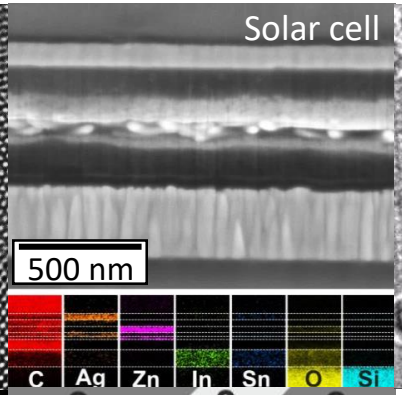

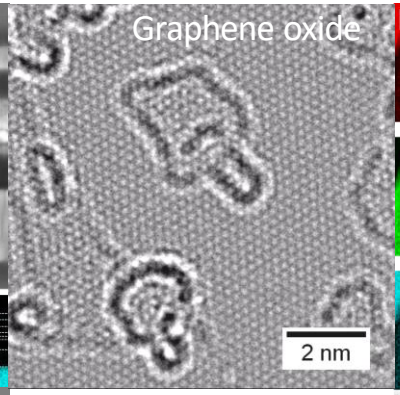

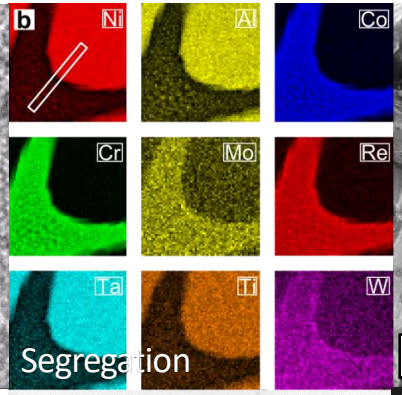

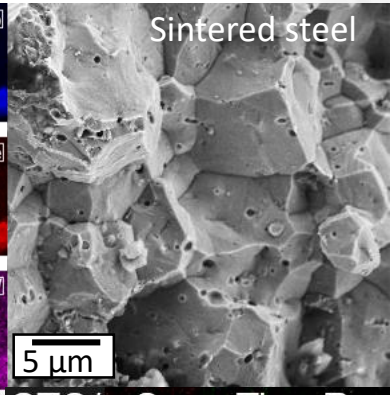

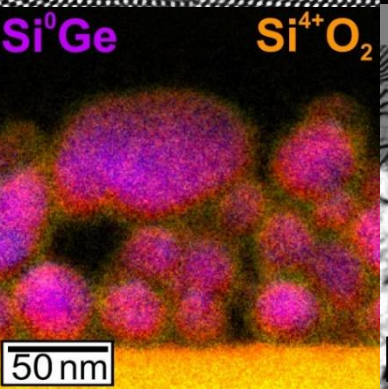

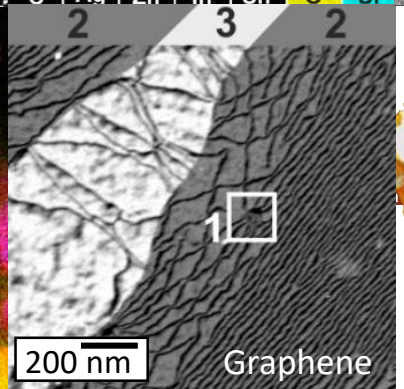

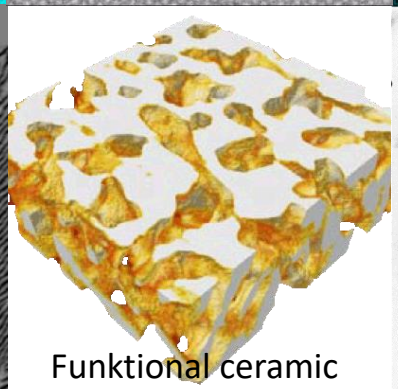

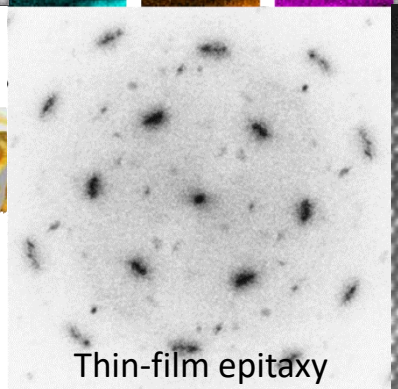

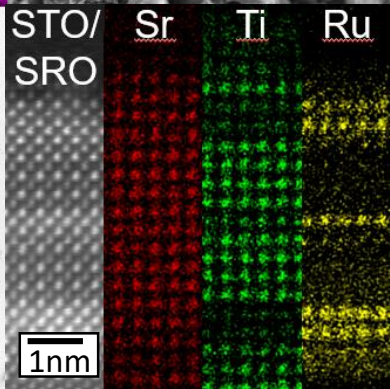

Size Scales

Electronic devices

Water bear

pFET

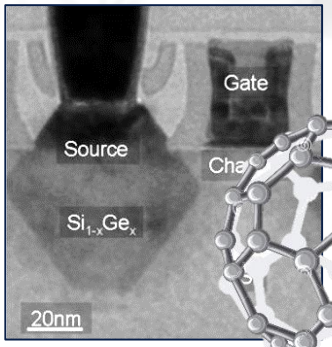

C_{60} molecule

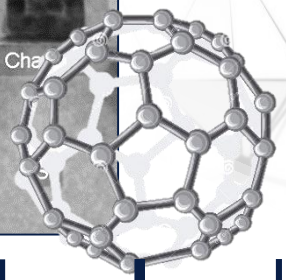

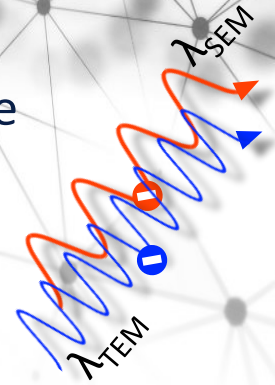

m mm µm nm Å pm

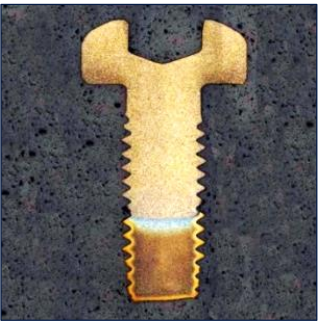

Screw

Parts in watch

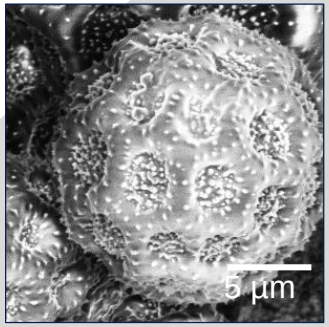

Pollen

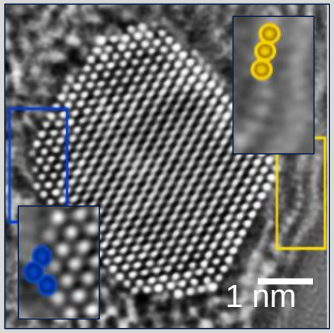

Nanoparticle

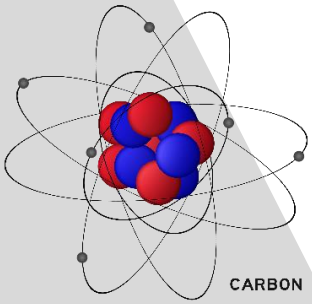

Atom

IR Visible light UV Hard X-rays

Diffraction

H. Quian et al., PNAS 2012, 109 (3) 696-700, wikipedia.com, piaget.de

Advantages of SEM

Microscopy with Electron Waves

Louis Victor Pierre Raymond Prince de Broglie, 1892 - 1987

LM is limited by the long wave length of visible light.
→Fast **electrons:** the faster the electron, the shorter the wave length.

„de Broglie“ – Wavelength
(postulated in 1924)

$$\lambda = \frac{h}{p} = \frac{h}{mv} = \frac{h}{\sqrt{2mE_{kin}}}$$

The Fathers of SEM

1935: First SEM built by von Ardenne

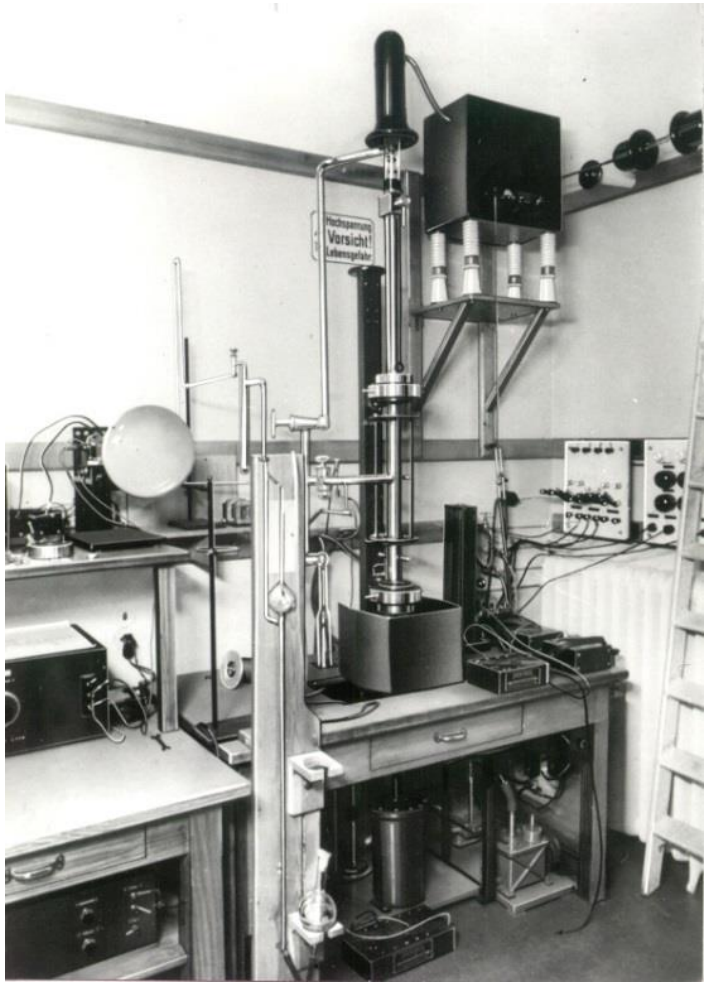

Manfred von Adrenne (1907-1997)

Charles William Oatley (1904-1996)

built the first commercial SEM

The development of SEMs was fuelled by the simultaneous development of TVs (e.g. work of *Vladimir Kosmich Zworykin)*

wikipedia.de

SEM Development

1935: First SEM built by von Ardenne

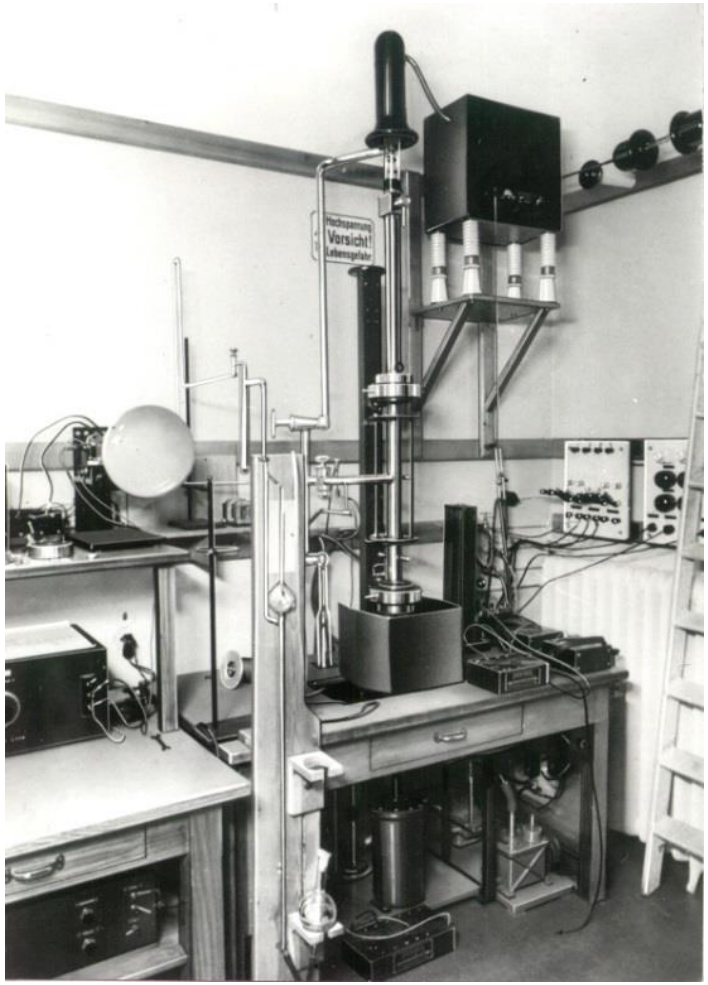

Cambdrige Scientific Instrument Co. - Mark I “Steroscan” (1965): first commercial available instrument

Comparison of EM and OM

	SEM/FIB	OM
Resolution	high (~ 1 nm)	low (~µm)
Depth of field	large	small
Spectroscopy		
Usage	complicated and easy	complicated and easy
Costs	high	depends

OM: limited resolution and DOF

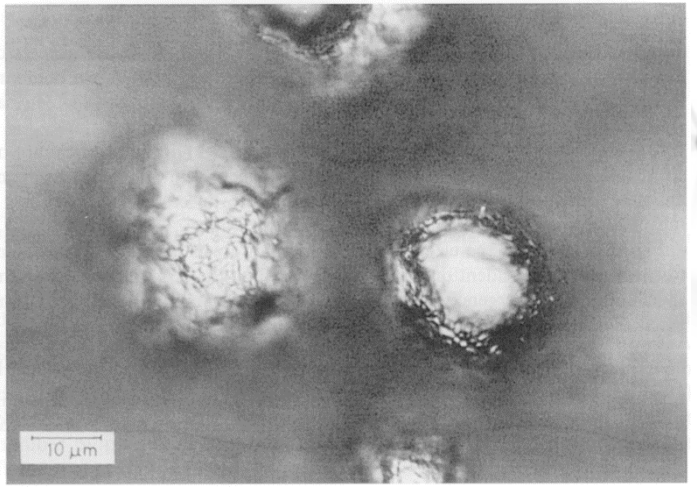

SEM: high res. and DOF

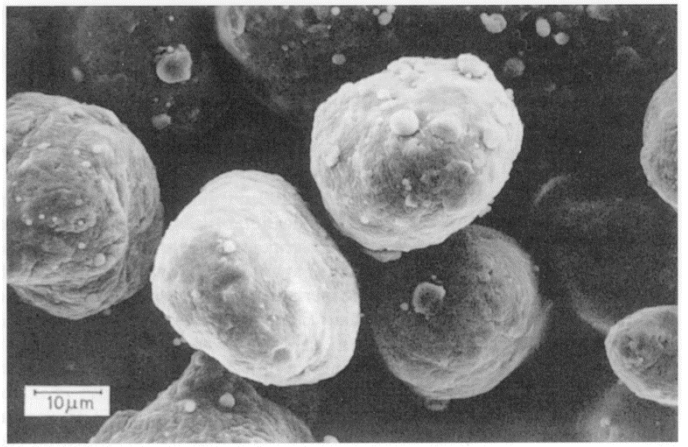

SEM / FIB Methods

Conventional imaging

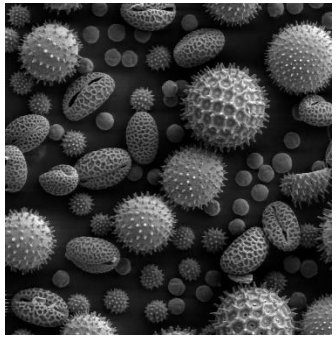

- Topography
- Z-contrast
- Electric/ magnetic fields

Cutting / manipulation

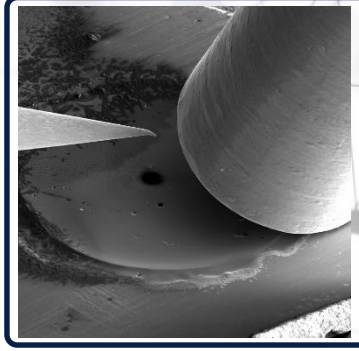

- TEM-sample preparation
- Manipulation
- Depth profiling
- Imaging

SEM/ FIB

EBSD

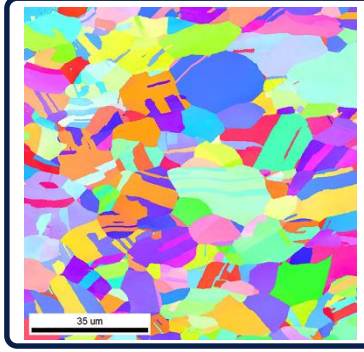

- Crystal structure
- Mirco-structure
- Strain

gatan.com

Chemical analysis

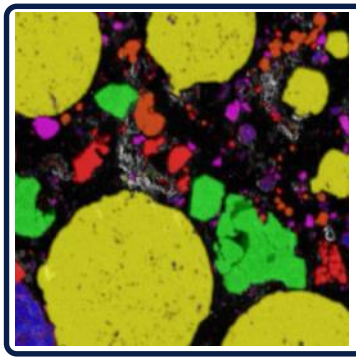

- Composition
- Combination EBSD / EDS

fei.com

In situ microscopy

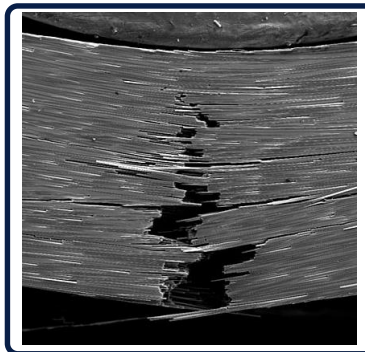

- Mechanical/ electrical testing
- Heating
- Cooling
- Environment

kammrath&weiss

Tomography

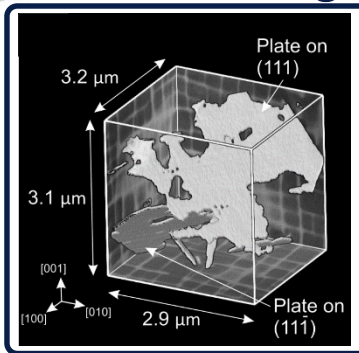

- 3D morphology
- 3D chemistry
- Phase/pore distributions

Topography

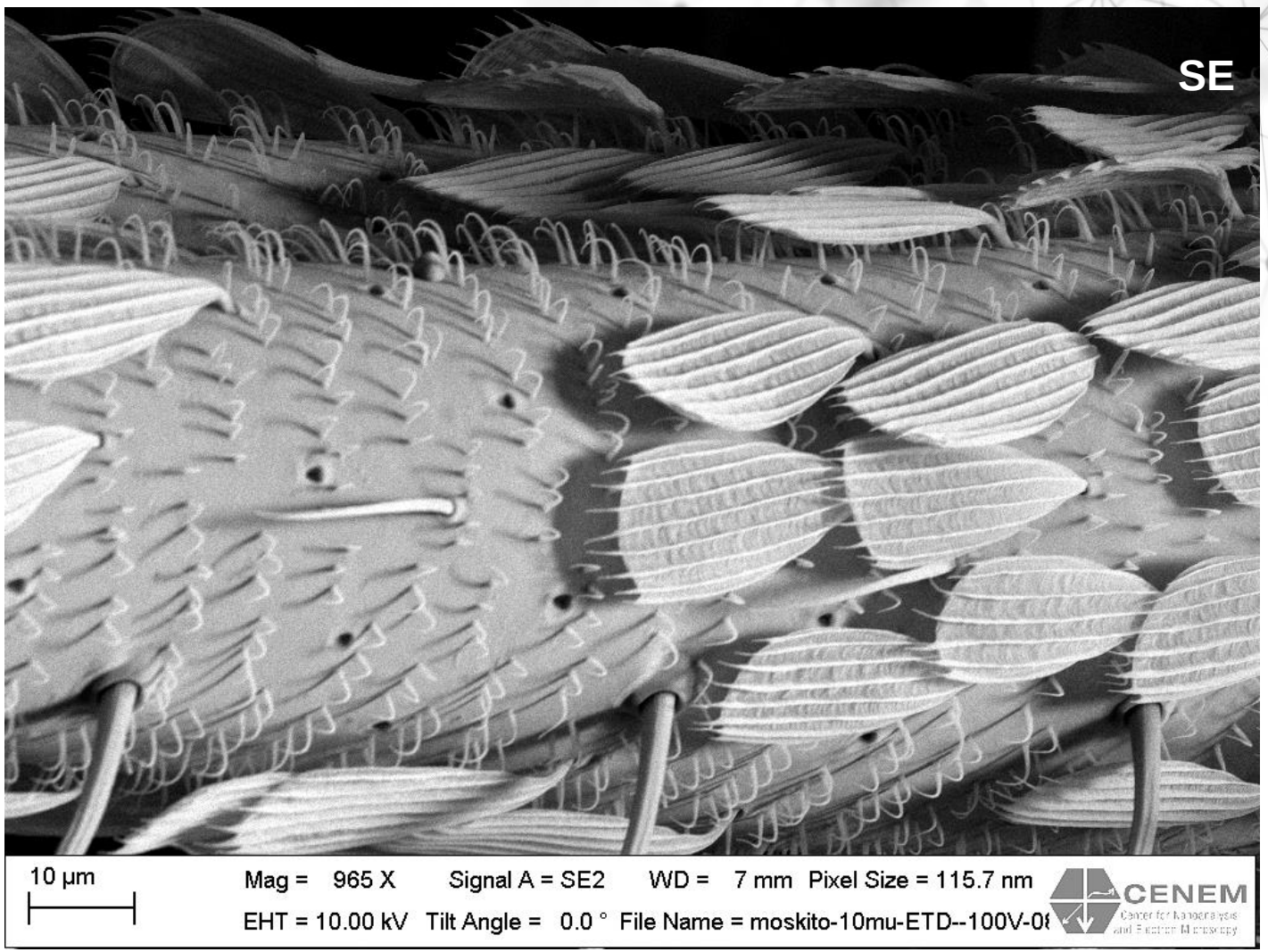

Shadowing
Transparency

Leg of mosquito

Chemical Imaging

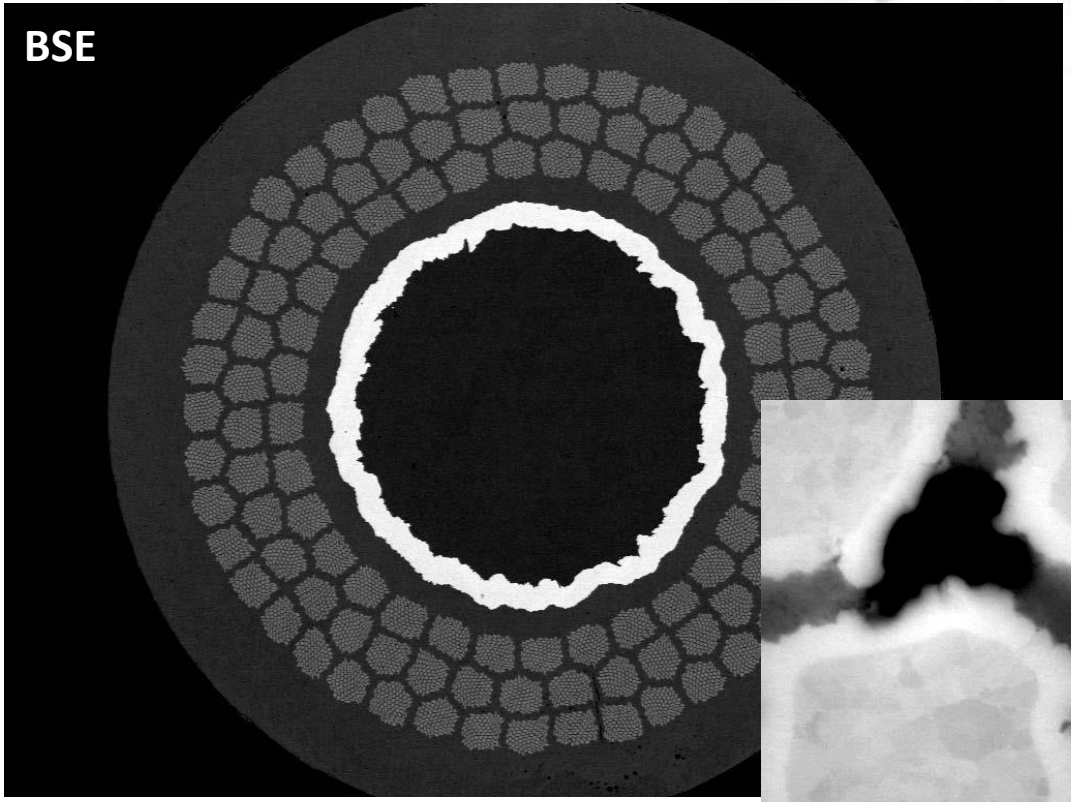

Nb_3Sn superconductor wire

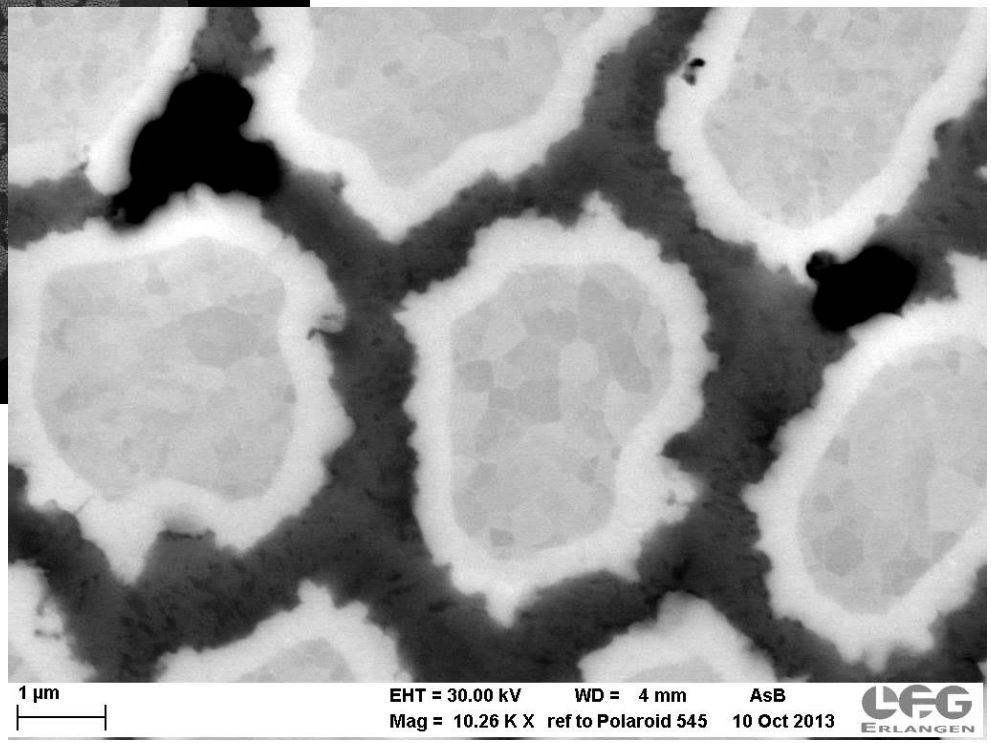

Chemical Contrast

Crystallographic Contrast

Polycrystalline CeO_2

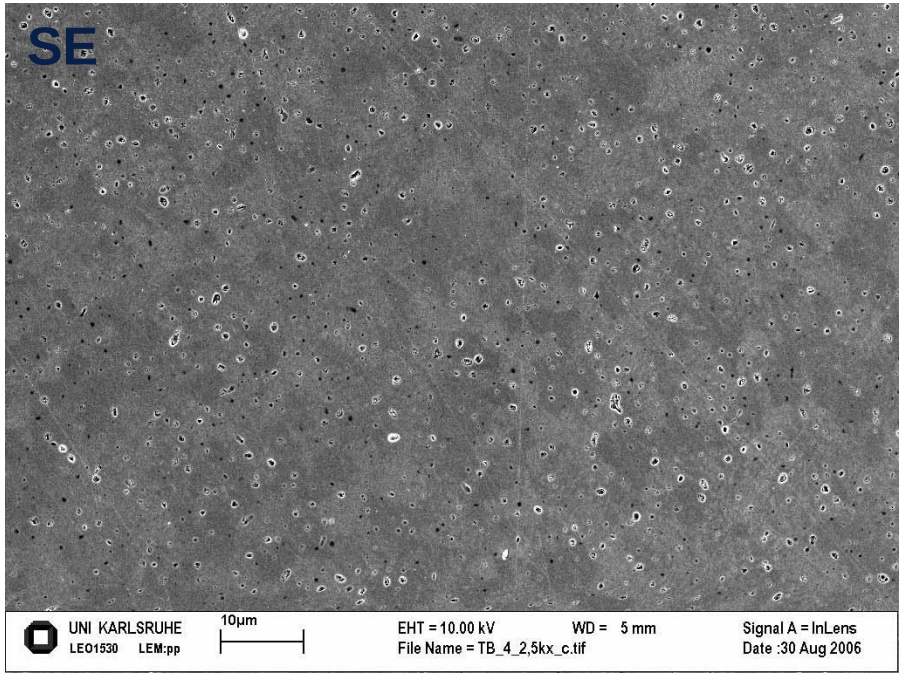

Polished surface

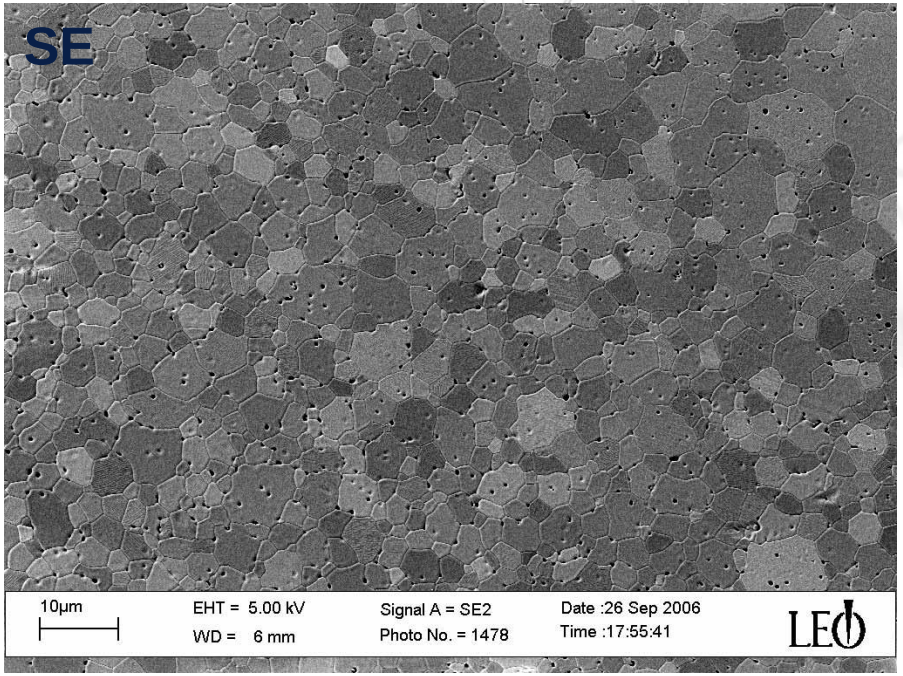

Thermally etched surface

Crystallographic Contrast

X-ray Spectroscopy

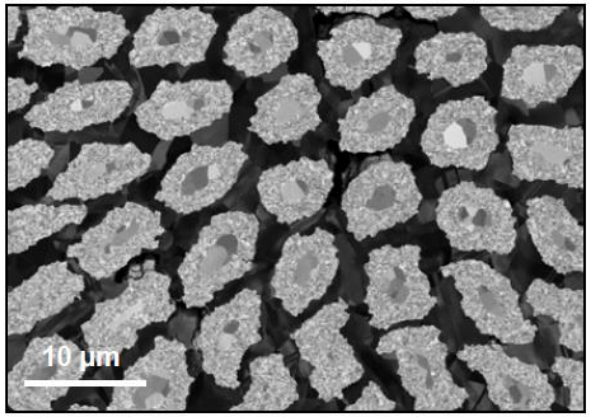

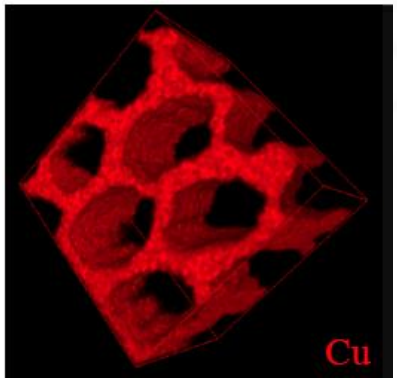

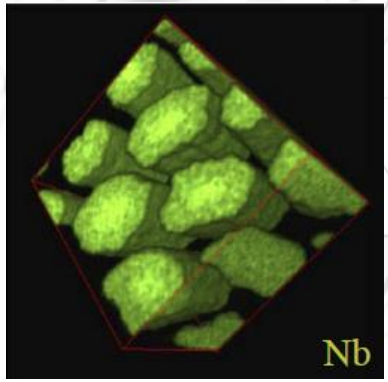

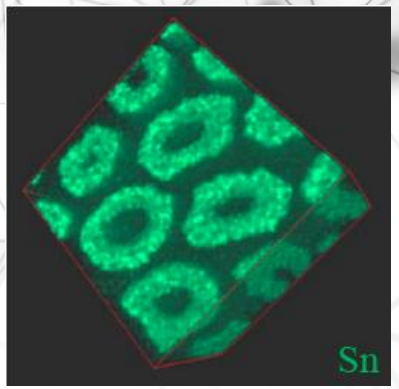

EDXS-tomo. of
superconducting material

X-Ray Emission

γ (**E**γ=hν)

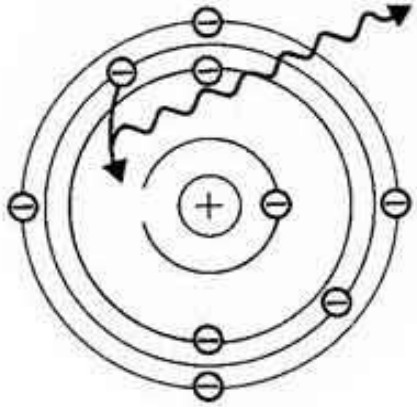

EDXS

Energy-Dispersive
X-Ray Spectroscopy

$$h\nu = E_i - E_f$$

E. Fuchs, H. Oppolzer, H. Rehme,
Particle Beam Microanalysis, Fig. 2.43
Pavia et al. – Microsc. Mircoanal. 21 (Suppl 3), 2015

Focused Ion-beam Microscopy

DualBeam set up

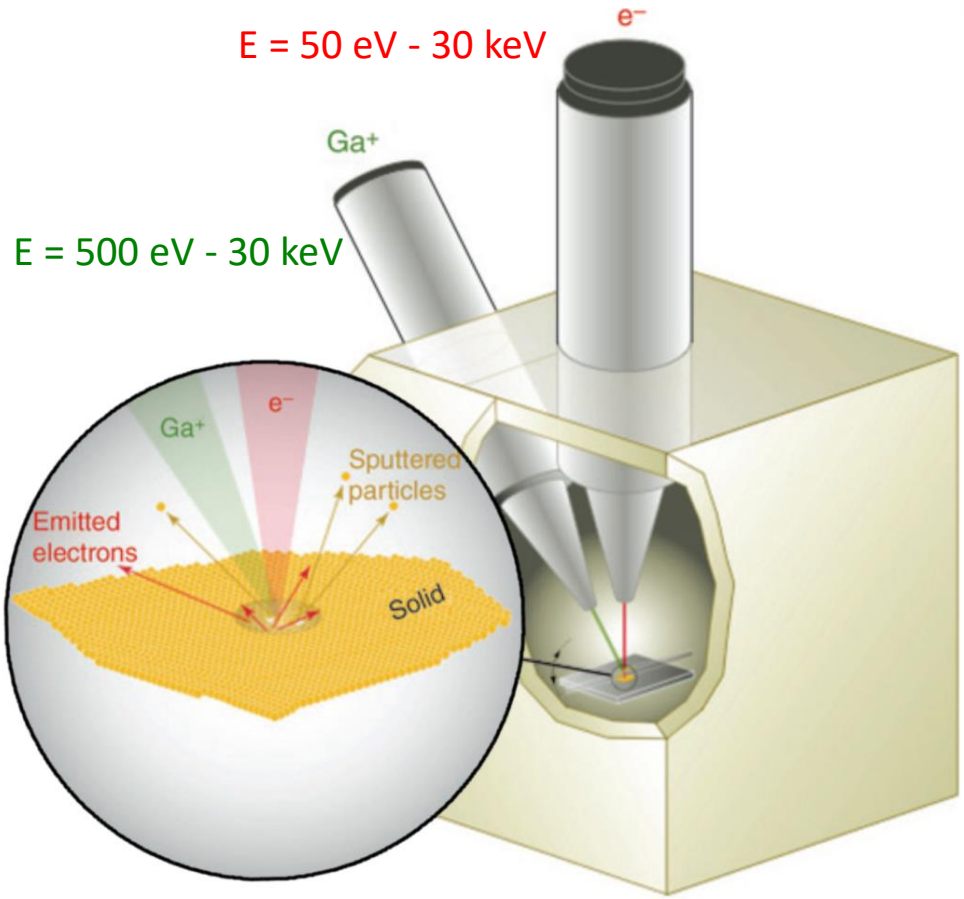

Volkert and Minor (2007)

Youtube.com, from Alexander Laqueree

Scanning Electron & Ion Microscope

FEI Helios NanoLab 660 (monochromated)

Outline

1. **Scanning Electron Microscopy**
   1. **Basic Instrumentation**
      - Electron source + acceleration, optics (lenses, deflectors)
      - Lens aberrations — **Minimum probe size — Resolution**
      - Convergence angle — **Depth of field (DOF)**
   2. **Electron Sample Interaction:** Primary electron — Atom — Sample
      - Elastic + inelastic scattering
      - Multiple scattering → **Interaction volume — Resolution**
      - Generation of backscattered electrons (BSE), secondary electrons (SE) — Charging
   3. **Imaging Modes**
      - SE-imaging: topographic contrast
      - BSE-imaging: density/atomic-number contrast, orientation contrast (channeling)
      - Scanning transmission electron microscopy (STEM)
      - Electron backscattered diffraction (EBSD)
      - Advanced techniques
   4. **X-ray Spectroscopy**
      - Excitation X-rays
      - Energy-dispersive (EDXS) vs. wave-length dispersive (WDXS) X-ray spectroscopy
2. **Focused Ion Beam (FIB)**
   - Basic instrumentation: Liquid-metal Ga-ion source + ion optics
   - Interaction of Ga ions with sample
   - Modes of operation: Imaging (SE, secondary ions)
     Milling (Nanostructuring, TEM sample preparation)
     Beam-induced deposition

Basic Instrumentation

FEI Helios NanoLab 660

Image Formation

Image formation:

- Scanning electron probe on sample through sequence of positions (1..9)

Magnification M = **L/l**
Scale bar!

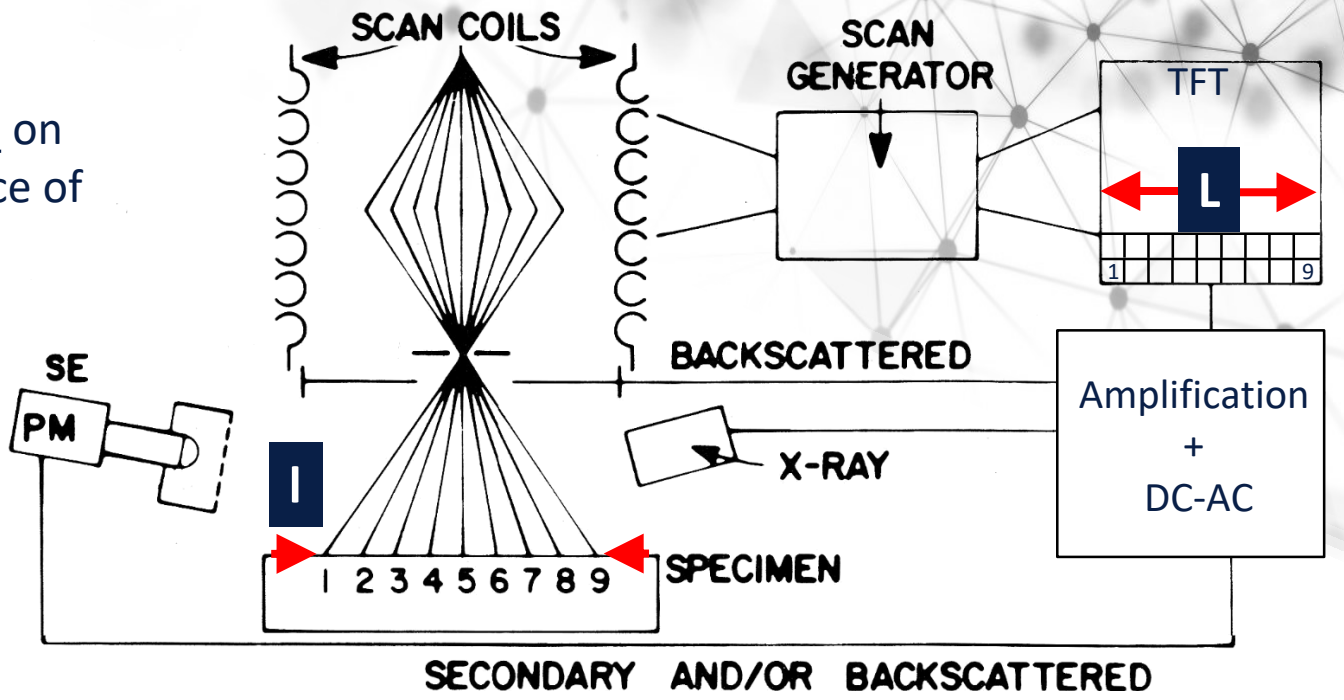

after Goldstein et al., *Scanning Electron Microsopy and X-ray Microanalysis* (p. 102)

Image Formation

Image formation:

- Scanning electron probe on sample through sequence of positions (1..9)

Magnification M = **L/l**
Scale bar!

- Each measuring point: (dwell time few 10 µs)
  - Signal collection
  - Amplification
  - Analog → Digital signal

Serial image build-up by assigning digital signal to related pixel

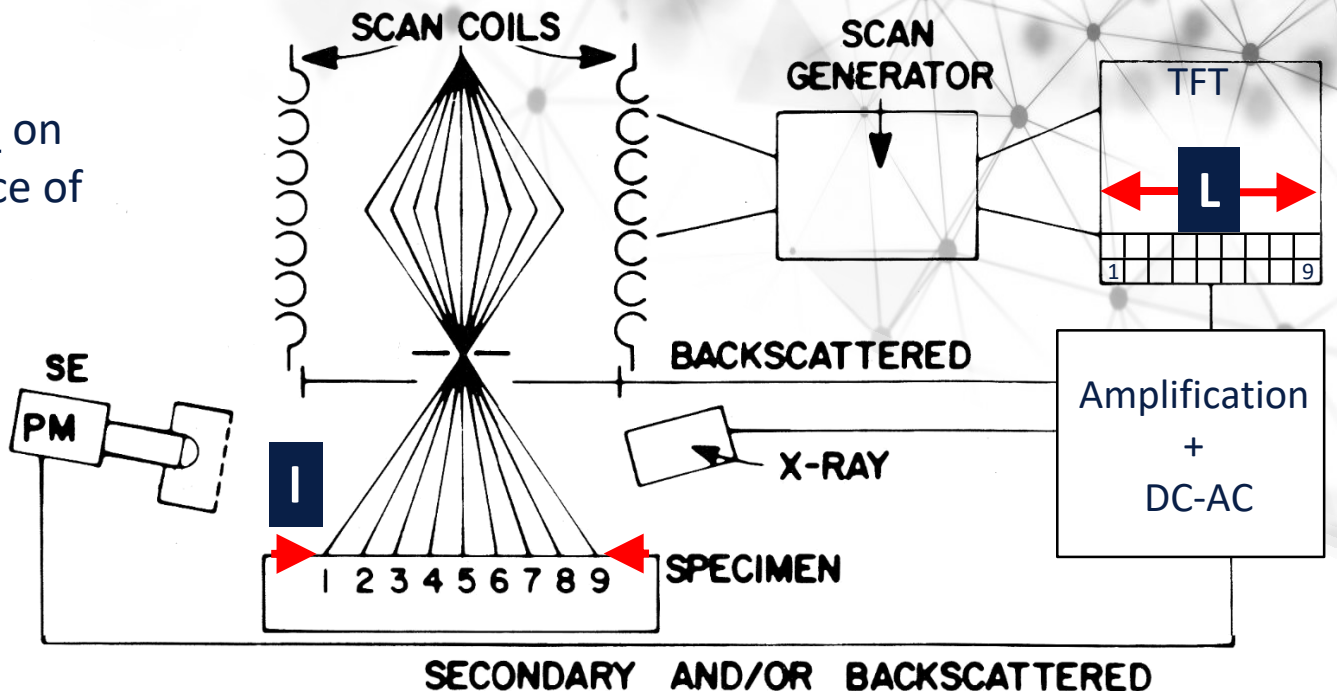

after Goldstein et al., *Scanning Electron Microsopy and X-ray Microanalysis* (p. 102)

Image Formation

Image formation:

- Scanning electron probe on sample through sequence of positions (1..9)

Magnification M = **L/l**
Scale bar!

- Each measuring point: (dwell time few 10 µs)
  - Signal collection
  - Amplification
  - Analog → Digital signal

Serial image build-up by assigning digital signal to related pixel

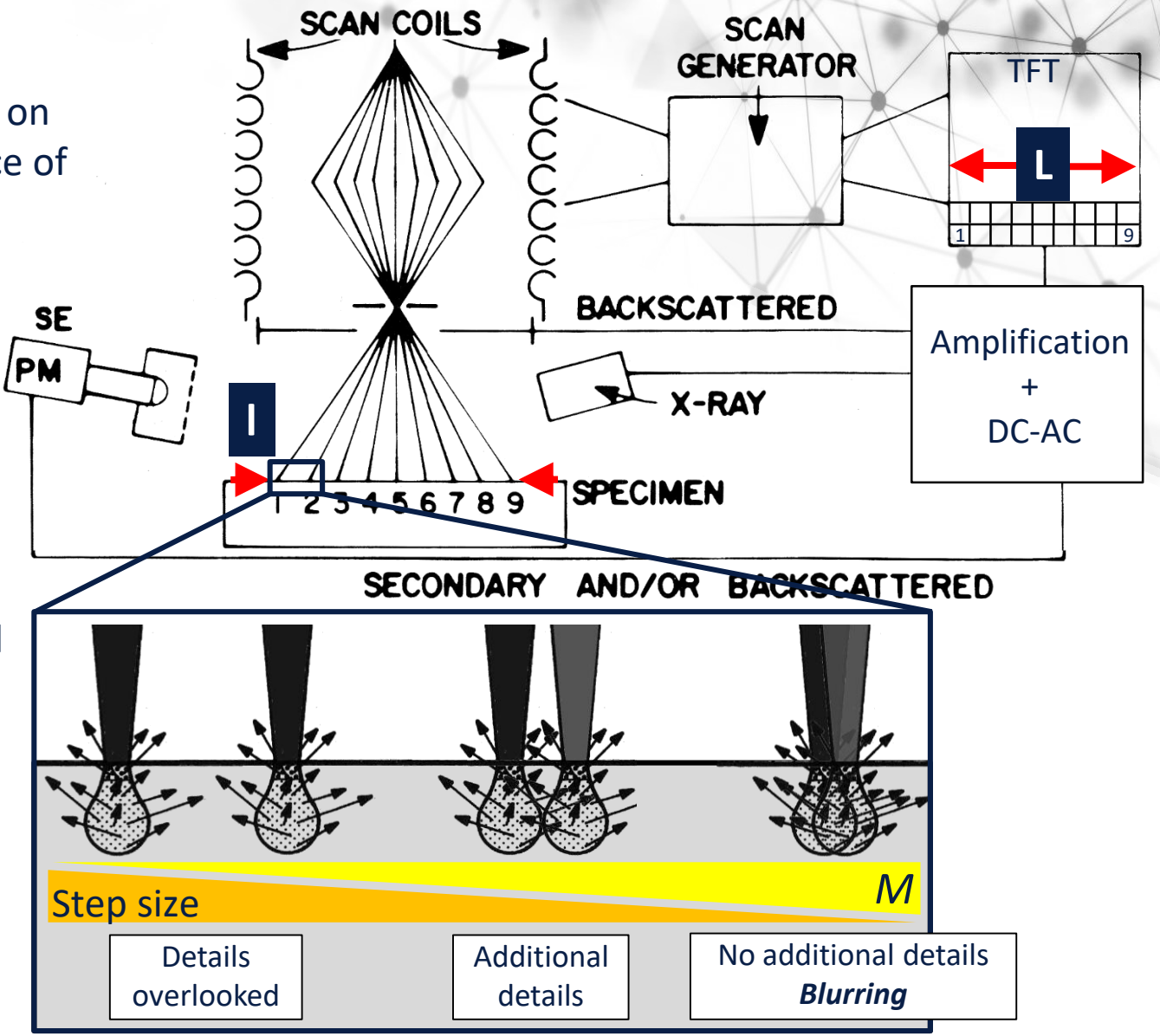

*Example: Undersampling of Object Details at Low Mag

Plasmonic gold discs on wafer

Courtesy S. Madsen, Prof. R. Sinclair (Stanford Univ.)

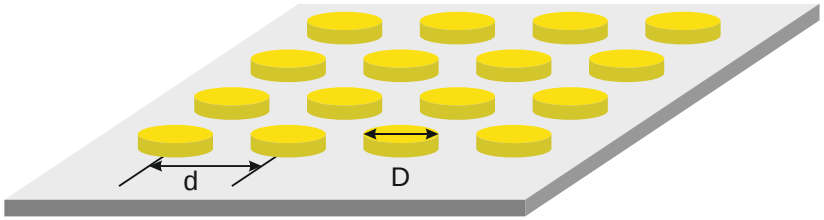

Au discs d=100 nm/D=66 nm (SEM step size ~2,5 nm)

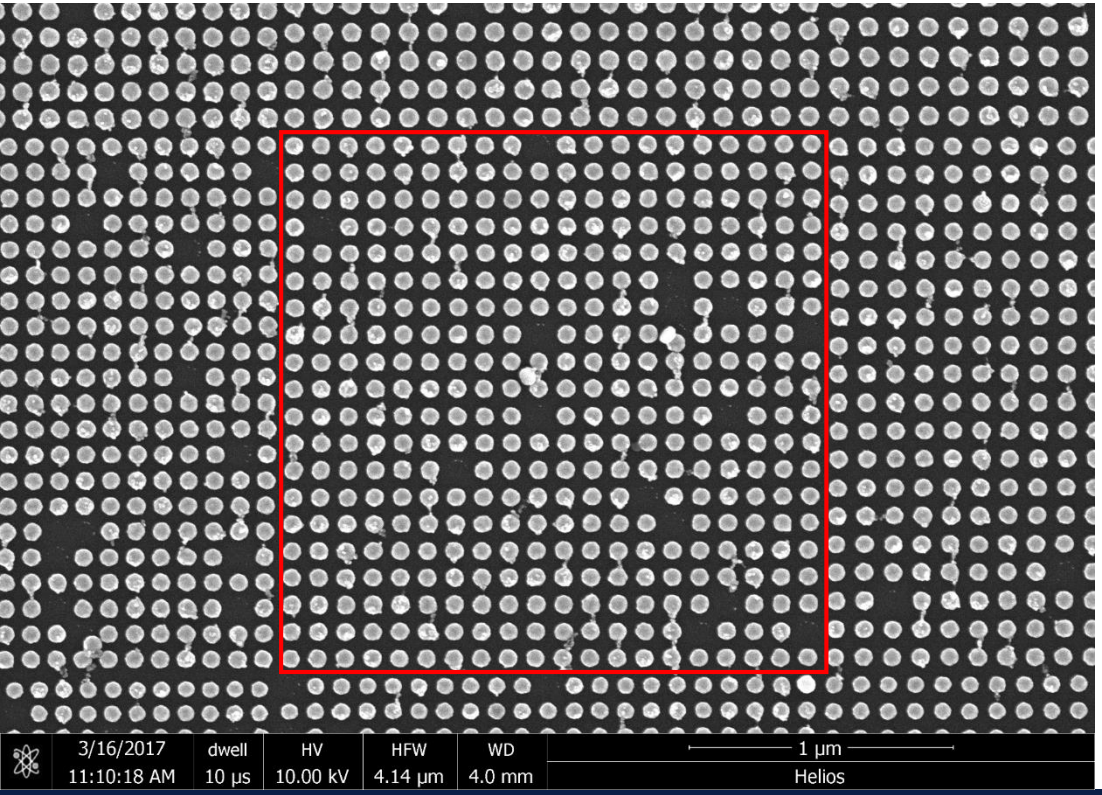

Low-mag overview scan
(SEM step size **95 nm**)

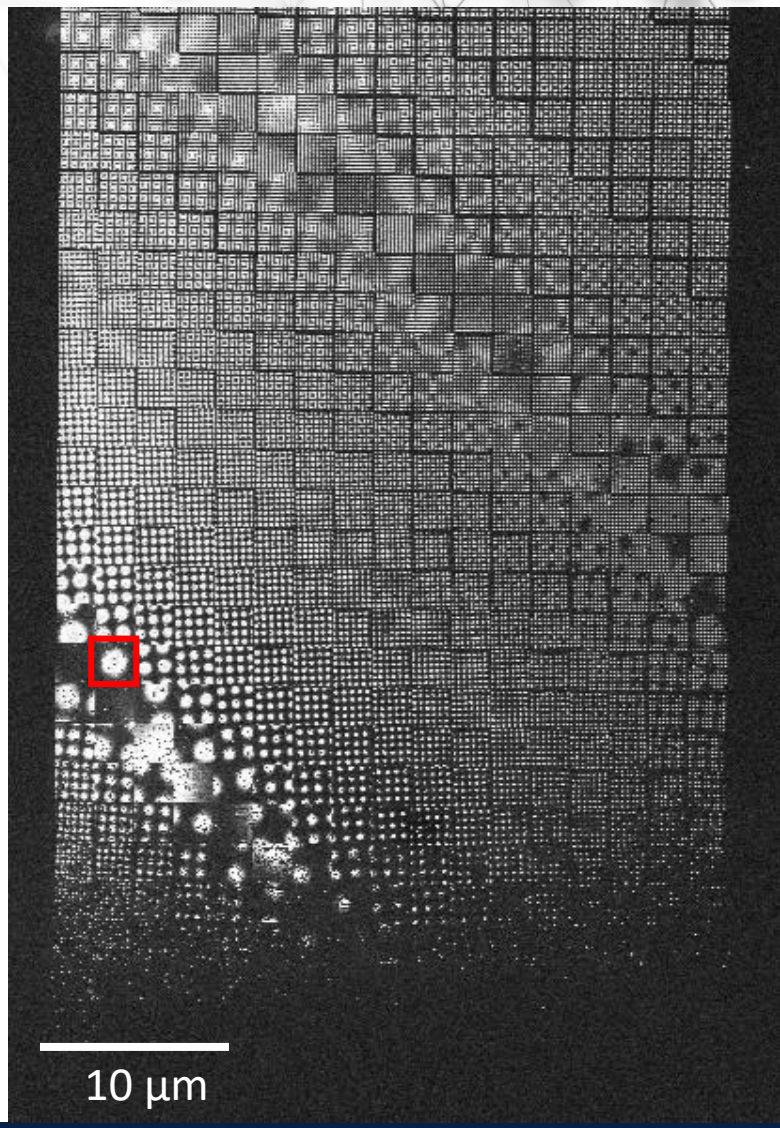

*Example: Undersampling of Object Details at Low Mag

Plasmonic gold discs on wafer

Courtesy S. Madsen, Prof. R. Sinclair (Stanford Univ.)

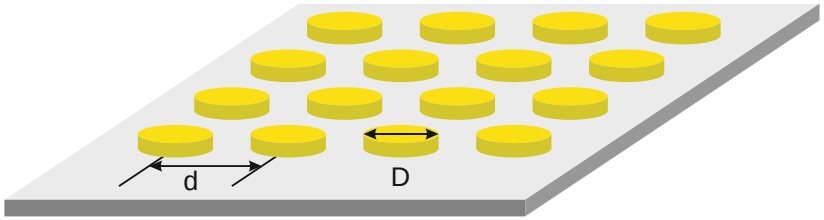

Au discs d=100 nm/D=66 nm (SEM step size ~2,5 nm)

Low-mag overview scan
(SEM step size **95 nm**)

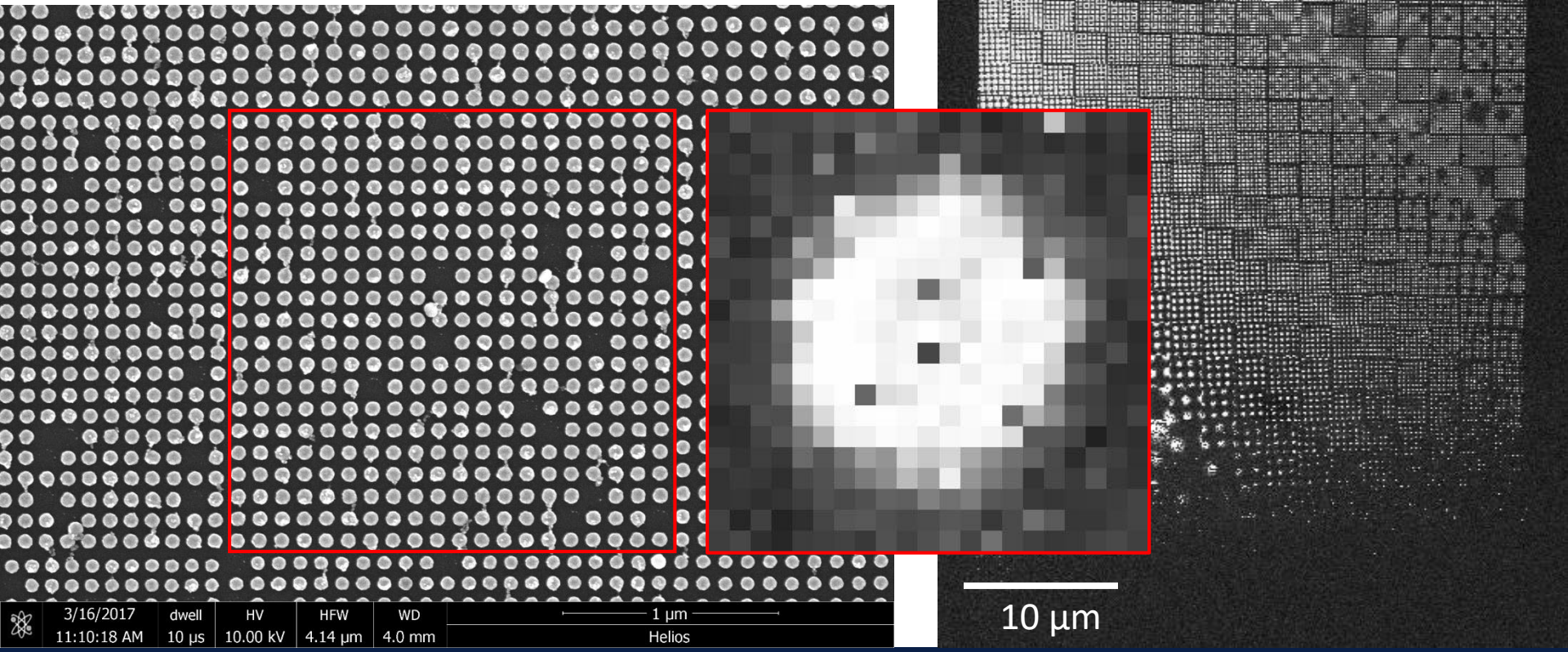

*Example: Undersampling of Object Details at Low Mag

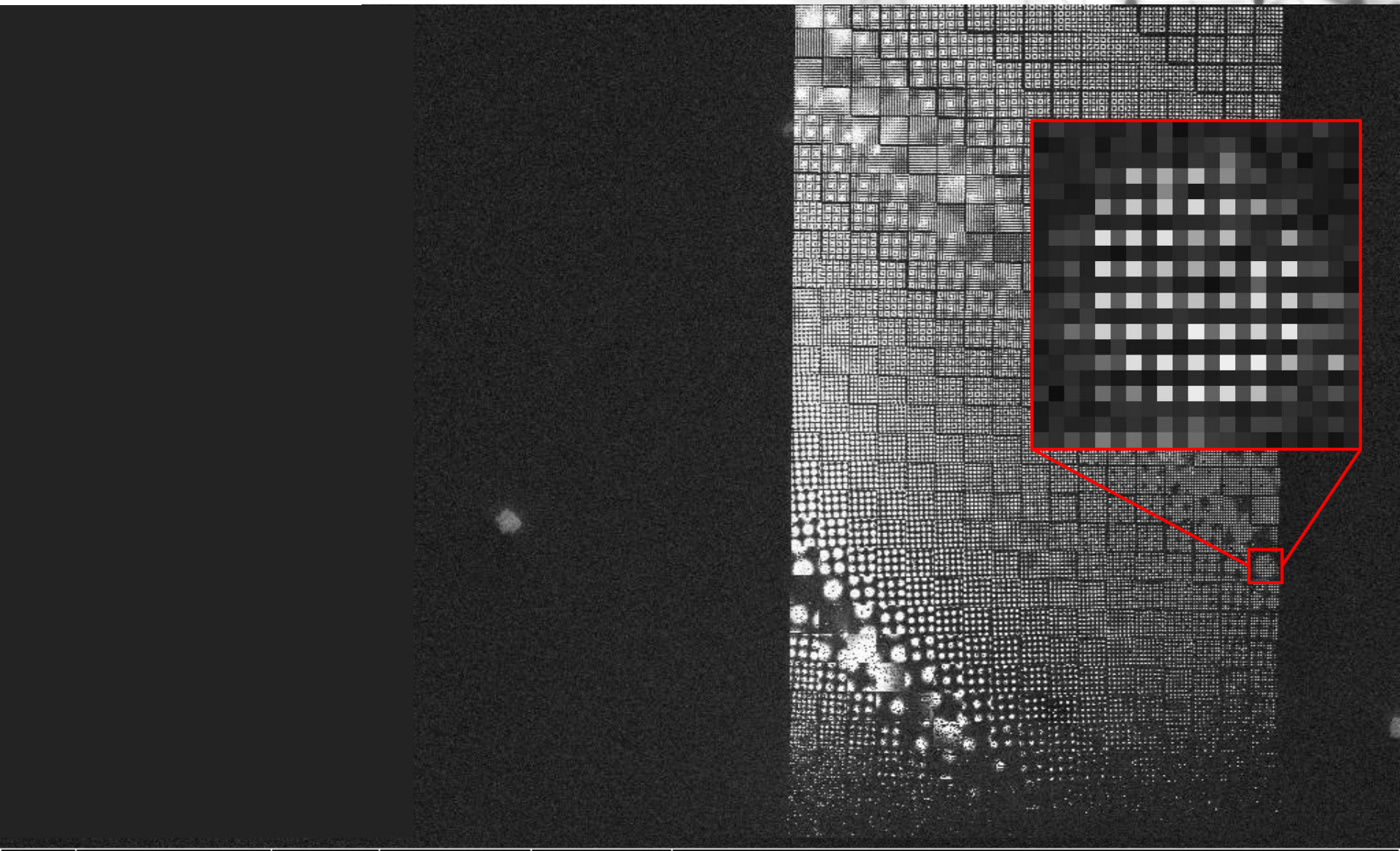

*Example: Undersampling of Object Details at Low Mag

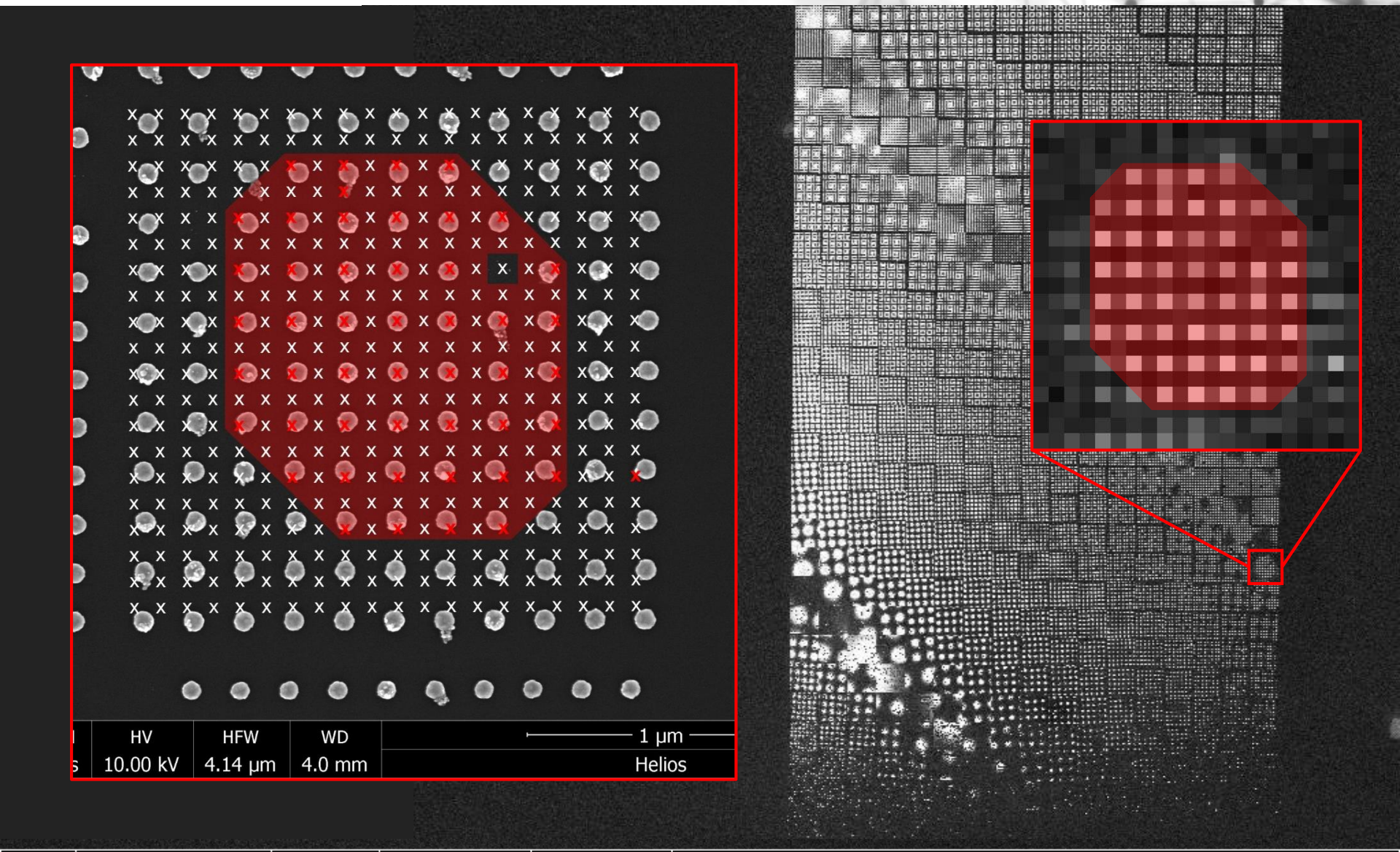

*Cathode Ray Tube – TV

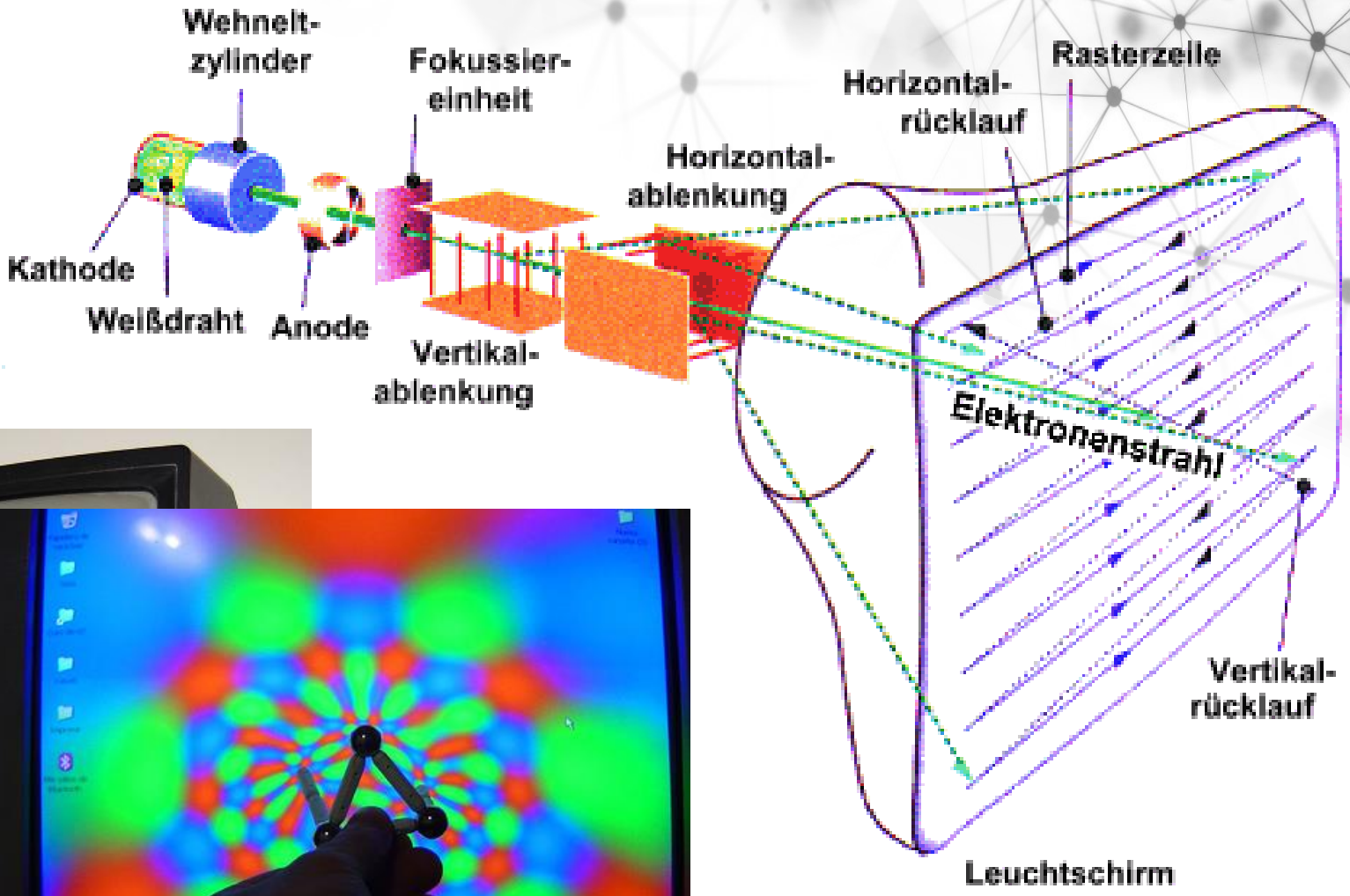

http://www.fachlexika.de/technik/mechatronik/monitor.html & de.wikipedia.org

Electron Sources for SEM/TEM

W hairpin filament

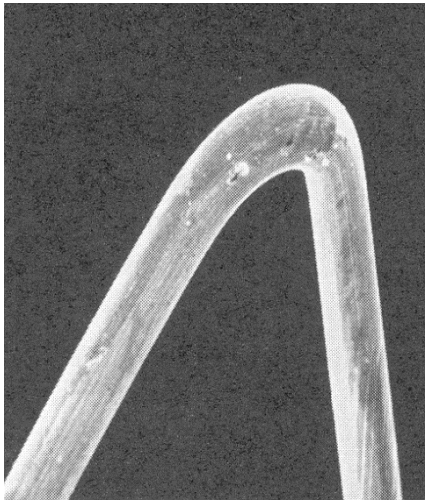

LaB_6 cathode

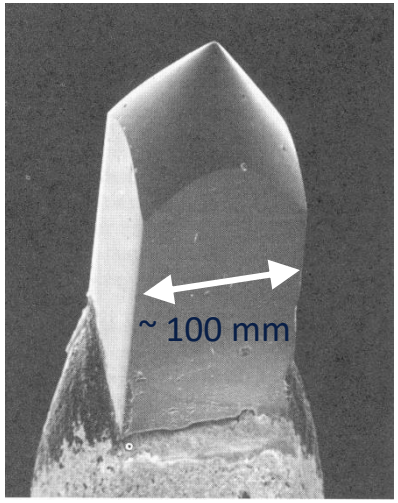

Thermionic emission

Schottky-emitter

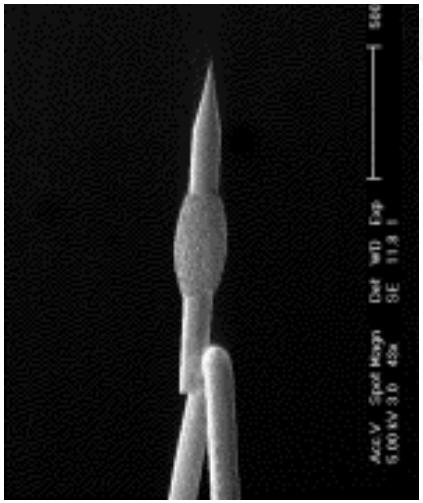

Field-assisted thermionic emission

Cold-FEG

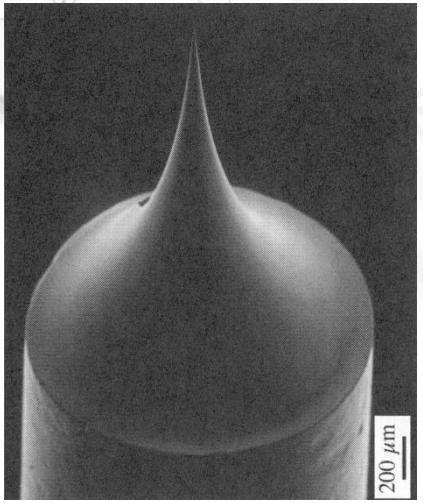

Field emission

Cook et al., Ultramicroscopy 109, 403 – 412 (2009)
Williams/Carter: Transmission Electron Microscopy

Principles of Electron Emission

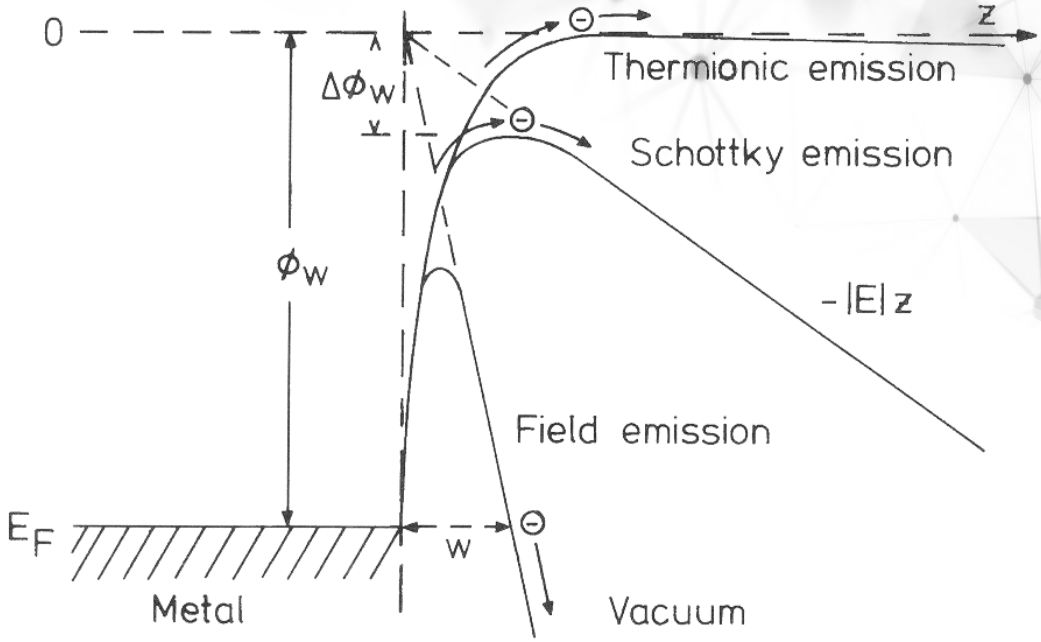

ϕ_w work function

Thermionic emission: $j_c = AT_c^{\,2} \exp(-\phi_w / kT_c)$ (Richardson's law)

Field emission: Tunneling of electrons through the barrier which is reduced by a very strong electric field (~ 10 V/nm)

Schottky emission: strong electric field (~ 0.5…1 V/nm) reduces the effective work function for thermionic emission

from Reimer, *Transmission Electron Microscopy*

Electron: Wave-Particle Dualism

Electron as particle

Rest mass $m_0 = 9.1091 \cdot 10^{-31} kg$

Charge $e = -1.602 \cdot 10^{-19} C$

Kinetic energy $E = |e|U = \frac{1}{2} m_0 v^2 = \frac{p^2}{2m_0}$

De Broglie (1924): $\vec{p} = h\vec{k} = m\vec{v}$ (as for light quanta)

Planck constant $h = 6.626 \cdot 10^{-34} Js$

with $|\vec{k}| = \frac{1}{\lambda}$ ⇒ $\lambda = \frac{h}{p} = \frac{h}{\sqrt{2m_0 E}}$

Electron as wave

Electron Wavelength in TEM

Relativistic correction of de-Broglie relation:

$$\lambda = \frac{h}{\sqrt{2m_0E}} \cdot \frac{1}{\sqrt{1+E/(2E_0)}}$$

$$E_0 = m_0c^2 = 511keV$$

$$c = 2.9979 \cdot 10^8 \, m/s$$

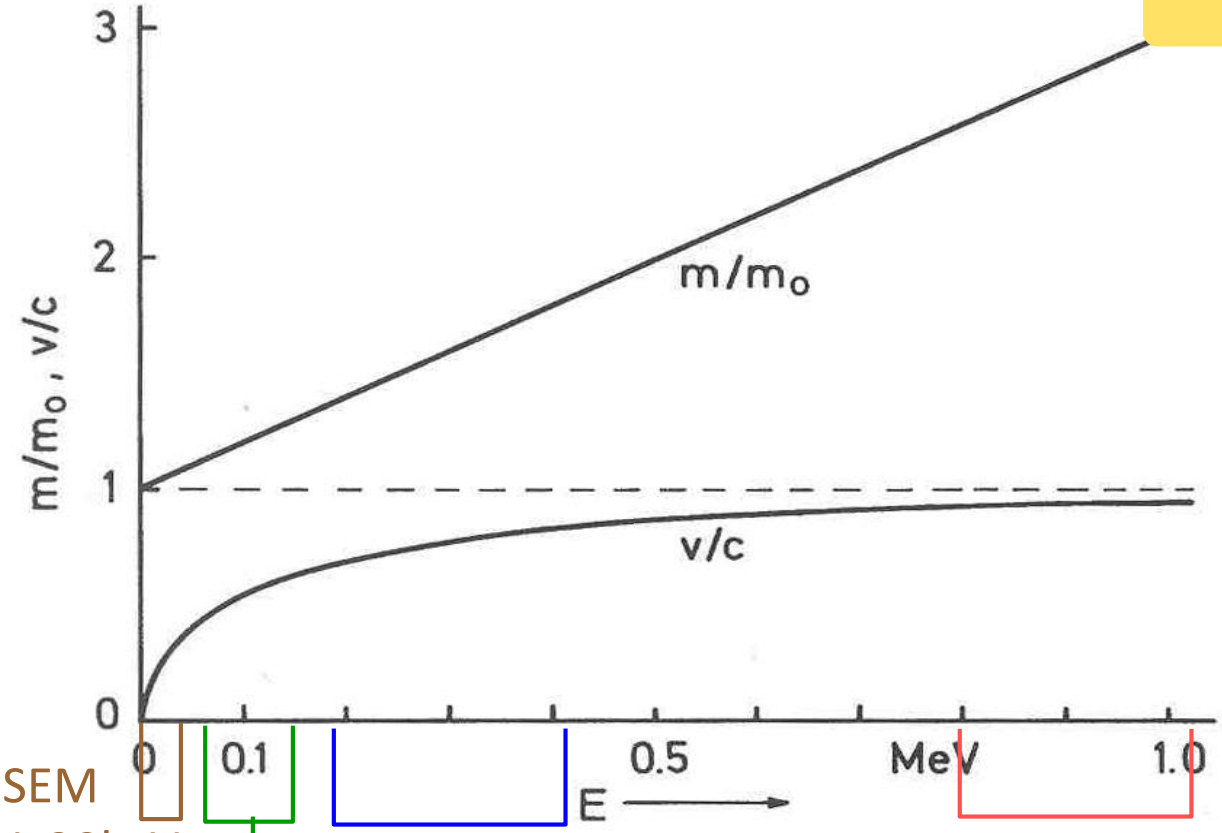

SEM
1-30keV

Biological TEM
80-120keV

medium-voltage TEM
(Material Science)
200-400keV

high-voltage TEM
800keV – 1.2MeV

Acceleration voltage	λ
1 kV	38.8 pm
30 kV	6.9 pm
100 kV	3.7 pm
200 kV	2.5 pm
300 kV	2.0 pm
1MV	0.9 pm

Reimer, *Transmission Electron Microscopy*

*Deflection in a Magnetic Field

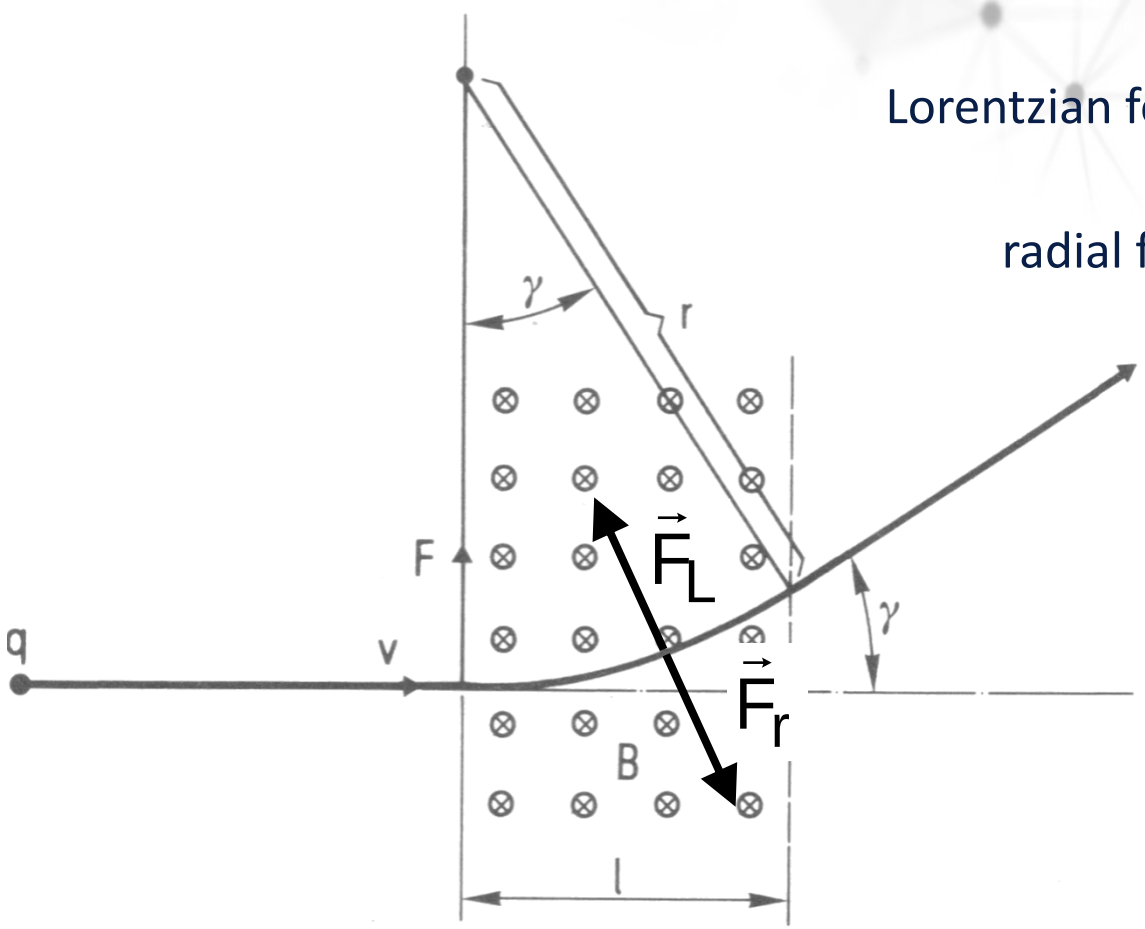

Lorentzian force: $\vec{F}_L = q \cdot (\vec{v} \times \vec{B})$

radial force: $\vec{F}_r = m \cdot v^2 / r$

balanced

$$q \cdot v \cdot B = m \cdot v^2 / r$$

Small-angle deflection:

$$\gamma \sim \frac{l}{r} = \frac{q \cdot l \cdot B}{m \cdot v} = \sqrt{\frac{q}{m}} \cdot \frac{l \cdot B}{\sqrt{2U_0}}$$

from Oppolzer, Rehme, *Particle Beam Microanalysis*

*Deflection in a Magnetic Field

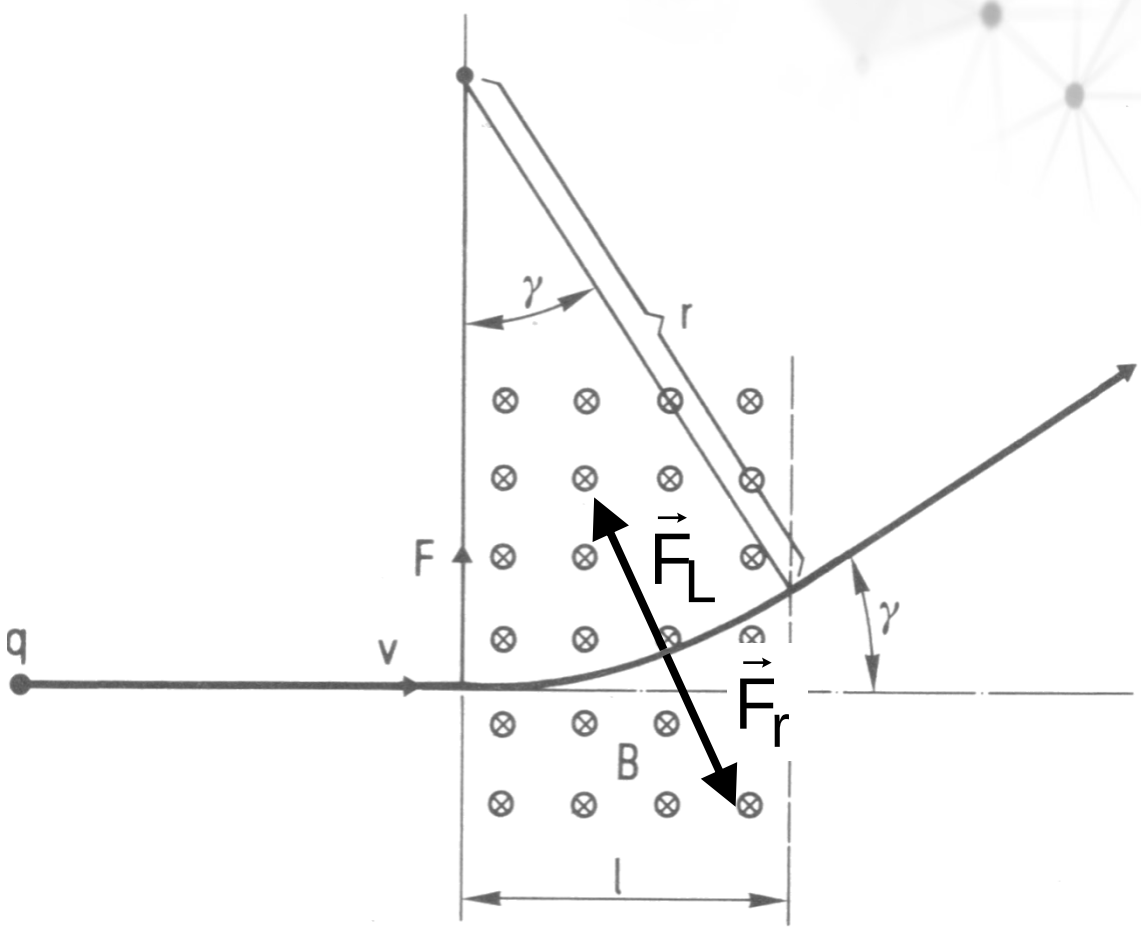

$$\gamma \sim \sqrt{\frac{q}{m}} \cdot \frac{I \cdot B}{\sqrt{2U_0}}$$

The deflection depends on $\sqrt{q/m}$.

Magnetic fields can be exploited for separating particles with respect to their mass, charge and energy! (but not independently)

Electromagnetic Lens

B constant:

$$\vec{F} = q\vec{v} \times \vec{B}$$ (Lorentz force)

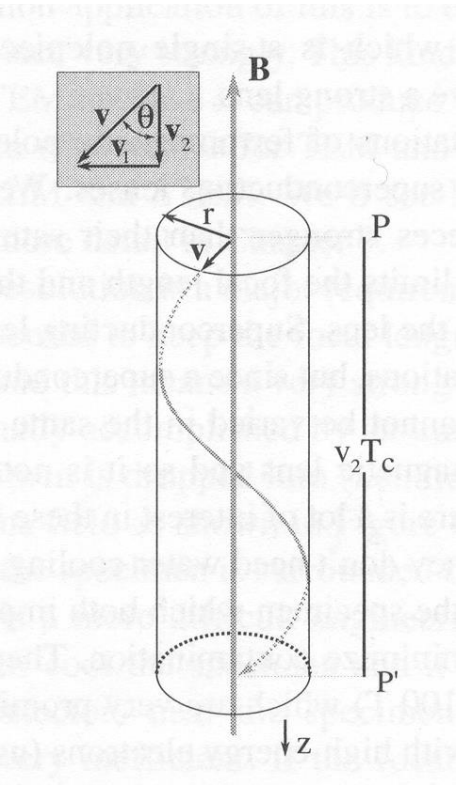

Spiral path

Electromagnetic lens

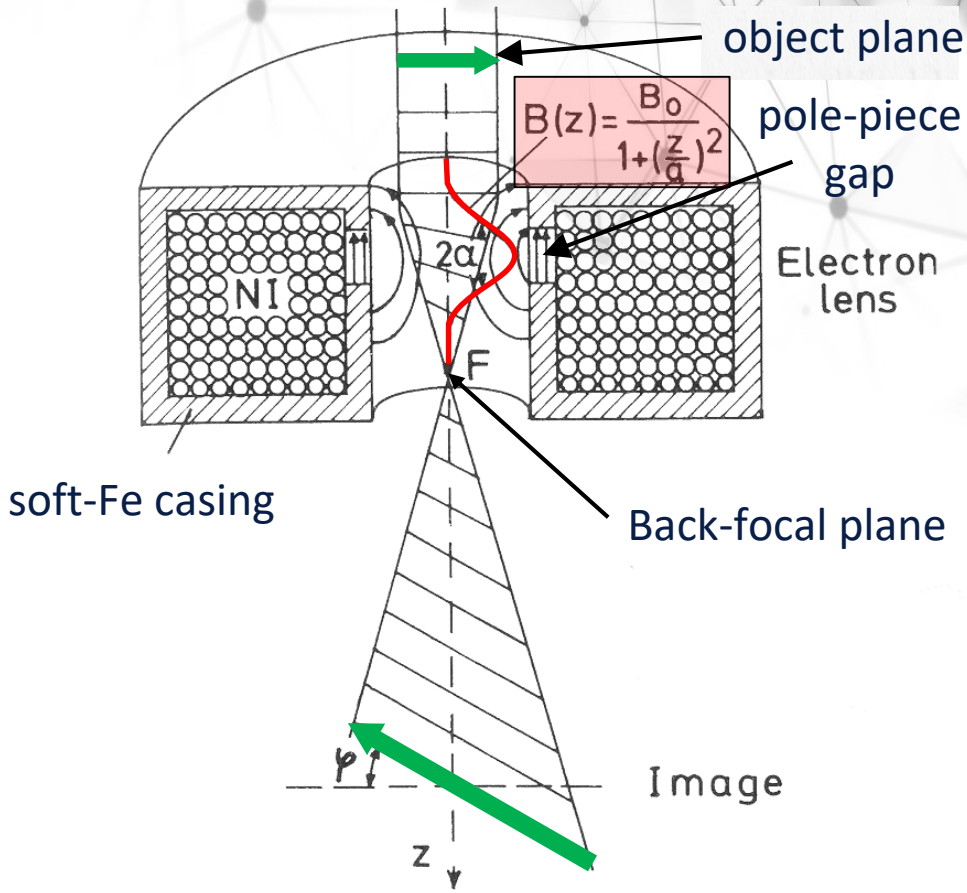

Spiral path + Focussing

Focal length can be controlled by lens current

Reimer, *Transmission Electron Microscopy*

Lens Equations

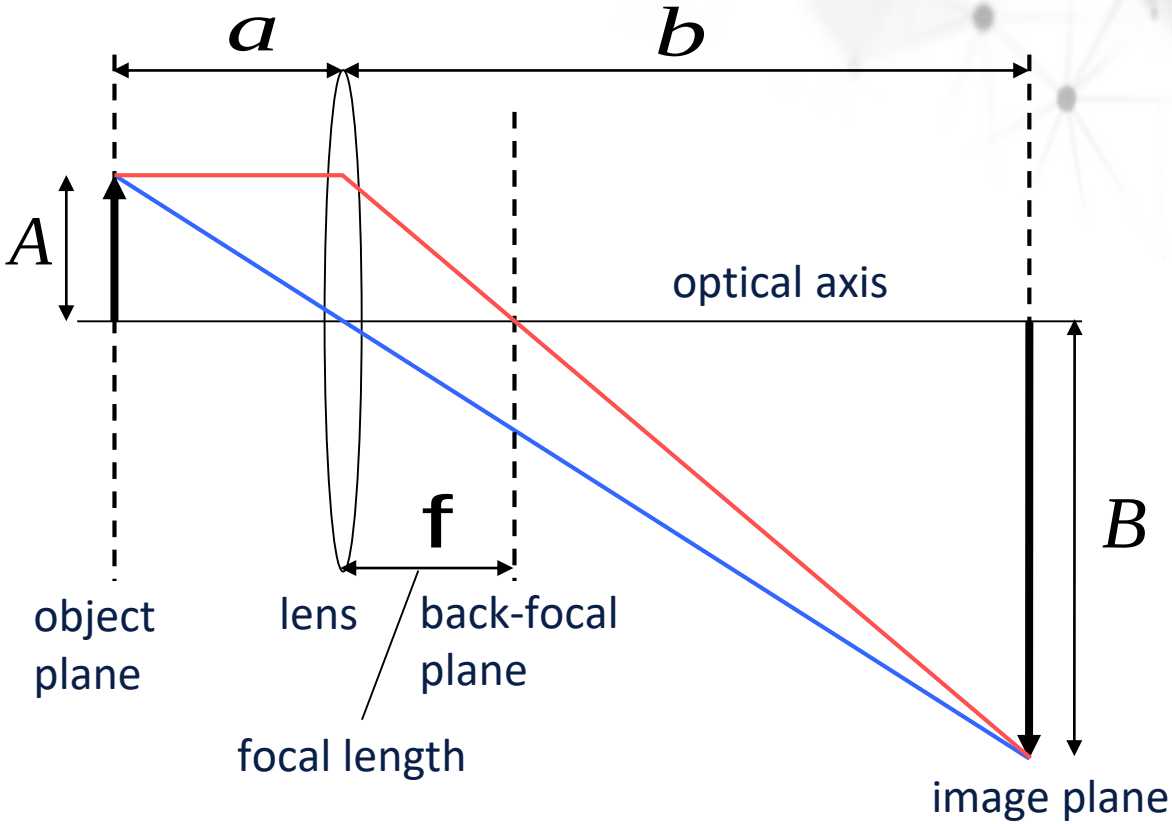

$$\frac{1}{f} = \frac{1}{a} + \frac{1}{b}$$

$$M = \frac{B}{A} = \frac{b}{a}$$

M: magnification

Constructing the image:

- Central beam unaffected by lens
- Axis-parallel beam crosses center of the back focal plane

a > f real images

a < f imaginary image

a = f image at infinite distance

Magnetic lenses in SEM used to demagnify electron source! → nm-sized electron probe

Spherical Aberration

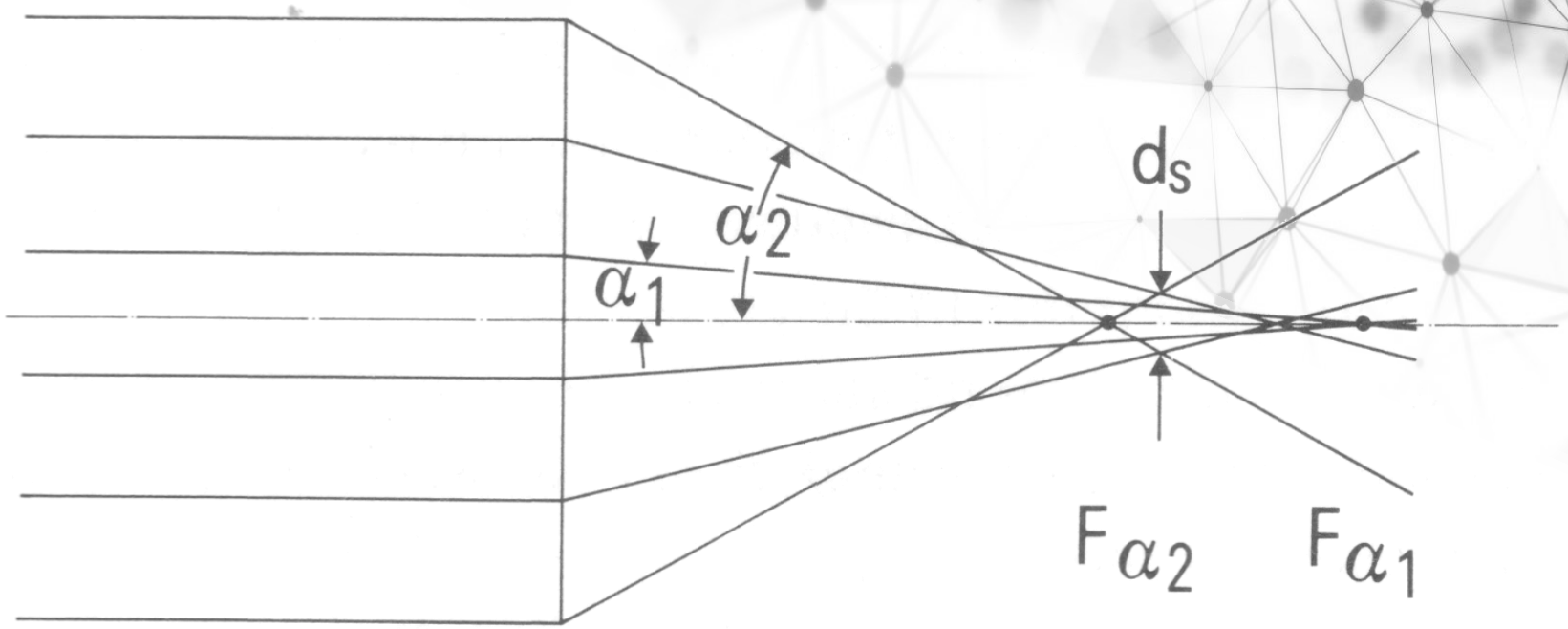

The focal point F_{a2} of rays with larger angles of divergence a_2 (off-axis rays) is closer to the lens than for paraxial rays (F_{a1})

$$d_s = \frac{1}{2} C_s \cdot \alpha^3$$

Chromatic Aberration

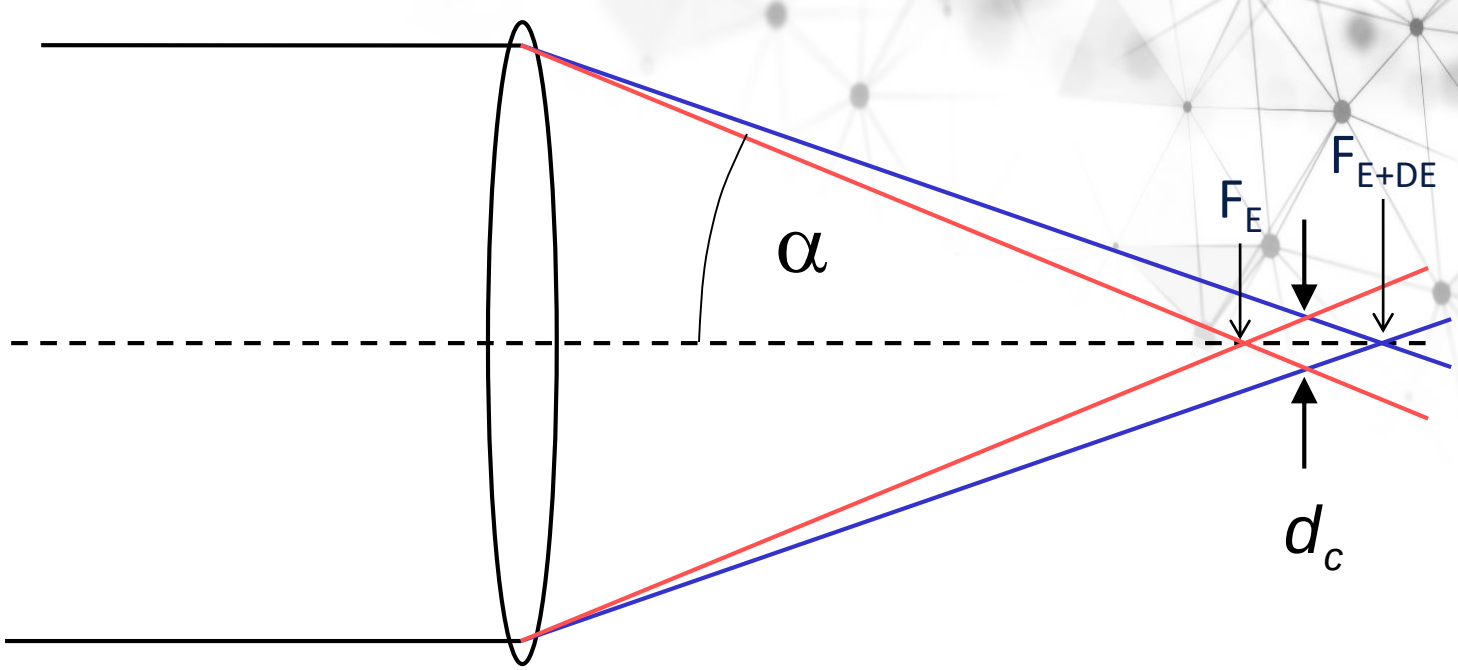

Electrons with different energies E and DE, i.e. different wavelength (represented by color), are focused at different focal points F_E and F_{E+DE}.

$$d_c = C_c \cdot (\Delta E / E) \cdot \alpha$$

Diffraction Error

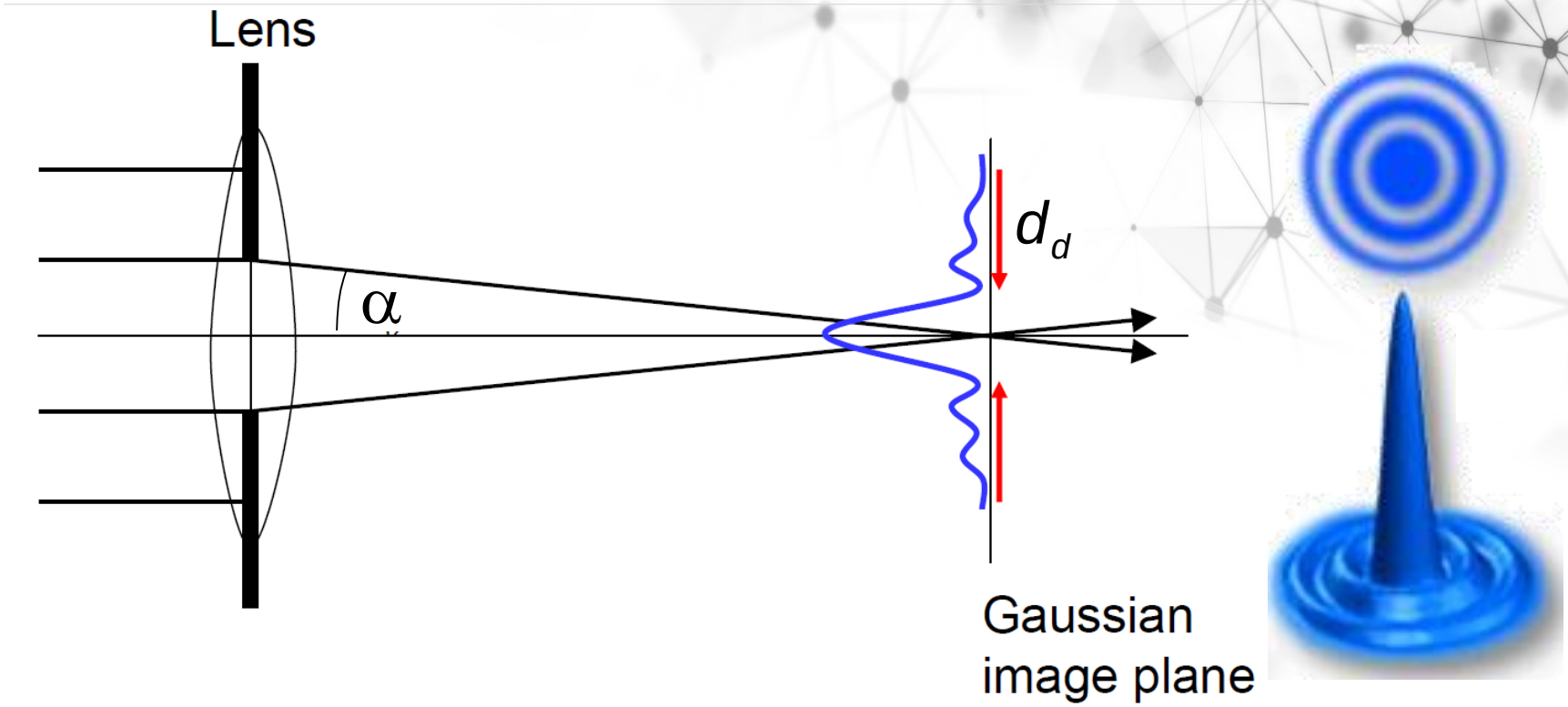

The limitation of the wavefront by the lens edge or aperture results in an intensity distribution (Airy disc) in the focal plane caused by diffraction.

$$d_d = 0.61 \cdot (\lambda / \alpha)$$

Optimum Probe Size

Relationship between probe size d_0, divergence α_p, and gun brightness β

$$d_0 = \frac{2}{\pi \alpha_p} \cdot \sqrt{\frac{I_p}{\beta}}$$

Lens aberrations lead to further beam broadening

$$d_0'^2 = d_0^2 + d_d^2 + d_s^2 + d_c^2$$

$$d_0'^2 = d_0^2 + \frac{(0.61 \cdot \lambda)^2}{\alpha_p^2} + \frac{1}{4} C_s^2 \cdot \alpha_p^6 + \left[C_c \cdot \frac{\Delta E}{E} \right]^2 \cdot \alpha_p^2$$

There is an optimum beam divergence α_{opt} for minimum probe size!

Optimum Probe Size

Find optimum convergence angle α_{opt} so that the probe size is minimized!

Often, only the spherical aberration and the diffraction error have to be considered:

$$\frac{d_{\min}}{m} = K\left(\frac{C_S}{m}\right)^{1/4}\left(\frac{\lambda}{m}\right)^{3/4}\left[\frac{I_p}{\beta\lambda^2}+1\right]^{3/8}$$

Optimal aperture for every microscope!

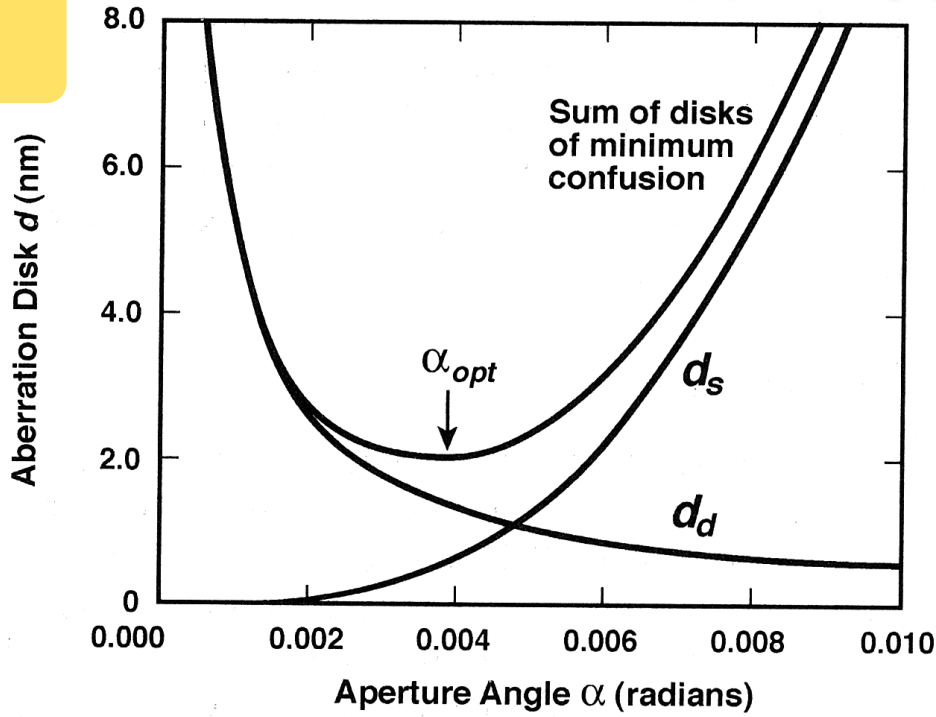

from Goldstein et al., *Scanning Electron Microscopy and X-ray Microanalysis*

$K \approx 1$ constant

β gun brightness

I_p probe current

λ electron wavelength

spherical aberration coeff.

Two-fold Astigmatism

Perfect lens

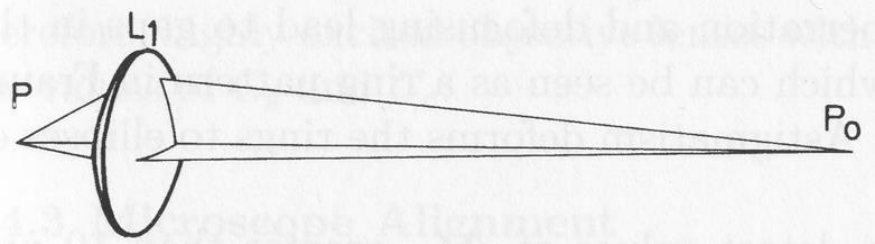

Lens with astigmatism

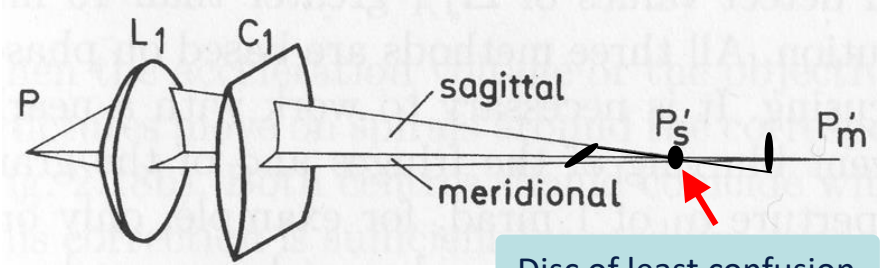

Disc of least confusion

Correction of astigmatism (schematic)

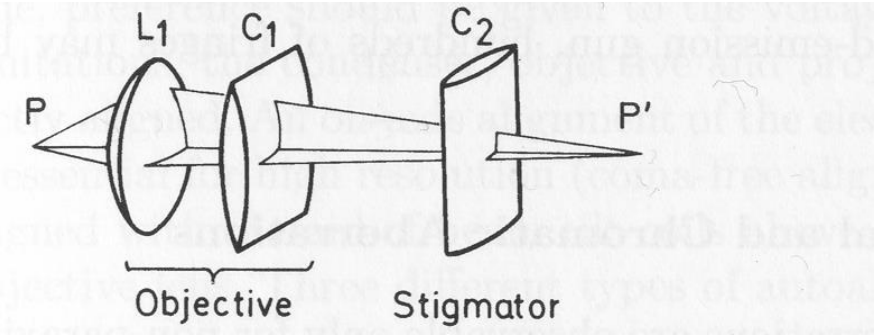

Stigmator

Fields & forces seen by the electron beam

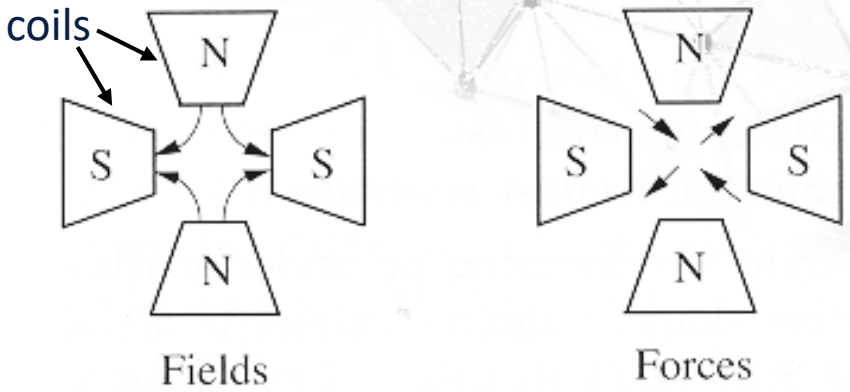

Beam shape before and after correction

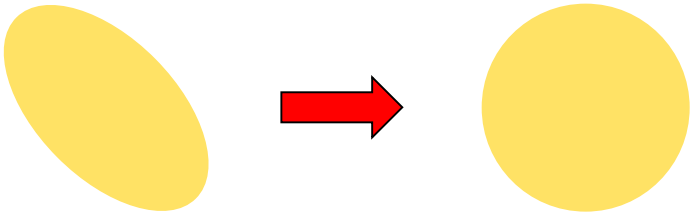

Reimer: Transmission Electron Microscopy

Microscope Alignment — Aberrations to be adjusted

Defocus **Astigmatism**

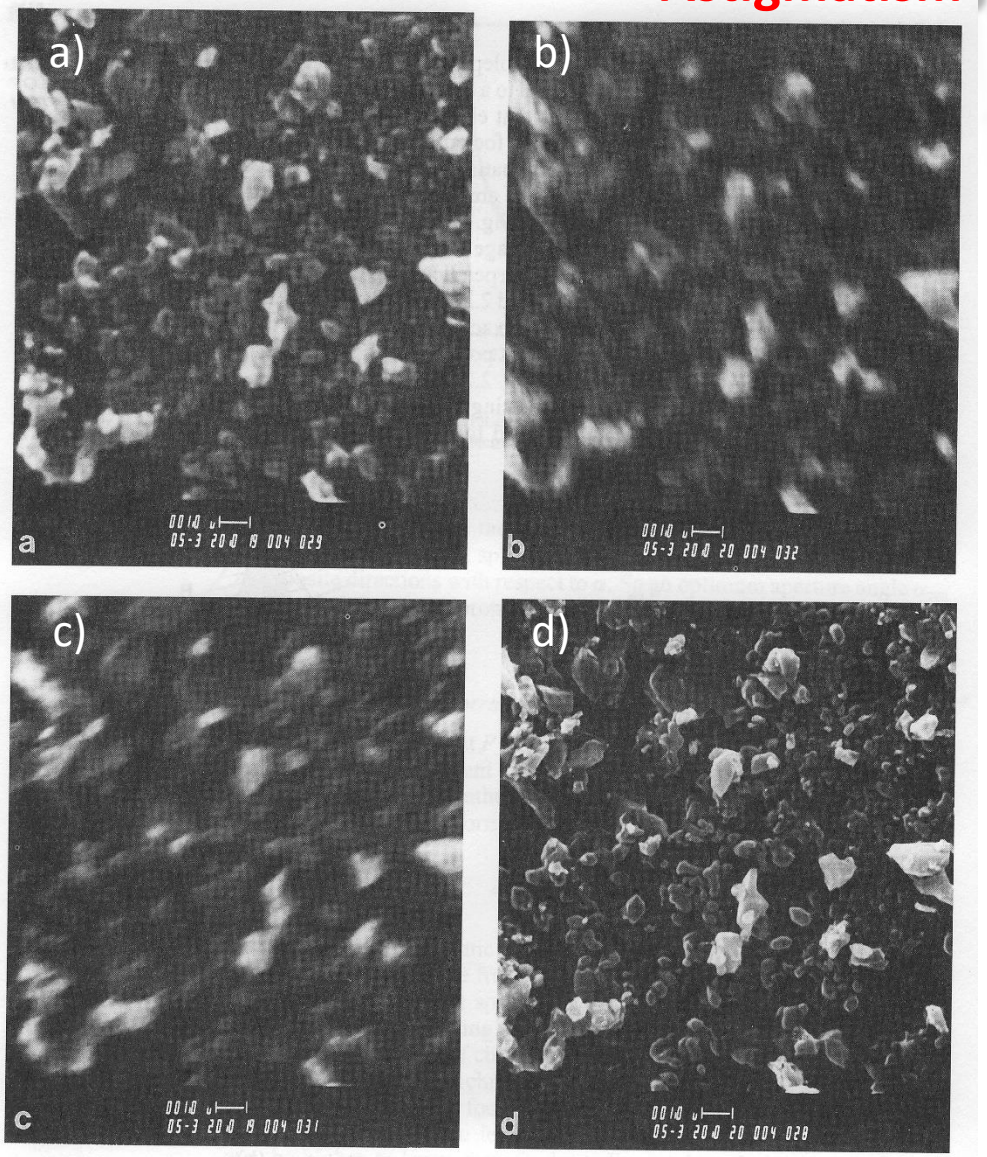

Beam shapes on the sample

a) initial situation

b) underfocus

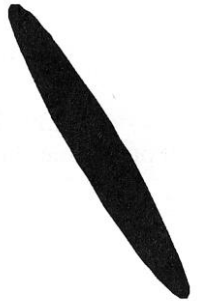

c) overfocus

d) corrected

from Goldstein et al., *Scanning Electron Microsopy and X-ray Microanalysis*

Resolution Definition in SEM

1. **Rayleigh criterion**
   Separation of point-like objects (well-separated, sub-nm small NP?)

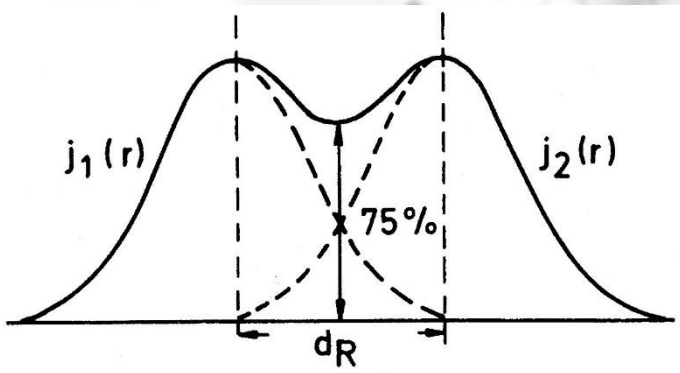

2. **Edge resolution**
   Intensity distribution across sharp edges (e.g., Au on C)

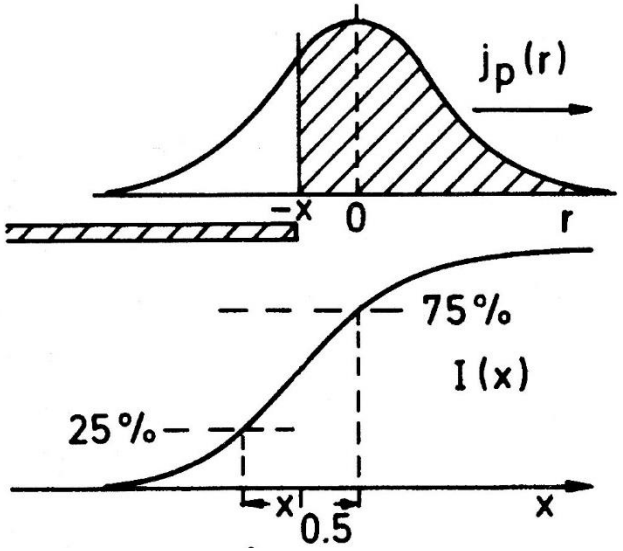

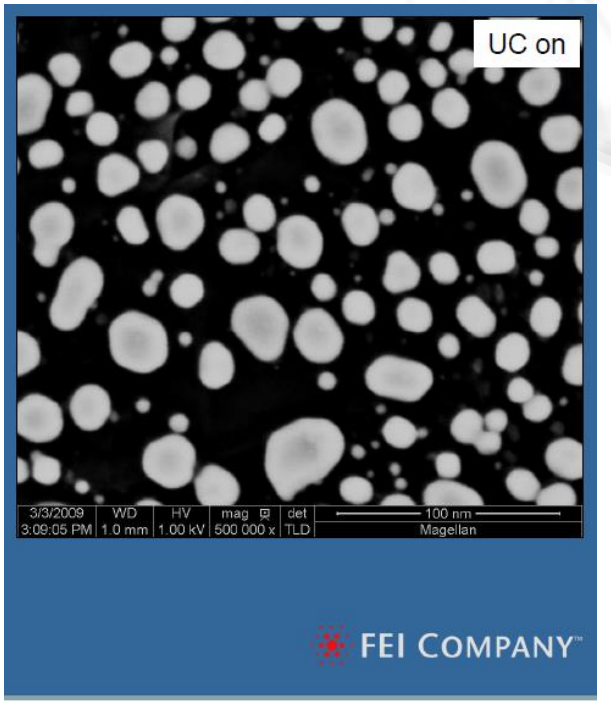

SE imaging
d_0 ~ resolution
(SE imaging mode)

in L. Reimer, *Scanning Electron Microscopy* (p. 53)

Resolution Definition in SEM

1. **Rayleigh criterion**
   Separation of point-like objects (well-separated, sub-nm small NP?)

Not applicable

2. **Edge resolution**
   Intensity distribution across sharp edges (e.g., Au on C)

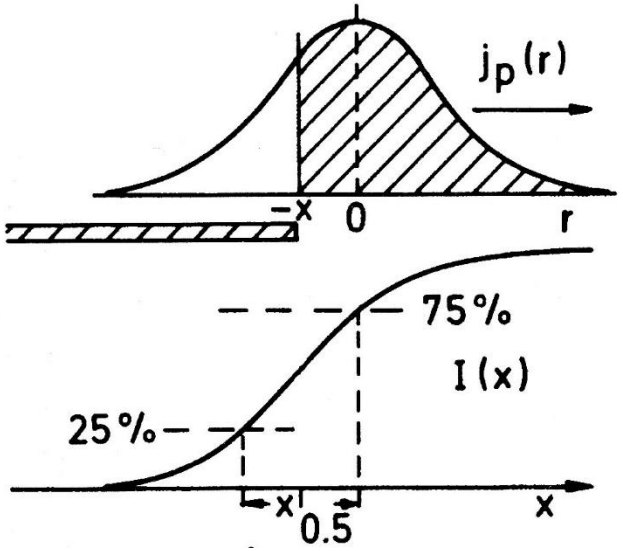

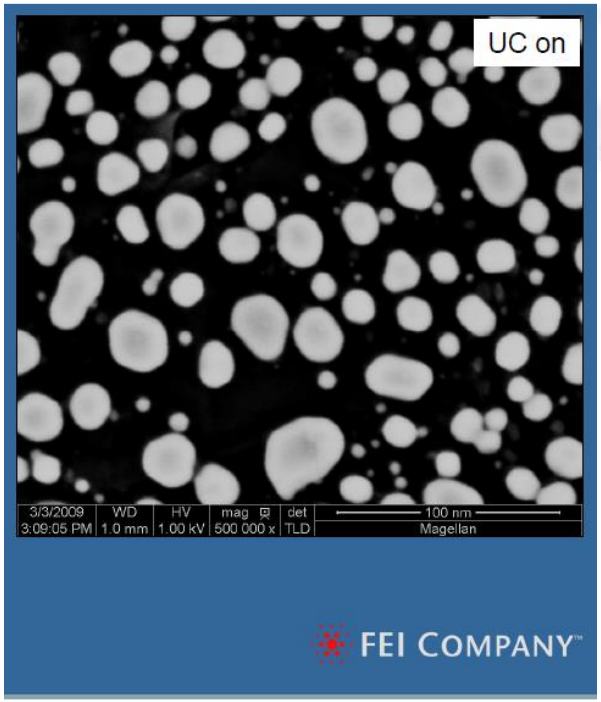

SE imaging
d_0 ~ resolution
(SE imaging mode)

in L. Reimer, *Scanning Electron Microscopy* (p. 53)

Depth of Field (DOF)

Alloy particles

Light Microscopy

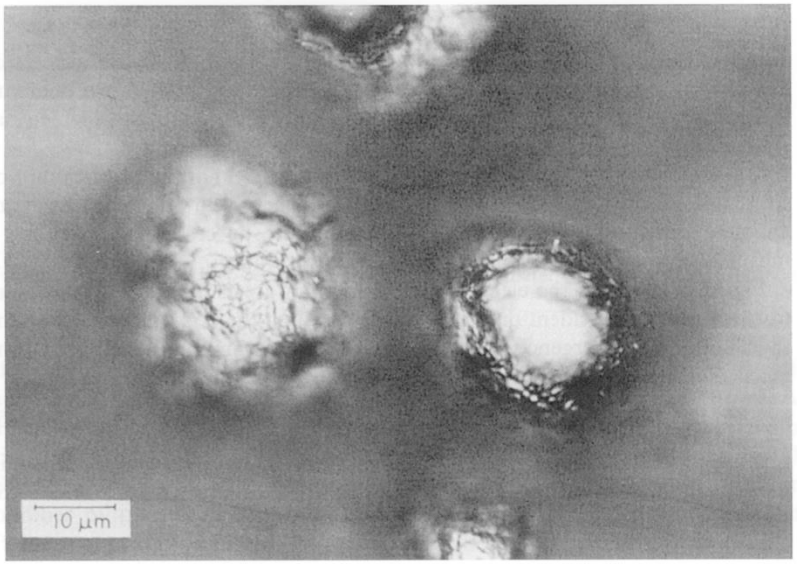

SEM

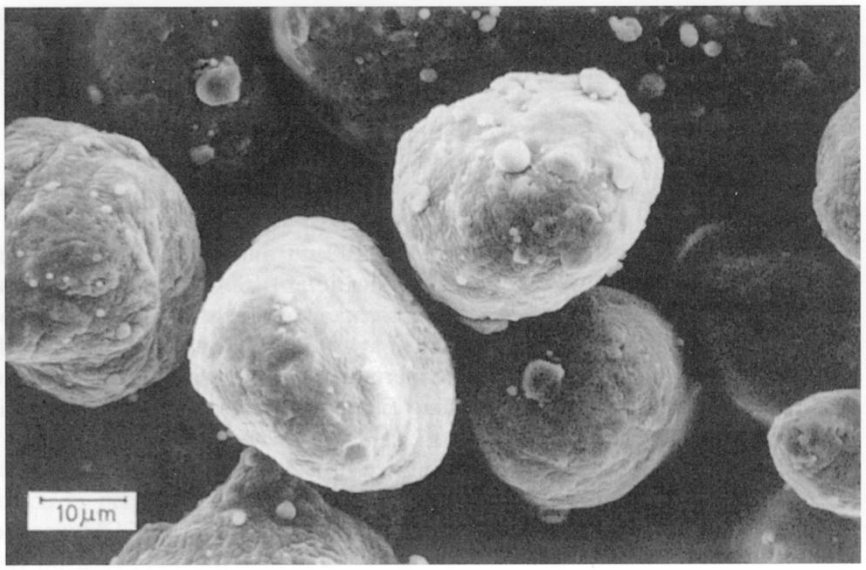

Why do we have such an incredible **depth of field (DOF)** in SEM images?

DOF

WD = 15 mm

d_{Ap} = 600 µm

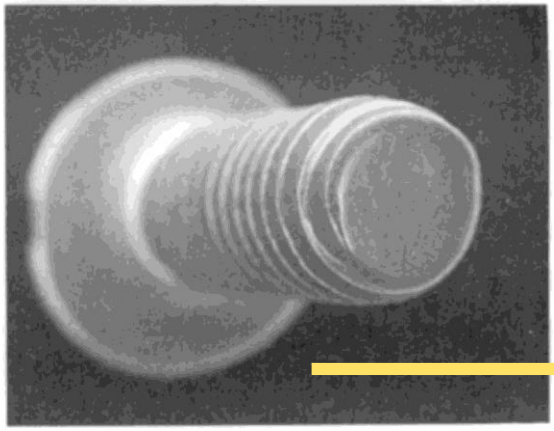

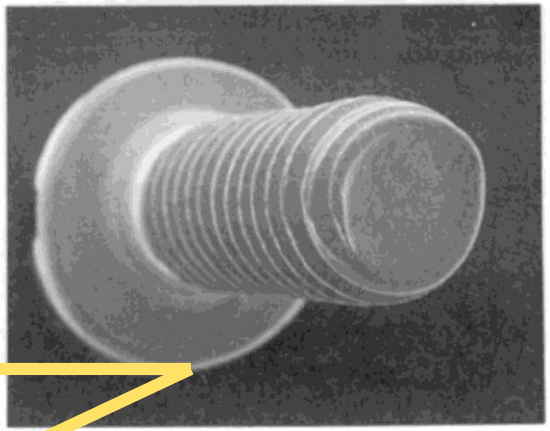

WD = 15 mm

d_{Ap} = 200 µm

Increasing DOF

WD = 15 mm

d_{Ap} = 100 µm

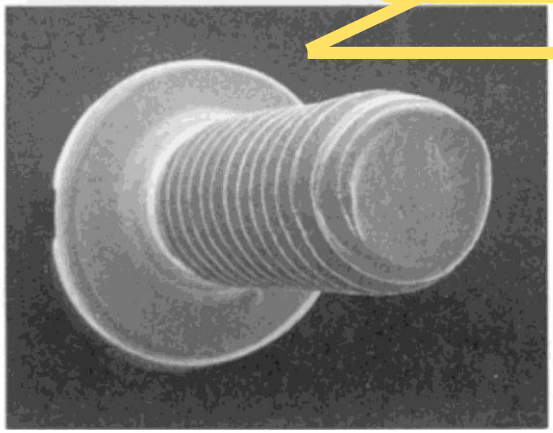

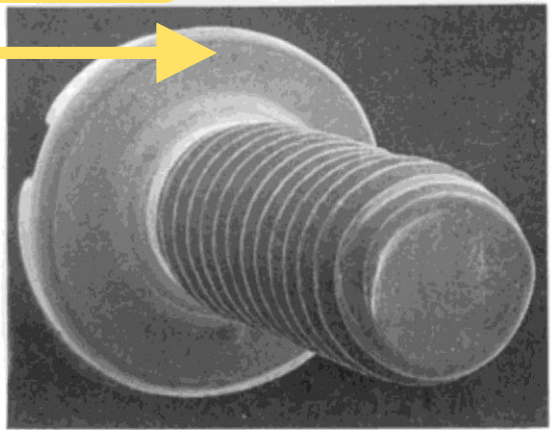

WD = 39 mm

d_{Ap} = 100µm

DOF

Details appear *sharp if* $2r \leq \frac{\text{size of picture element}}{M}$

$$DOF = \frac{2r}{\tan \alpha_P} \approx \frac{0.2 \text{ mm}}{\alpha_P \cdot M}$$

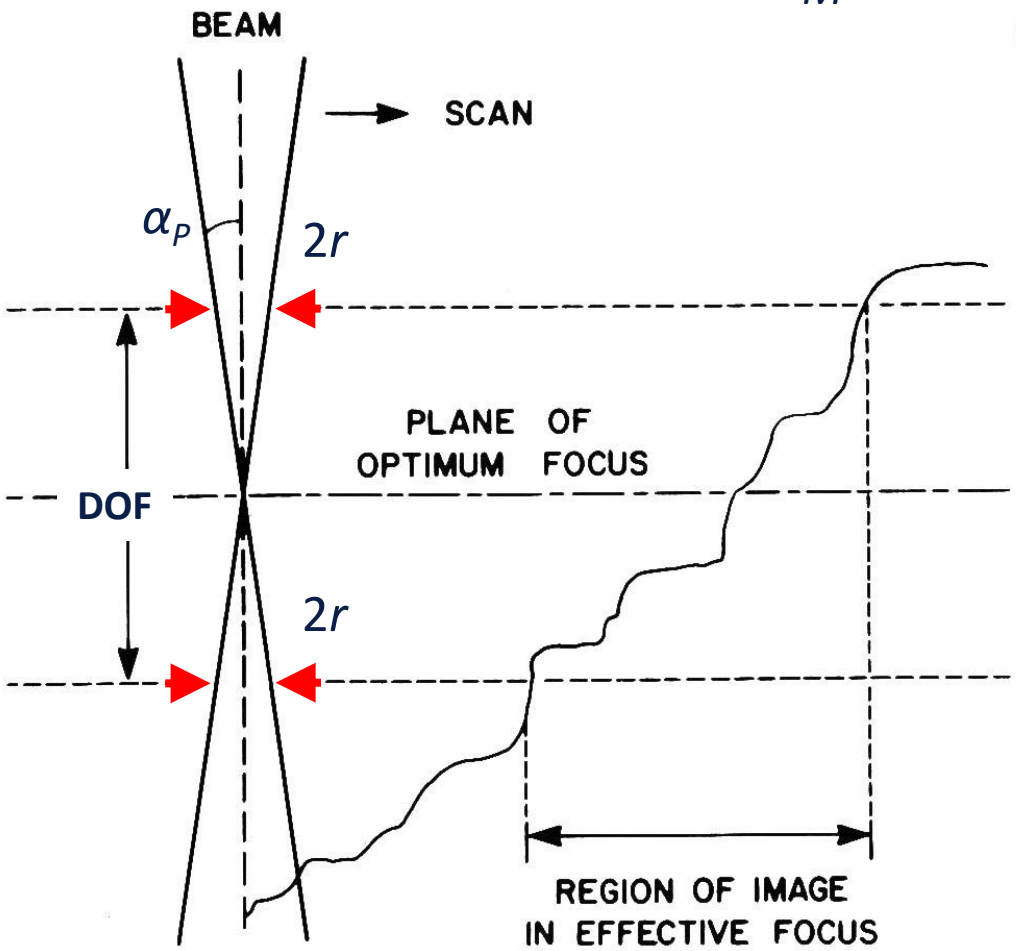

in Goldstein et al., *Scanning Electron Microscopy and X-Ray Microanalysis* (p. 134)

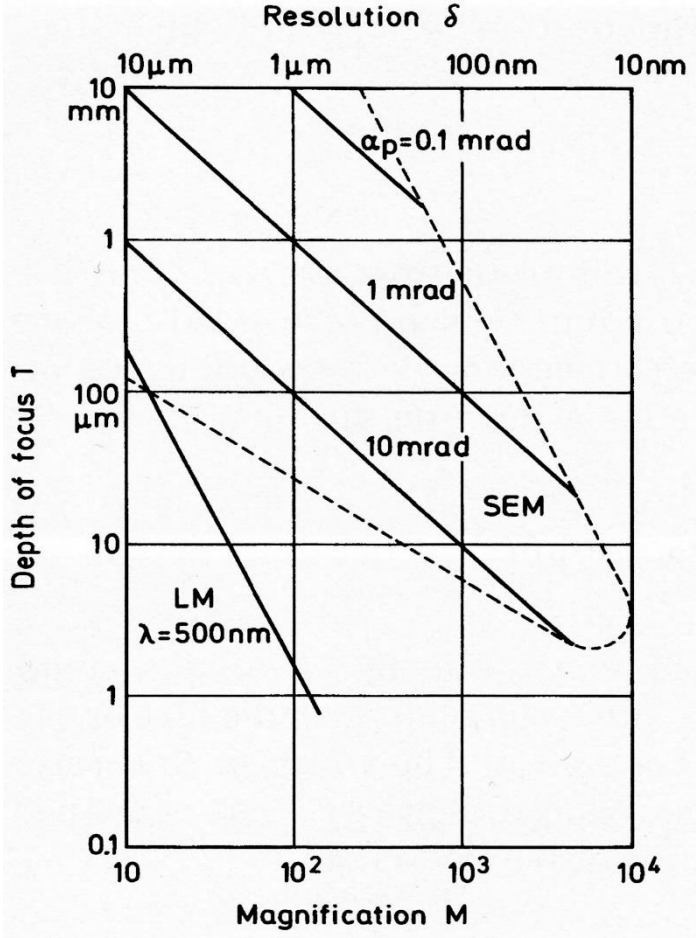

in L. Reimer, *Scanning Electron Microscopy* (p. 50)

DOF – **Condenser Aperture**

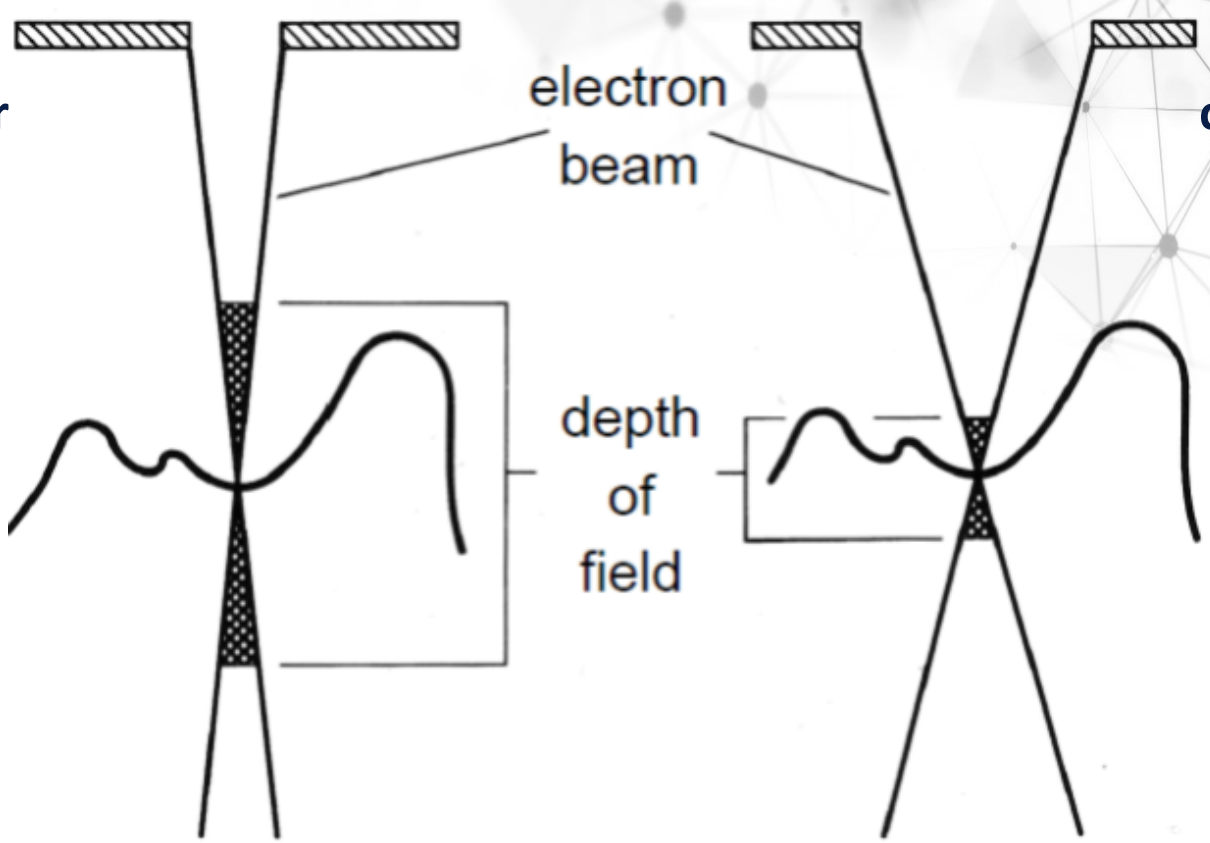

Gaining high DOF at an expense of beam current

DOF – **Working Distance**

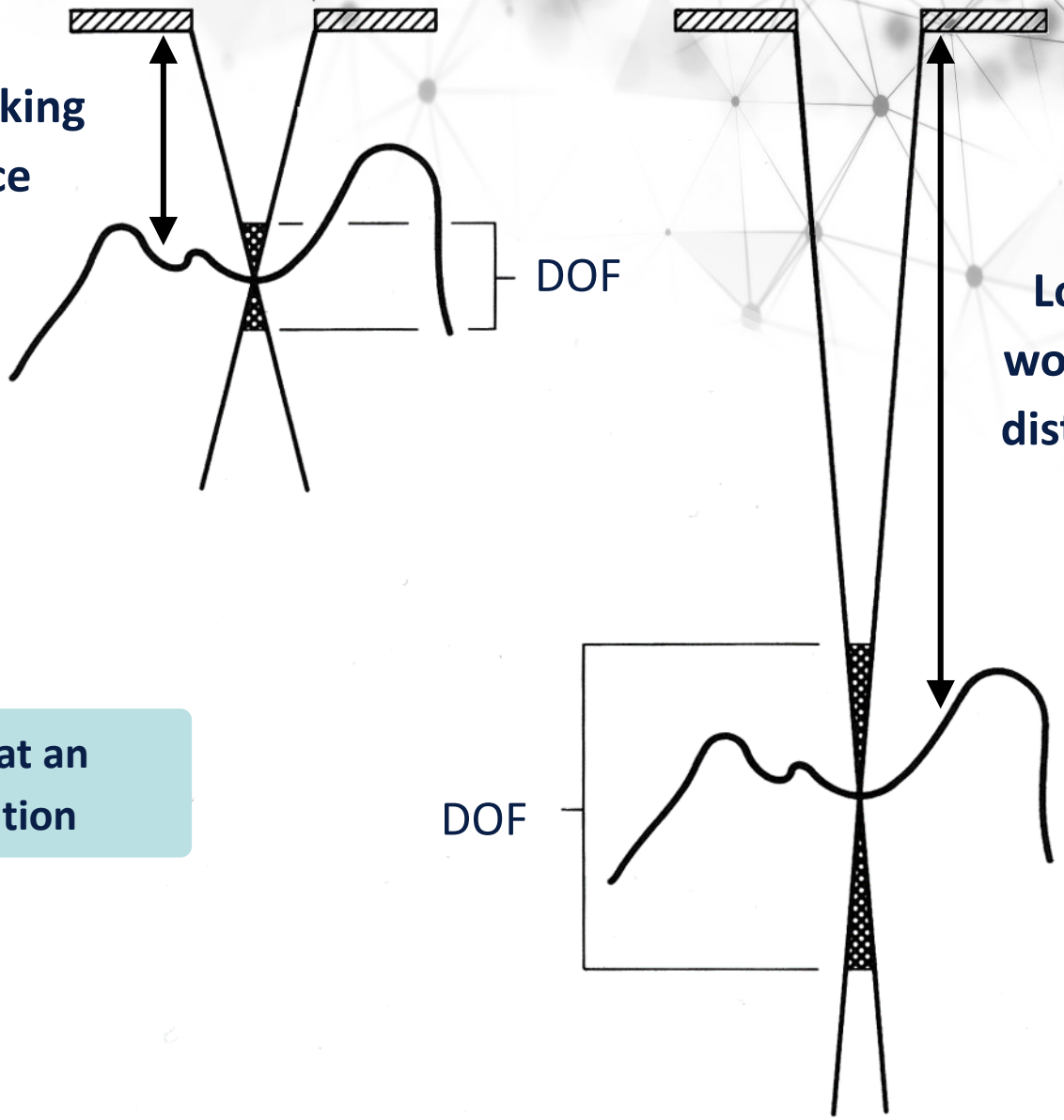

Gaining high DOF at an expense of resolution

Dynamic Focus

Tilted sample surface (insufficient DOF)

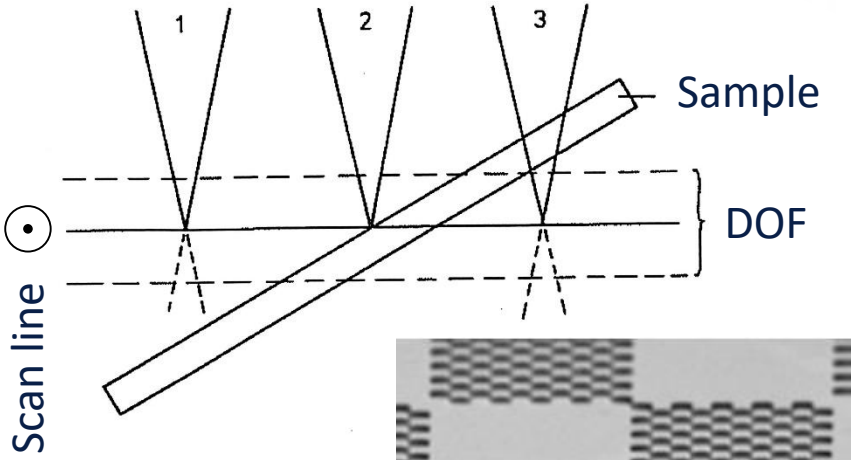

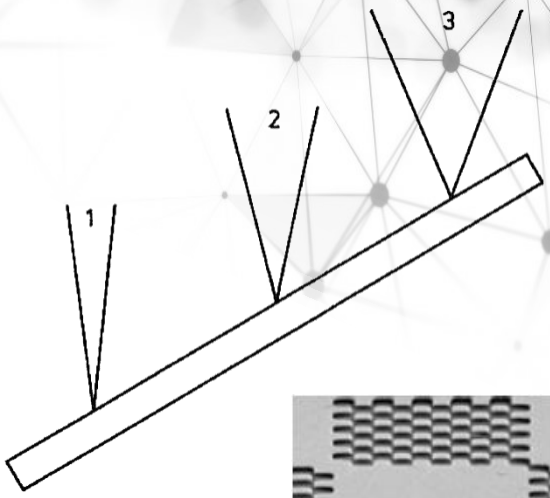

Dynamic Focus

OFF

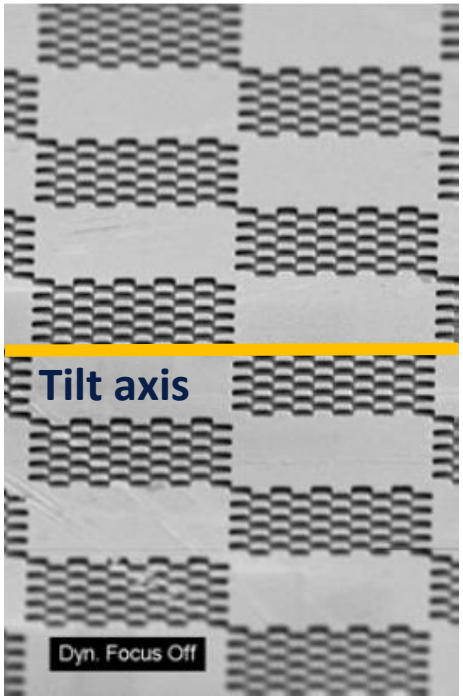

in Schmidt, *Praxis der Rasterelektronenmikroskopie und Mikrobereichsanalyse* (p. 64)

Dynamic Focus

ON

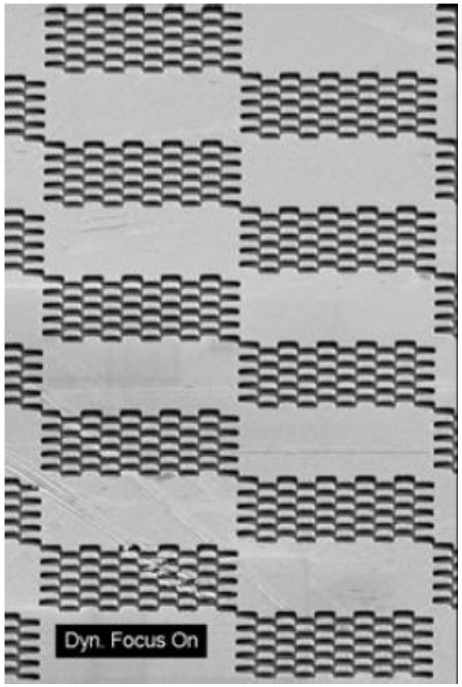

in Zeiss, *Supra Handbuch* (2004, p. 220)

Electron Sample Interaction

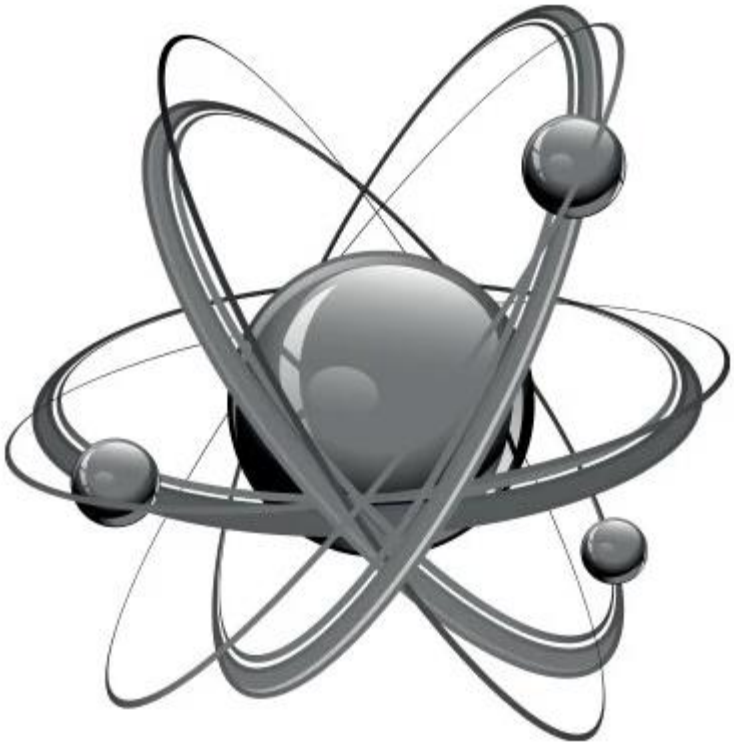

[sciencefocus.com]

Signals

Incident electron beam
(200 V — 30kV)

X-rays
- Energy-dispersive det.
- Wafe length-dispersive det.

Backscattered electrons (**BSE**)
- EsB® detector (Zeiss)
- Retractable BSE detector
- EBSD detector

Cathodoluminescence (**CL**)
- CL-detector

Secondary electrons (**SE**)
- Everhard-Thornley detector
- Inlens detector (Zeiss)

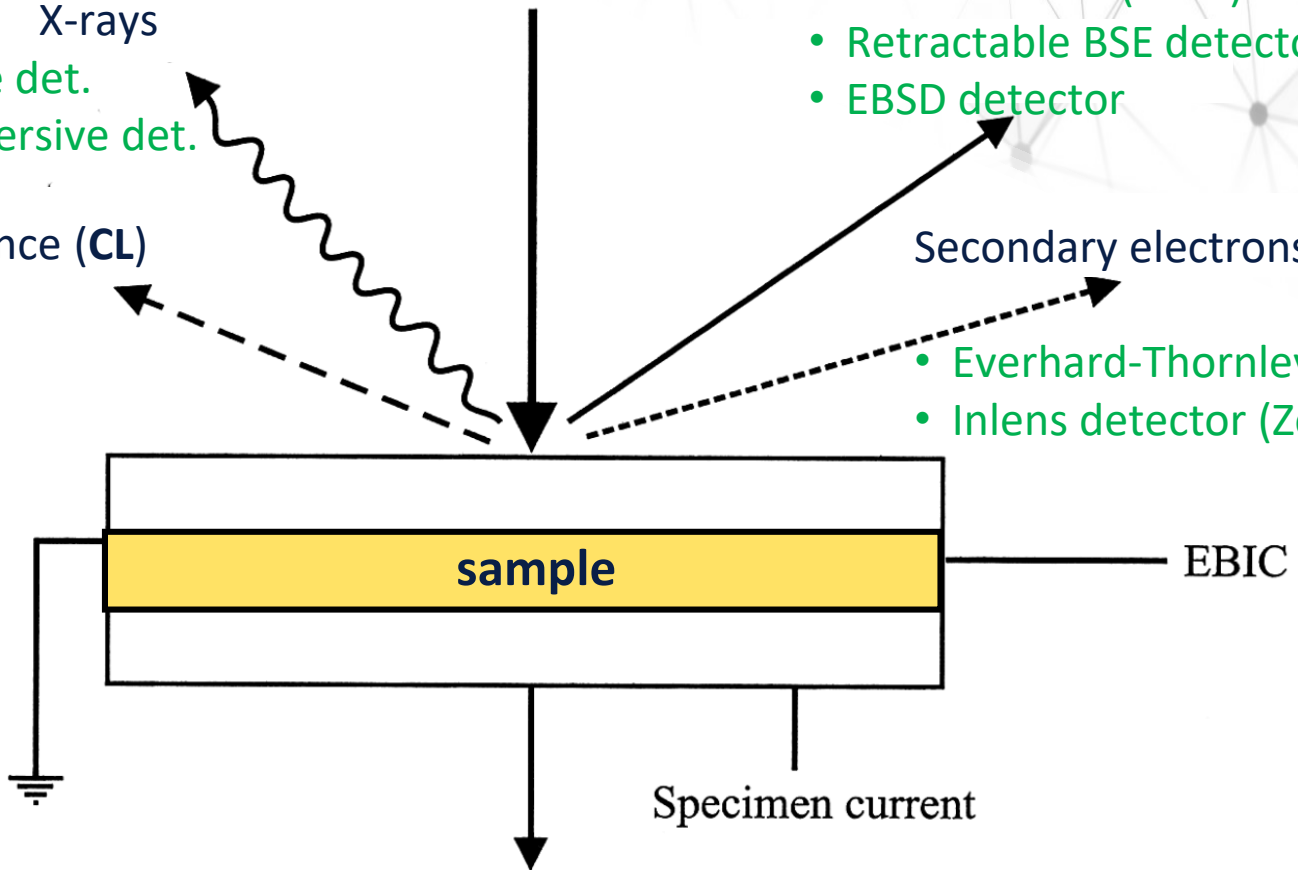

Transmitted electrons
- Bright-/dark-field STEM detector

FIB/SEM Chambers — Detektors

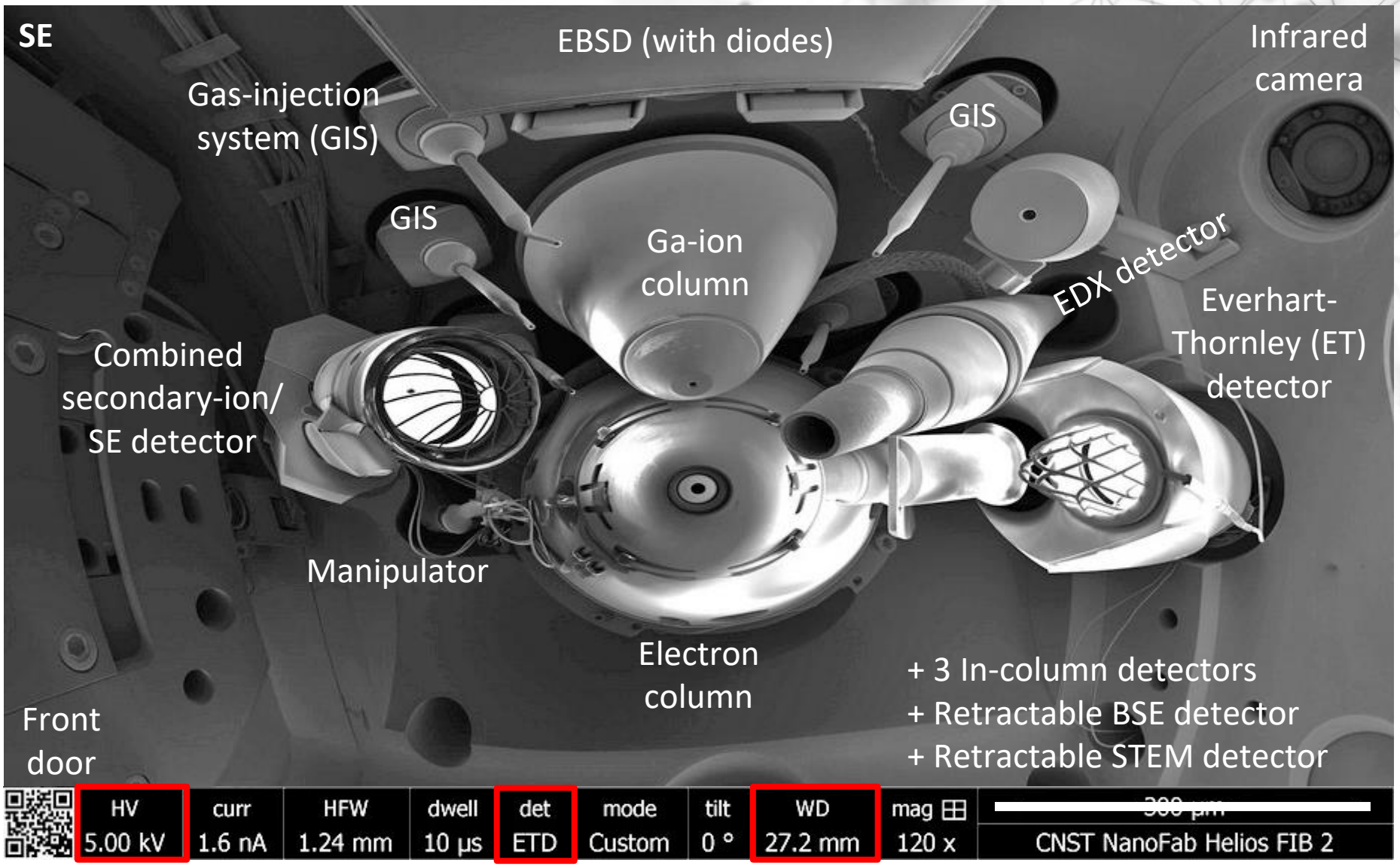

sample bias > HV

Couresy of Joshua Schumacher / FEI Company

Interaction volume — Distribution of PE in Sample

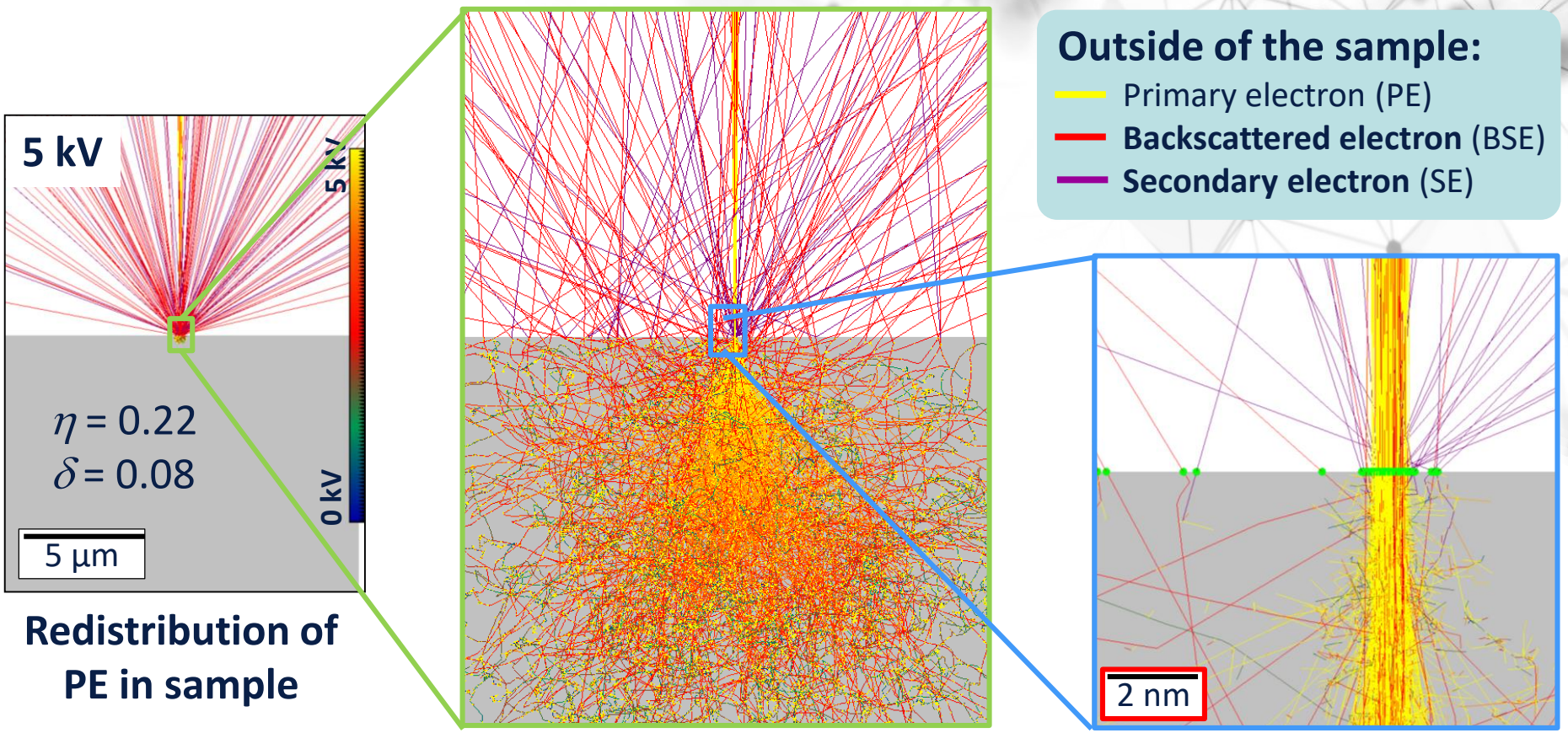

Trajectories of 500 electrons on Si (calculated with *Casino*):

α_p= 10 mrad, d_0 = 1 nm, trajectories rainbow-colored depending on the energy of the electron

Electron Scattering Processes

Elastic scattering → No detectable energy transfer

- Coulomb interaction with the attractive potential formed by the atomic nuclei of the target material

Inelastic scattering → Energy transfer to the specimen

- Phonon scattering → Excitation of lattice vibrations (contributes to sample heating)
- Plasmon scattering → Excitation of collective oscillations of the conduction electrons (in metals)
- Inner shell excitation → Ionization of inner shell electrons
  - ➢ emission of X-rays, Auger-Electrons
- Inner/inter-band transitions → Ionization of inner shell electrons
  - ➢ emission of light (Cathode luminescence)

*Electron Scattering Processes

Elastic scattering → No detectable energy transfer

- Coulomb interaction with the attractive potential formed by the atomic nuclei of the target material → **BSE**

Inelastic scattering → Energy transfer to the specimen

- Phonon scattering → **$\Delta E \approx k_B T$ (25 meV at 300 K)**
- Plasmon scattering → **ΔE: 5 — 50 eV** → **SE**
- Inner shell excitation → **ΔE: 100 eV — E_0** → **SE**
- Inner/inter-band transitions → **ΔE: few eV** → **SE**

Elastic Electron Scattering

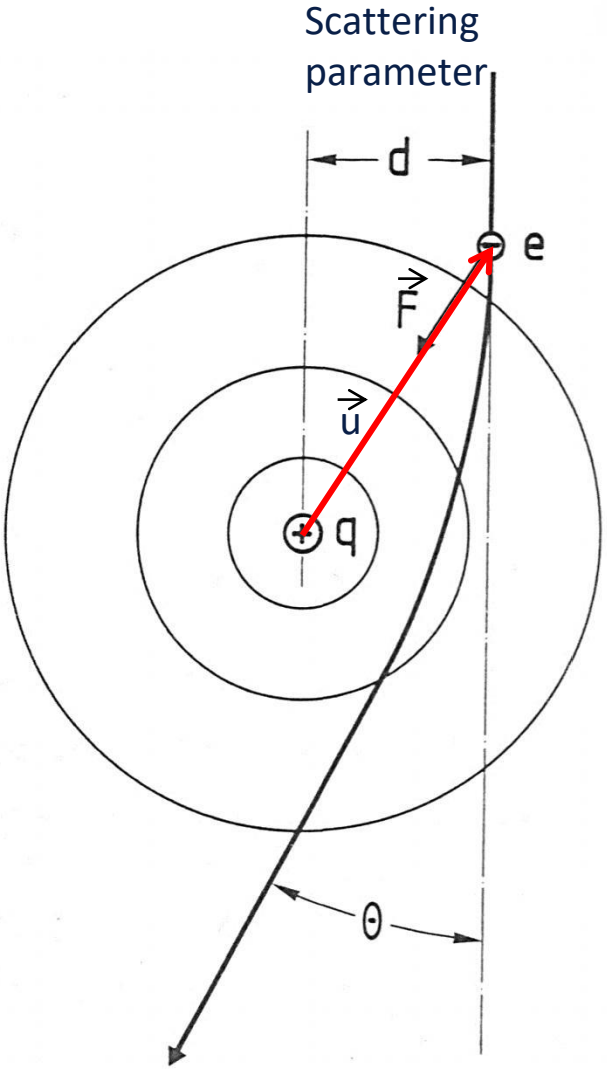

Elastic scattering of the primary electrons (PE) at the atomic nuclei of the target material or, more precisely, at the coulomb potentials of the positively charged nuclei:

$$\vec{F}_{\text{Coulomb}} = -\frac{e^2 Z}{4\pi\varepsilon_0 r^2}\vec{u}_r$$

= attractive force from the (unscreened) nucleus

Screening by electron cloud reduces the force!

Effect of Screening

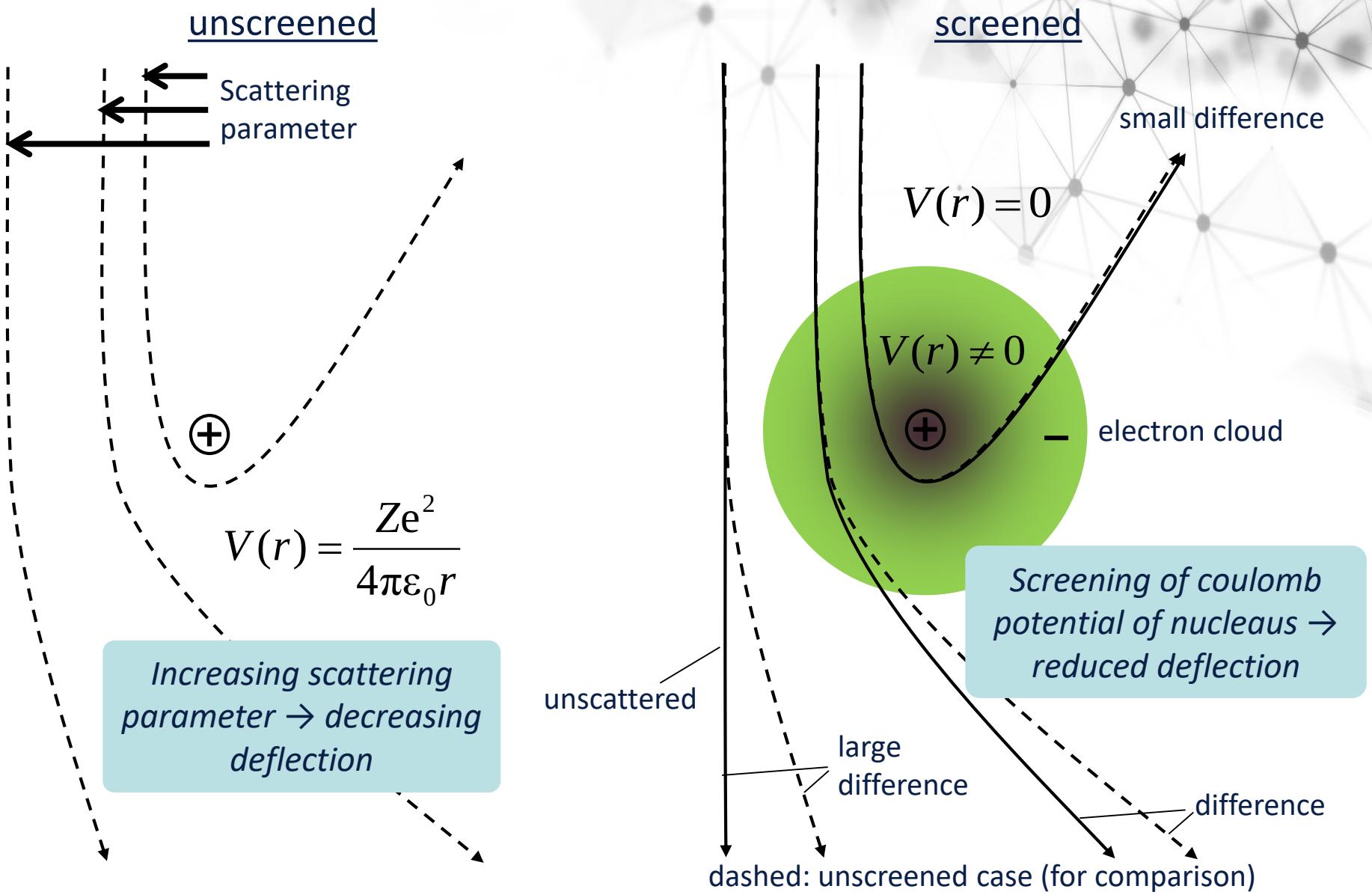

Atomic Scattering Amplitude

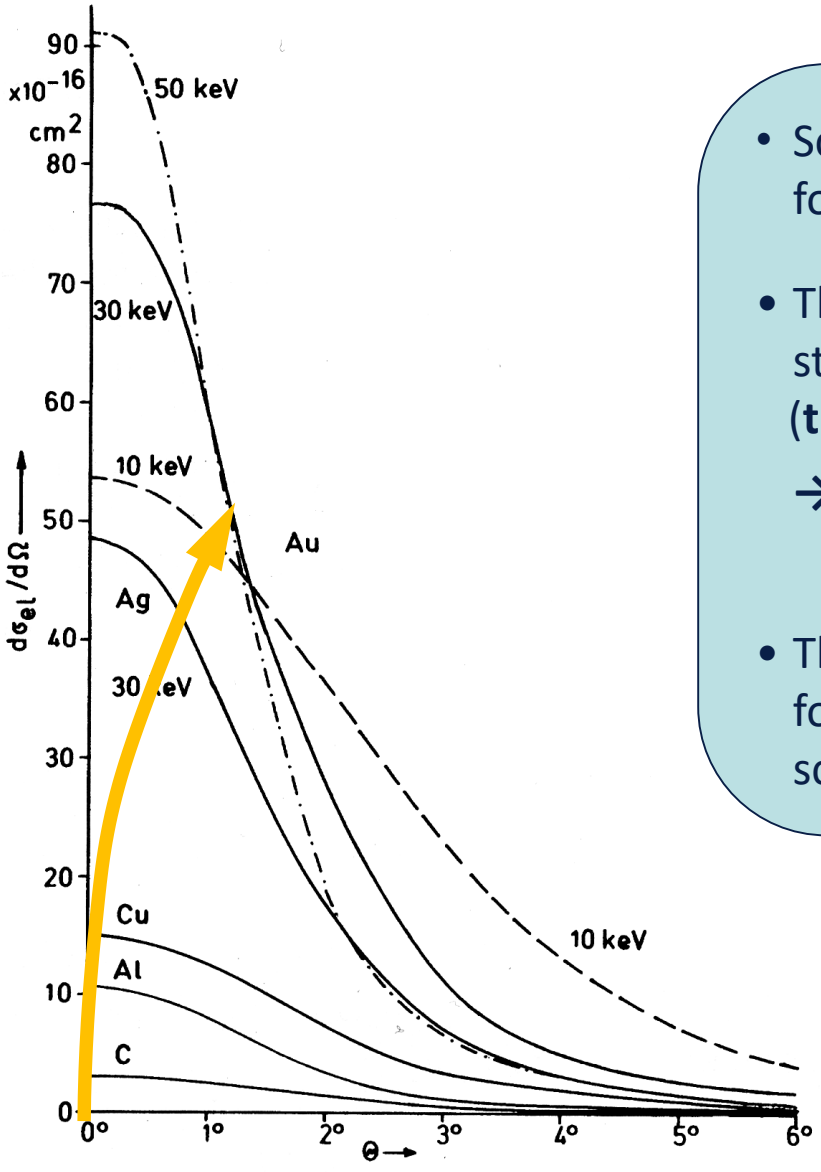

- Scattering of electrons is peaked in forward direction
- The higher the atomic number the stronger the scattering (**the higher the BSE yield**)

  → **Atomic number contrast in BSE imaging**
- The higher the beam energy the more forward-peaked is the elastic electron scattering

in L. Reimer, *Scanning Electron Microscopy* (p. 69)

Ionization

Primary process

Secondary processes

Ionization

Auger-electron emission

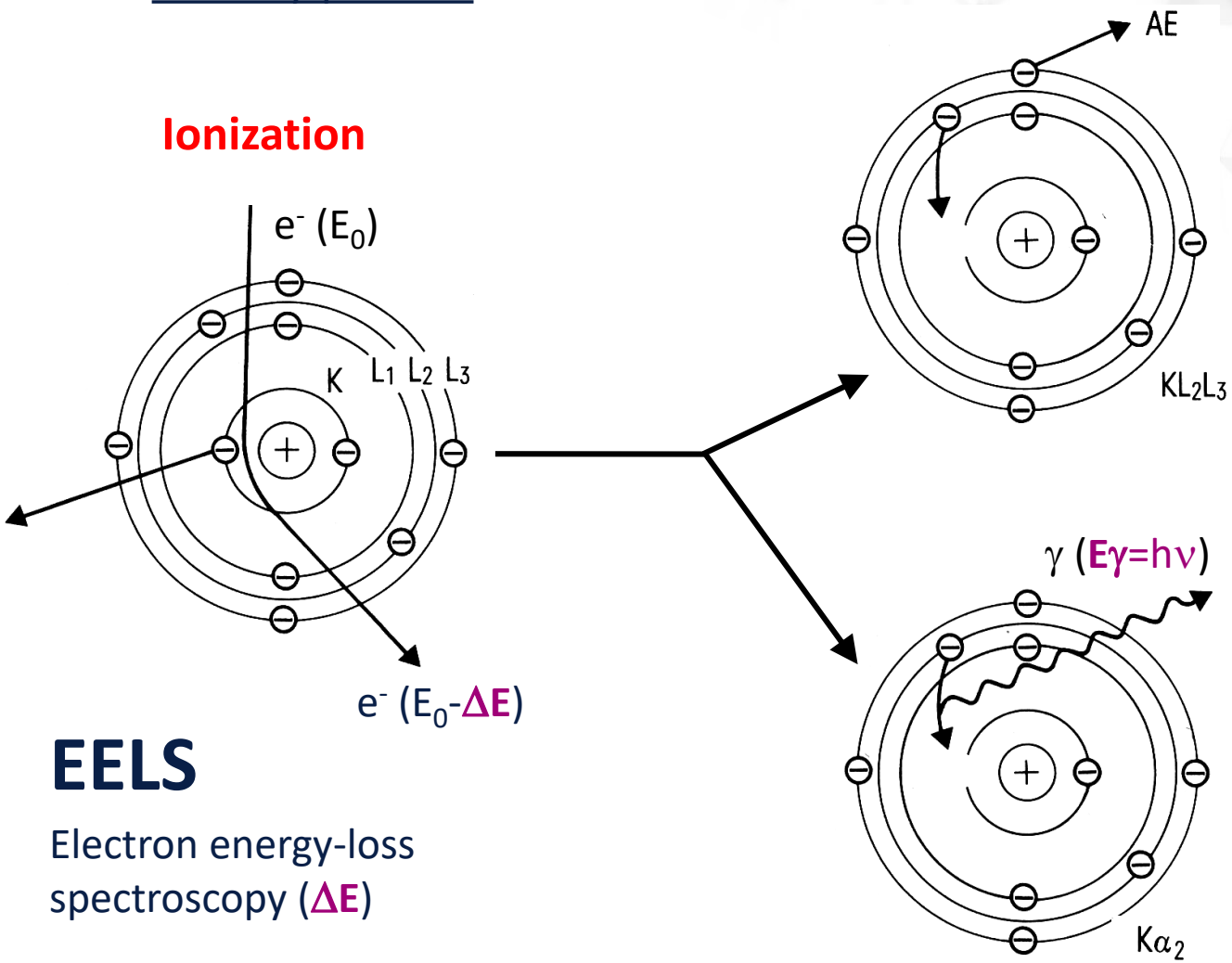

Characteristic X-ray emission

EELS

Electron energy-loss spectroscopy (**ΔE**)

EDXS

Energy-dispersive X-ray spectroscopy

$$h\nu = E_i - E_f$$

in Fuchs, Oppolzer, Rehme, *Particle Beam Microanalysis* (p. 52)

Total Scattering Cross-Section

Probability of electrons being scattered

Total scattering cross-section
(takes all possible inelastical processes into account)

$$\sigma_t = \sigma_{el} + \sigma_{inel} = 2\pi \int_0^{\pi} \left(\frac{d\sigma_{el}}{d\Omega} + \frac{d\sigma_{inel}}{d\Omega} \right) \sin\theta d\theta$$

Unscattered intensity

$$I(t) = I_0 \exp(-N\sigma_t t) = I_0 \exp(-t/\Lambda_t)$$

N Number of atoms per volume
I_0 Incident beam current
L_t Mean-free-path length

$$\Lambda_t = \frac{1}{\sigma_t N}$$

Total mean-free-path length in *nm*

	C	Al	Cu	Ag	Au
5 keV	2.3	2	1.1	1.0	0.9
10 keV	4.5	4	2.0	1.7	1.3
20 keV	9	8	3.5	2.8	2.1

in L. Reimer, *Scanning Electron Microscopy* (p. 83)

Monte-Carlo Simulation of Interaction Volume

For each electron iterative calculation of ist trajectory using Monte-Carlo methods:

- ***Propagation* of electron** depending on its energy and the material – free path length s_i
- After propagation **calculation of scattering event** (scattering angle + energy loss, based on σ_{el}, σ_{inel})
- Respective correction of energy + momentum
- Repetition until E < ε or escape from sample

Monte-Carlo simulation software:

***DTSA-II* (NIST)** (02/2018)
Casino (02/2018)

Trajectories + X-ray spectra

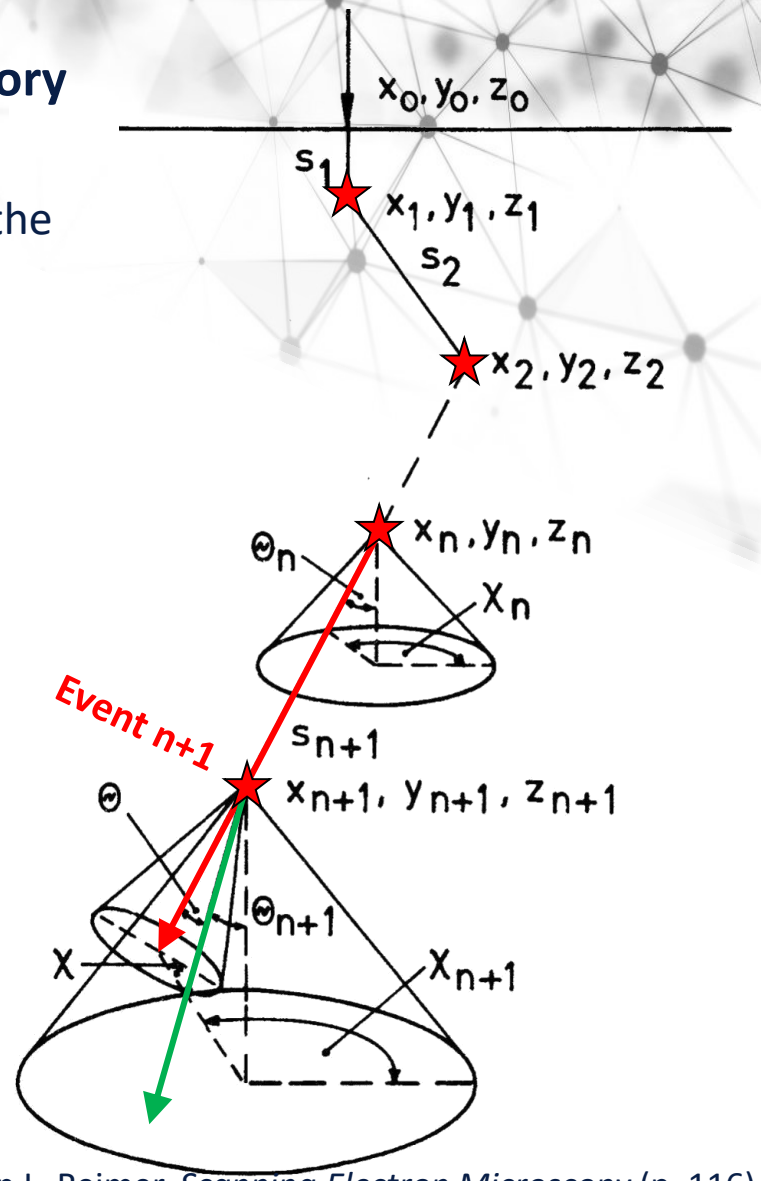

Fig. 3.30. Sequence of scattering processes in a Monte Carlo simulation with s_i = free path lengths, x_i, y_i, z_i. = coordinates of electron at the ith collision, θ_i and χ_i = scattering and azimuth angles after the ith collision

in L. Reimer, *Scanning Electron Microscopy* (p. 116)

Primary Energy – Penetration Depth

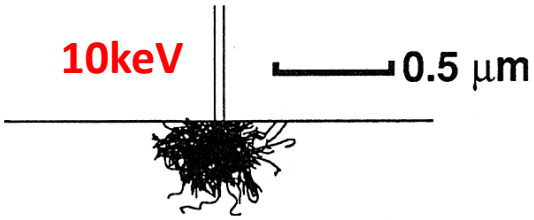

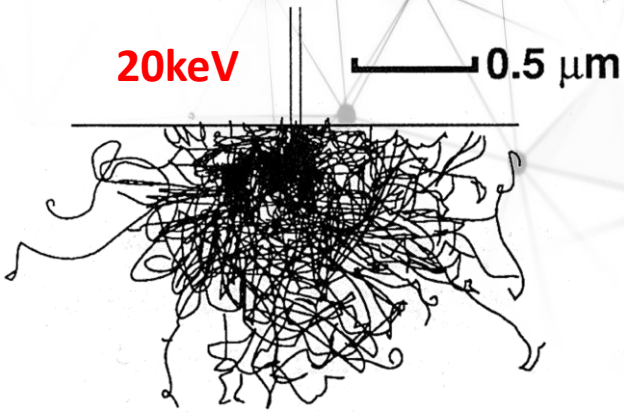

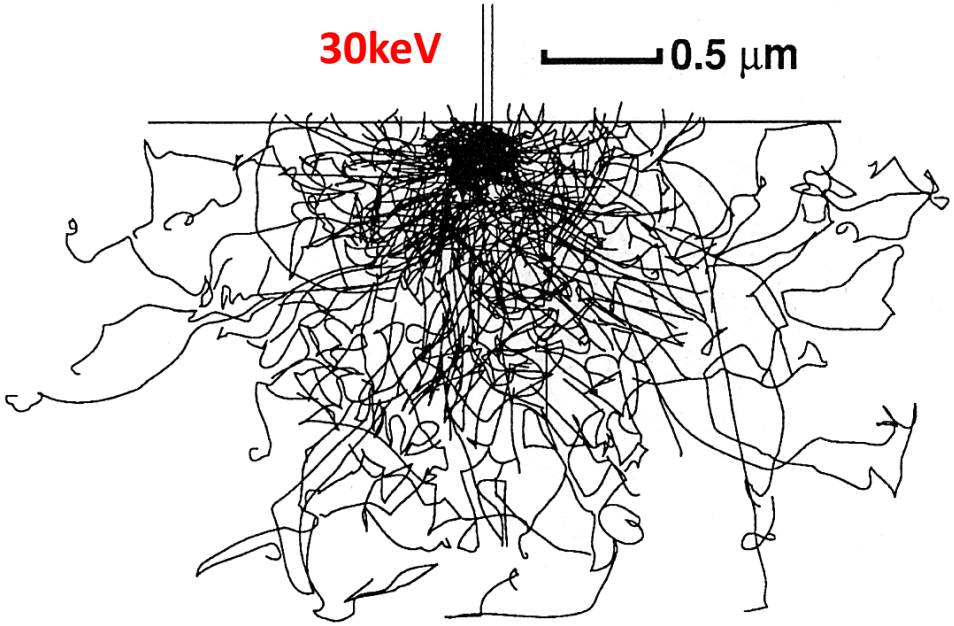

Target material: Iron

The higher the primary energy is, the larger is the penetration depth

Atomic Number – Penetration Depth

Carbon (Z=6)

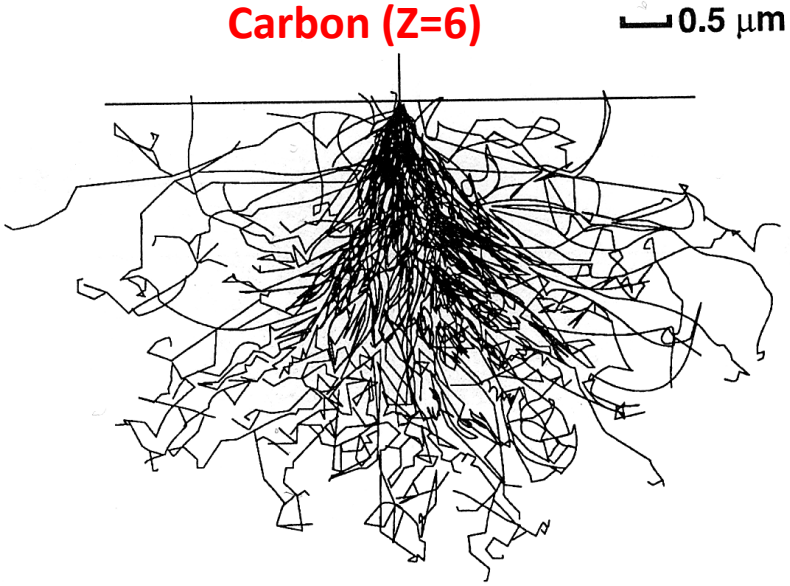

High Voltage: 30 kV

The higher Z, the smaller is the penetration depth

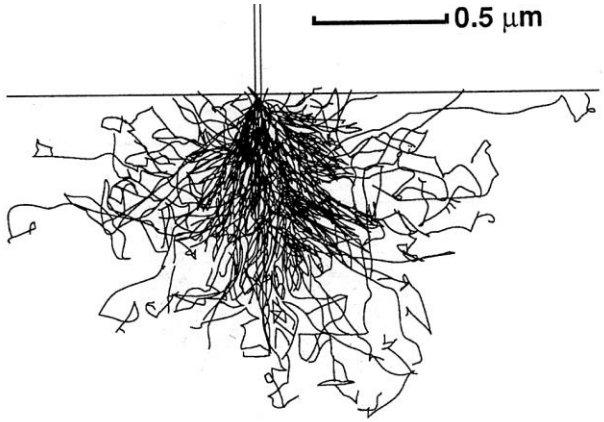

Iron (Z=26)

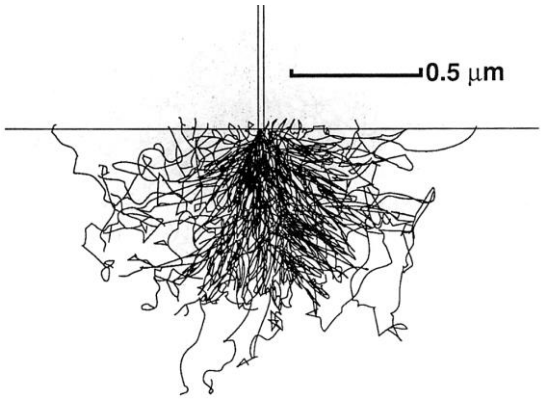

Silver (Z=47)

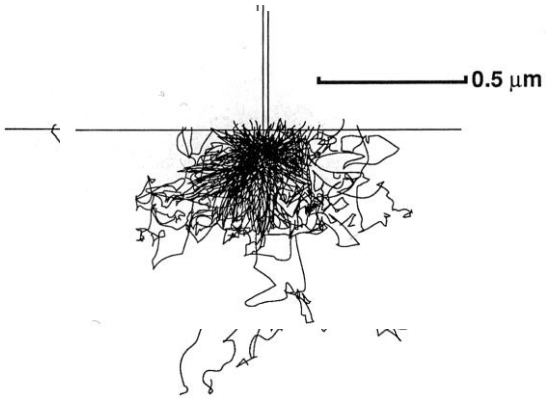

Uranium (Z=92)

Interaction Volume: Visualization

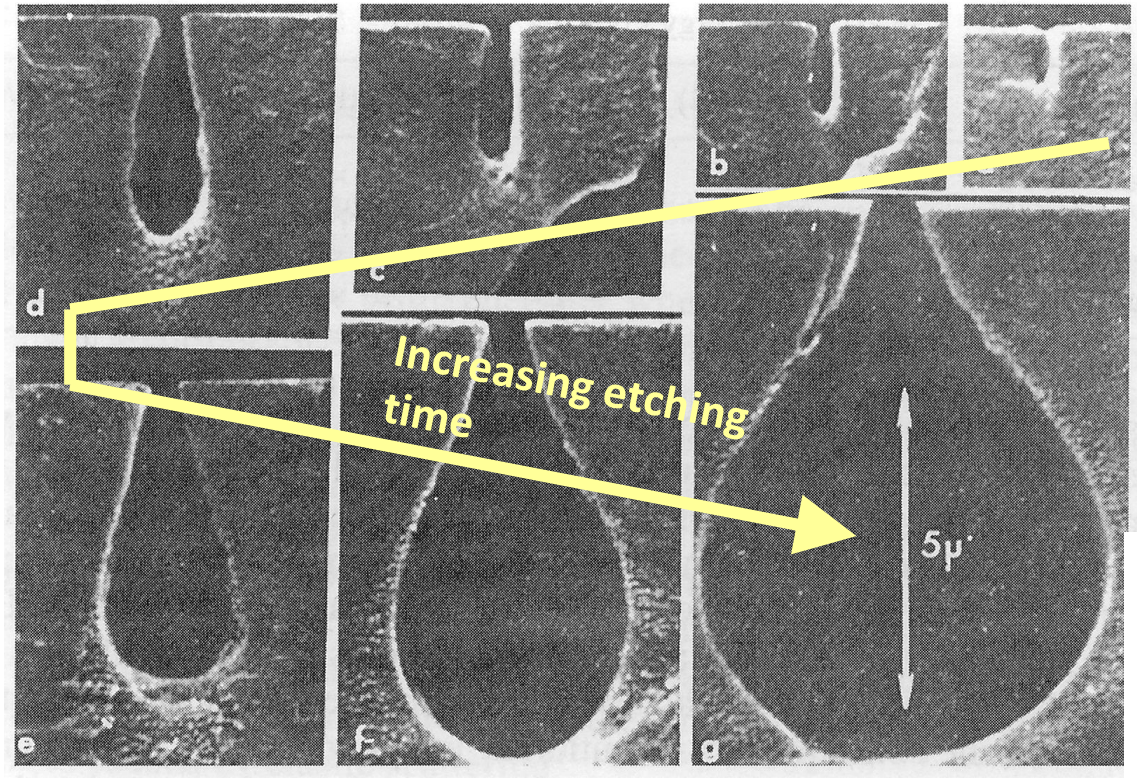

Decreasing energy deposition with increasing distance to impact point

Revealing decreasing energy deposition contours:

Etching of PMMA after 20keV electron irradiation

Contours of constant energy deposition:

Experiment

Monte-Carlo simulation

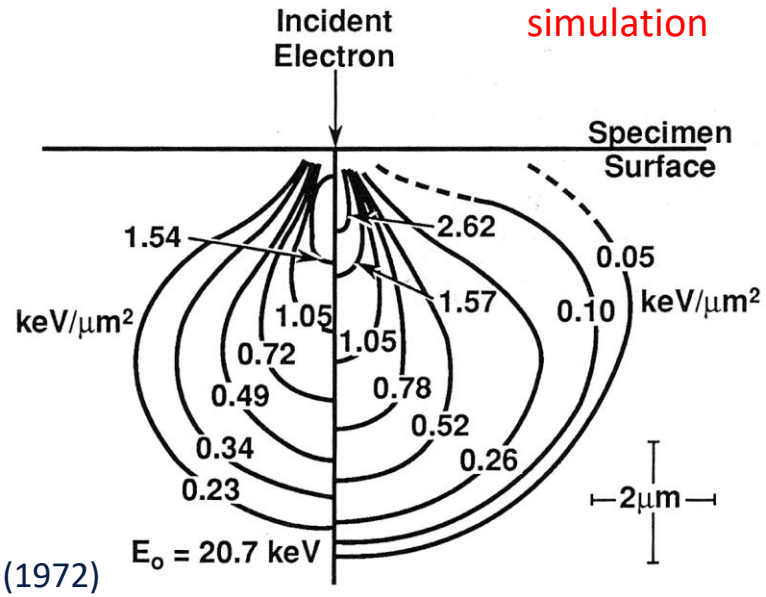

T.E. Everhart et al., *Proc. 6th Intl. Conf. On X-Ray Optics and Microanalysis* (1972)
or Goldstein et al., *Scanning Electron Microscopy and X-Ray Microanalysis* (pp. 60+63)

BSE / SE Yield

Trajectories of 500 electrons on Si (calculated with *Casino*):

α_P= 10 mrad, d_0 = 1 nm, trajectories rainbow-colored depending on the energy of the electron

Outside of the sample: PE BSE SE

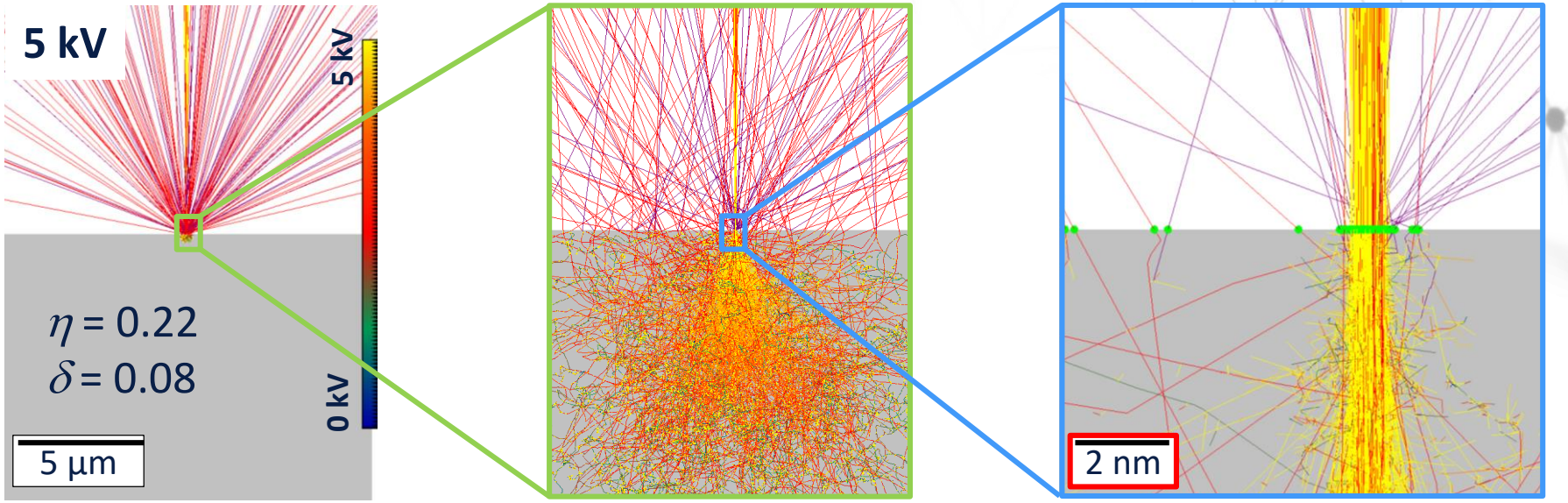

Backscattering coefficient

$$\eta = \frac{\text{number of backscattered electrons}}{\text{number of primary electrons}} = \frac{I_{BSE}}{I_{PE}}$$

SE yield

$$\delta = \frac{\text{number of secondary electrons}}{\text{number of primary electrons}} = \frac{I_{SE}}{I_{PE}}$$

BSE / SE Yield

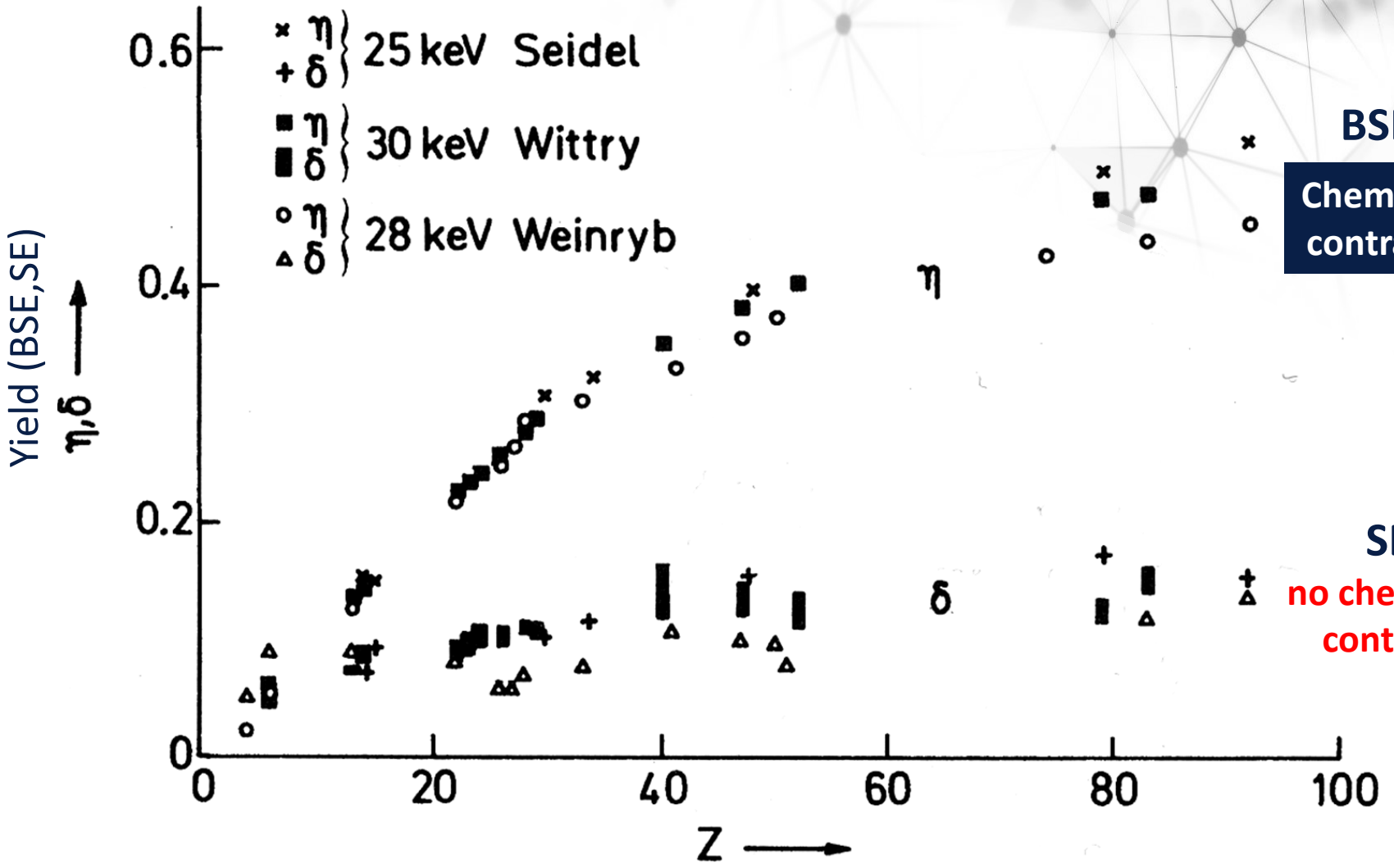

in L. Reimer

BSE — Chemical Contrast

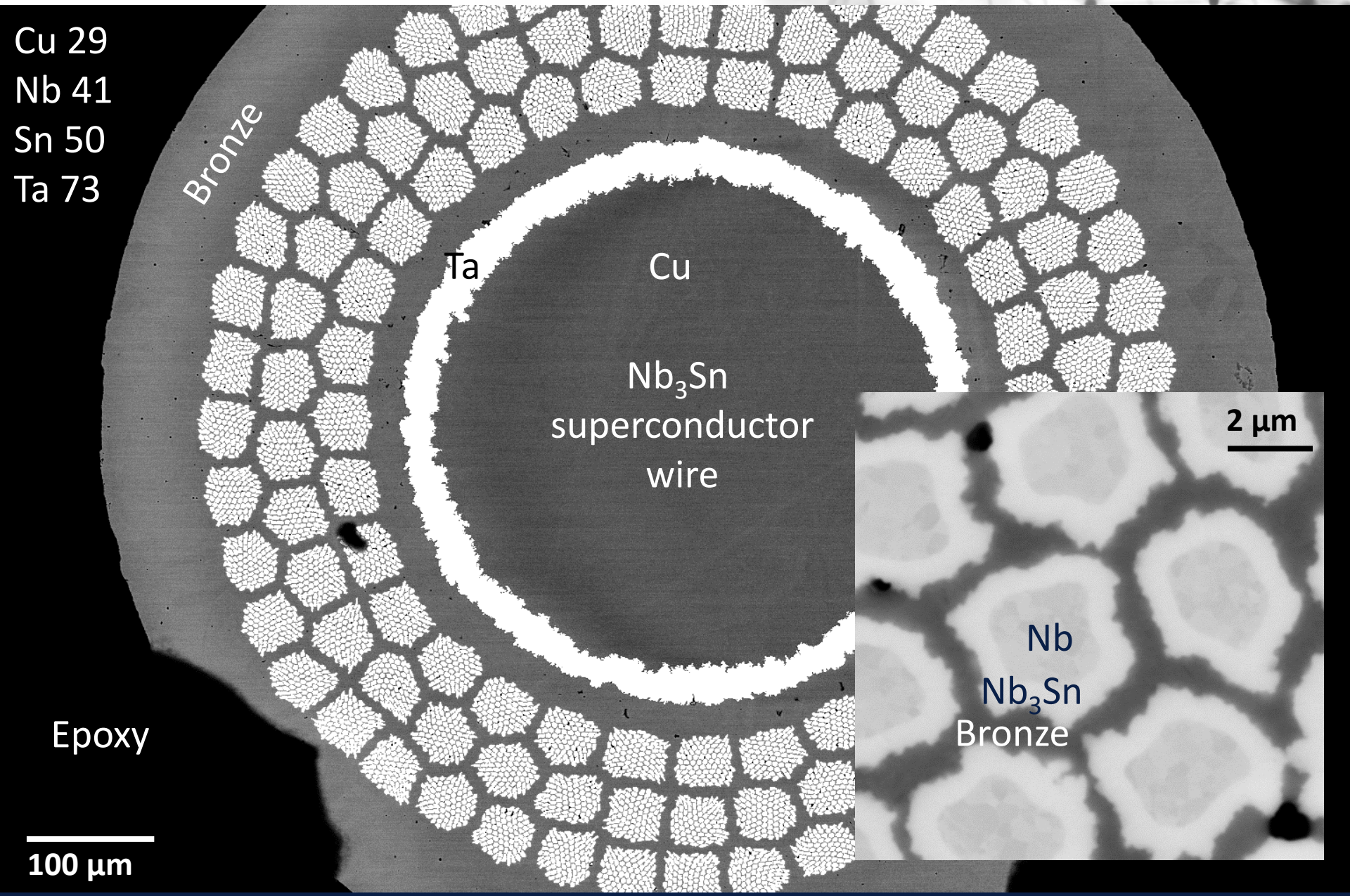

Electron Energy Distribution

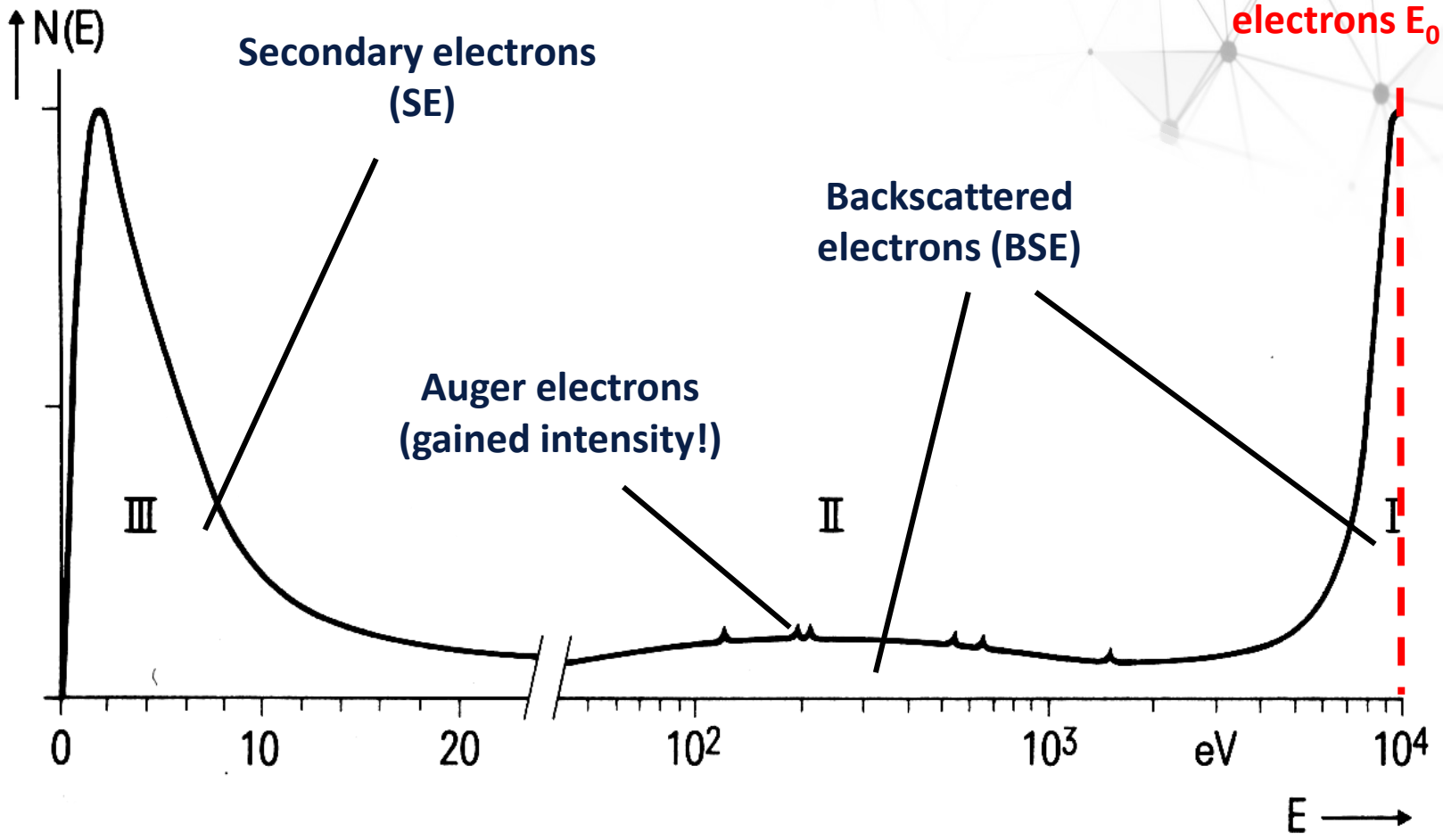

in Fuchs, Oppolzer, Rehme, *Particle Beam Microanalysis* (p. 50)

Backscattering Coefficient vs. ϕ + Z

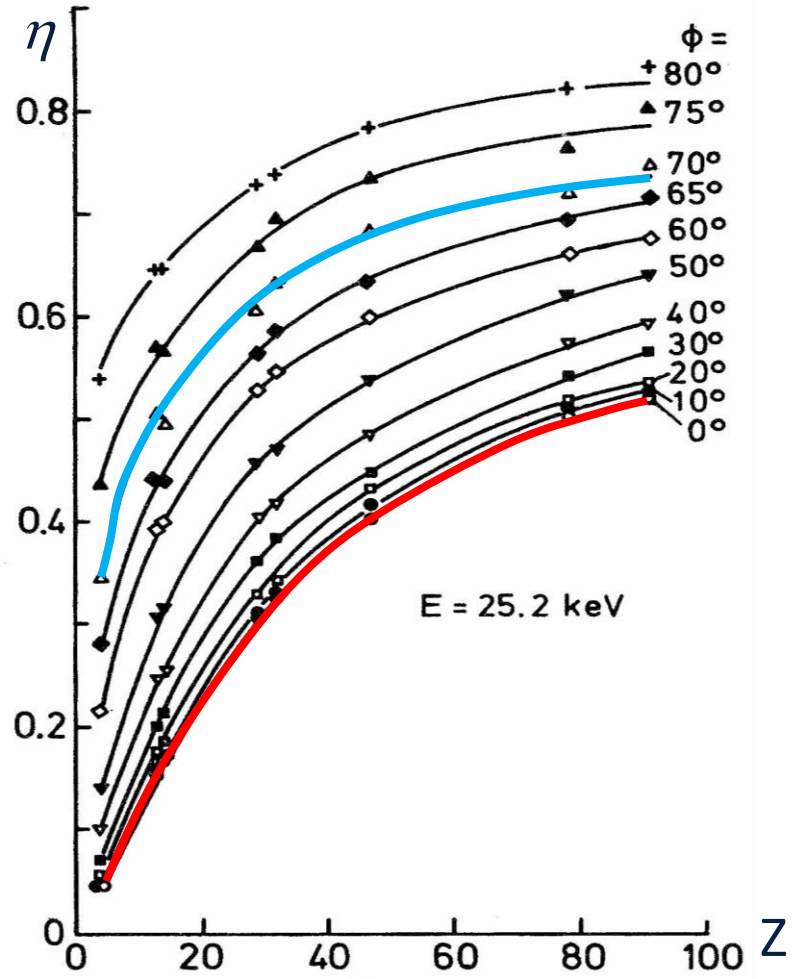

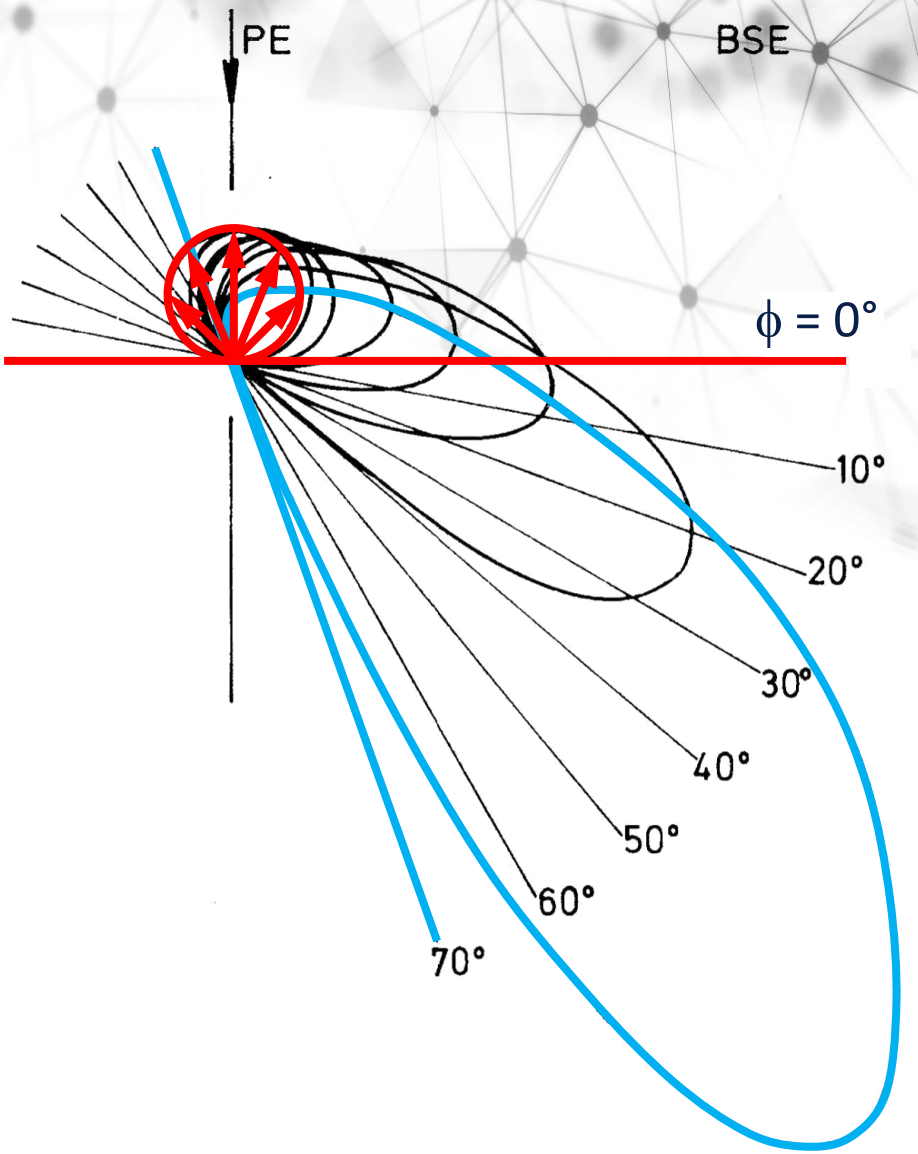

Oblique incidence greatly increases η
"Surface-near scattering"

in L. Reimer, *Scanning Electron Microscopy* (pp. 143+224)

BSE Energy

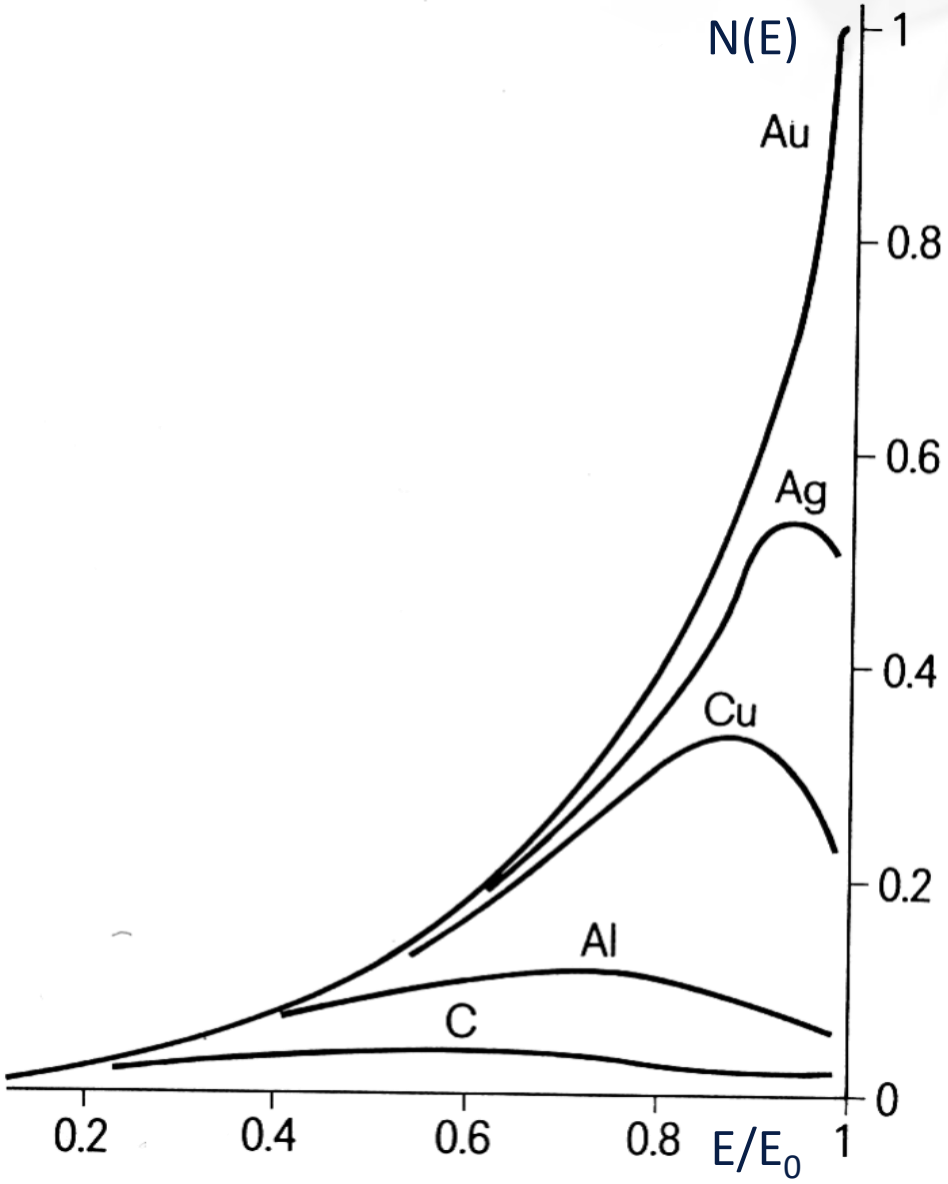

Energy loss by inelastic collisions before the BSE leave the sample

More pronounced for light elements (relatively)

But backscattering coefficient larger for heavier elements

in Fuchs, Oppolzer, Rehme, *Particle Beam Microanalysis* (p. 46)

BSE Imaging – Resolution

The resolution in BSE imaging is limited by the **escape area of BSE electrons (~R)**

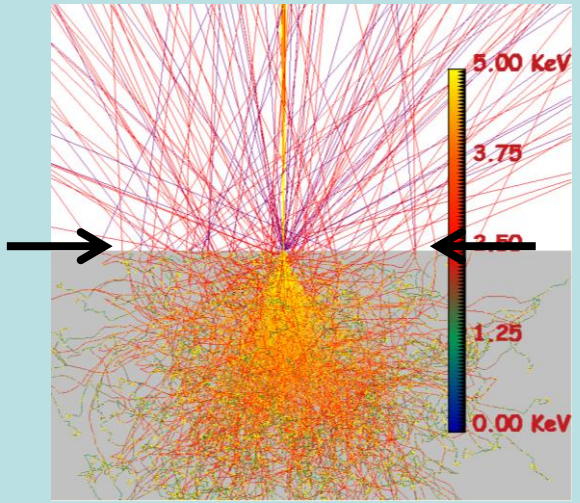

Particular structures can be imaged with a better resolution when their

topographic or material contrast significantly exceeds

the background signal of BSE from the whole interaction volume.*

(e.g., high-Z regions in/on low-Z matrix, polycrystalline material: change in crystallographic orientation)

- **The lower E_0 the smaller is the escape area!**
- **The higher the local variations in Z the better is the resolution**

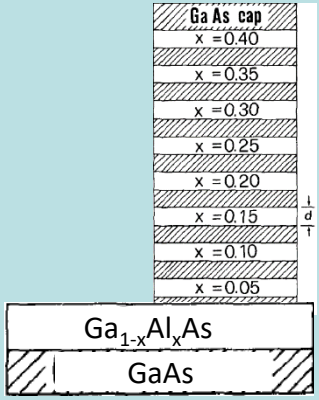

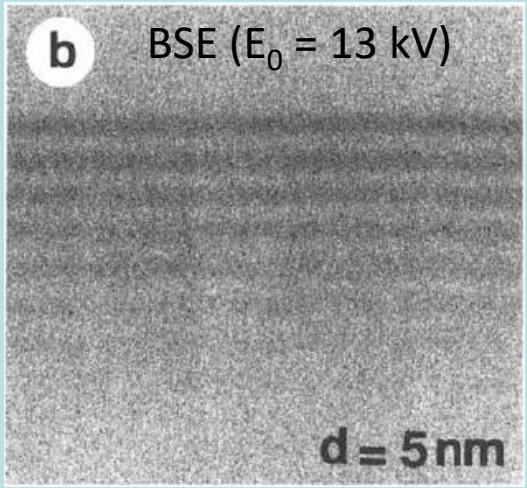

Merli, Nacucci, Ultramicroscopy 50 (1993), pp. 83

* L. Reimer, *Scanning Electron Microscopy* (p. 144)

BSE Imaging – Summary

Dependency of η on

Atomic number Z	⇒	**Chemical/compositional contrast**
Angle of incidence	⇒	Topographic contrast
Crystallographic orientation in polycrystals	⇒	Channeling contrast

Drawbacks

- Limited resolution in BSE imaging due to interaction of PE with sample

Escape area of BSE >(>) Illuminated area (d_0)

- Highly energetic BSE cannot be electrostatically deflected towards any detector like low-energy SE

Limited solid angle covered by available BSE detectors

⇓

Generally lower count rates than in SE imaging

SE Signal

SE are produced in the whole interaction volume (E < 50 eV)

Due to the low energy only SE with

$E > \Phi_W$ (Work function)

produced in the

topmost layer (~5–50 nm)

may escape from the sample. Final kinetic energy is reduced by Φ_W! (for AE it can be even less)

BSE: the escape depth is much higher

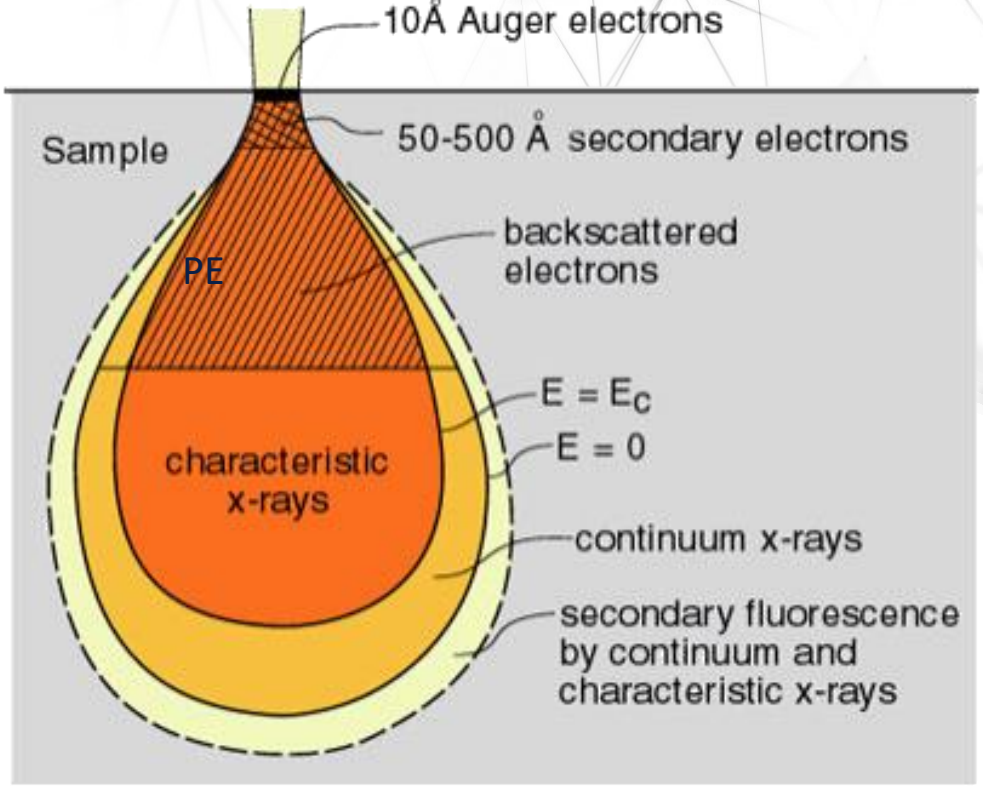

from http://www4.nau.edu/microanalysis/Microprobe/NewOverview.html

Contributions to SE Signal

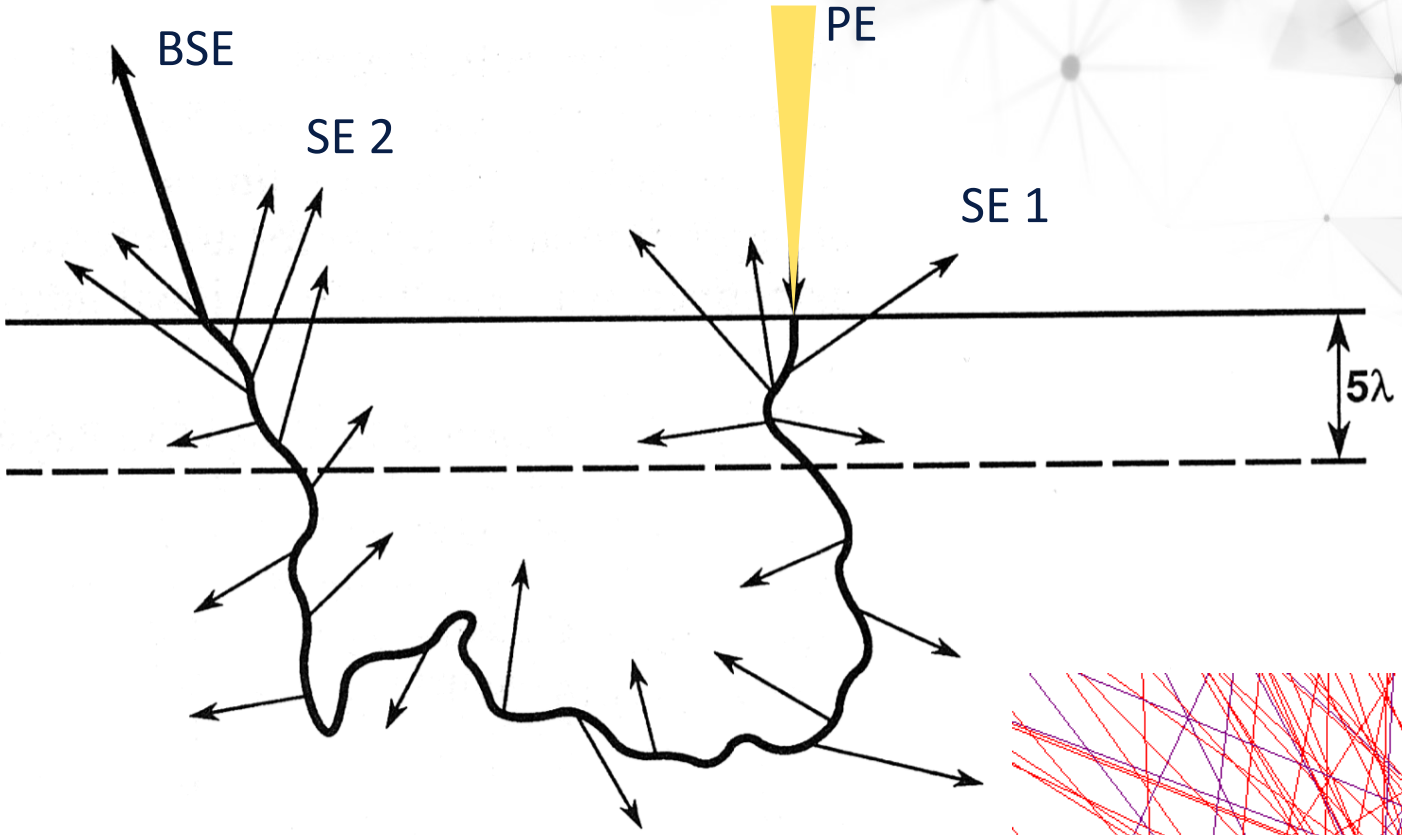

$I_{SE\,1} < I_{SE\,2}$

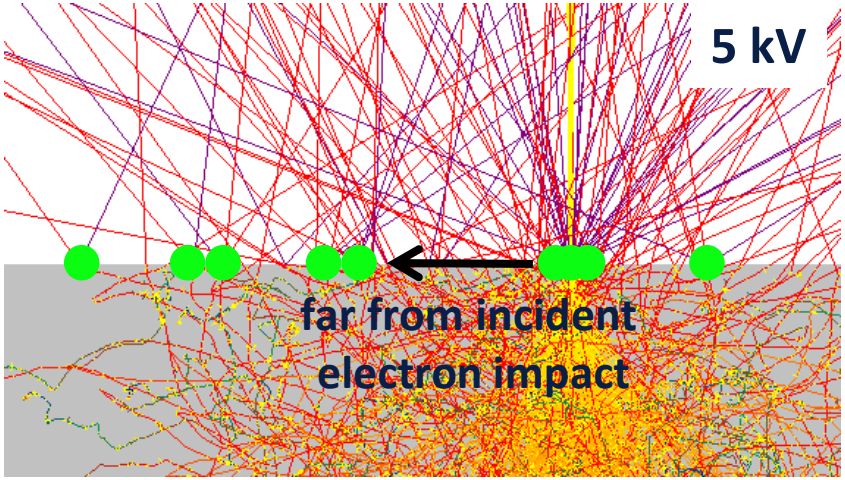

Contributions to SE Signal

Artificial contributions to SE signal:

- SE 3 Unwanted SE excited by BSE
- SE 4 Stray electrons (aperture)

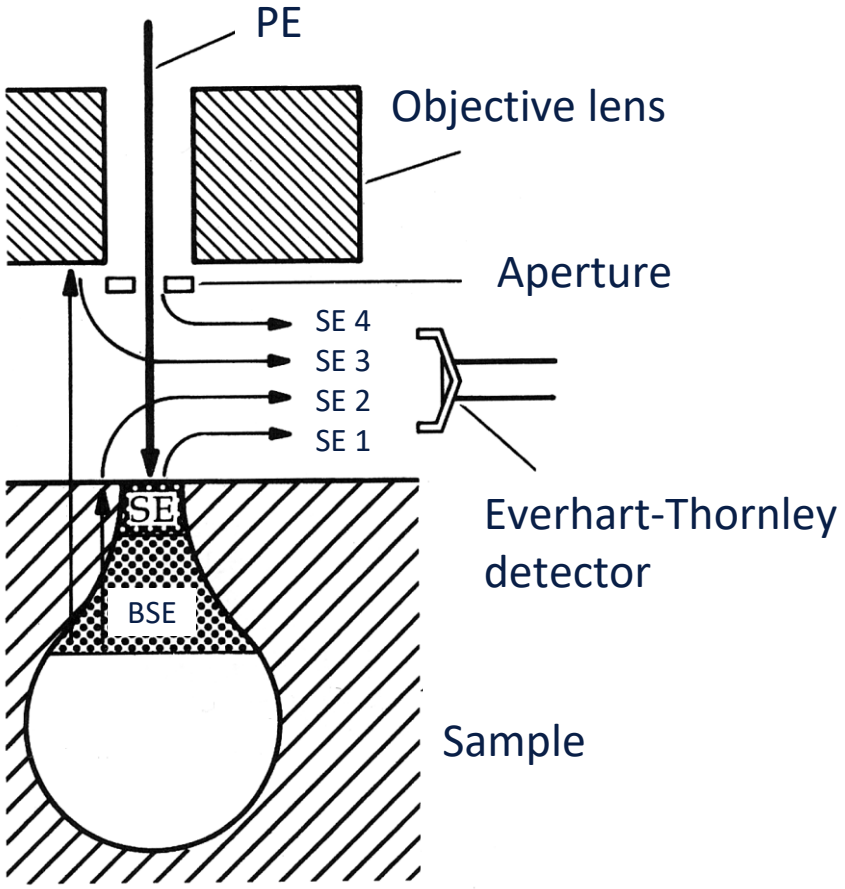

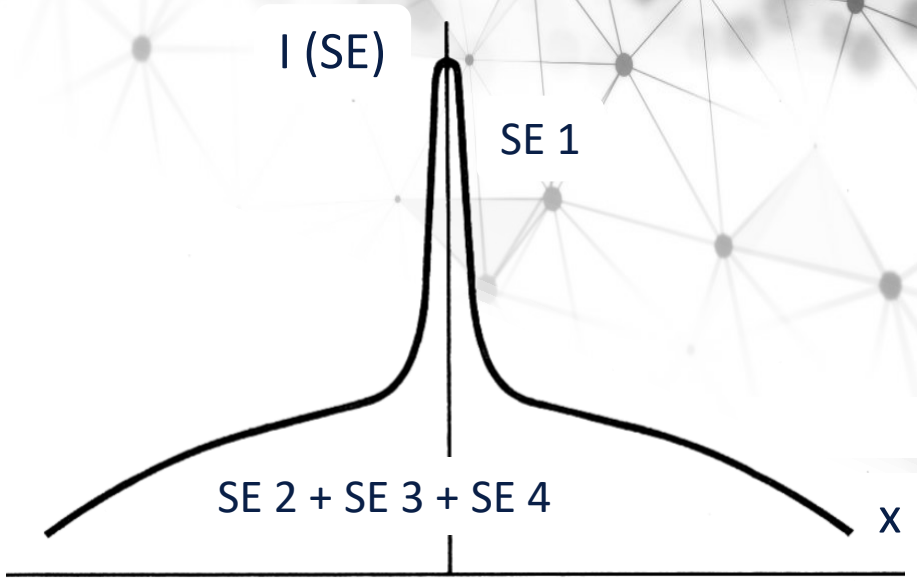

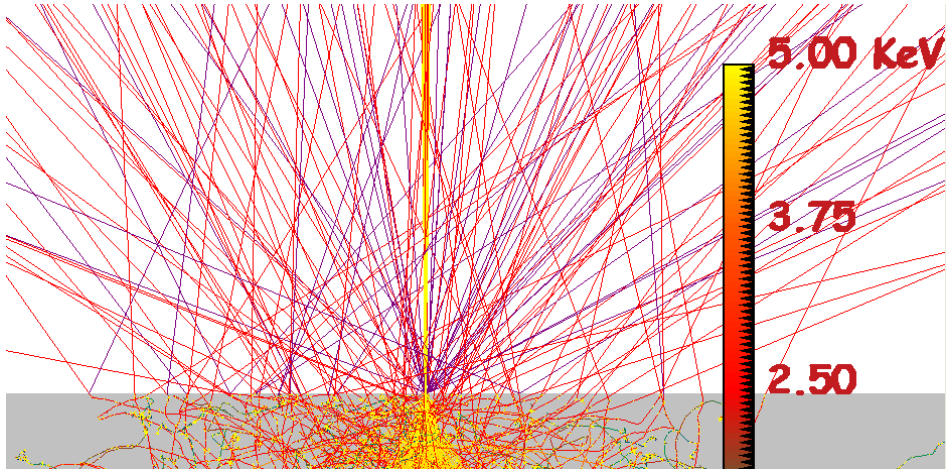

in Fuchs, Oppolzer, Rehme, *Particle Beam Microanalysis* (p. 106)

Contributions to SE Signal

Artificial contributions to SE signal:

- SE 3 Unwanted SE excited by BSE
- SE 4 Stray electrons (aperture)

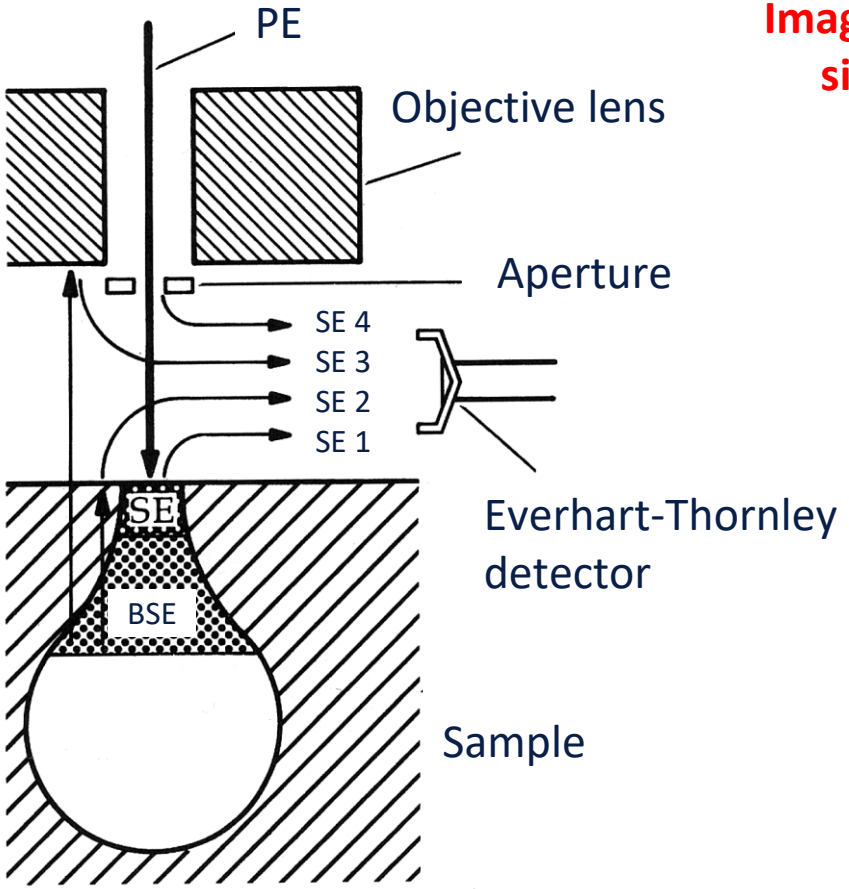

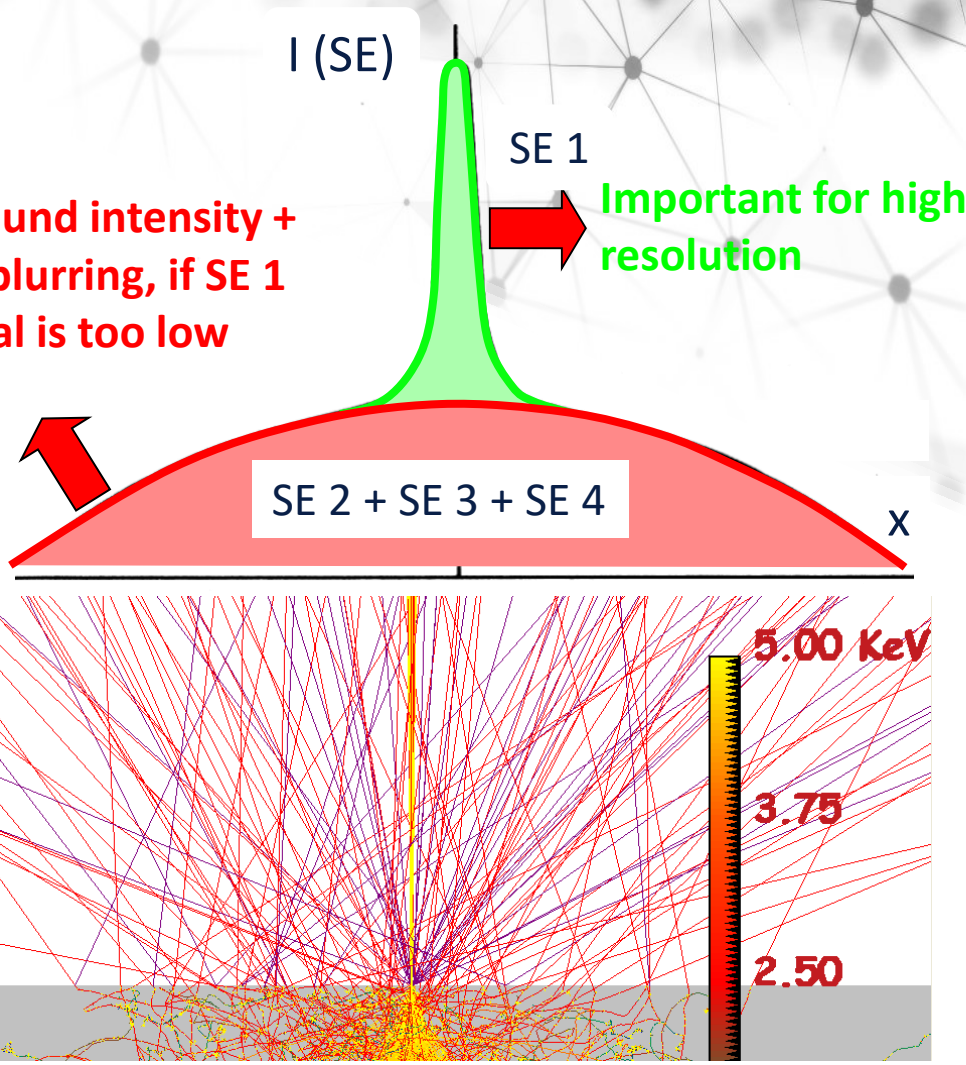

in Fuchs, Oppolzer, Rehme, *Particle Beam Microanalysis* (p. 106)

SE Imaging – Resolution

Despite the expansion of the interaction volume the

resolution in SE imaging is of the order of the initial beam size (d_0)

if the contribution of SE 1 electrons is sufficient.

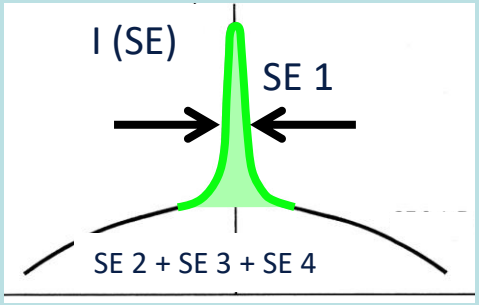

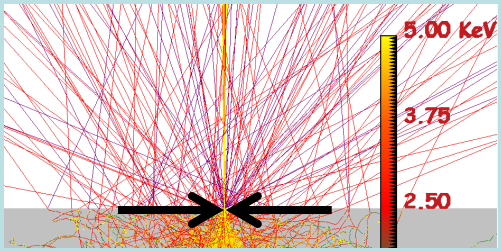

* L. Reimer, *Scanning Electron Microscopy* (p. 144)

SE Imaging – Summary

Dependency of δ on

Angle of incidence	→	**Topographic contrast**
(Work function Φ_W)	→	(Chemical contrast)
Crystallographic orientation in polycrystals	→	Channeling contrast
(Local) electric potential	→	Voltage contrast (Contrast due to charging)
Interaction of local magnetic potential with low-energetic SE	→	Magnetic contrast

Everhart-Thornley detector: SE are "collected" by attractive potential → **High count rates!**

Drawbacks

- No real Z-contrast
- Charging: Low-energetic electrons are strongly deflected by local electric potentials (Charging) + Strong enhancement of SE yield (negative charging) leading to oversaturation

How to Prevent Charging — Tailoring Landing Energy

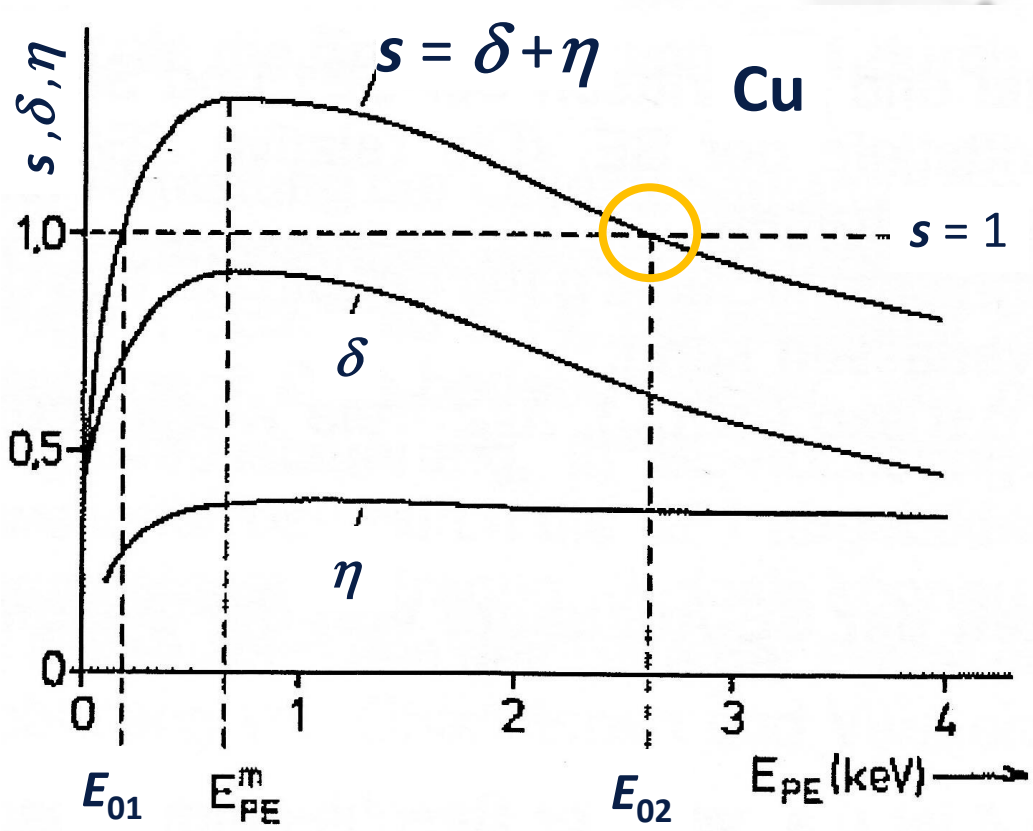

Material	E_{02} [keV]
gold	8
copper	2.8
aluminum	2.8
GaAs	4.3
silicon	1.6
SiO_2	3.0
passivation	2.0
polyimide	0.6
AZ1470 resist	1.0
epoxy	1.1
ceramics	2

Sample charging may be prevented by balancing incoming and outgoing currents:

$I_{PE} = I_{BSE} + I_{SE}$ ⇒ $s = \delta + \eta = 1$!

in P. Schmidt, *Praxis der Rasterelektronenmikroskopie und Mikrobereichsanalyse A* (p. 160)

in Fuchs, Oppolzer, Rehme, *Particle Beam Microanalysis* (p. 114)

Sample Charging

Glass fibers

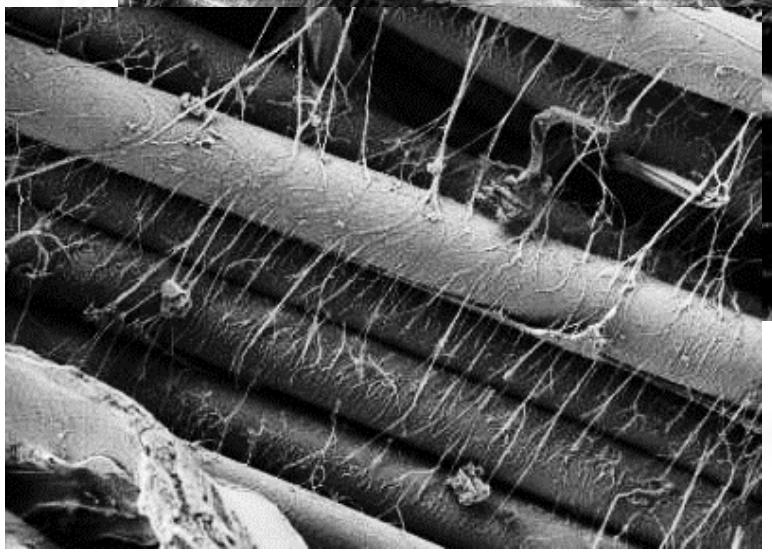

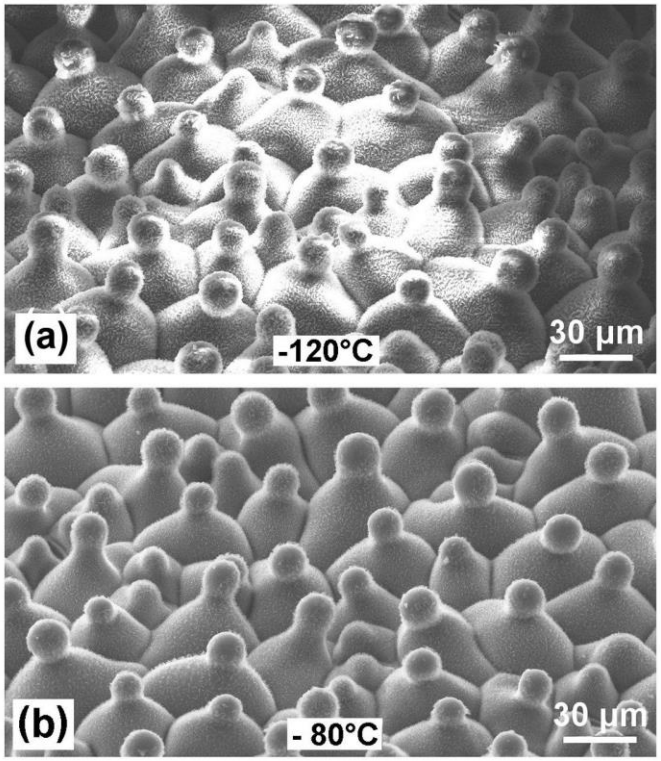

Biological specimen

Lithographic structures on glass substrate

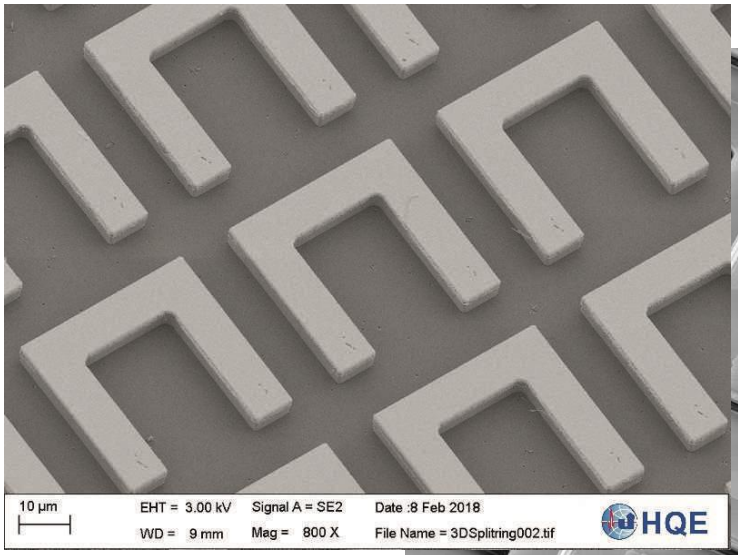

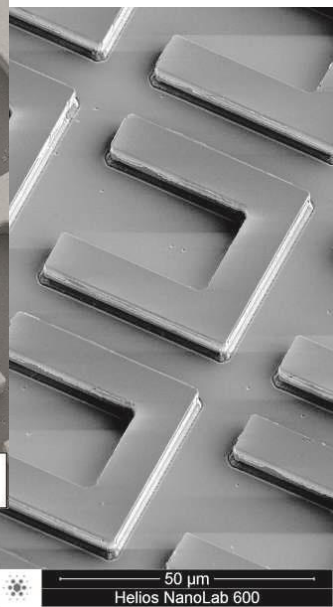

Example of current balancing

Non-conducting cellulose filter paper at different energies:

- Uncoated cellulose
- Region coated with silver paste

→ **No charging** at ~1.65 keV

→ Almost **not contrast** because $\delta + \eta = 1$, where the local beam current is constand

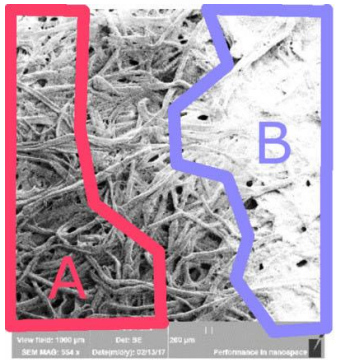

0.5 kV

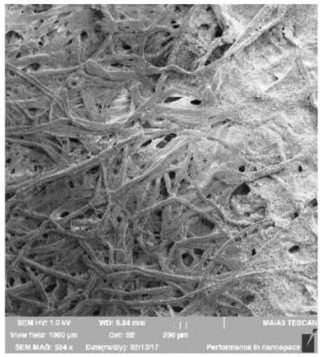
1.0 kV

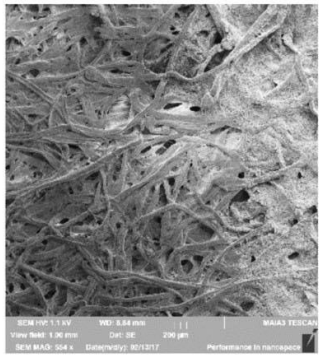
1.1 kV

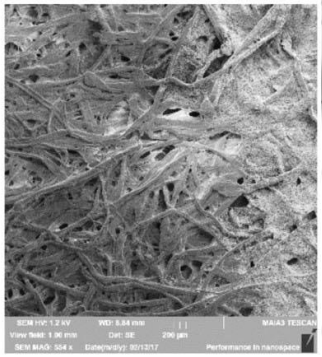
1.2 kV

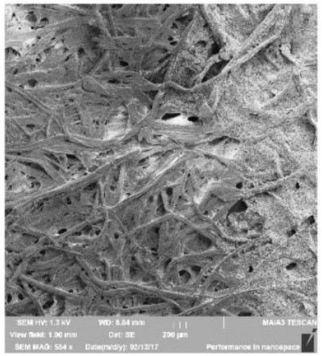
1.3 kV

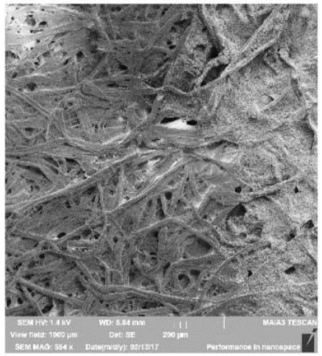
1.4 kV

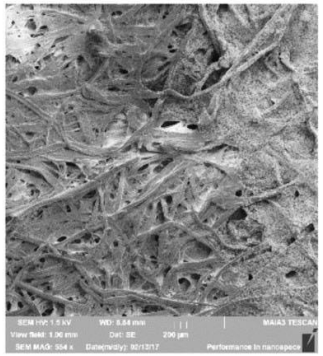
1.5 kV

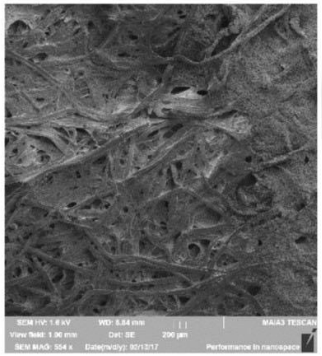
1.6 kV

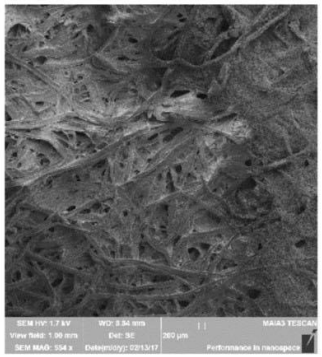
1.7 kV

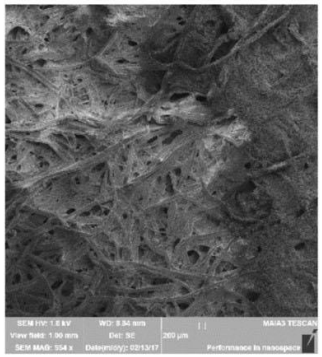
1.8 kV

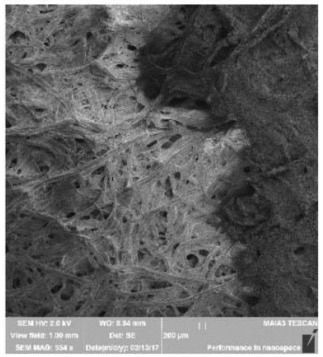
2.0 kV

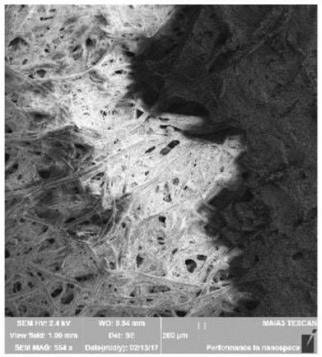
2.4 kV

Dr. M. Hummelgård
Mid Sweden University
Note via LinkedIn

Example of current balancing

Non-conducting cellulose filter paper at different energies:

- Uncoated cellulose
- Region coated with silver paste

→ **No charging** at ~1.65 keV

→ Almost **not contrast** because $\delta + \eta = 1$, where the local beam current is constand

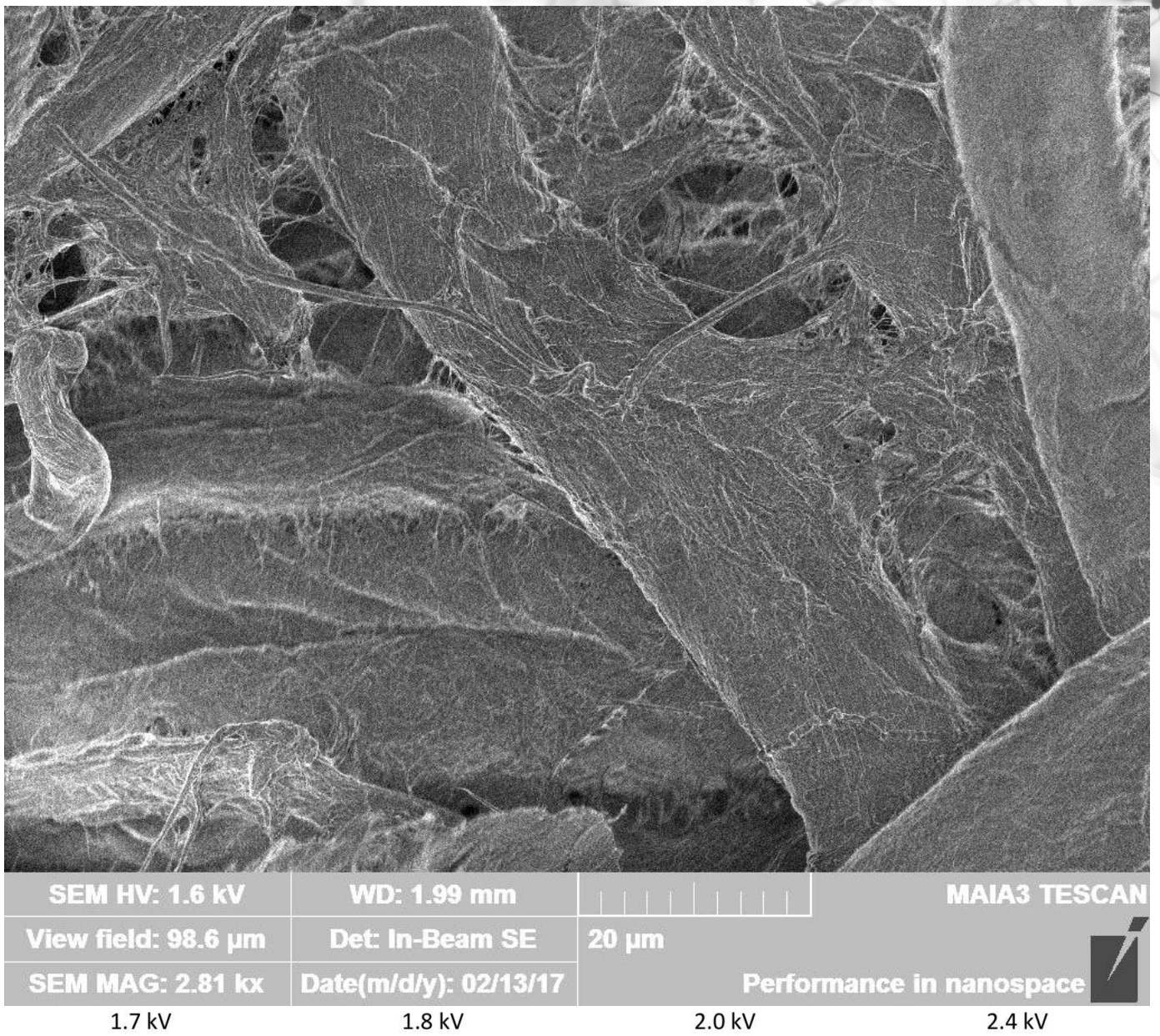

Dr. M. Hummelgård
Mid Sweden University
Note via LinkedIn

How to Prevent Charging — Sample Coating/Contacting

- **Au, Pt** (finer grain size)
  not optimal for EDXS
- **C-coating**
  → Contamination, additional plasma cleaning may be needed

How to Prevent Charging — Beam Current & Fast Scanning

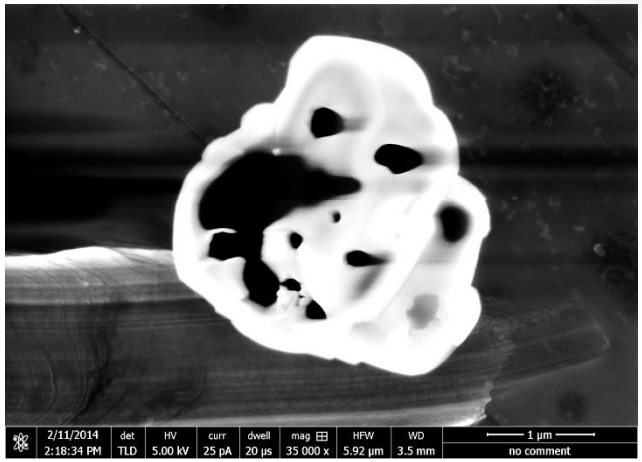

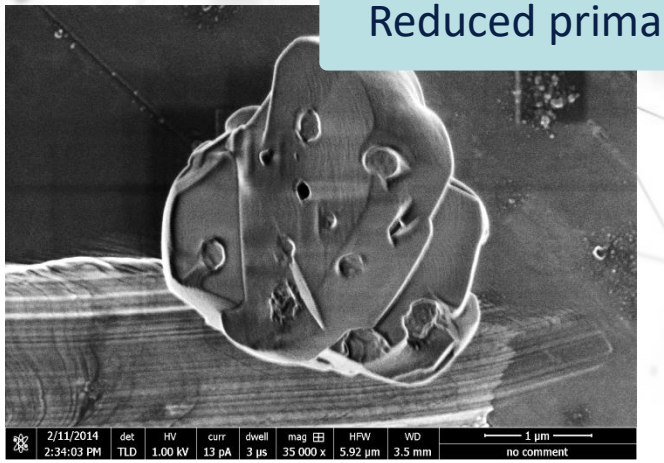

Reduced primary energy

Reduced dwell time

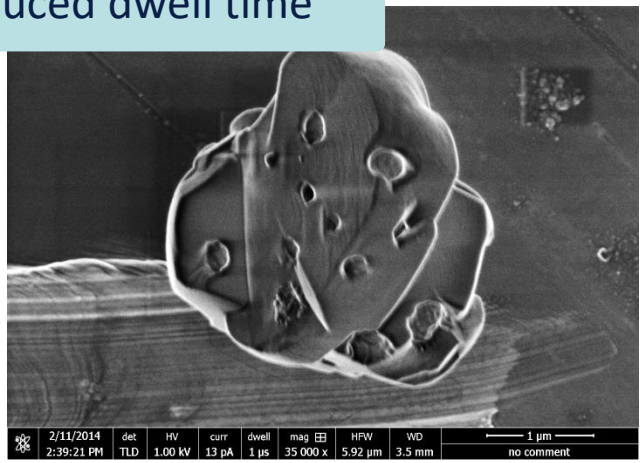

Reduced current

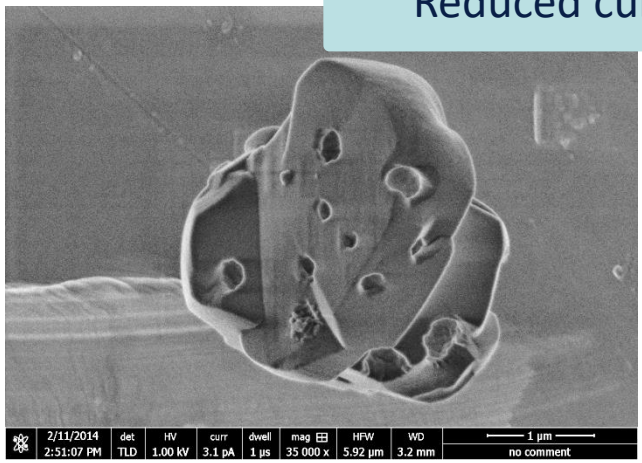

How to Prevent Charging — Alternative Techniques

- **Charge compensation by gas injection**
  (locally with a gas capillary,
  or environmental/variable-pressure SEM)
- **e^--flooding for positive charging**
  (e.g., during FIB milling)

Kleindiek Nanotechnik

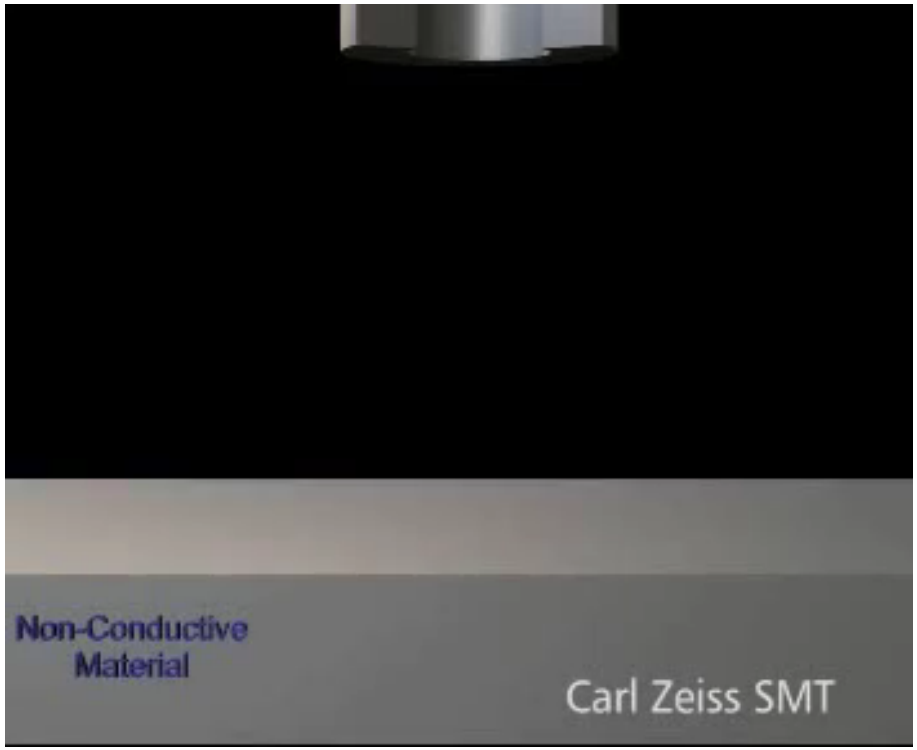

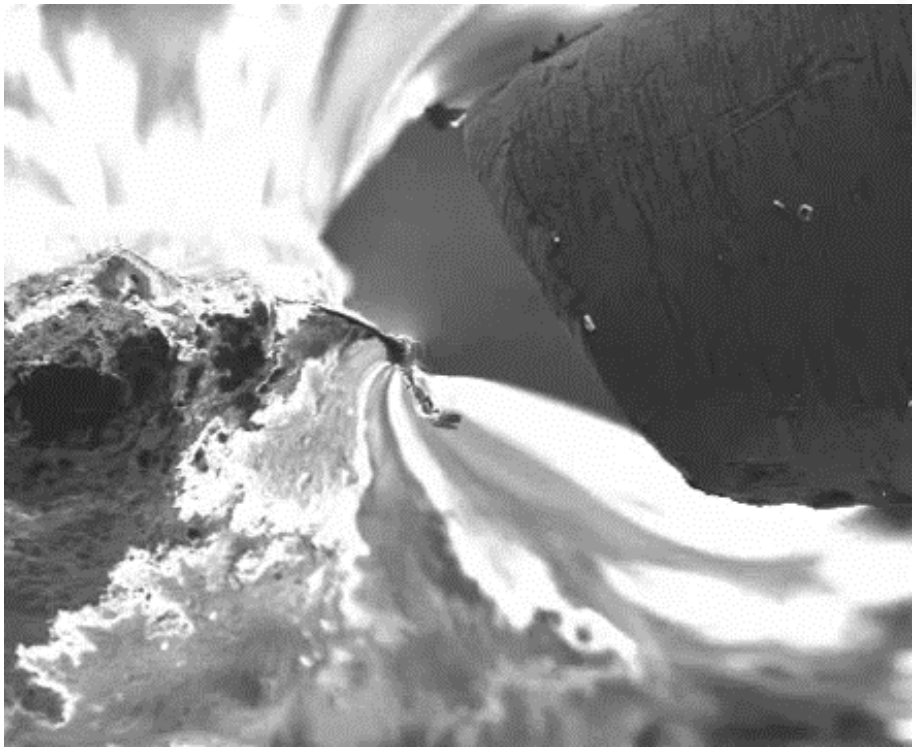

Carl Zeiss AG/Youtube

Imaging Modes

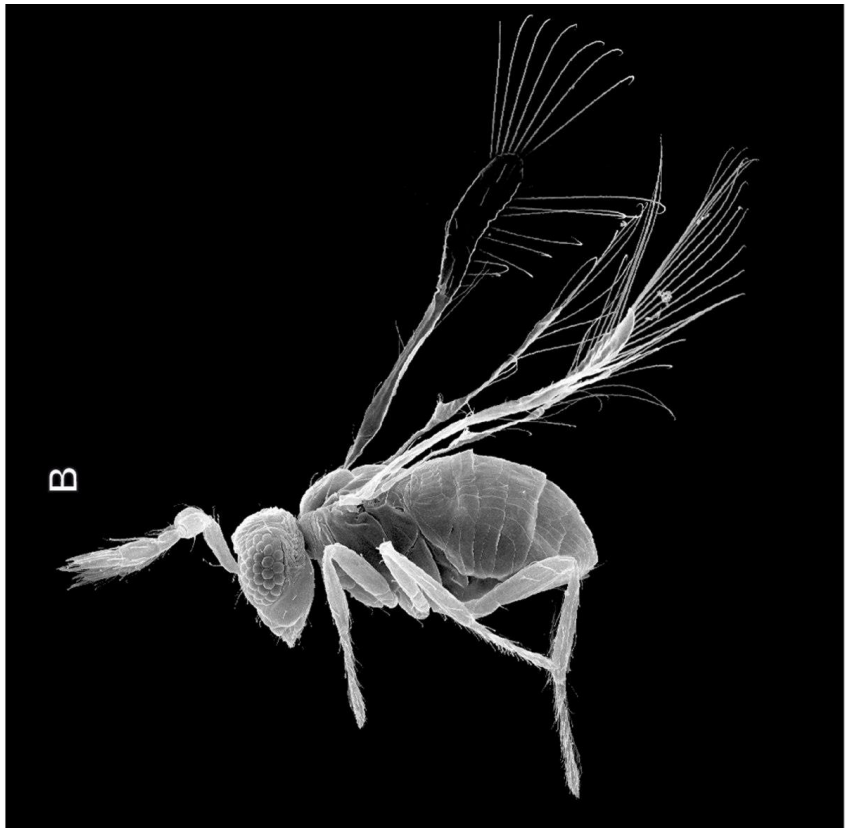

Megaphragma mymaripenne is a microscopically sized wasp. [wikipedia]

Electron Energy Distribution

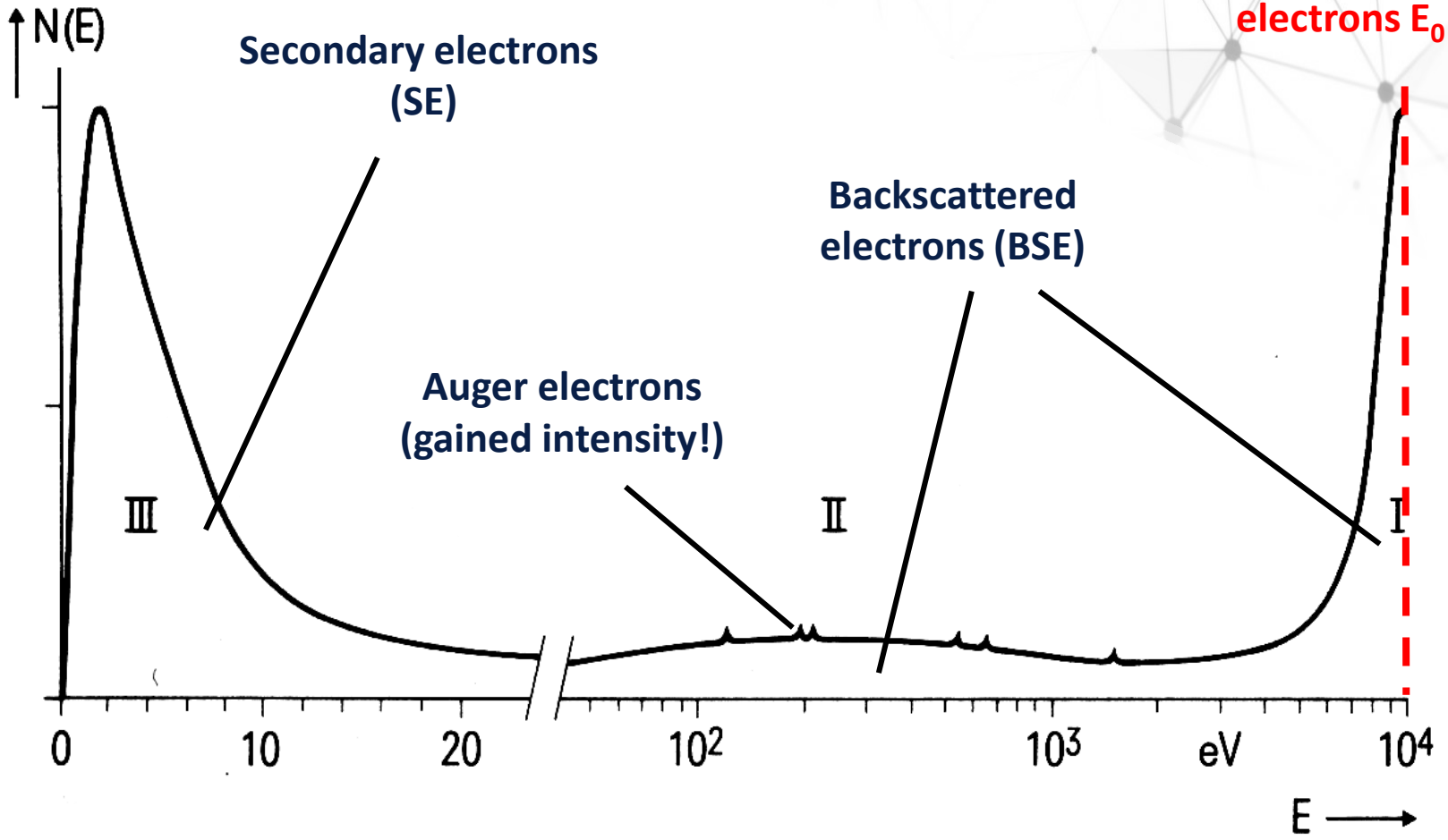

in Fuchs, Oppolzer, Rehme, *Particle Beam Microanalysis* (p. 50)

Detectors I

Everhart-Thornley detector (ETD)
(**SE/BSE**)

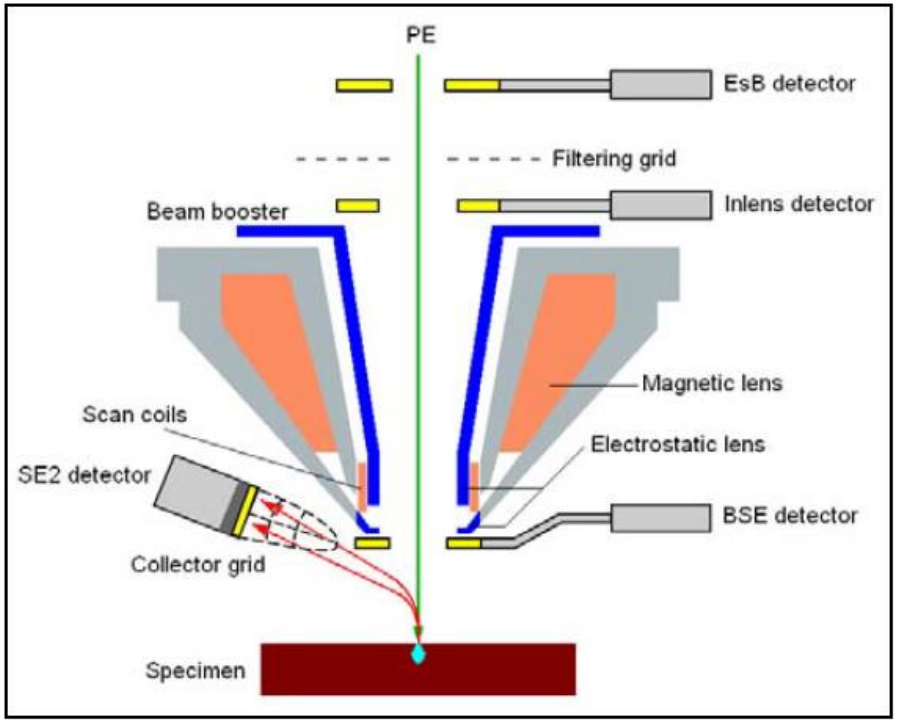

Retractable BSE detector
(**BSE**)

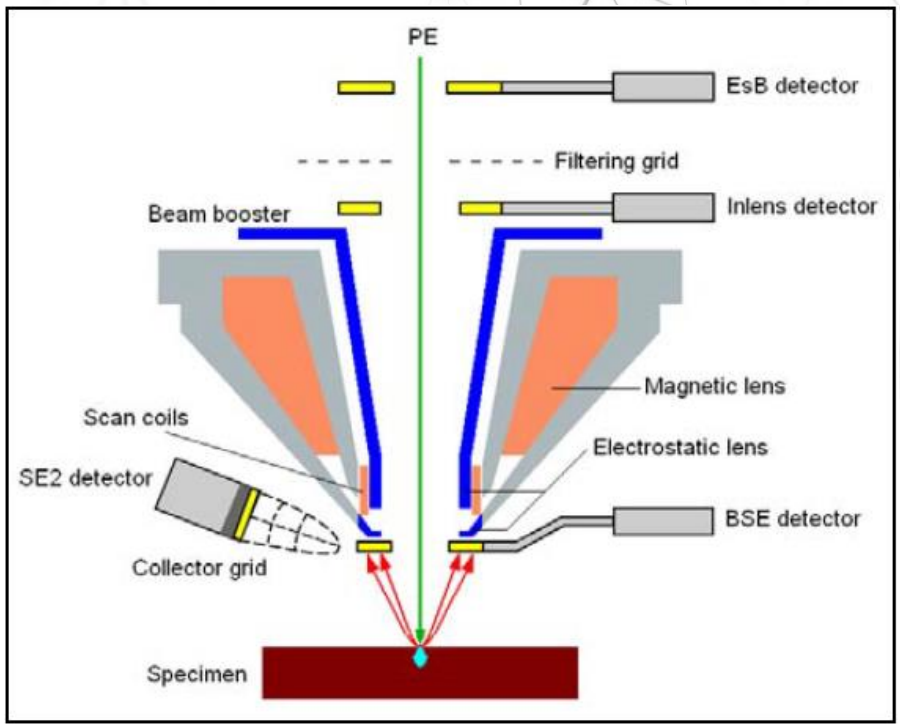

in Zeiss, *Supra Handbuch* (2004)

Detectors II (Zeiss)

InLens detector (**SE**)

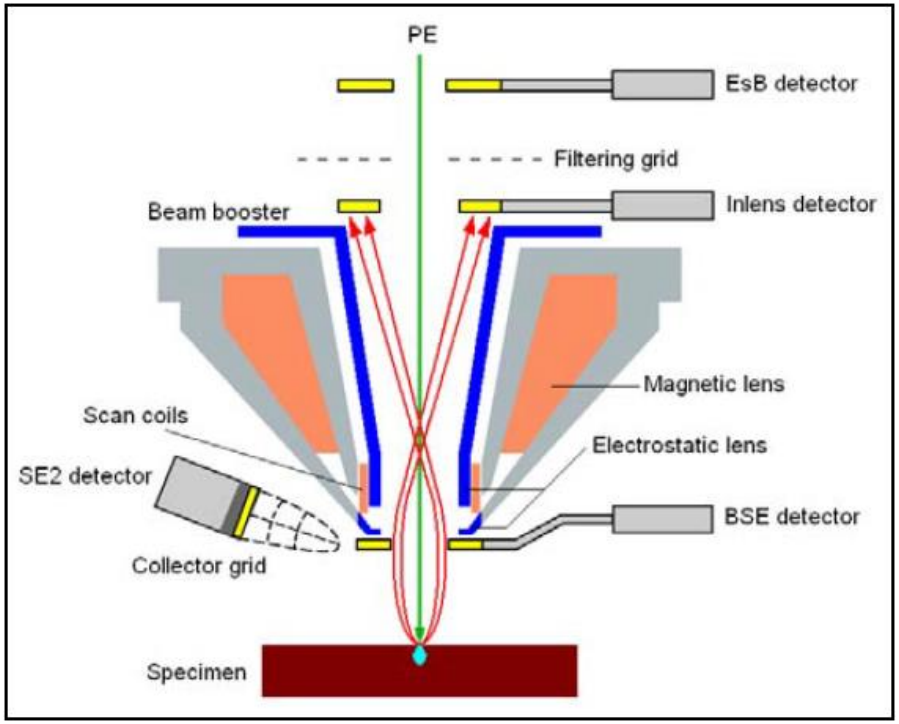

EsB detector (**E**nergy-**S**elective **B**SE detector) (**BSE**)

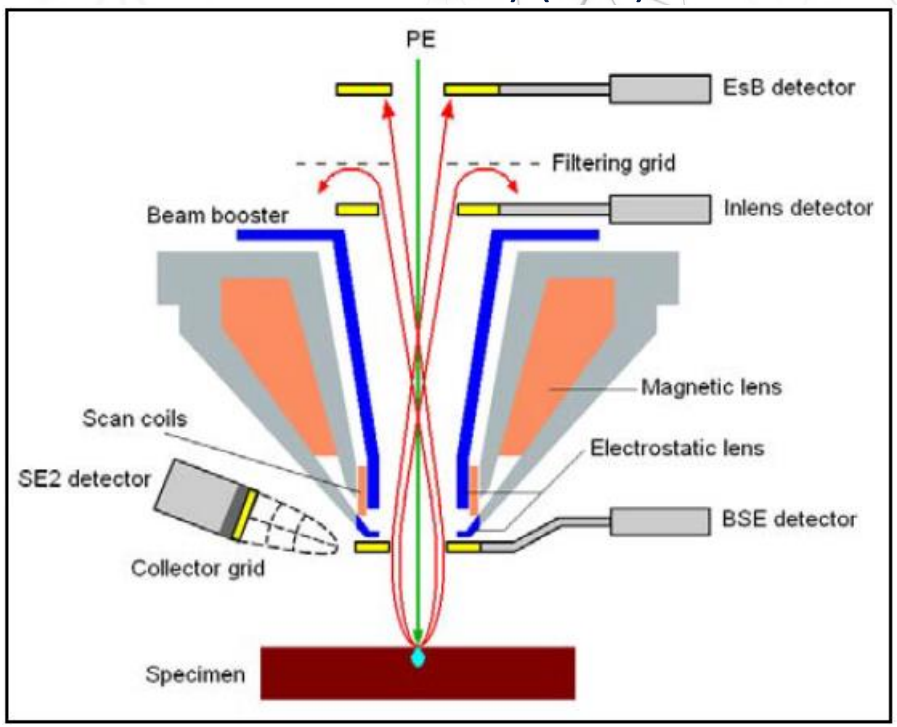

$E_0 \leq 20$ kV ➡ **Beam Booster**:

- +8 kV in electron column
- deceleration of PE by electrostatic potential of objective lens

in Zeiss, *Supra Handbuch* (2004)

Everhart-Thornley Detector (ETD)

Functional Principle

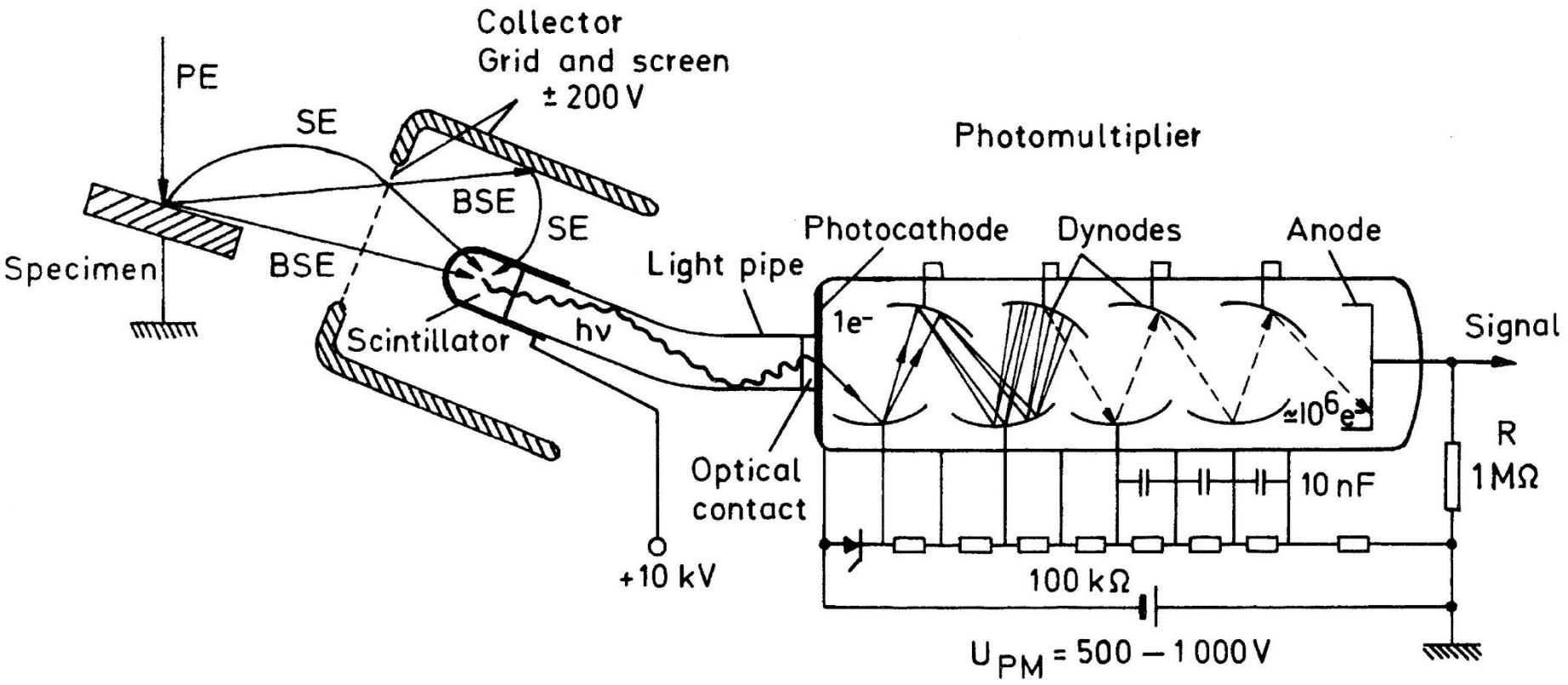

- Coupling of SE/BSE current into **photomultiplier**
  (double signal conversion: initial electron → light → electron)
- **Multiple signal amplification (x10^6):** acceleration of initial electrons + SE generation at dynodes

in L. Reimer, *Scanning Electron Microscopy* (p. 174)

Everhart-Thornley Detector (ETD)

Everhart-Thornley detector (ETD) used for SE or BSE imaging

Positive grid potential
- Attraction of SE (low energy)
- Collection efficiency depends on applied voltage
- BSE in respective solid angle detected as well

Negative grid potential
- Detection of BSE which leave which leave the sample in the direction of the E-T detector
- Repulsion of SE

Asymmetric arrangement of beam-sample-detector

↓

Topographic contrast

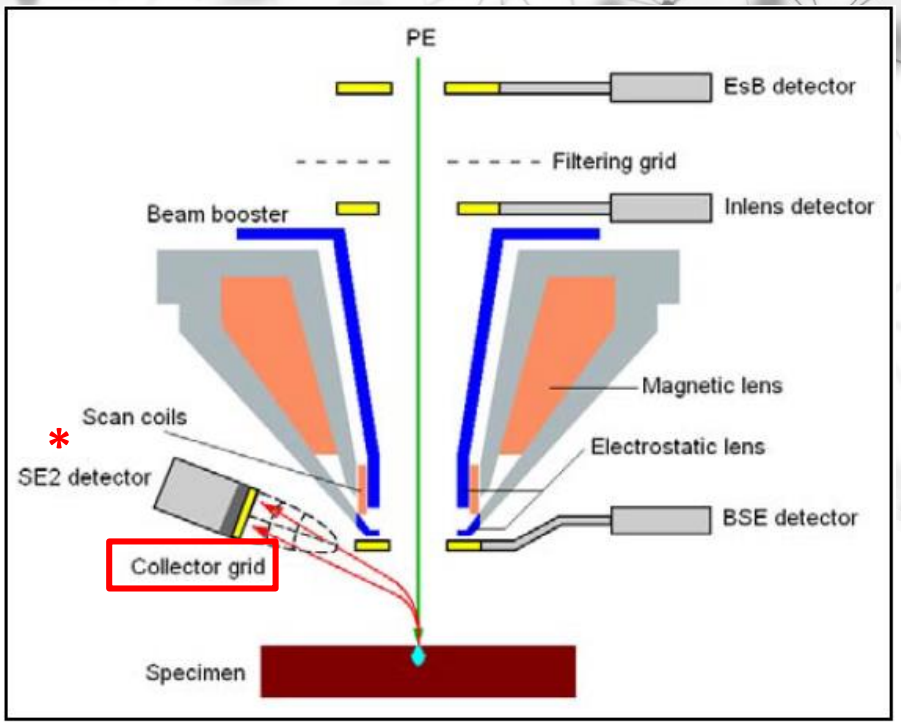

***Zeiss naming**
It doesn't exclusively collect SE 1!

in Zeiss, *Supra Handbuch* (2004)

Topographic imaging

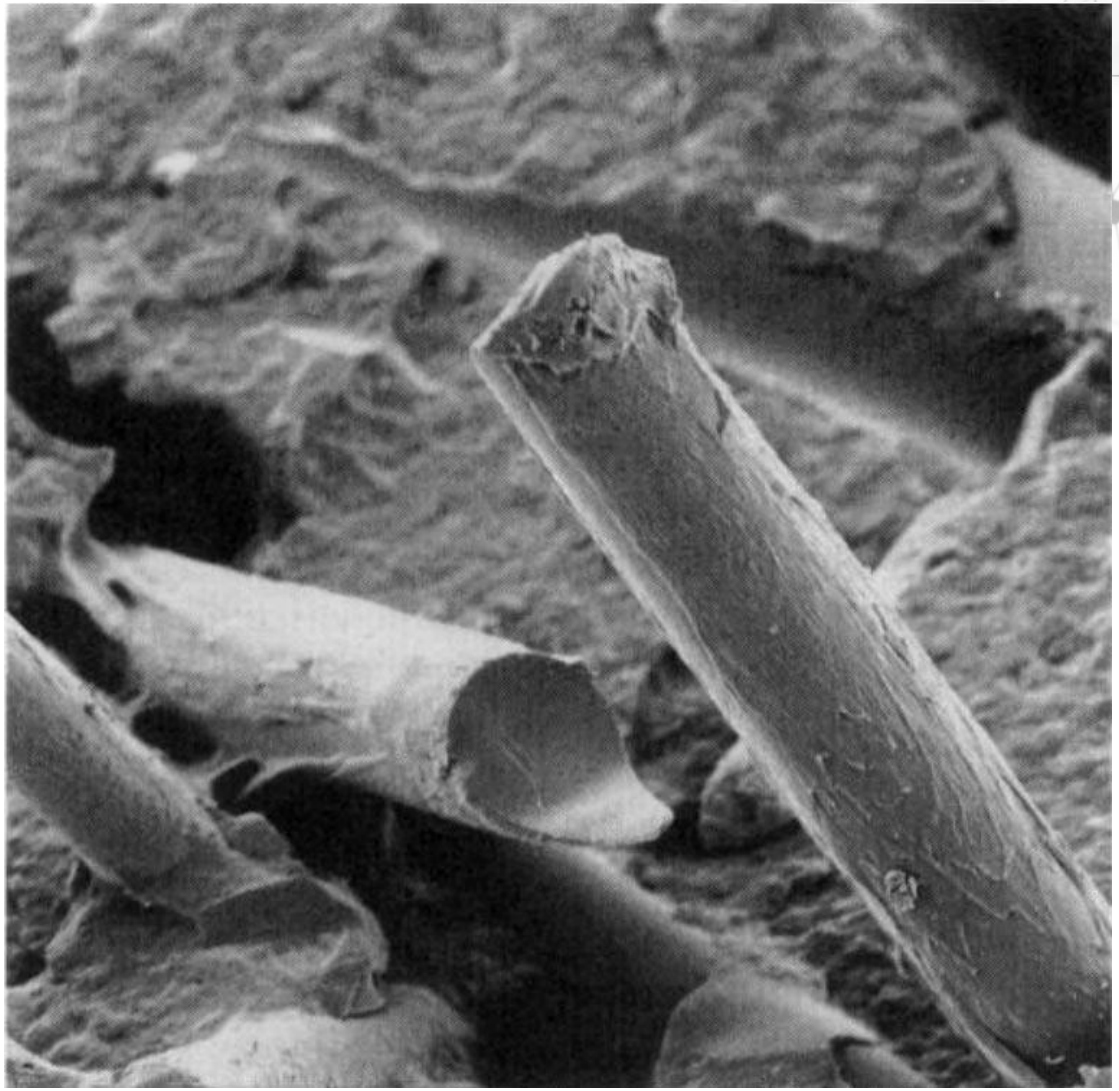

Edges
Local inclination

Glass fibre reinforced plastic

Illumination

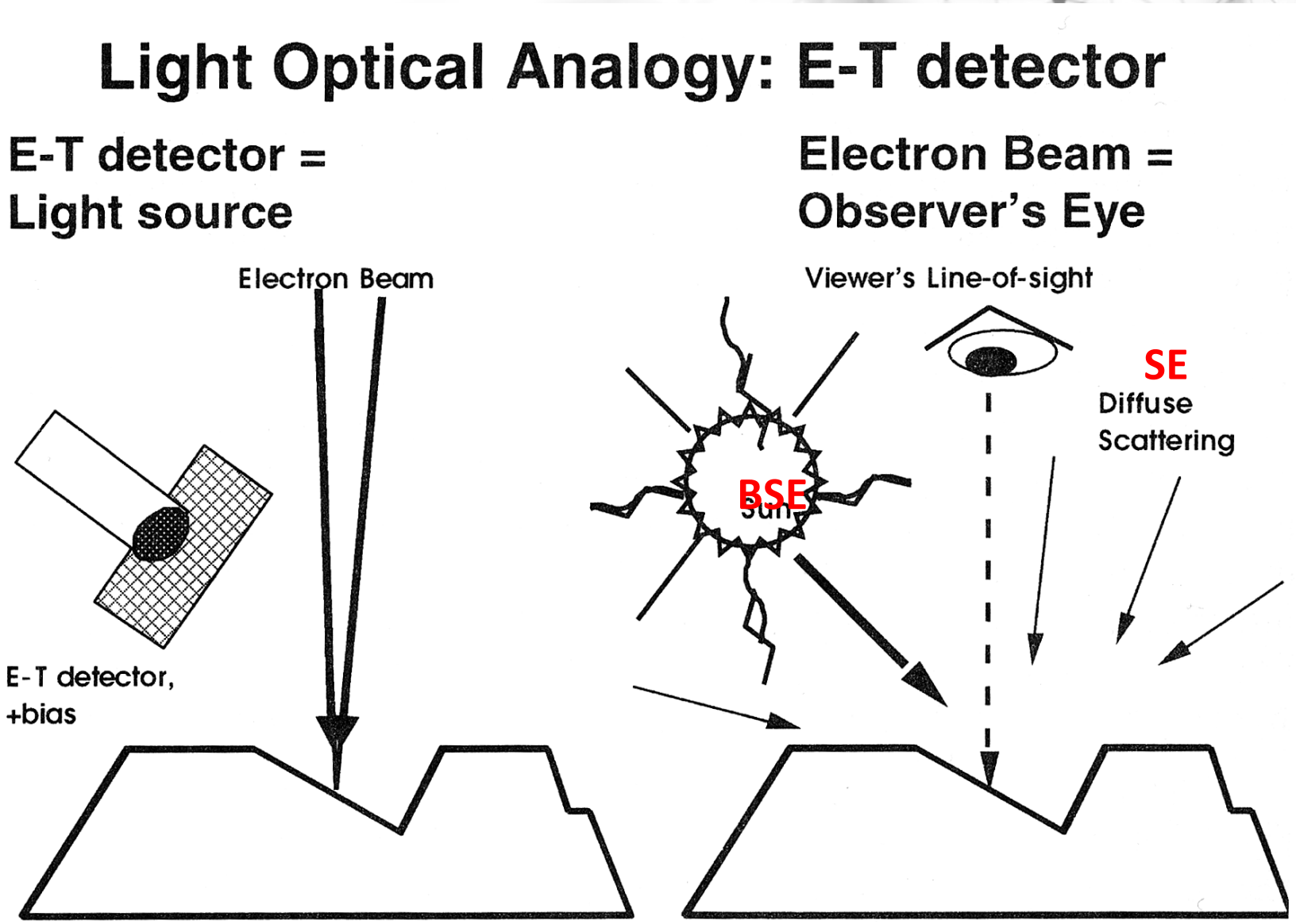

Topographic Contrast (BSE)

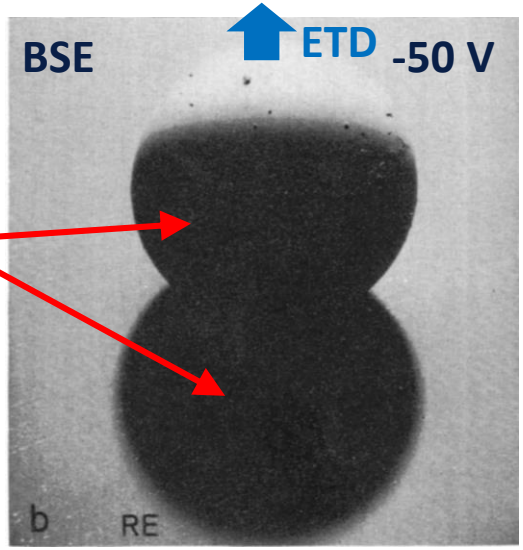

Shadowing contrast

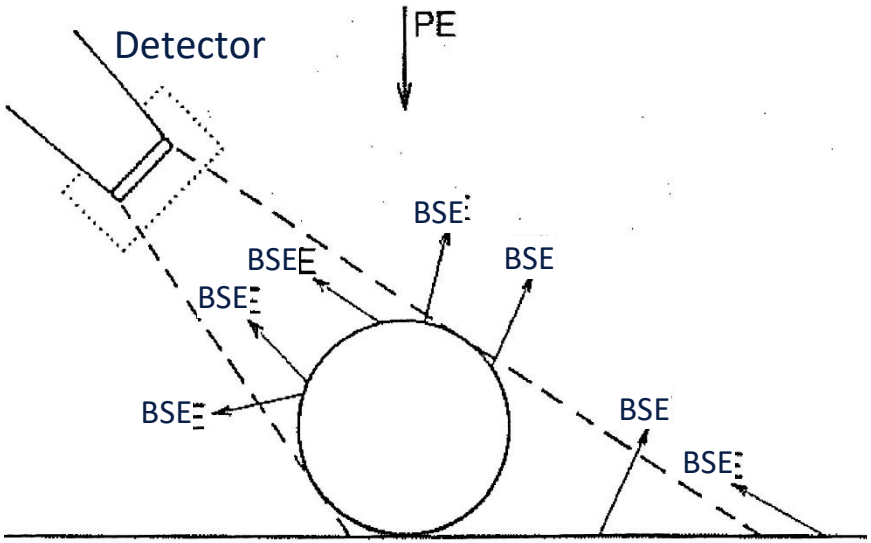

in P. Schmidt, *Praxis der Rasterelektronenmikroskopie und Mikrobereichsanalyse A* (pp. 148+167)

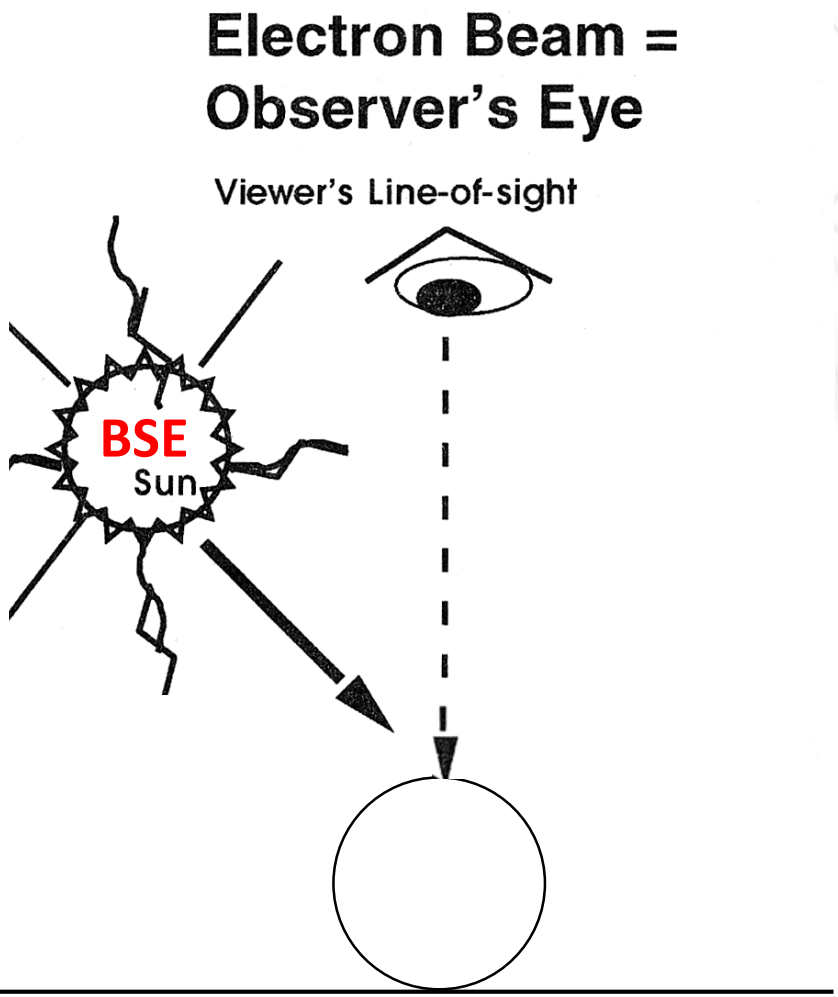

in L. Reimer, *Scanning Electron Microscopy* (p. 210)

Topographic Contrast (BSE/SE)

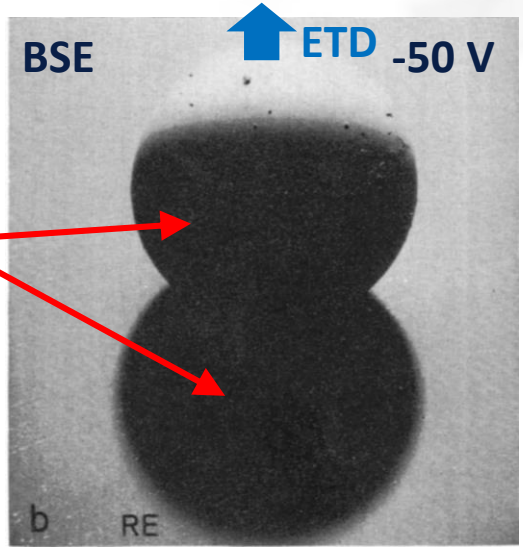

Shadowing contrast

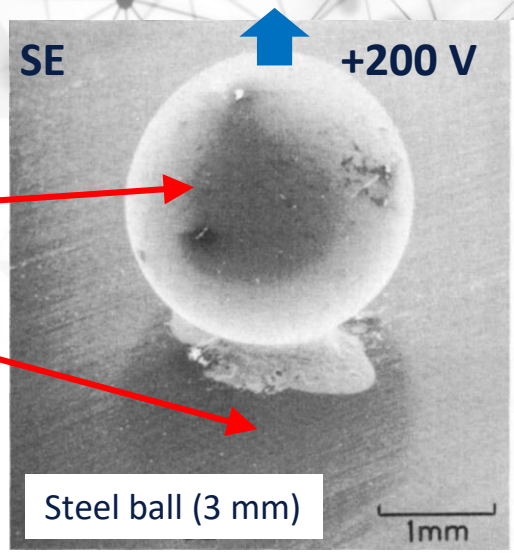

Surface tilt + Shadowing contrast

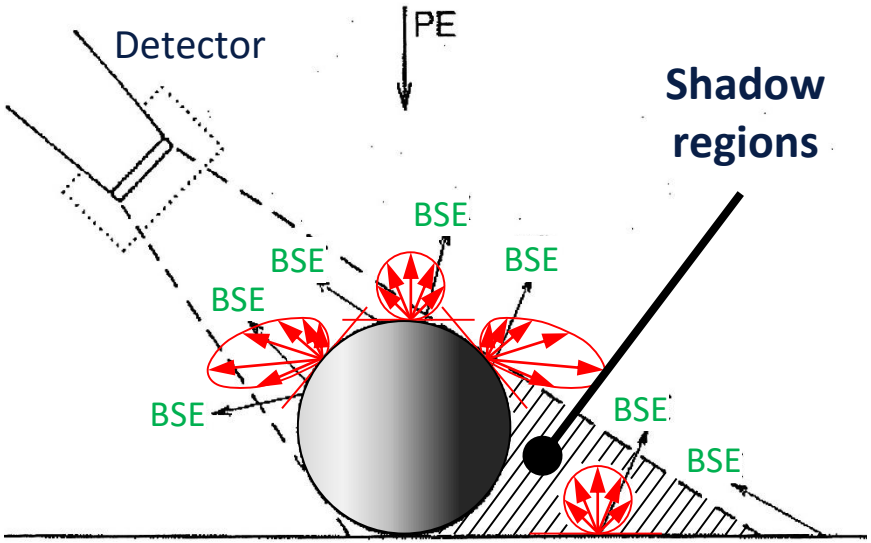

in P. Schmidt, *Praxis der Rasterelektronenmikroskopie und Mikrobereichsanalyse A* (pp. 148+167)

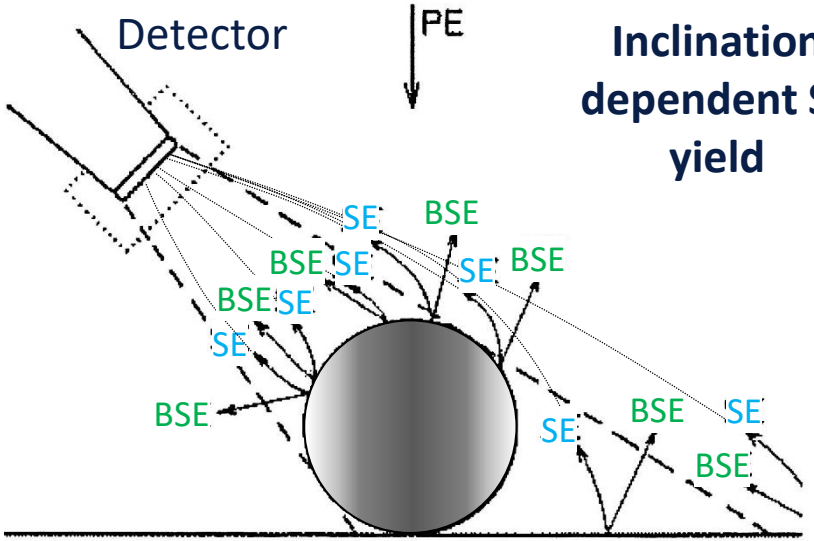

in L. Reimer, *Scanning Electron Microscopy* (p. 210)

Topographic Contrast (BSE/SE)

ETD

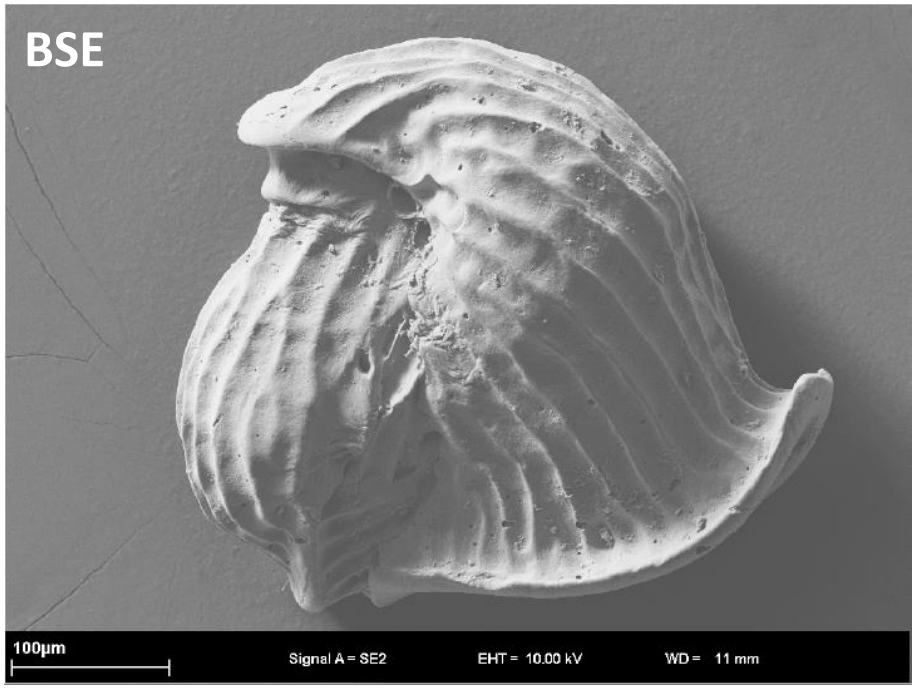

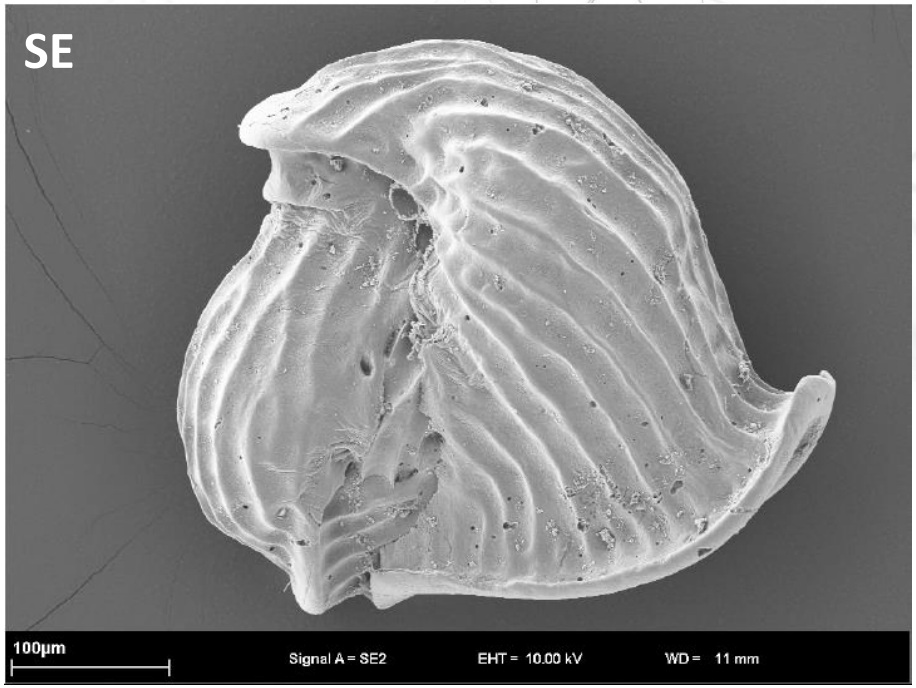

Snail shell

in Zeiss, *Supra Handbuch* (2004)

Edge Contrast (SE)

Edge contrast

Excessive intensity increase due to high SE yield

- **At an edge:** Large surface with respect to IV (1)
- Scattering of BSE into adjacent regions
  → High probability of SE 2 generation (2)

The higher E_0 the wider is the intensity increase!

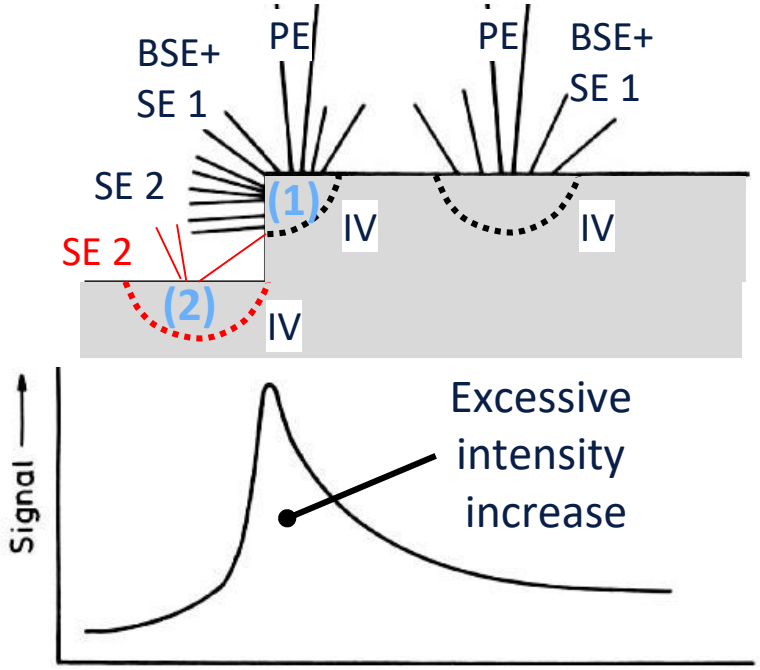

in P. Schmidt, *Praxis der Rasterelektronenmikroskopie und Mikrobereichsanalyse A* (pp. 164+165)

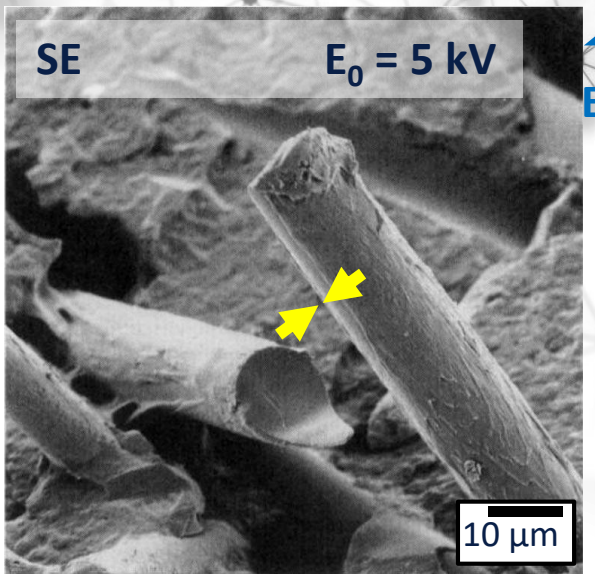

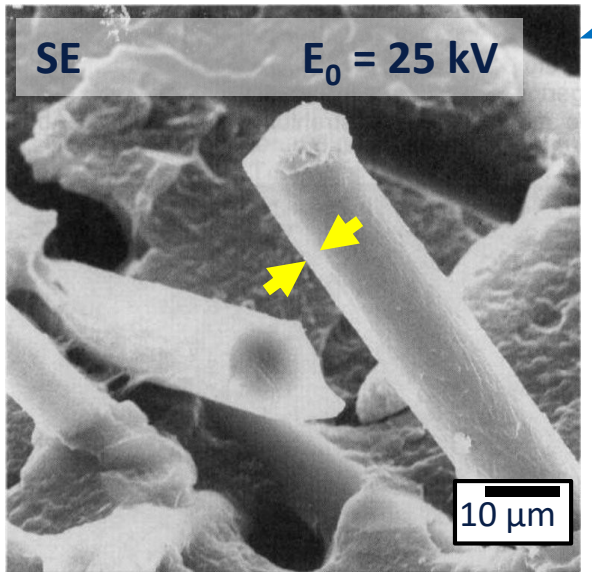

Glass fibre reinforced plastic

Transparency

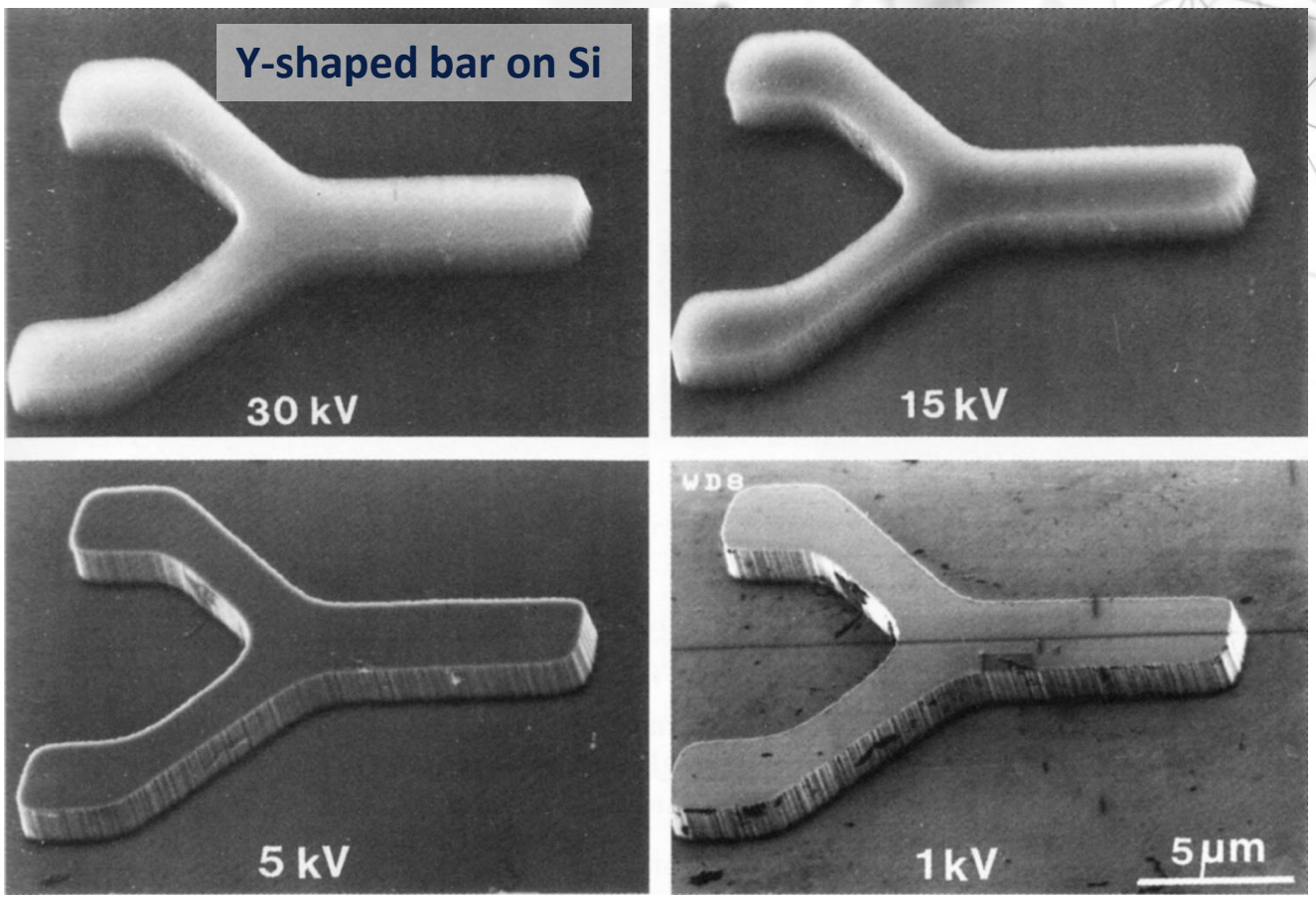

The larger IV (high E_0) the more "*transparent*" does the sample appear: contributions of SE 2 and SE 3

Localized surface information at low E_0

in L. Reimer, *Scanning Electron Microscopy* (p. 215)

Retractable BSE Detectors

Retractable annular or quadrant BSE detector used for BSE imaging

Detection of strongly backscattered electrons

Robinson-type szintillator detector

Symmetric arrangement around the optical axis

↓

Chemical contrast

Solid-state silicon detector

Symmetric arrangement around the optical axis

↓

Chemical contrast

Detector area separable into quadrants

↓

Topographic contrast

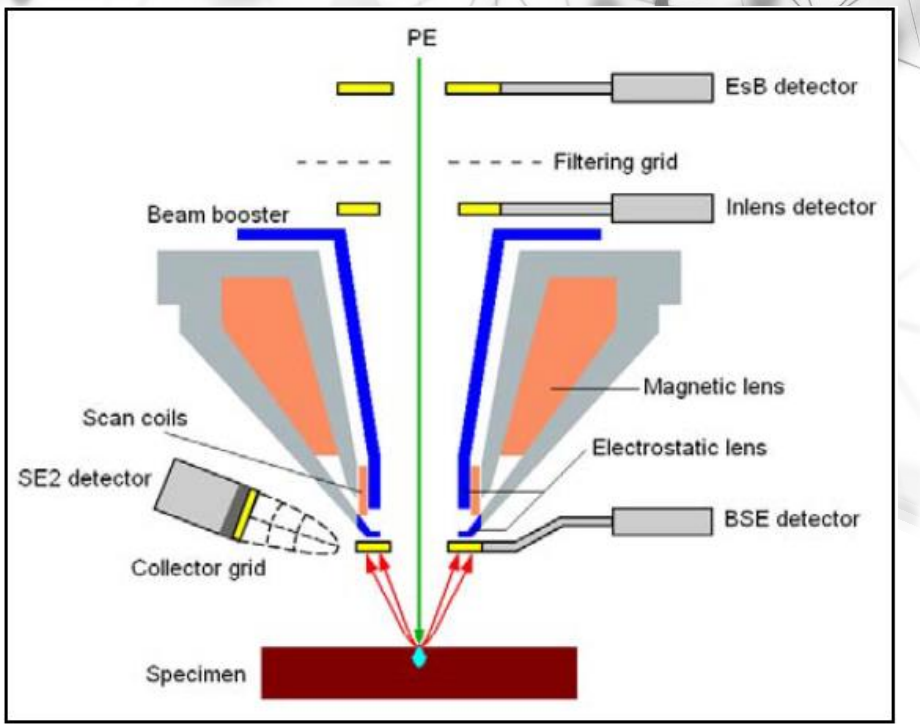

in Zeiss, *Supra Handbuch* (2004)

Retractable BSE Detector

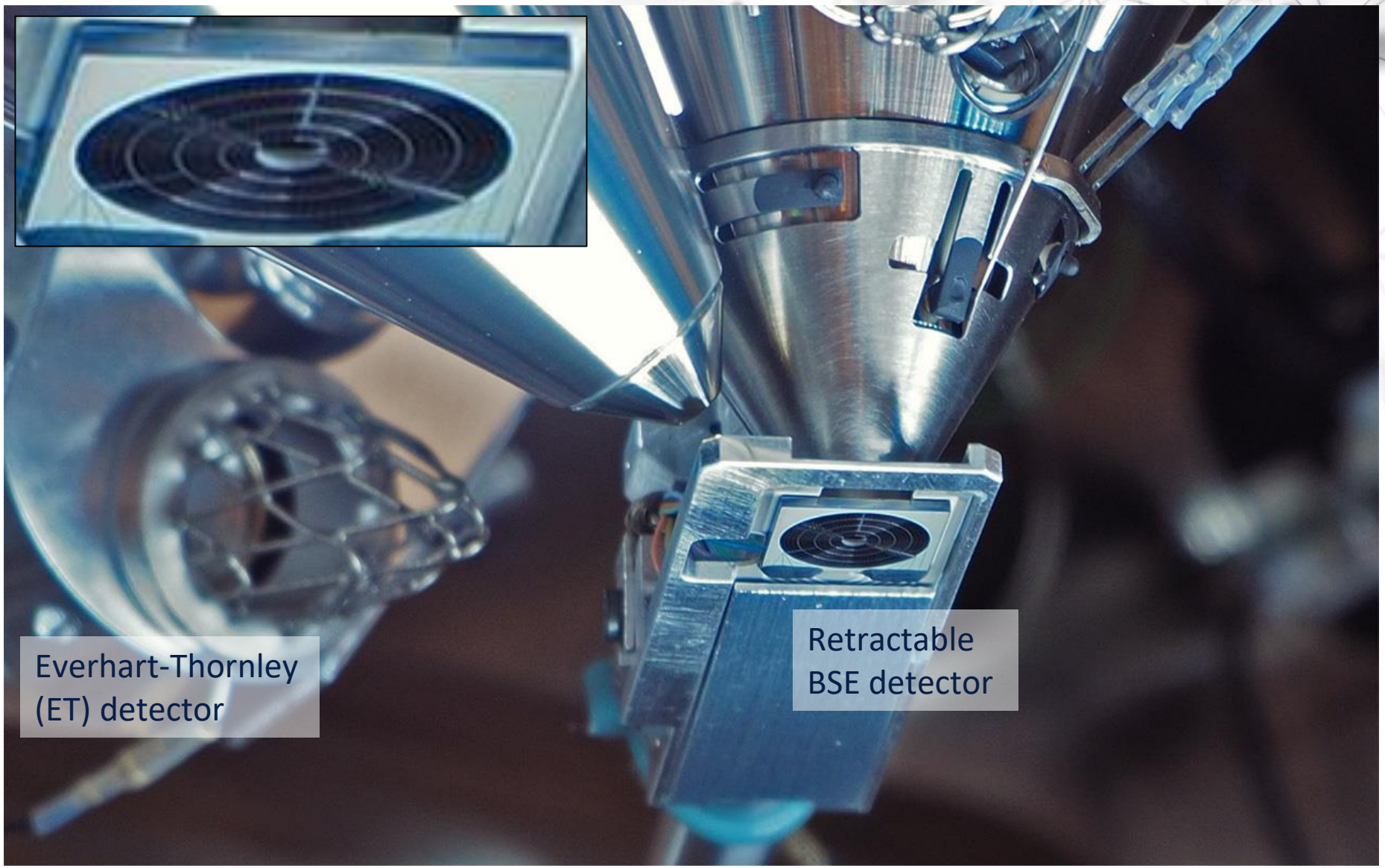

Annular BSE Detector

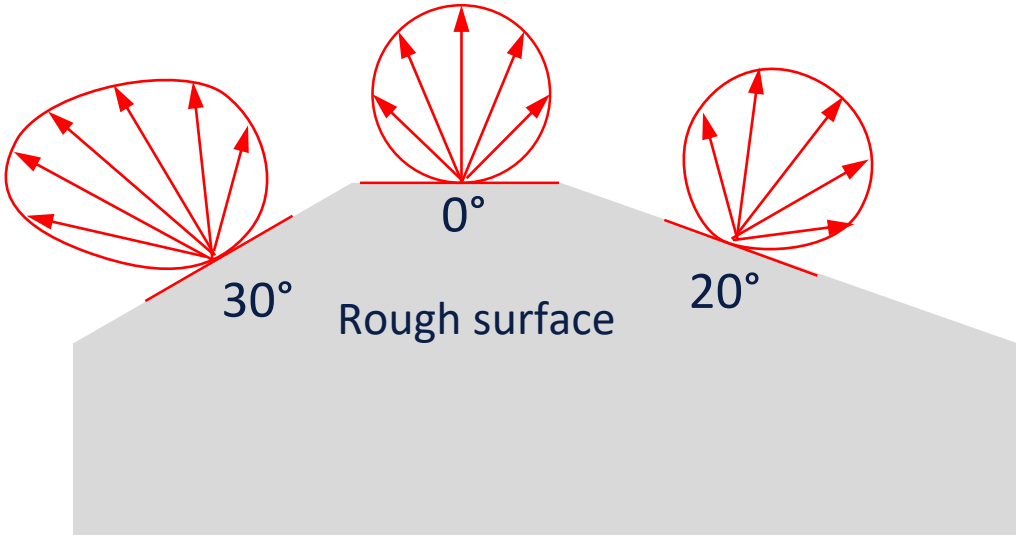

in L. Reimer, *Scanning Electron Microscopy* (p. 224)

Annular BSE Detector

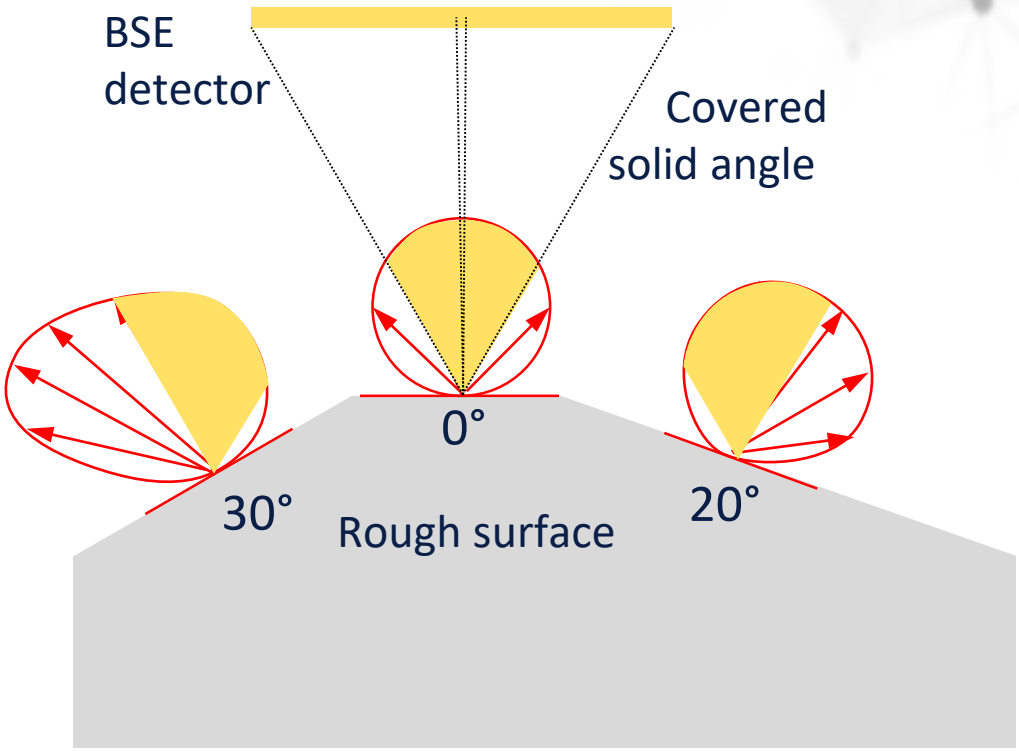

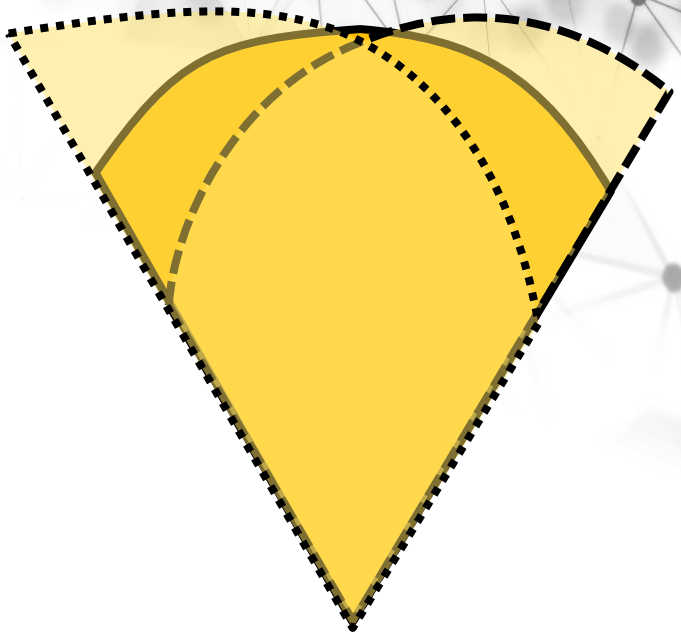

Annular BSE detector
Contrast contributions caused by varying topography minimal as long as inclination smaller than ~ 30°–40°
Flat surface optimal (polished sample)

Pure chemical contrast

Similar propability of BSE emission in covered solid angle
(independent on surface inclination)

Similar Intensity

Pure Chemical Contrast

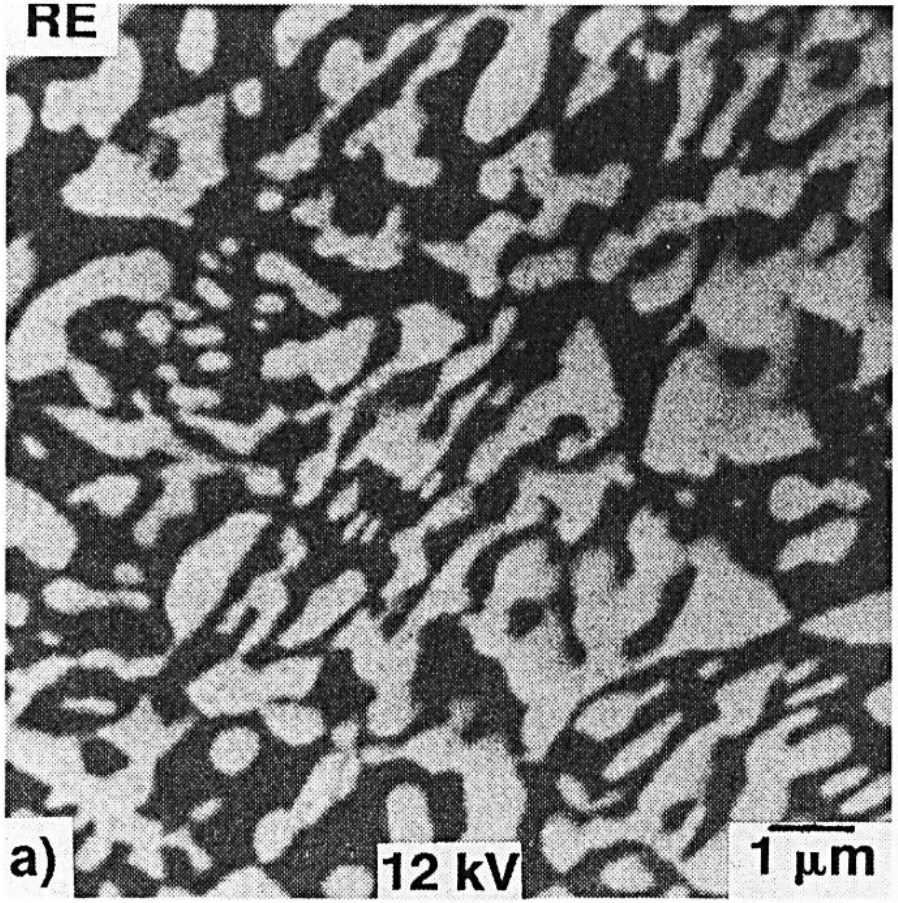

Sn-Pb alloy

Sn dark regions
Pb bright regions

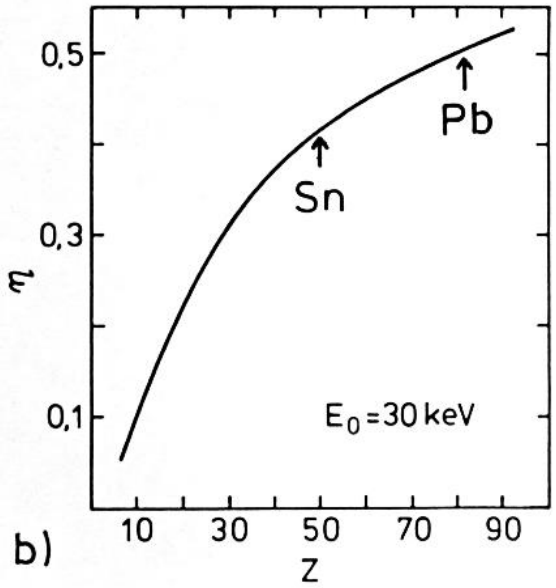

in P. Schmidt, *Praxis der Rasterelektronenmikroskopie und Mikrobereichsanalyse A* (pp. 149)

Pure Chemical Contrast

Cleaved SiO_2/Ta_2O_5-multilayer (BSE: SiO_2 dark, Ta_2O_5 bright)

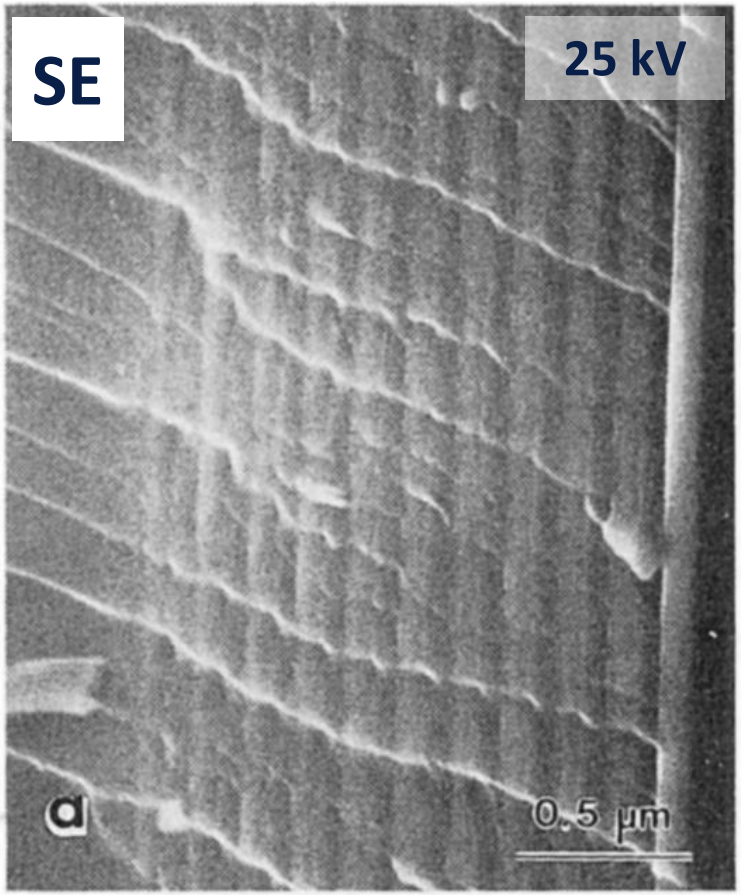

Material contrast +
surface topography contrast

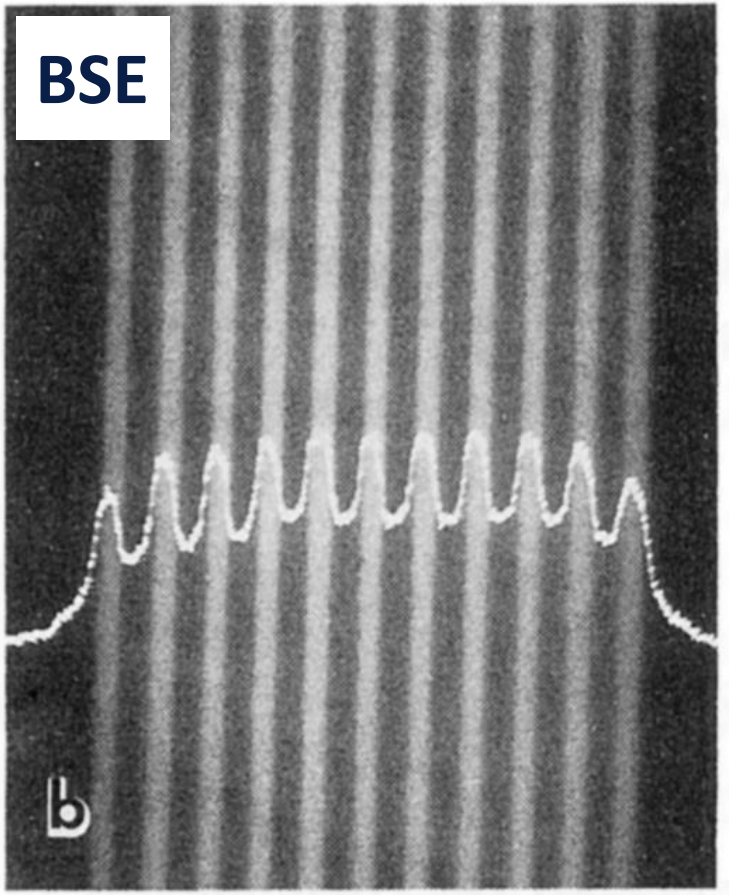

Pure material contrast

in Fuchs, Oppolzer, Rehme, *Particle Beam Microanalysis* (p. 110)

Quadrant BSE Detector

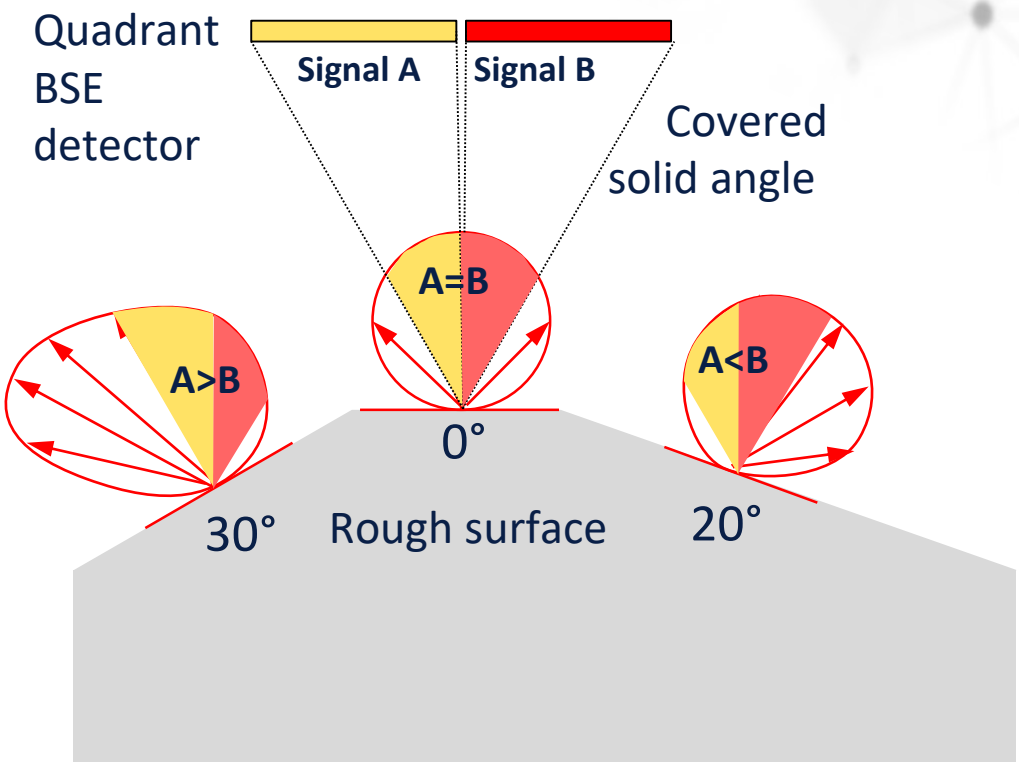

Chemical contrast
(annular BSE detector)

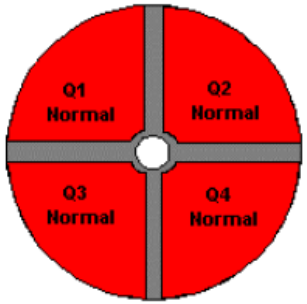

Topographic contrast
(Signal inversion of selected quadrants)

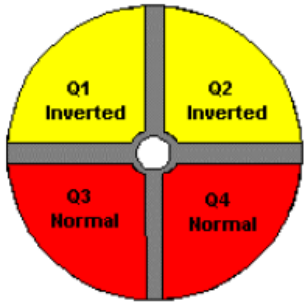

(e.g., **(Q3+Q4)-(Q1+Q2)**)

Quadrant BSE detector

<u>Normal mode</u>

Minimal topography contrast (as annular BSE detector)

<u>Topographic mode</u>

Signal inversion of part of the **quadrants (net signal for inclined surfaces)**

Gain of topographic contrast

in Zeiss, *Supra Handbuch* (2004)

Topographic vs. Chemical Contrast

Polished silver-soldered joint (Ag-rich: bright, Cu-rich: dark)

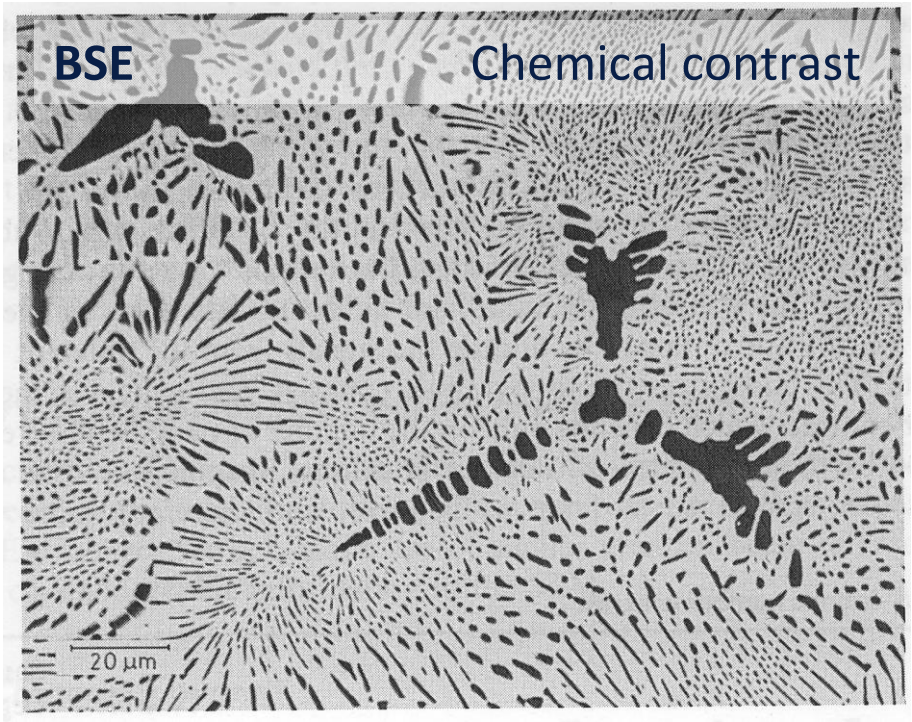

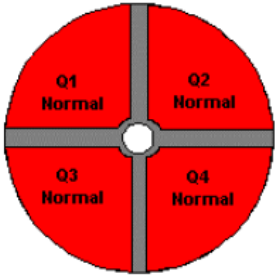

Goodhew, Humphreys, Beanland, *Electron Microscopy and Analysis*, S.147

Topographic vs. Chemical Contrast

Polished silver-soldered joint (Ag-rich: bright, Cu-rich: dark)

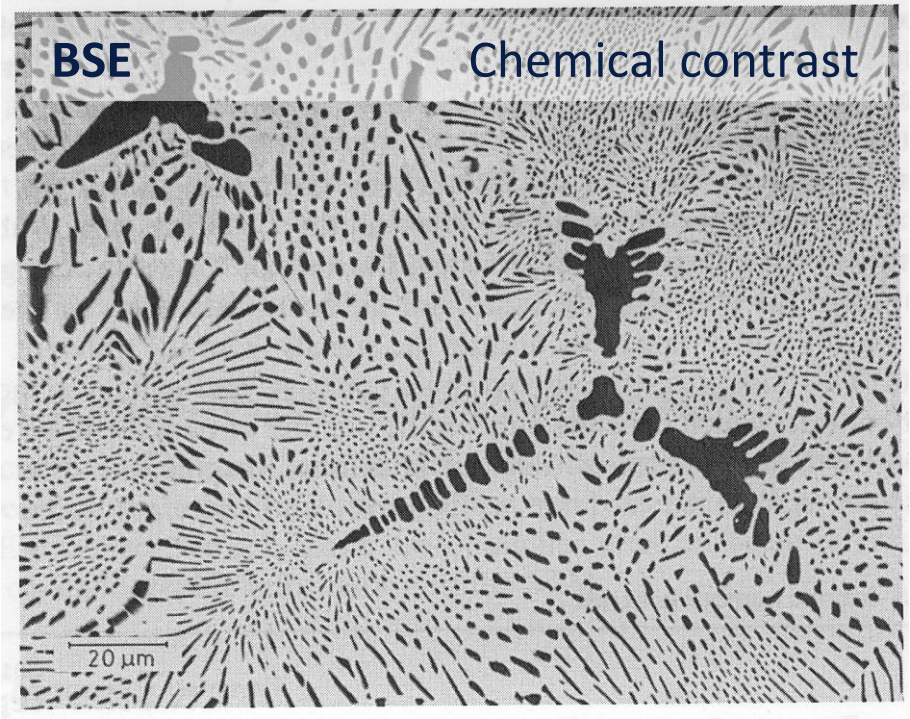

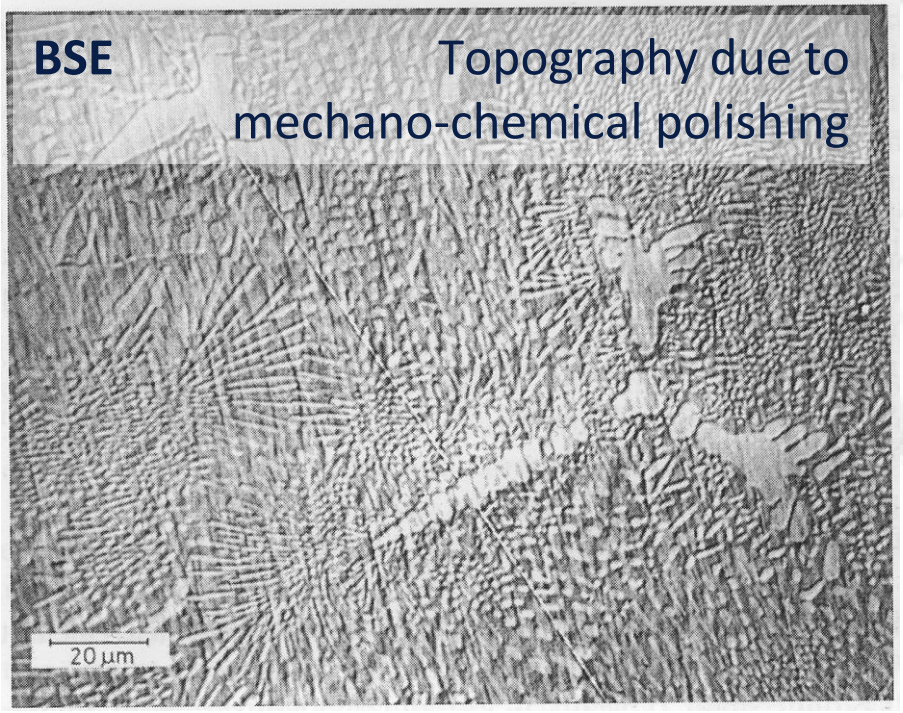

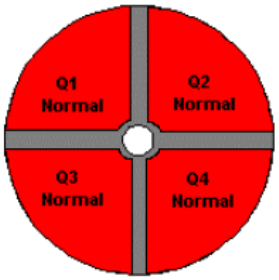

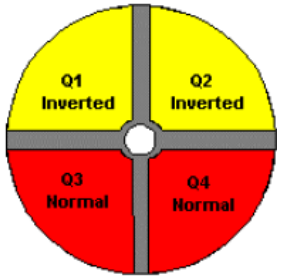

Goodhew, Humphreys, Beanland, *Electron Microscopy and Analysis*, S.147

BSE Imaging – Resolution

The resolution in BSE imaging is limited by the **escape area of BSE electrons (~R)**

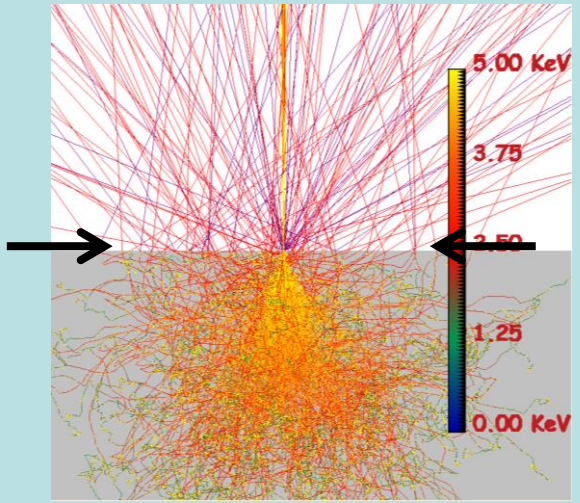

Particular structures can be imaged with a better resolution when their

topographic or material contrast significantly exceeds

the background signal of BSE from the whole interaction volume.*

(e.g., high-Z regions in/on low-Z matrix, polycrystalline material: change in crystallographic orientation)

- **The lower E_0 the smaller is the escape area!**
- **The higher the local variations in Z the better is the resolution**

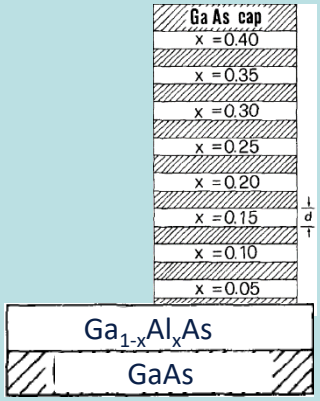

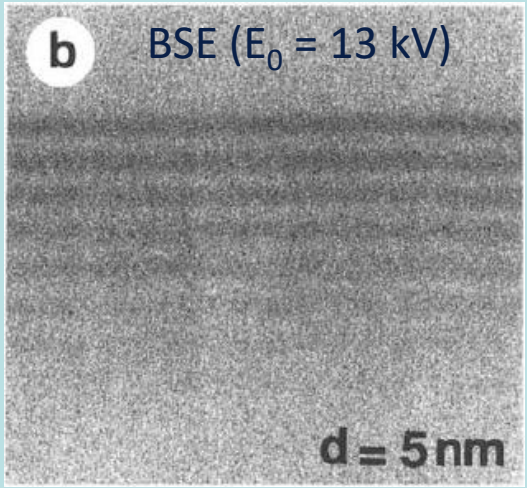

Merli, Nacucci, Ultramicroscopy 50 (1993), pp. 83

* L. Reimer, *Scanning Electron Microscopy* (p. 144)

Lessons learned

SE imaging

- **Excellent resolution (beam diameter)**
- **Topography contrast:**
  inclined surfaces are brighter
- **Edges appear brighter!**
- Changing the ETD grid voltage, one can **switch between topography contrast** (SE) **and chemical contrast** (BSE)

BSE imaging

- **Resolution ↔ Size of interaction volume**
- **Topographic diminishes up to medium inclinations**
  Even “rough” surfaces exclusively show chemical contrast
- Excellent chemical resolution of better than 1% Z-difference

*Detectors II (ZEISS)

In-lens SE detector
(**SE**)

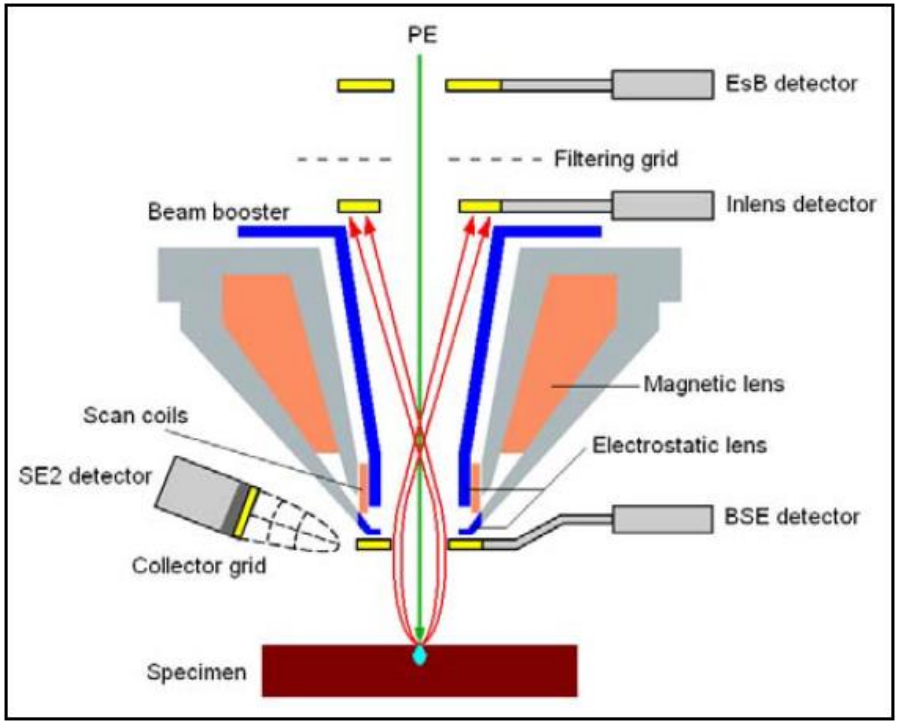

In-lens EsB detector
(**E**nergy-**S**elective **B**SE detector) (**BSE**)

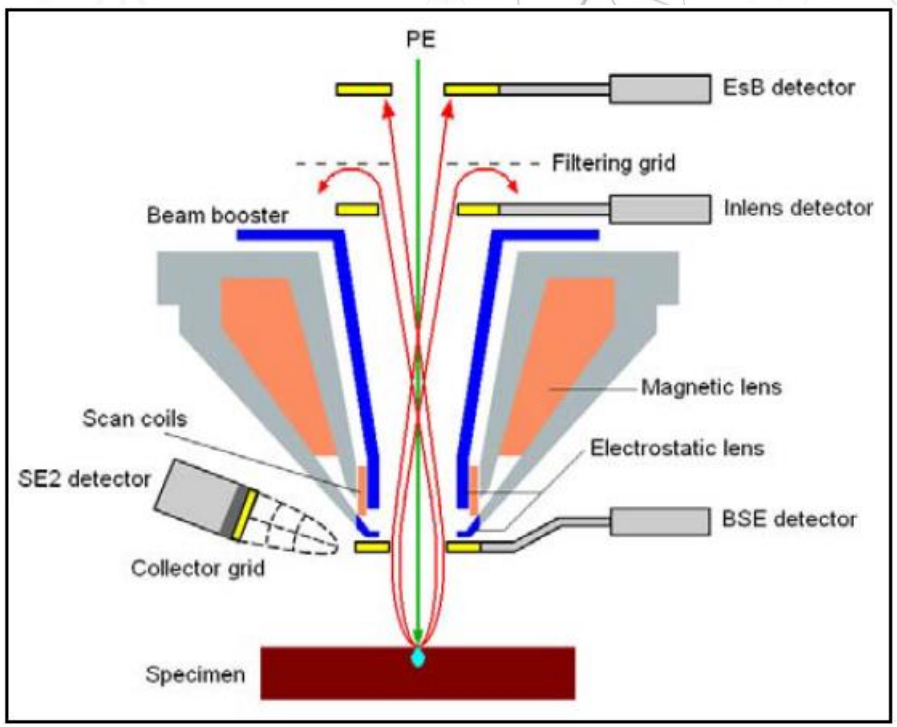

$E_0 \leq 20$ kV ➡ **Beam Booster**:

- +8 kV in electron column
- deceleration of PE by electrostatic potential of objective lens

in Zeiss, *Supra Handbuch* (2004)

*Zeiss GEMINI® Column

- **Beam booster ($E_0 \leq 20$ kV)**

+ Magnetic/electrostatic objective

- **+8 kV** in electron column (U_B)
- Deceleration of PE by electrostatic potential of objective lens

Minimized influence of stray radiation on PE even at low E_0 → **High resolution**

+

High efficiency of In-lens SE detector due to attraction of SE

- U_{ex} Extraction voltage
- U_{pe} Primary beam voltage
- U_B Booster voltage
- U_F EsB filtering grid voltage

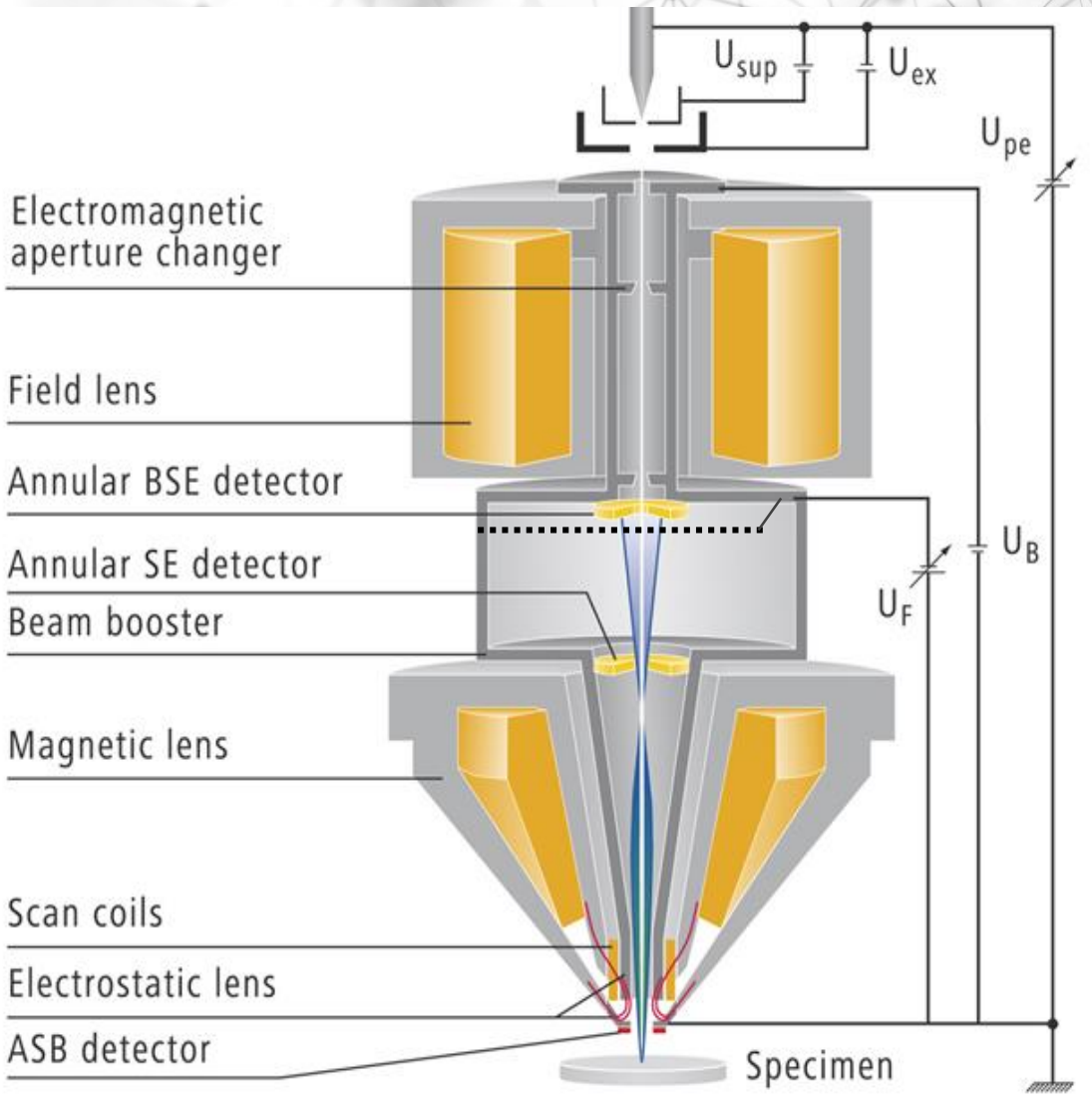

*Magnetic / Electrostatic Objective

Beam booster ➡ far-reaching electrostatic potential of objective lens
(decelerating impact on PE, **SE accelerated towards column**)

High efficiency of In-lens SE detector due to collection of SE

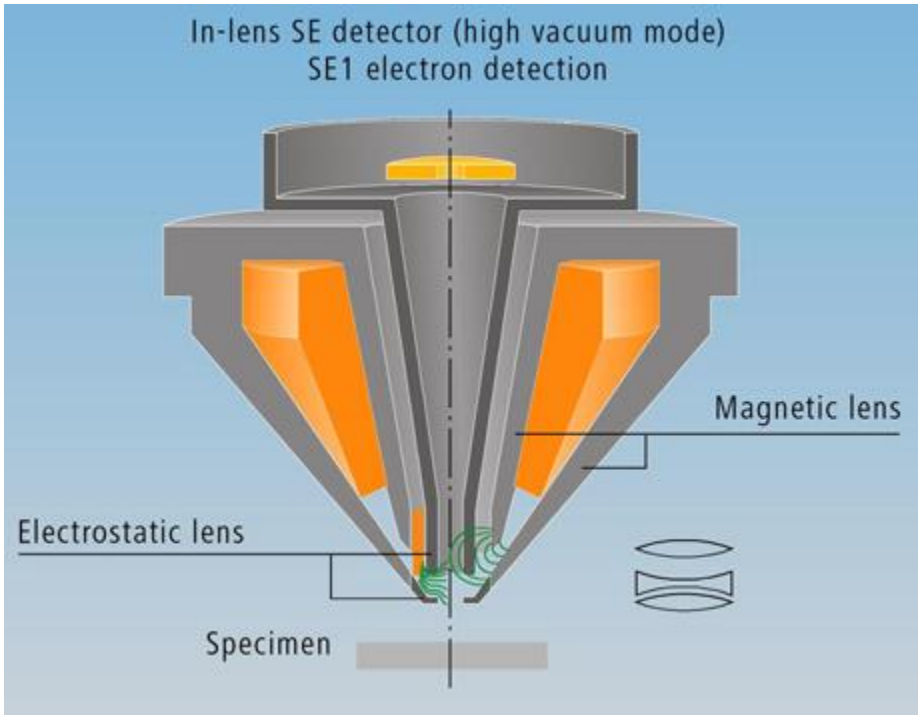

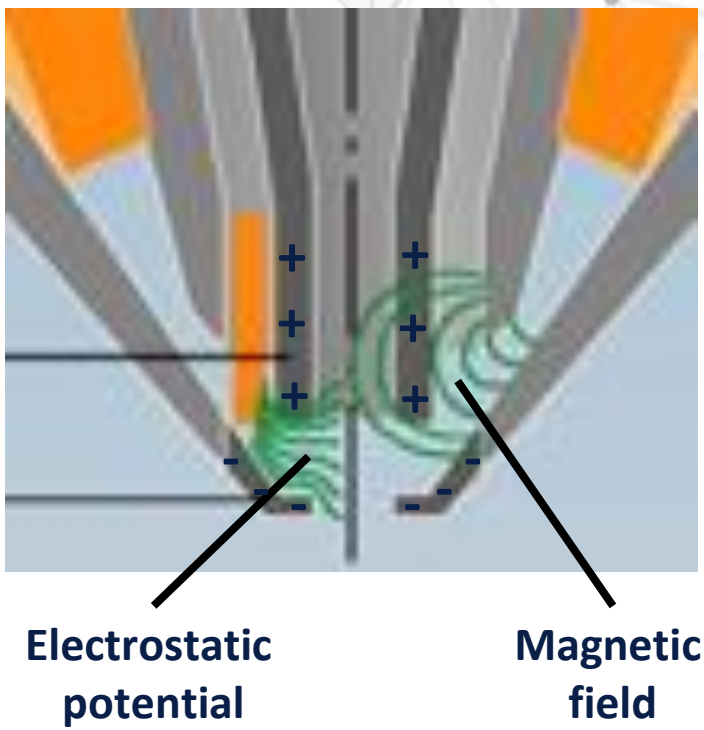

*Separation of BSE/SE

Energetic difference

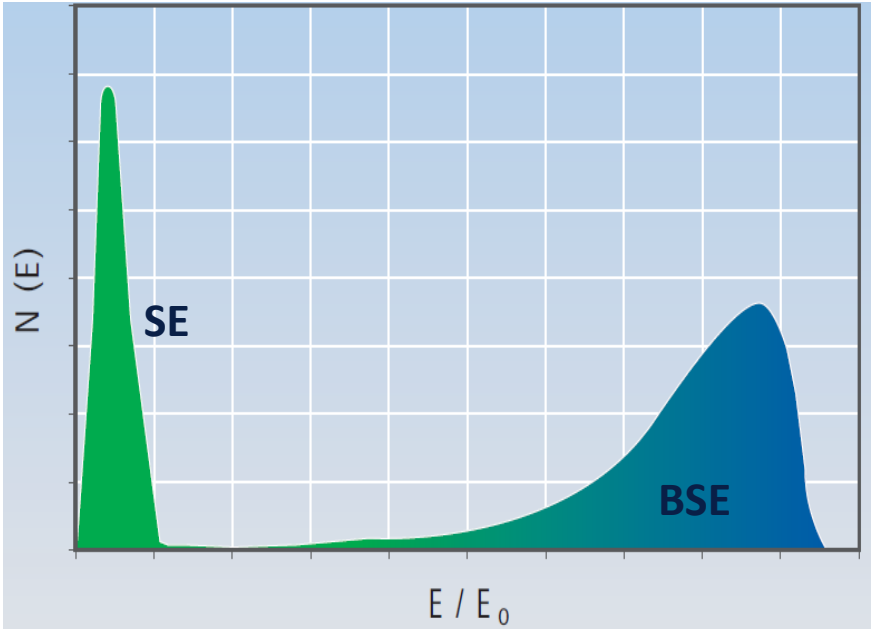

Annular separation

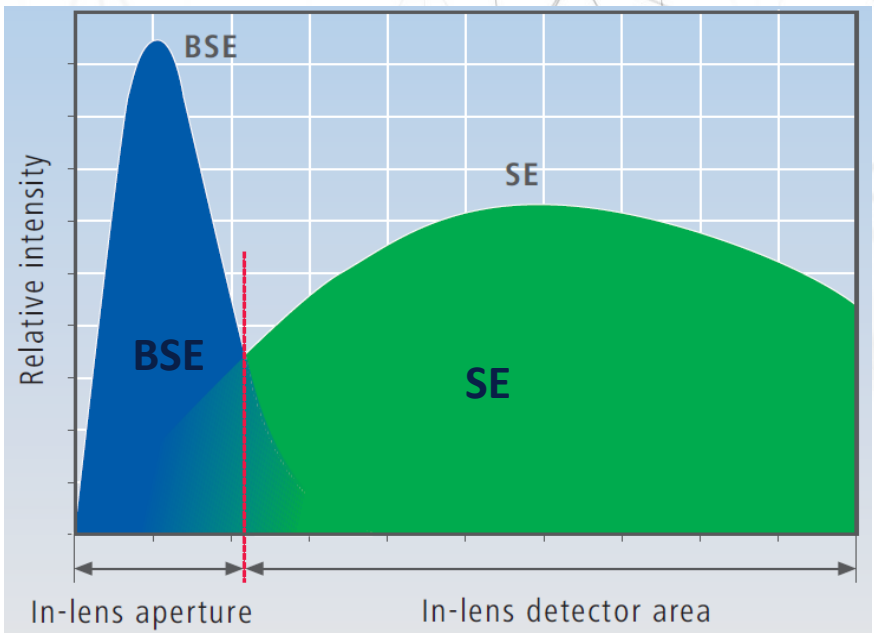

Focussing impact on SE is higher than on BSE

Stronger deflection of SE in electron column

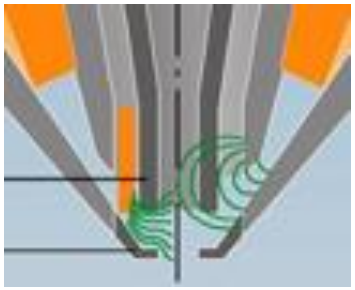

*Separation of BSE/SE

BSE

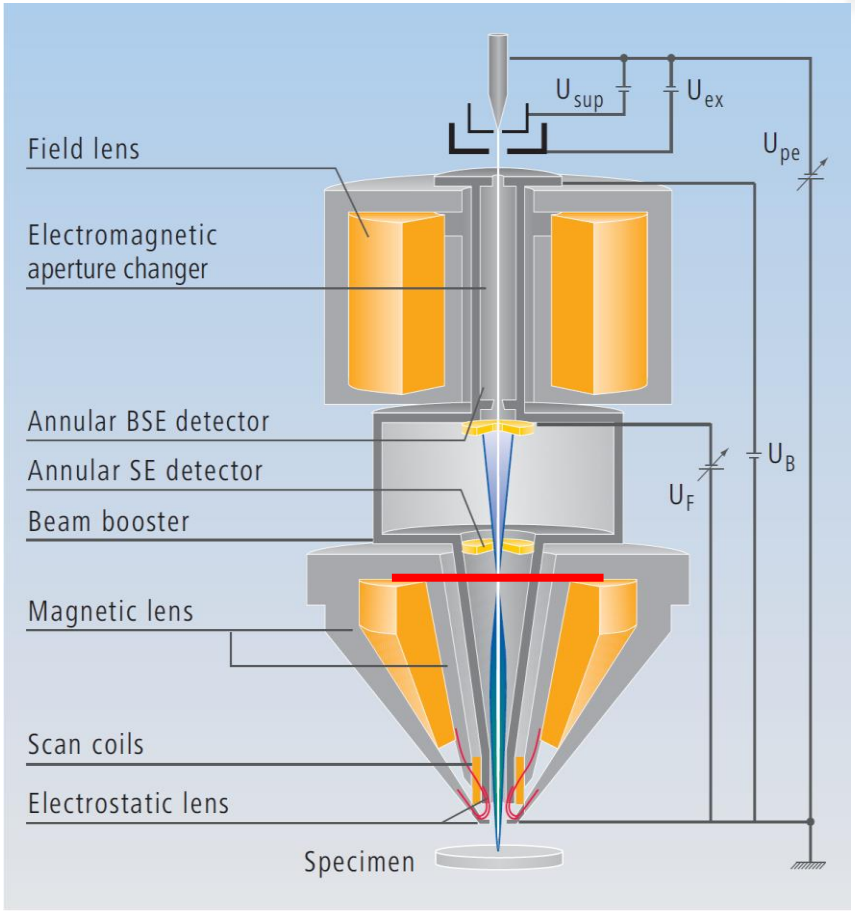

SE

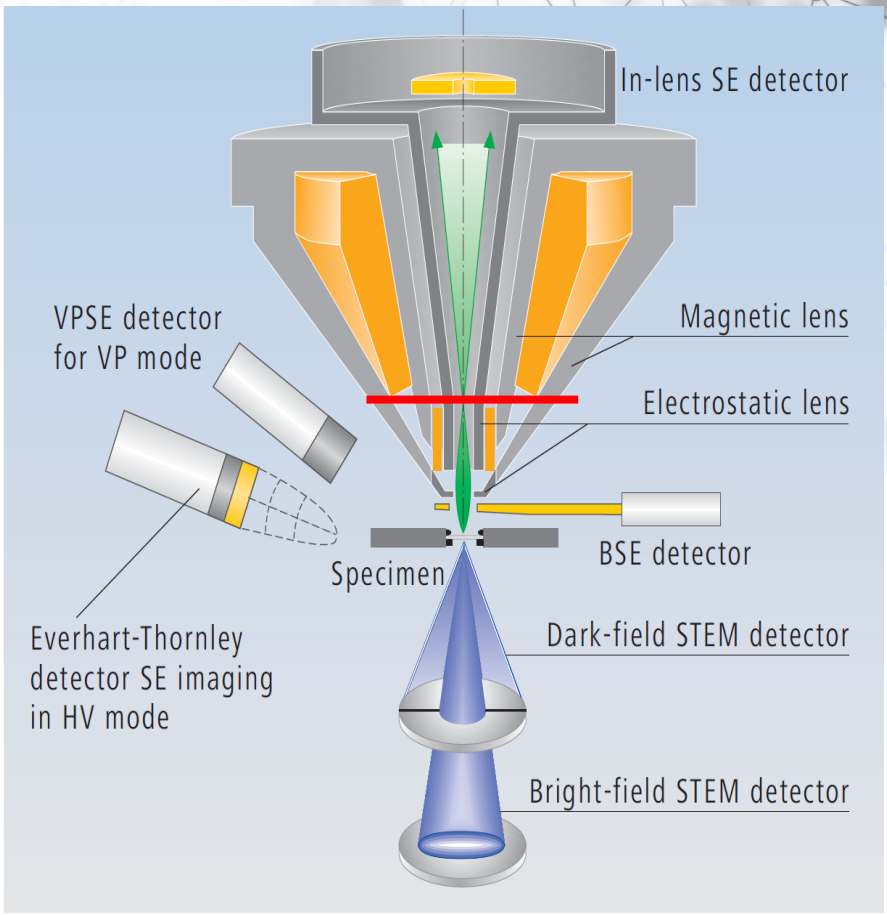

Lower cross-over of SE in column → Angular separation of BSE and SE

*In-lens SE vs. EsB Detector

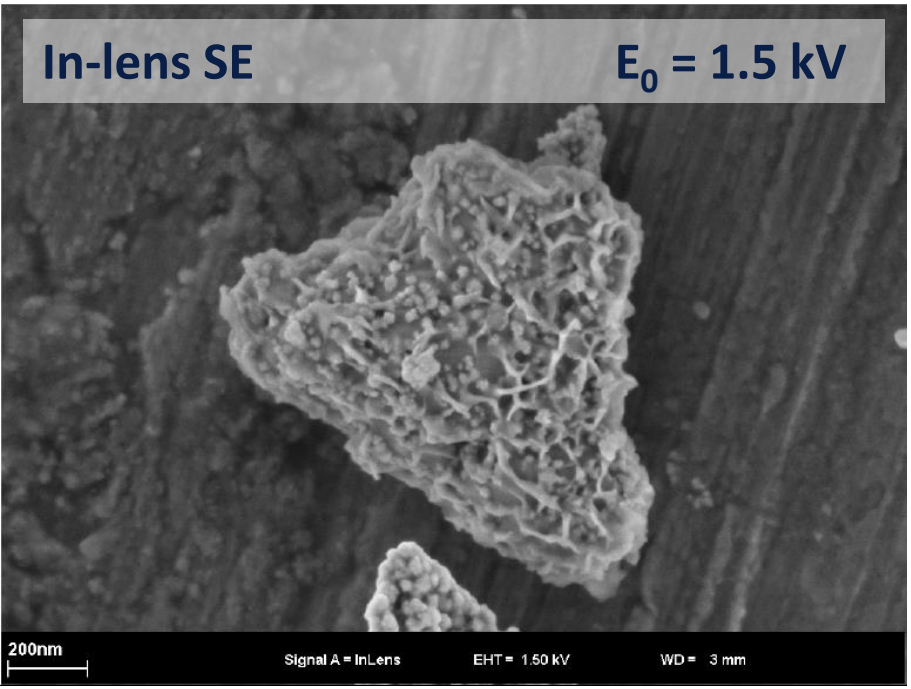

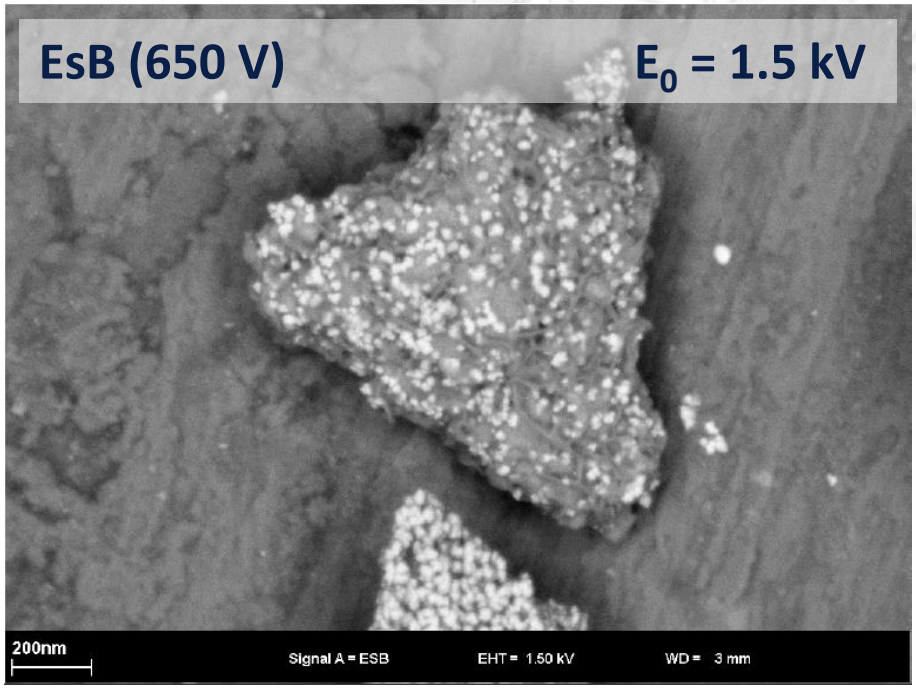

in Zeiss, *Supra Handbuch* (2004)

*In-lens SE vs. EsB Detector

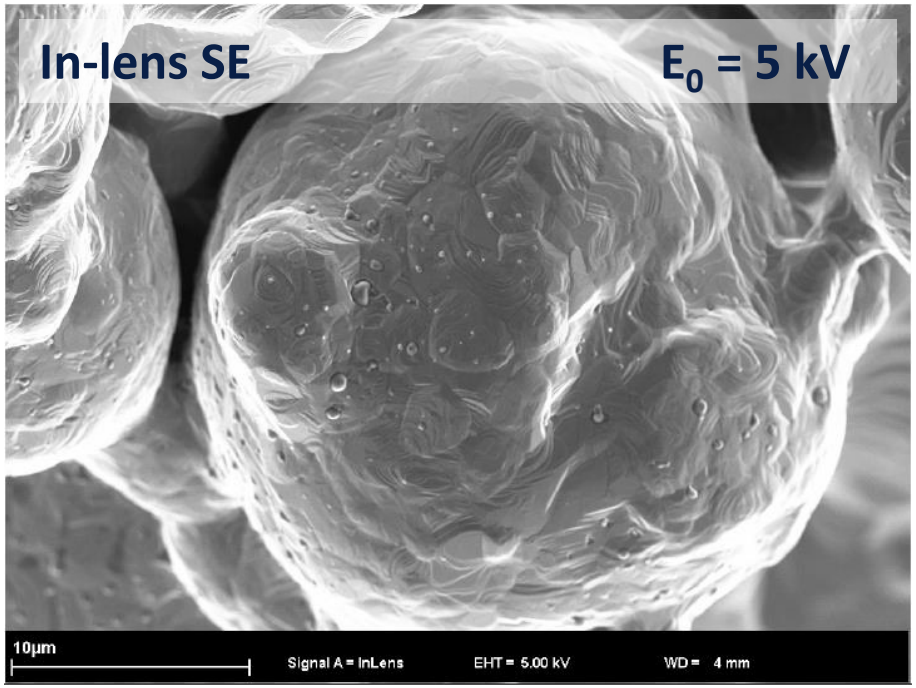

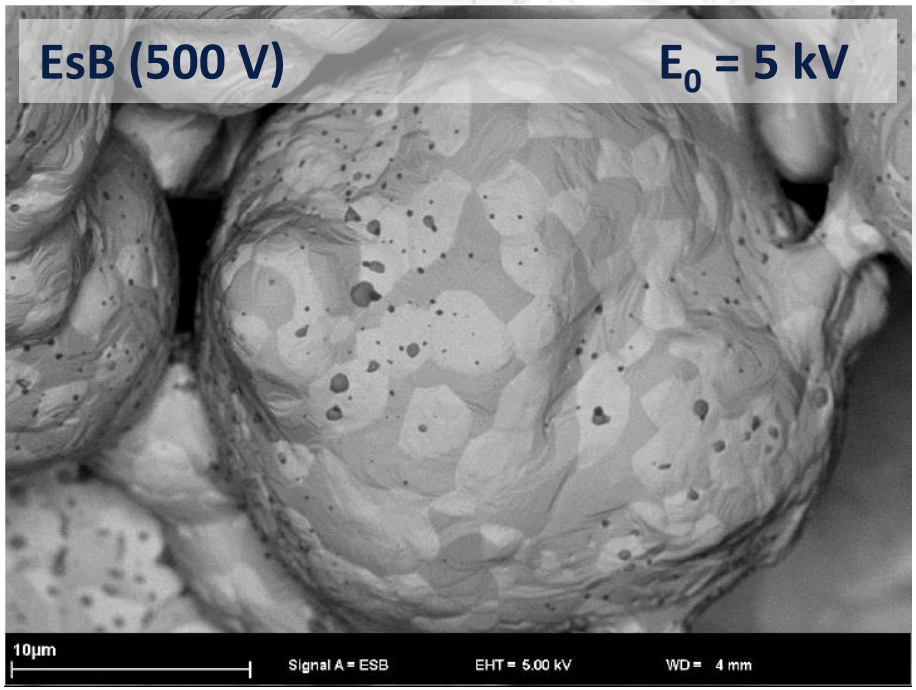

in Zeiss, *Supra Handbuch* (2004)

*EsB Detector: Grid Potential

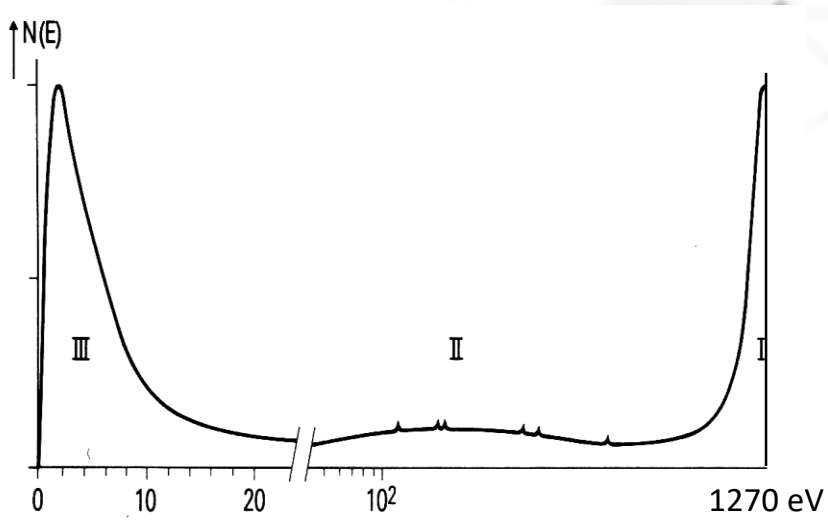

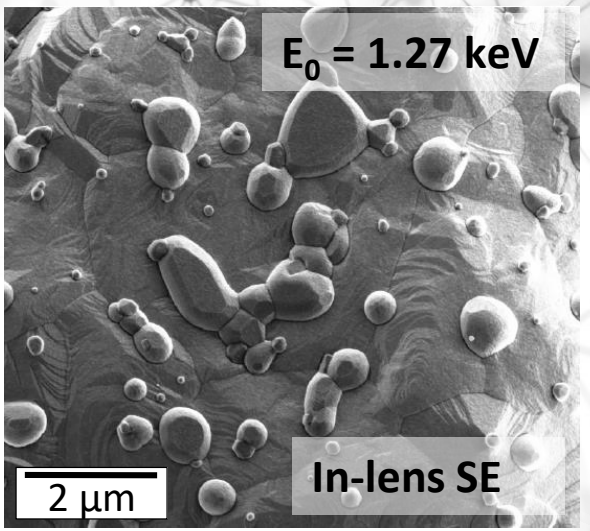

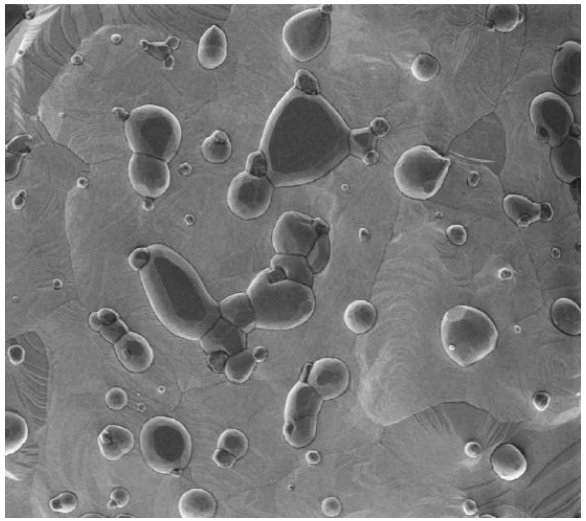

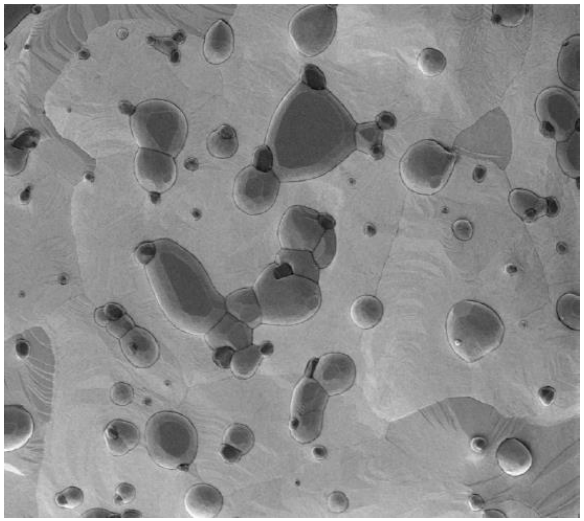

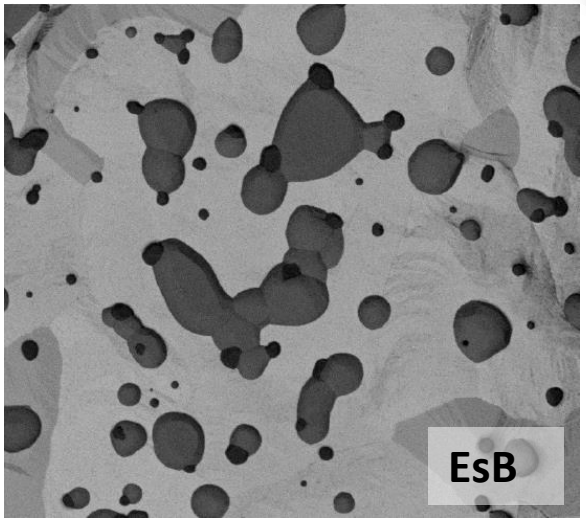

Grid potential	-0 V	-100 V	-1177 V
Max. energy loss		1.17 keV	100 eV

in Zeiss, *Supra Handbuch* (2004)

*EsB Detector: Grid Potential

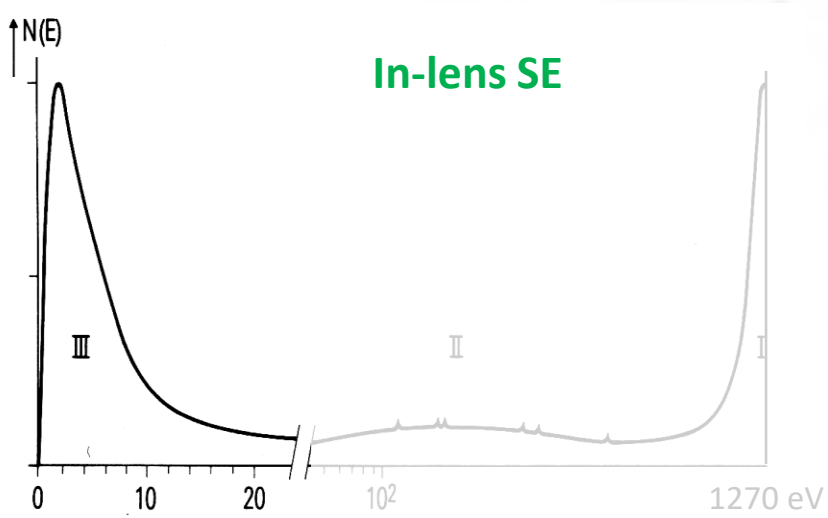

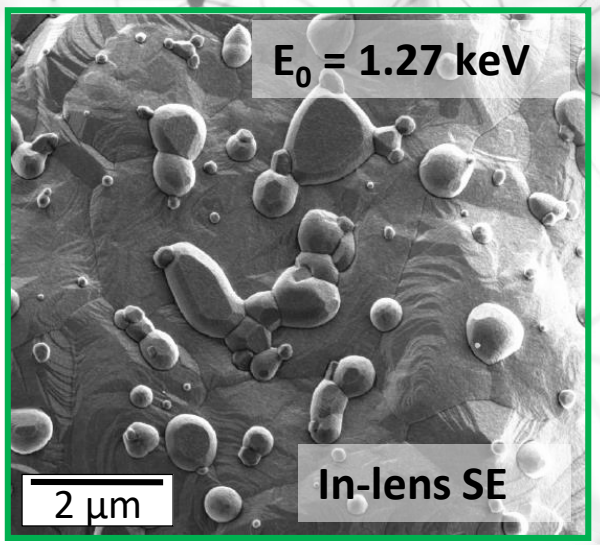

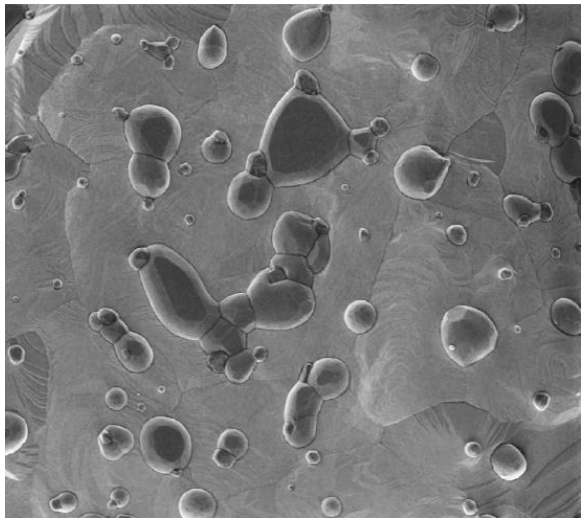

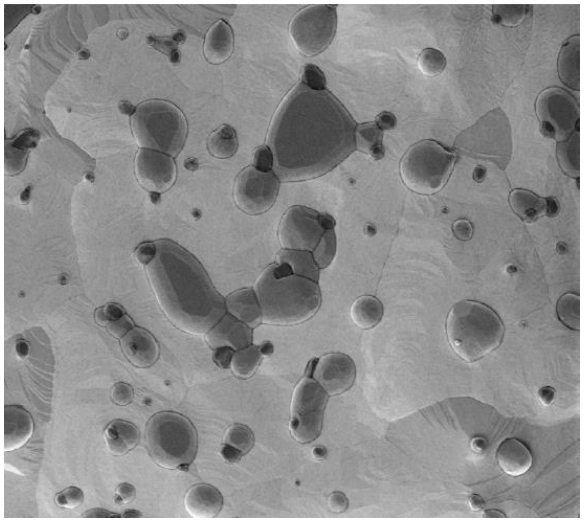

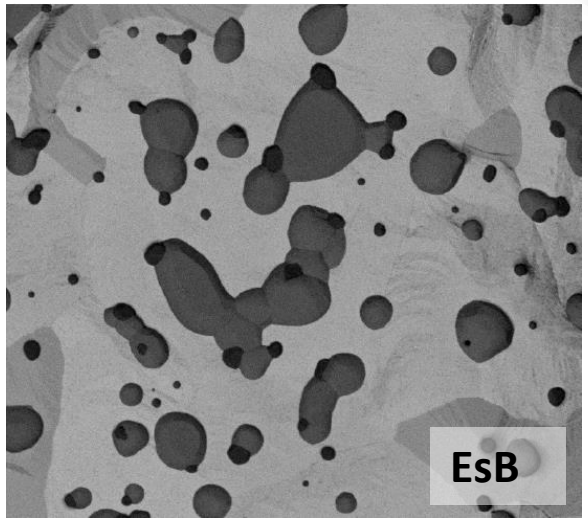

Grid potential **-0 V** **-100 V** **-1177 V**

Max. energy loss **1.17 keV** **100 eV**

in Zeiss, *Supra Handbuch* (2004)

*EsB Detector: Grid Potential

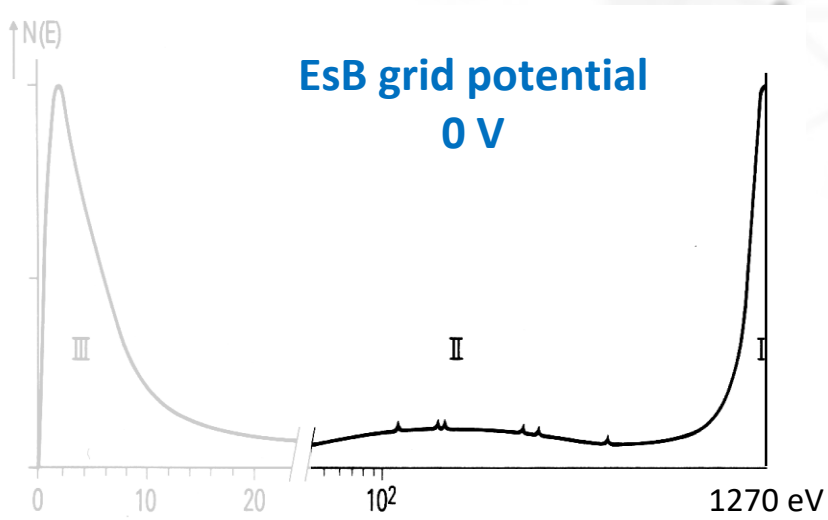

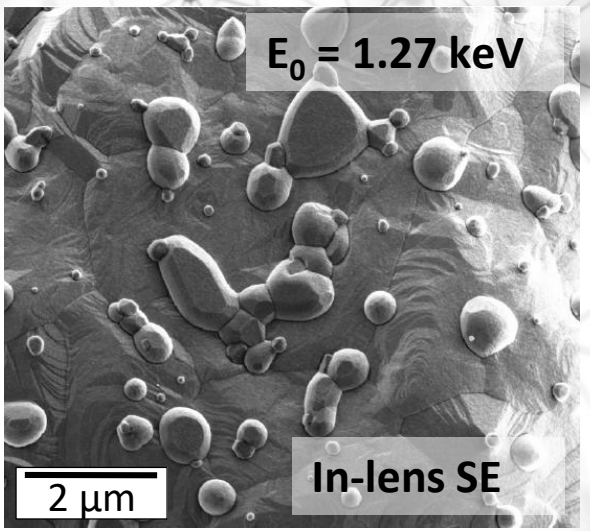

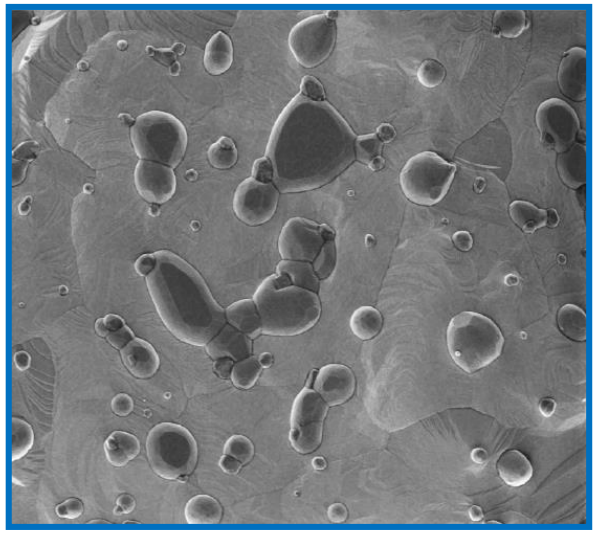

Grid potential -0 V

Max. energy loss

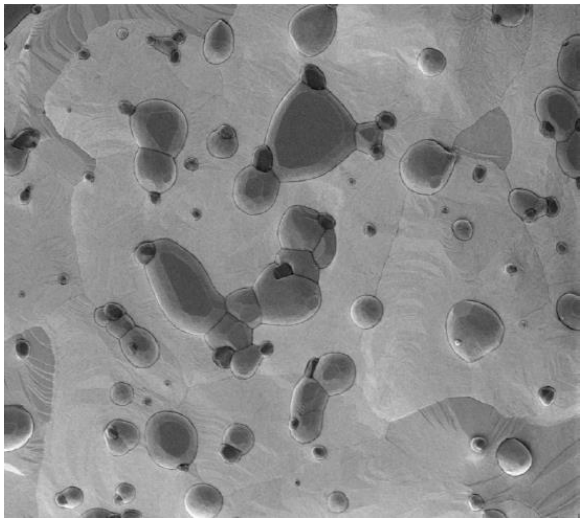

-100 V

1.17 keV

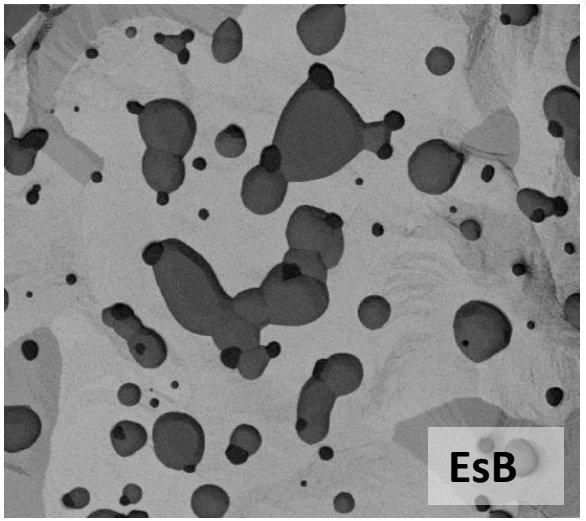

-1177 V

100 eV

in Zeiss, *Supra Handbuch* (2004)

*EsB Detector: Grid Potential

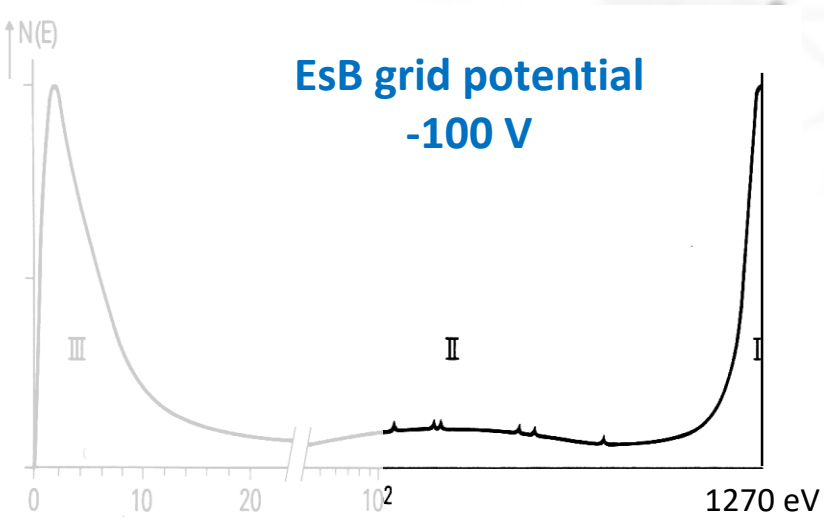

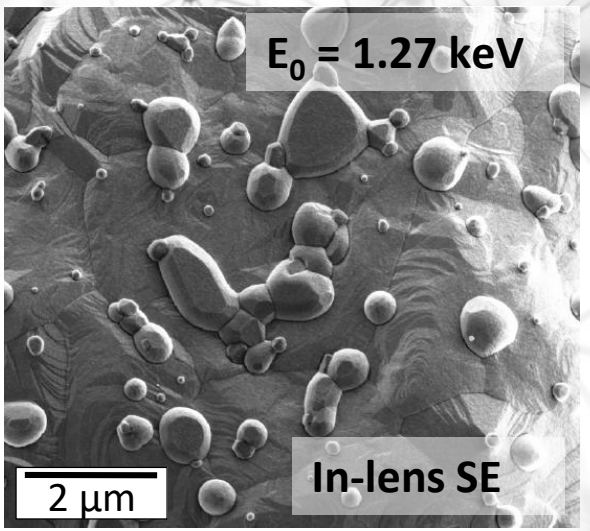

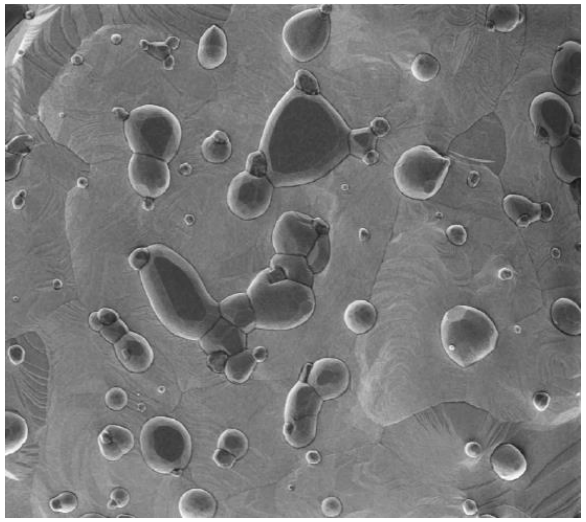

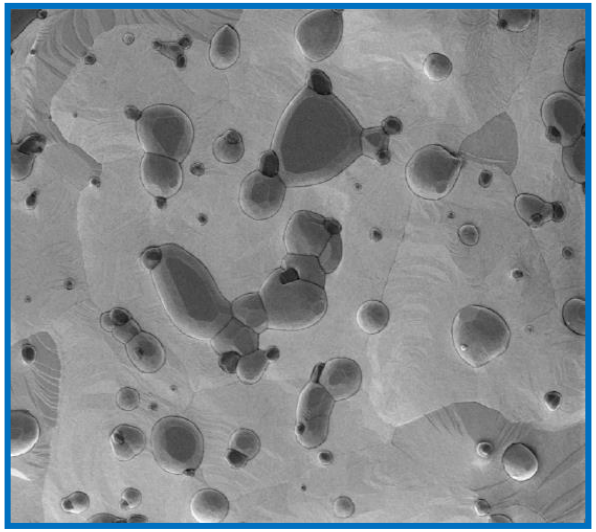

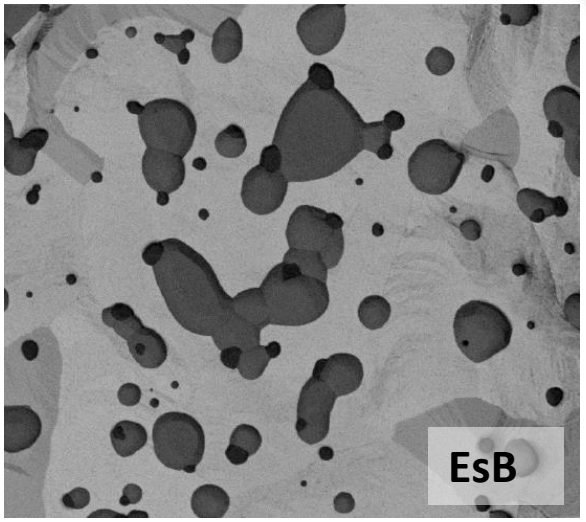

Grid potential **-0 V** **-100 V** **-1177 V**

Max. energy loss **1.17 keV** **100 eV**

in Zeiss, *Supra Handbuch* (2004)

*EsB Detector: Grid Potential

EsB grid potential
-1177 V

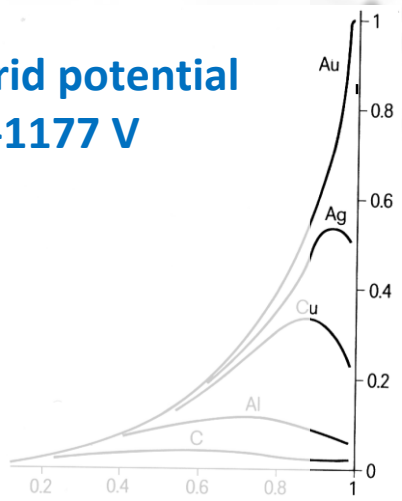

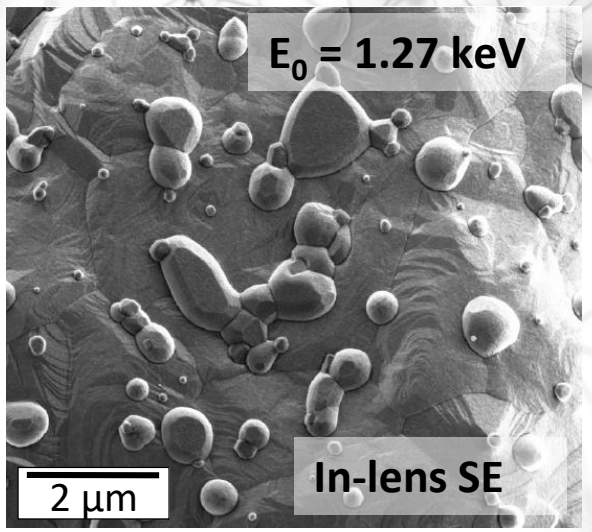

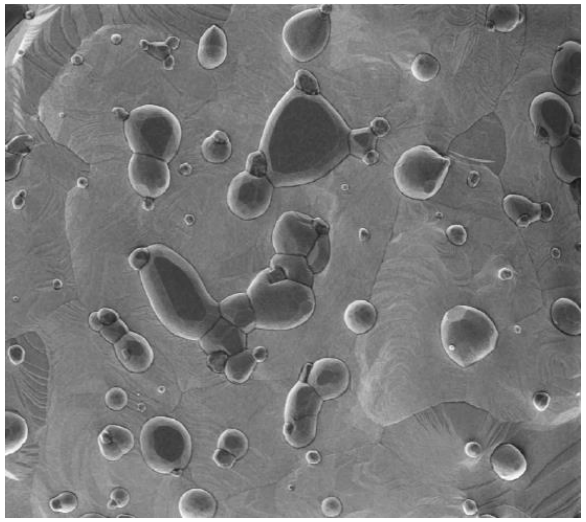

Grid potential **-0 V**
Max. energy loss

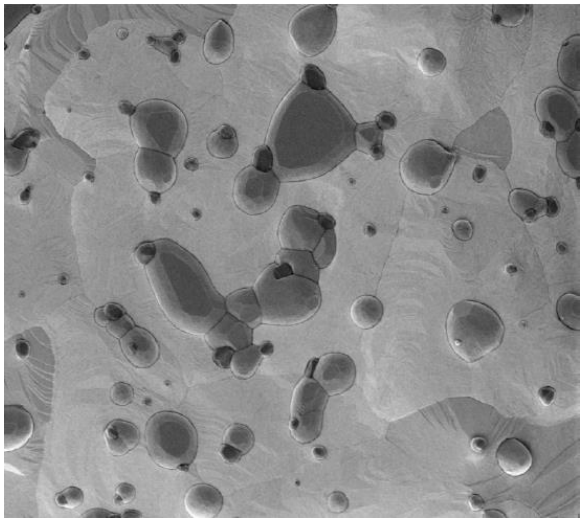

-100 V
1.17 keV

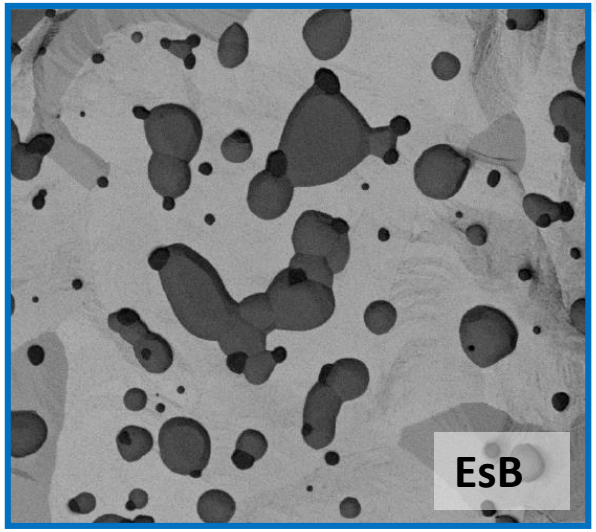

-1177 V
100 eV

in Zeiss, *Supra Handbuch* (2004)

*EsB Detector: Grid Potential

High grid potential with respect to E_0
(low-loss BSE imaging (ll-BSE))

Enhanced chemical contrast, minimized topographic contributions

Better resolution due to less interactions

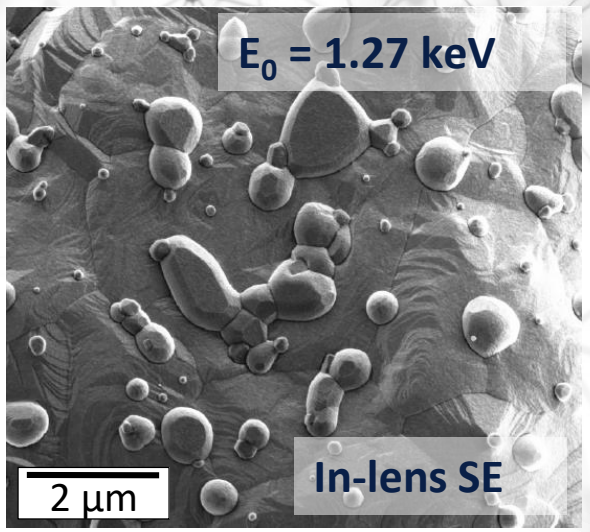

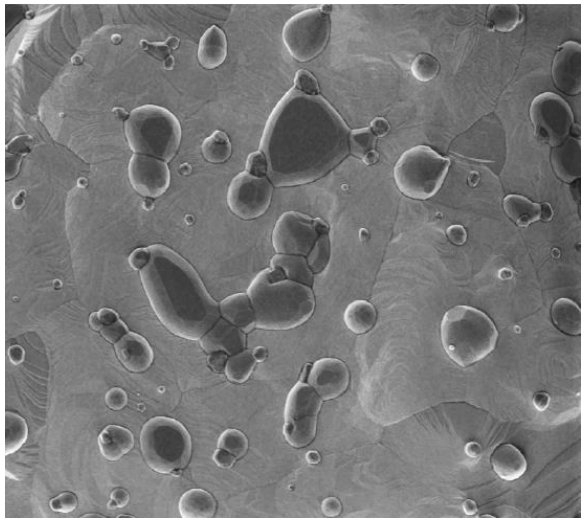

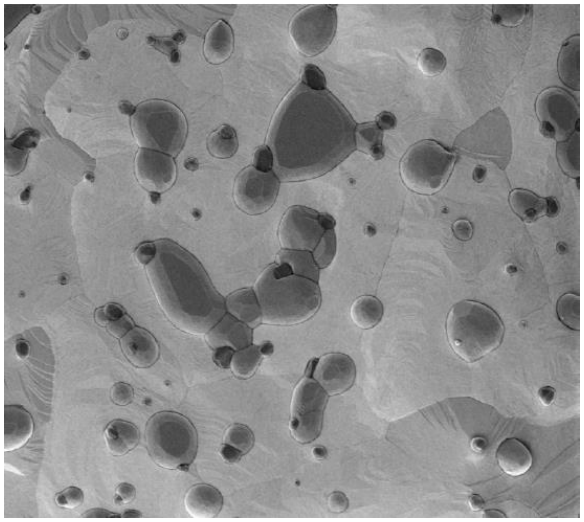

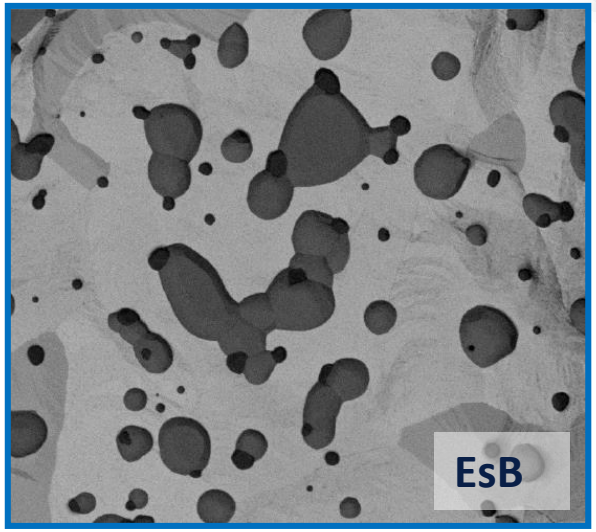

Grid potential **-0 V** **-100 V** **-1177 V**

Max. energy loss **1.17 keV** **100 eV**

in Zeiss, *Supra Handbuch* (2004)

*EsB Detector: Grid Potential

Rock containing silicated, oxides, mica, feldspars (+rare elements)

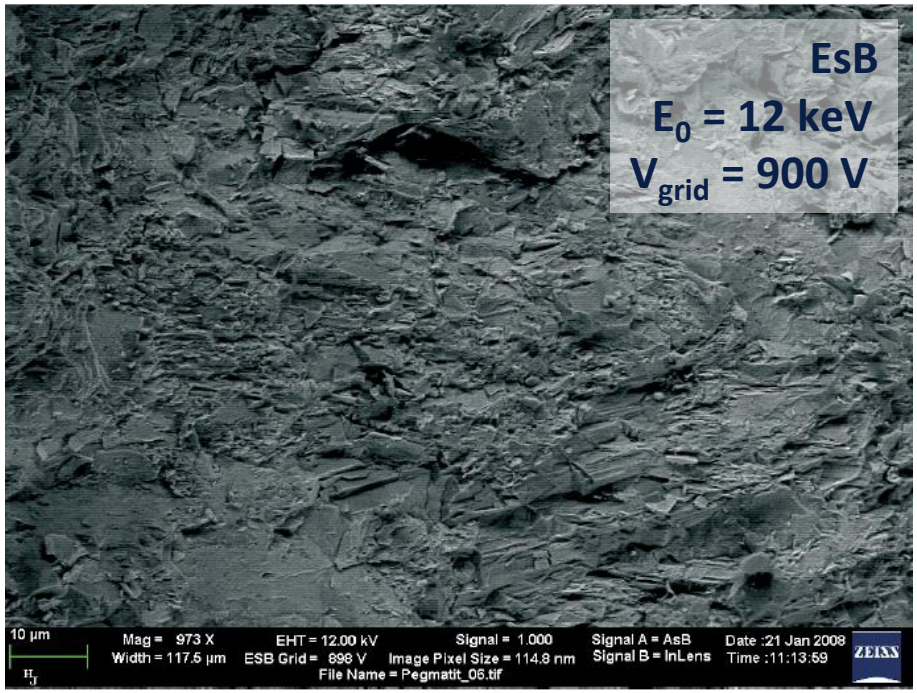

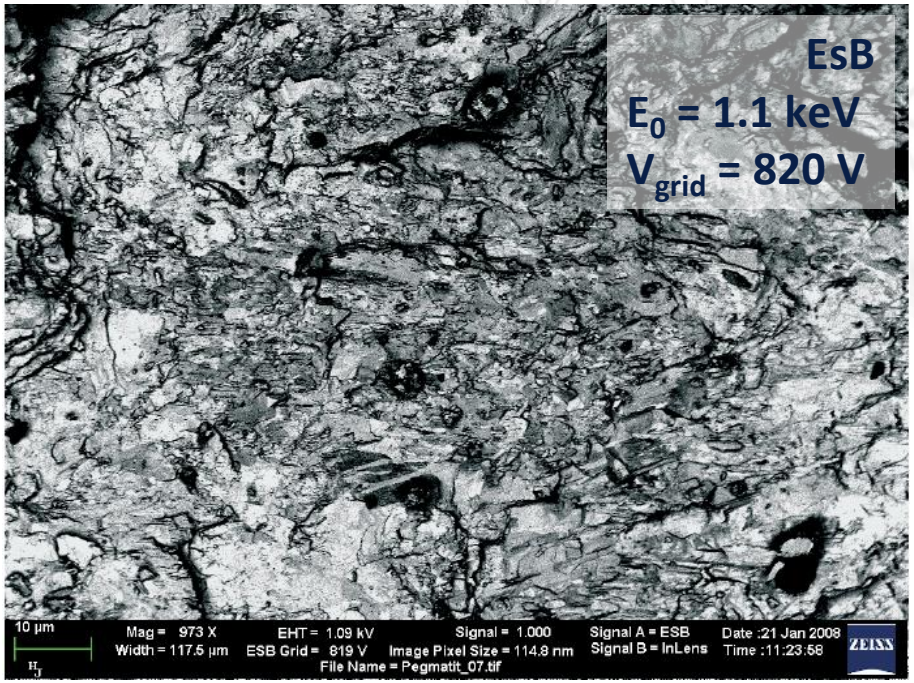

II-BSE: Low E_0 ⟺ smaller interaction volume ⟺ Reduced chemical averaging

STEM

Scanning transmission electron microscopy (STEM)

- Detection of **transmitted electrons**
- **Sample thickness < 100nm** @30 kV (e.g., TEM samples)
- **STEM detector** with various sectors
  - bright-field (**BF**),
  - annular dark-field (**ADF**)
  - high-angle annular DF (**HAADF**)

Parameter to adjust covered solid angles: camera length

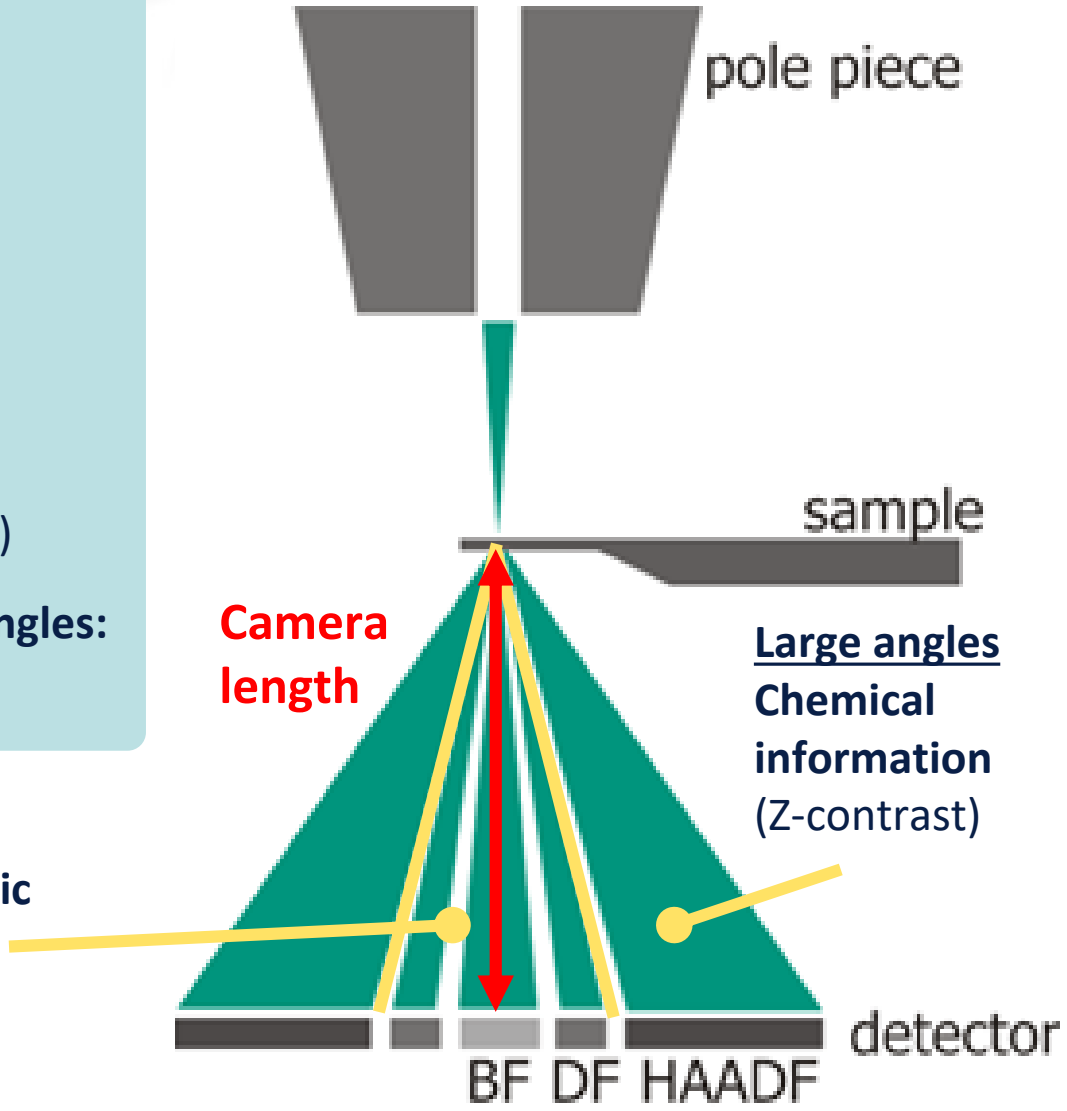

http://www.cfn.kit.edu/1004.php

FEI STEM Detector

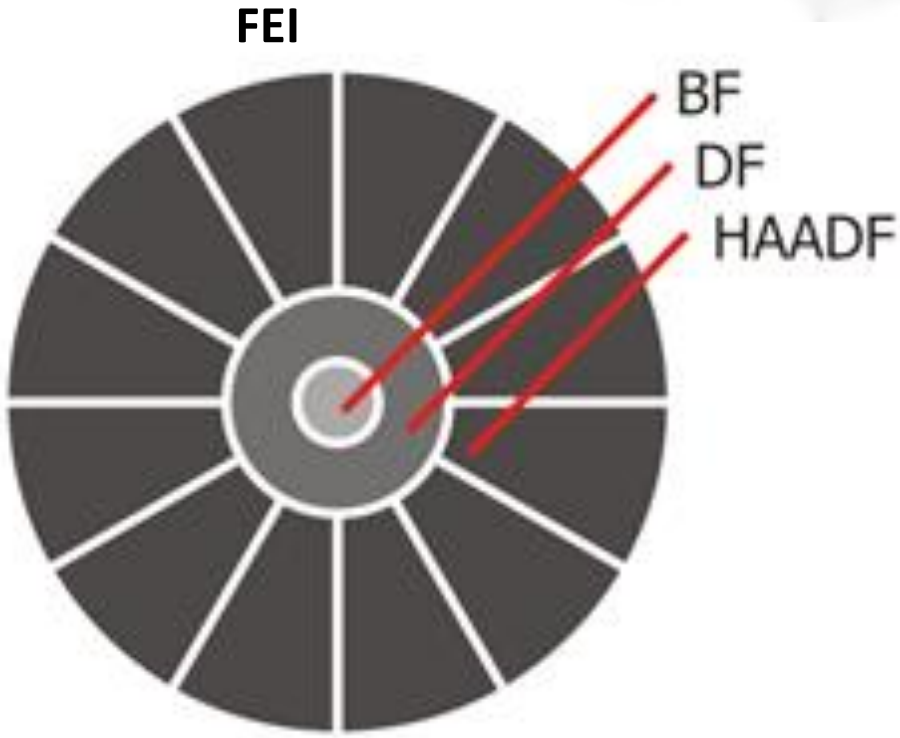

BF, DF: mass-thickness, Bragg/orientation contrast
HAADF: chemical contrast

Various opportunities to combine sectors, e.g. crystallographic (orientation) analysis — **texture analysis**

FEI Helios User's Guide

STEM Sample Holder

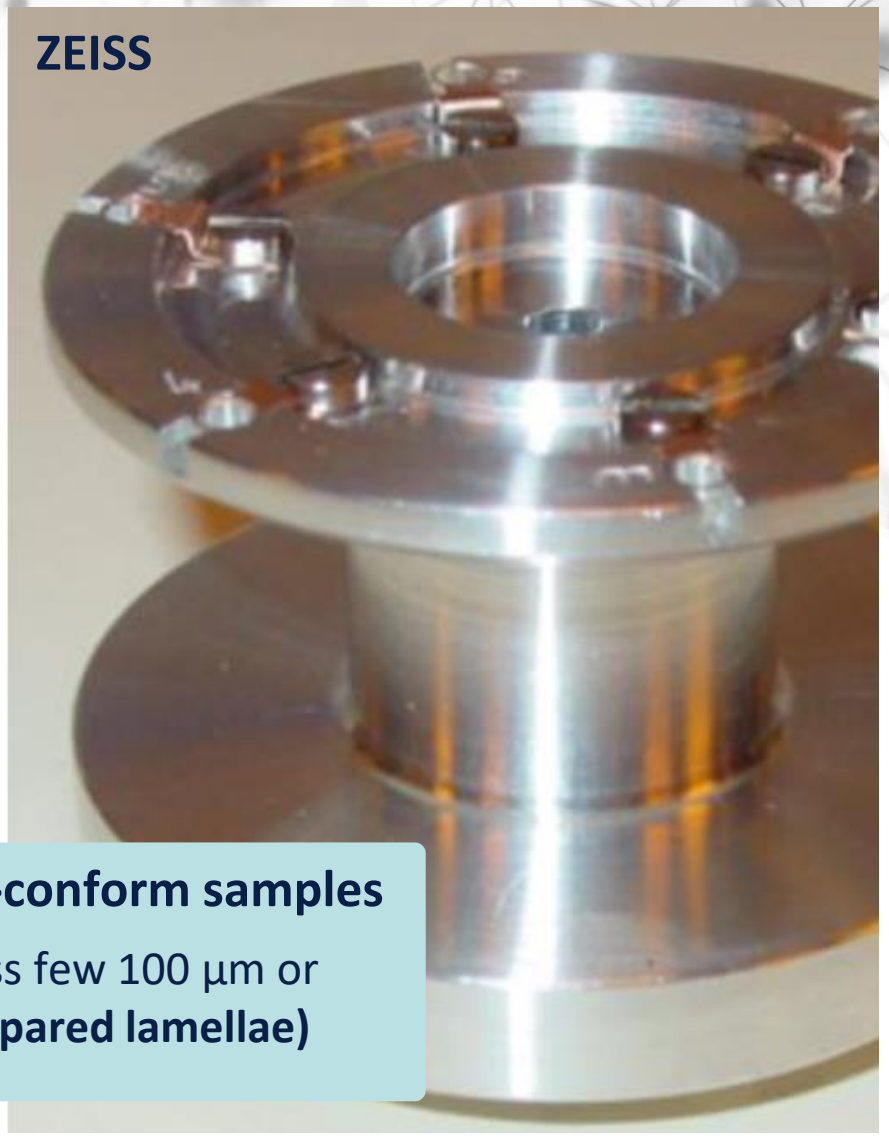

Special holder for **TEM-conform samples**

- **Disk**: Ø 3 mm * thickness few 100 µm or
- **TEM-/FIB-grids (FIB-prepared lamellae)**

FEI Helios User‘s Guide

http://www.utdallas.edu/~rar011300/SEM/Scanning%20Electron%20Microscope%20Operation.pdf

IV: Bulk vs. Thin Sample

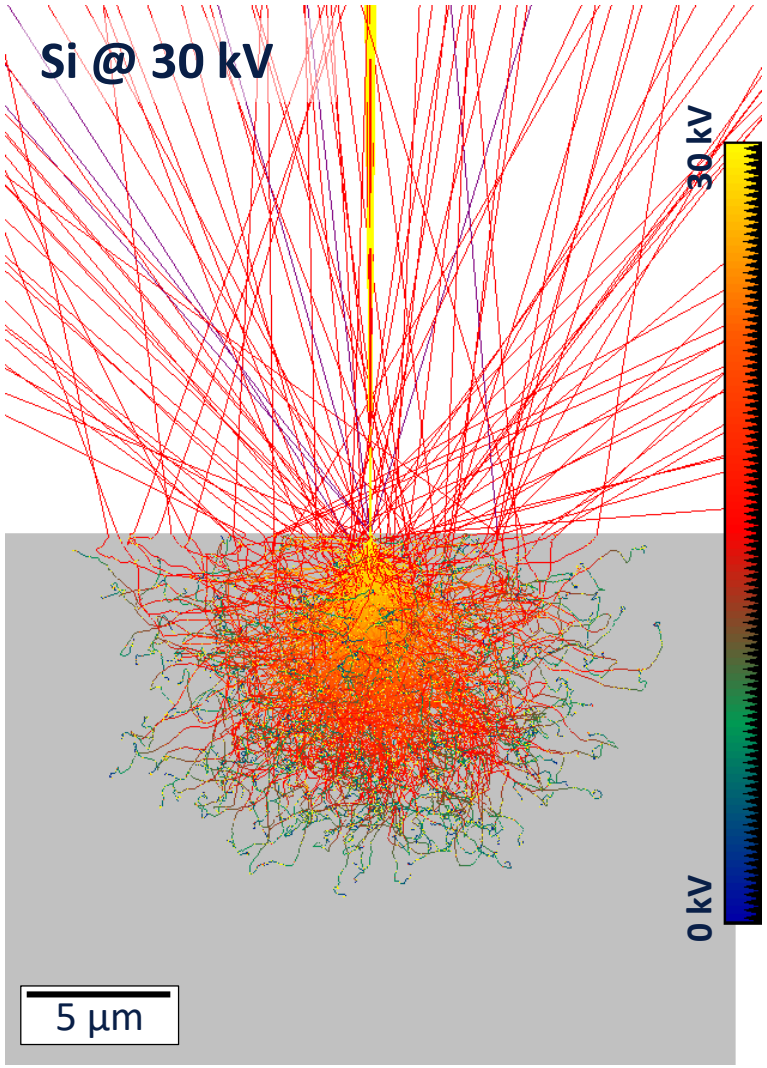

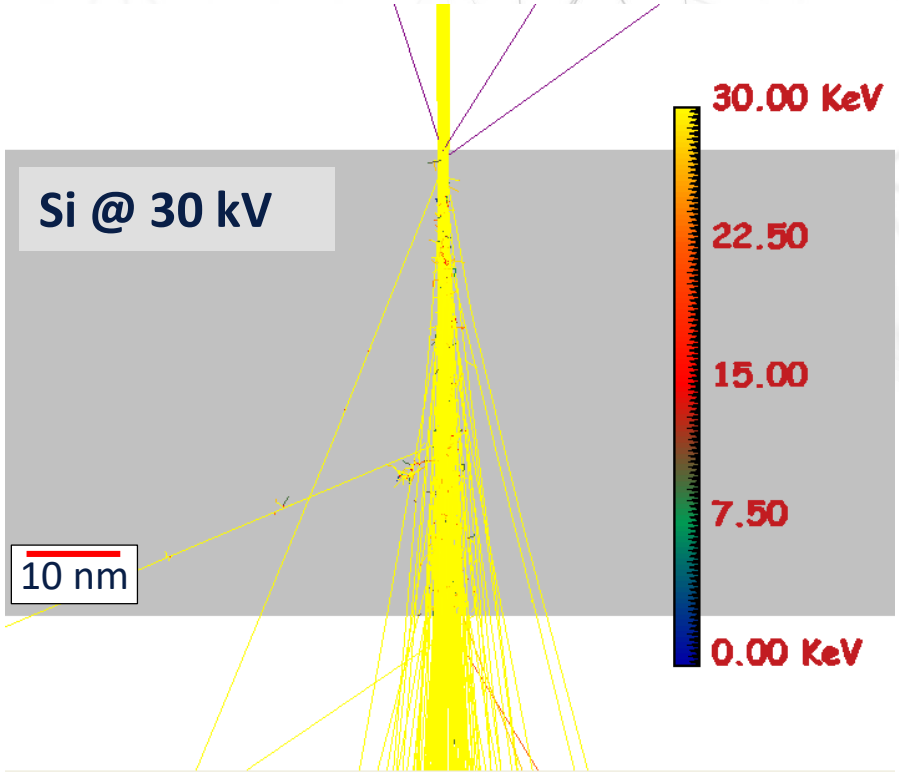

IV: Z-dependency

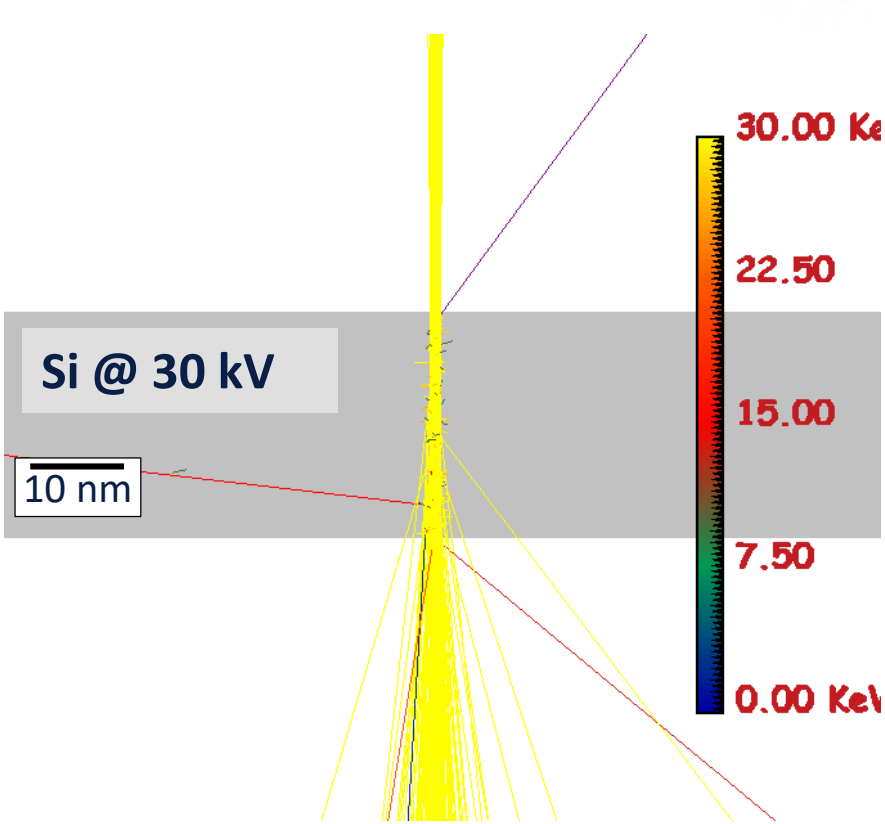

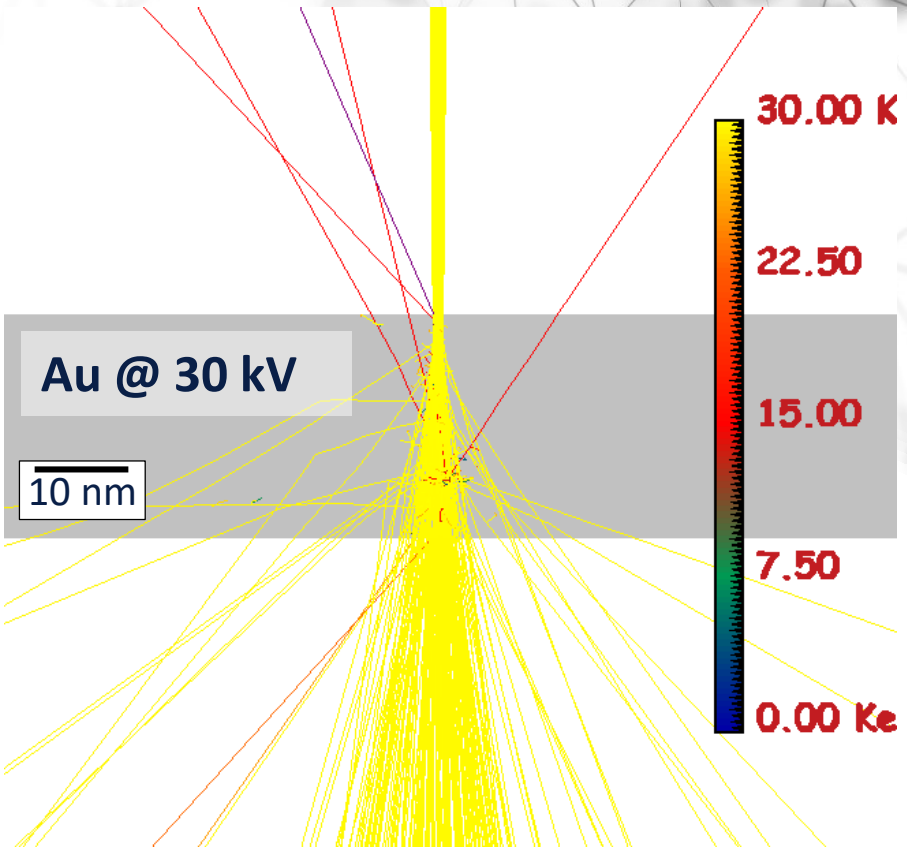

Strongly limited beam broadening

High resolution (~1nm) in imaging and analytics!

CIGS Solar Cell — **STEM in SEM** vs. TEM

Characterization TEM lamellae in FIB-SEM by STEM

Microstructural, (structural), chemical analysis of TEM-samples /FIB lamellae on the nm scale!

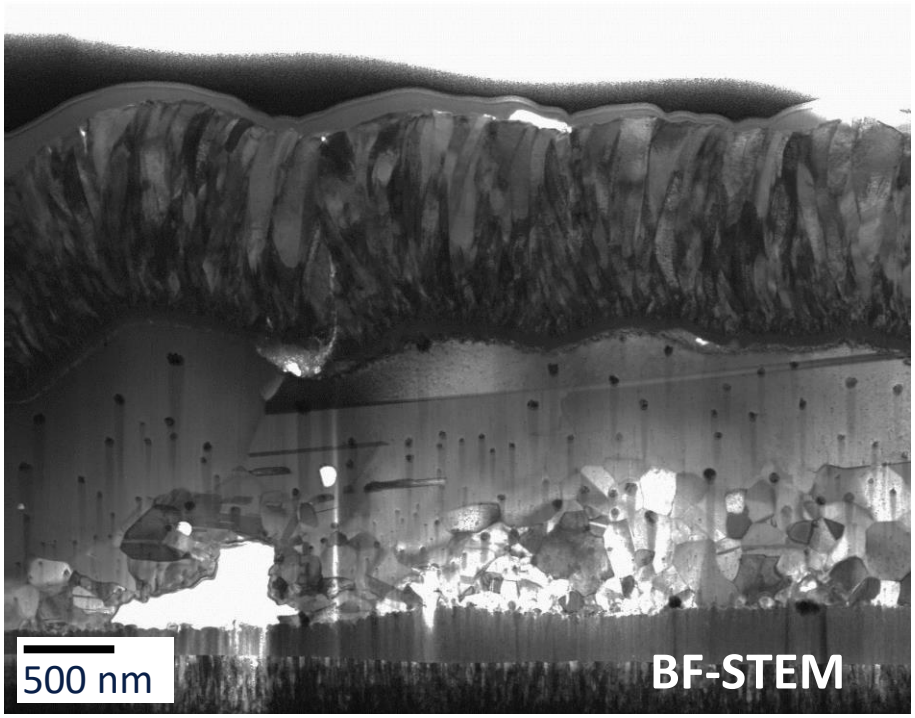

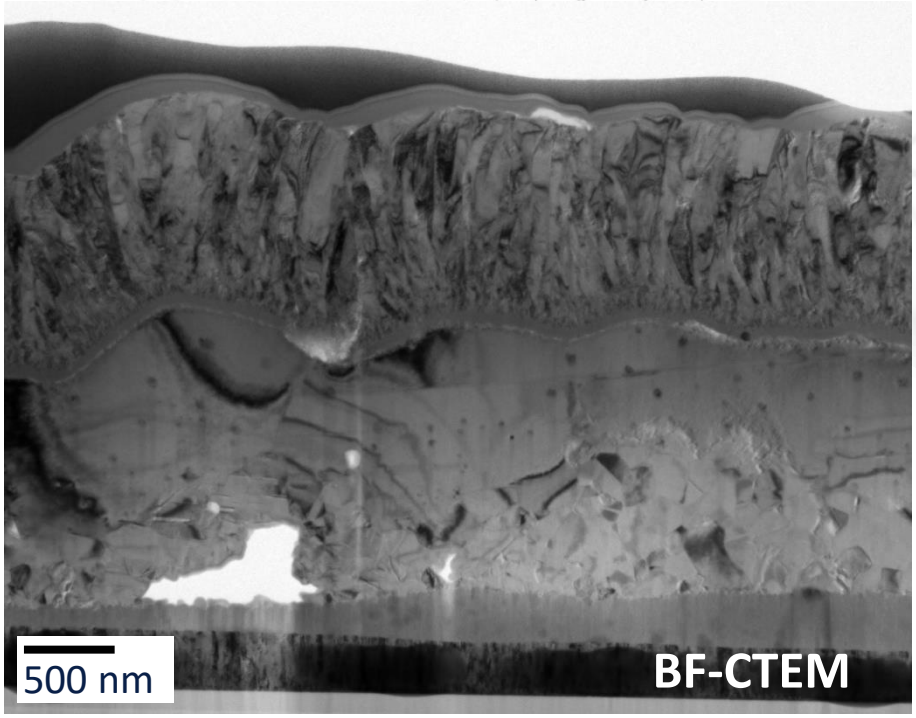

BF-STEM image (Helios @**30 kV**)

- Unscattered electrons
- Serial image formation (BF-STEM detector)

Bright-field TEM image (Titan @**200 kV**)

- Selection of undeflected electrons propagating on optical axis
- Parallel image formation (CCD camera)

FIB demo, FEI company

CIGS Solar Cell — **STEM in SEM** vs. STEM in TEM

Characterization TEM lamellae in FIB-SEM by STEM

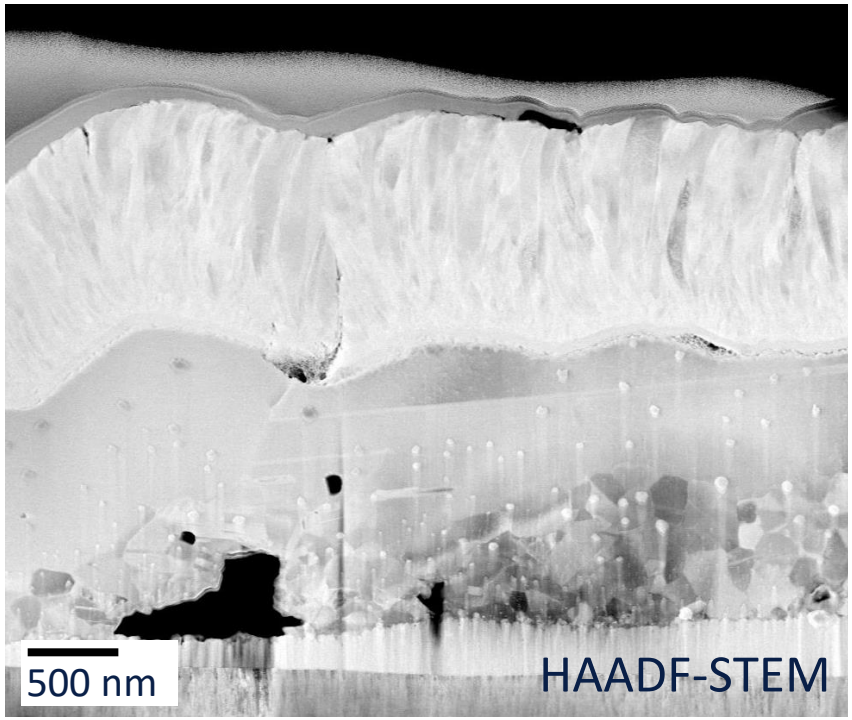

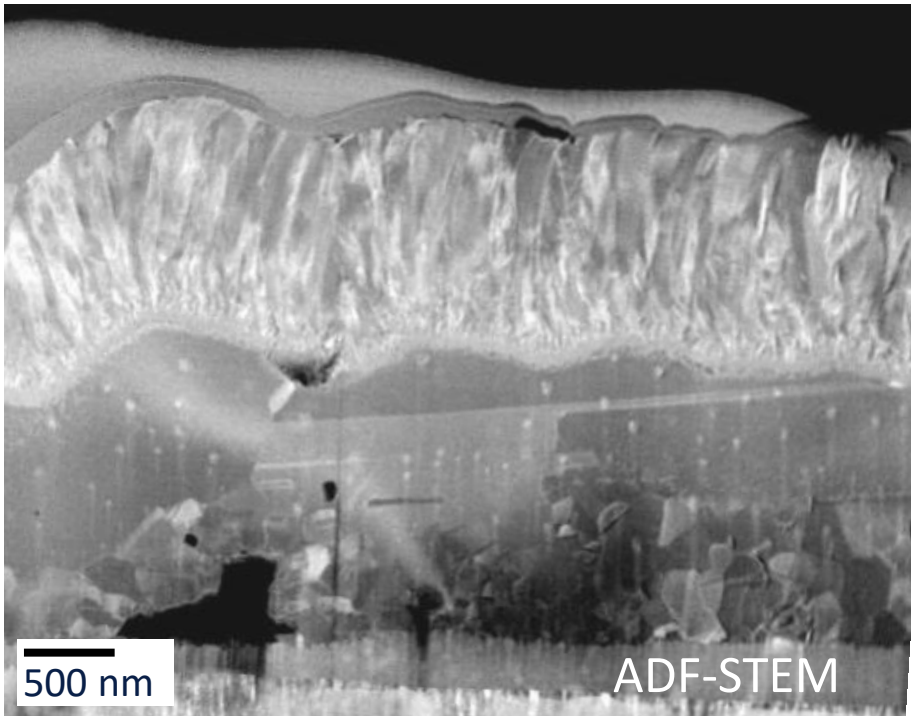

HAADF-STEM image (Helios @**30 kV**)

- Electrons scattered in large angles
- Serial image formation (DF-STEM detect

ADF-STEM image (Titan @**200 kV**)

- Selection of small-angle scattered electrons
- Serial image formation (DF-STEM detector)

FIB demo, FEI company

Channeling Contrast

Electro-polished Cu **(tilted through 1°)**

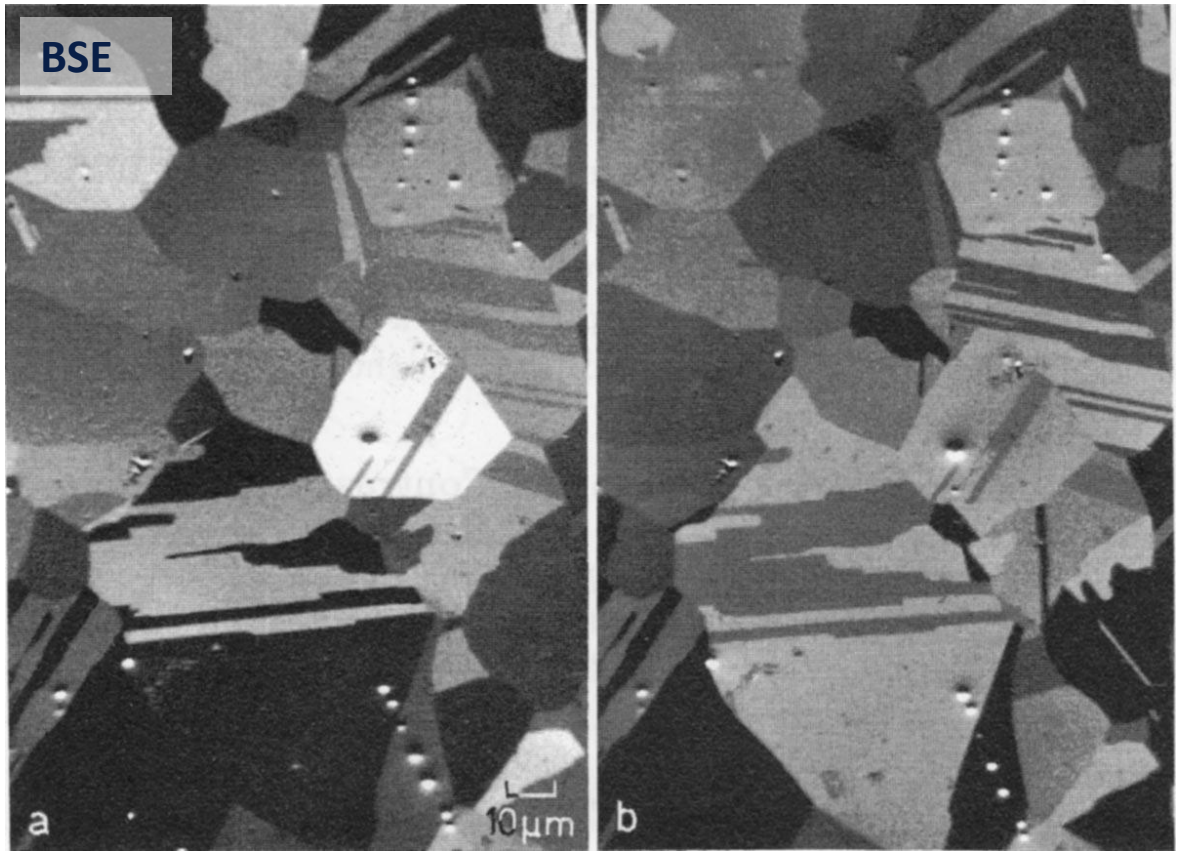

in L. Reimer, *Scanning Electron Microscopy* (p. 226)

Dependency of δ / η on PE incidence with respect to local crystal orientation (lattice planes)

Visualization of
- **grains in polycrystals**
- **lattice defects (twins)**
- **surface-near dislocations**

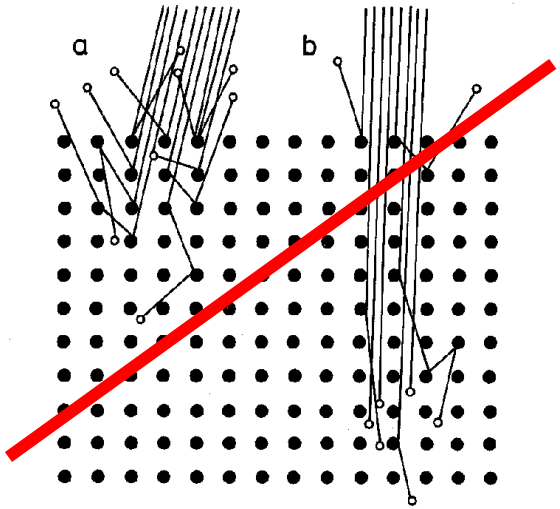

in P. Schmidt, *Praxis der Rasterelektronenmikroskopie und Mikrobereichsanalyse A* (p. 176)

Kinematic Theory

Bragg's law

Constructive interference of elementary waves

λ	Wave length
d_{hkl}	Distance between planes (h,k,l)
υ	Bragg angle

$$2x = 2d_{hkl} \cdot \sin\vartheta = n\lambda$$

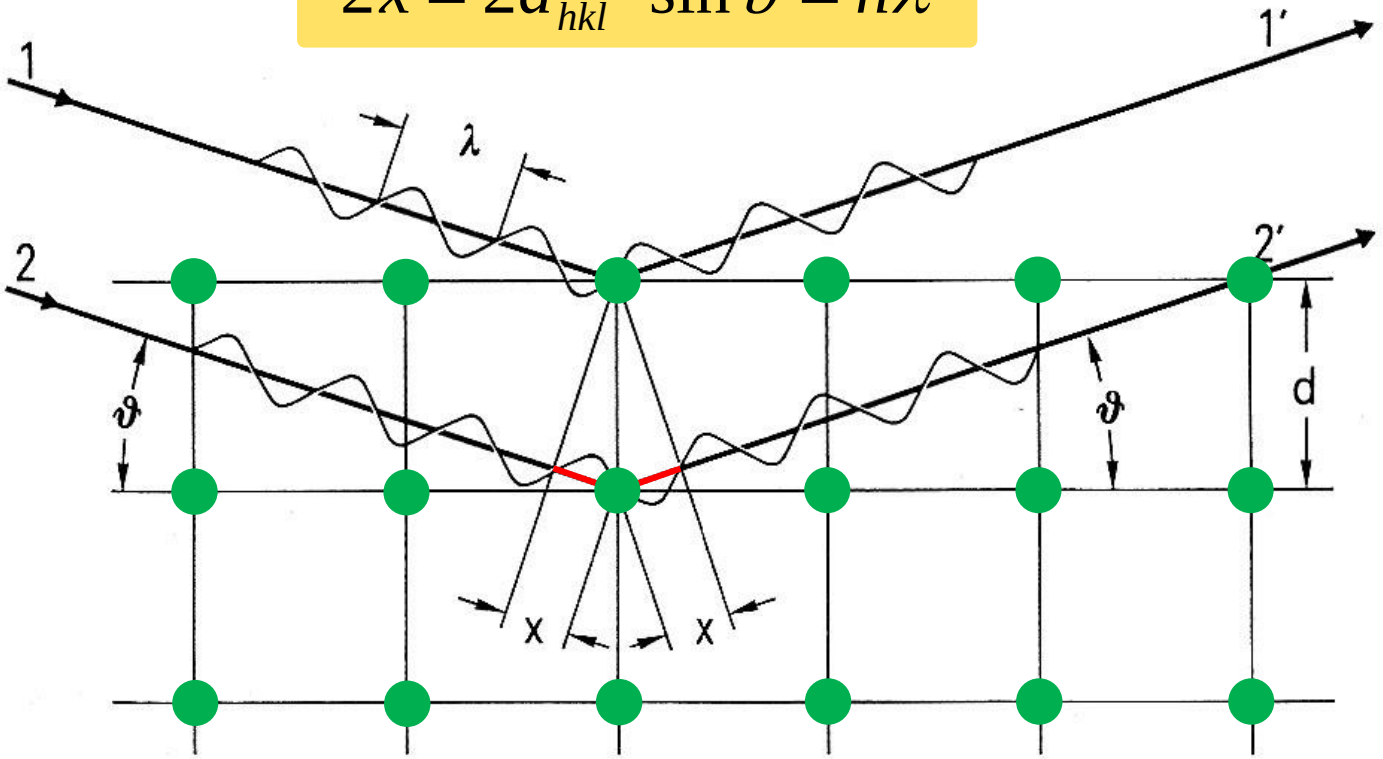

in Fuchs, Oppolzer, Rehme, *Particle Beam Microanalysis* (p. 15)

Electron Backscatter Diffraction (EBSD)

- **Electron backscatter diffraction (EBSD)**
- (1) Elastic scattering event + (2) Bragg diffraction → Diffraction pattern

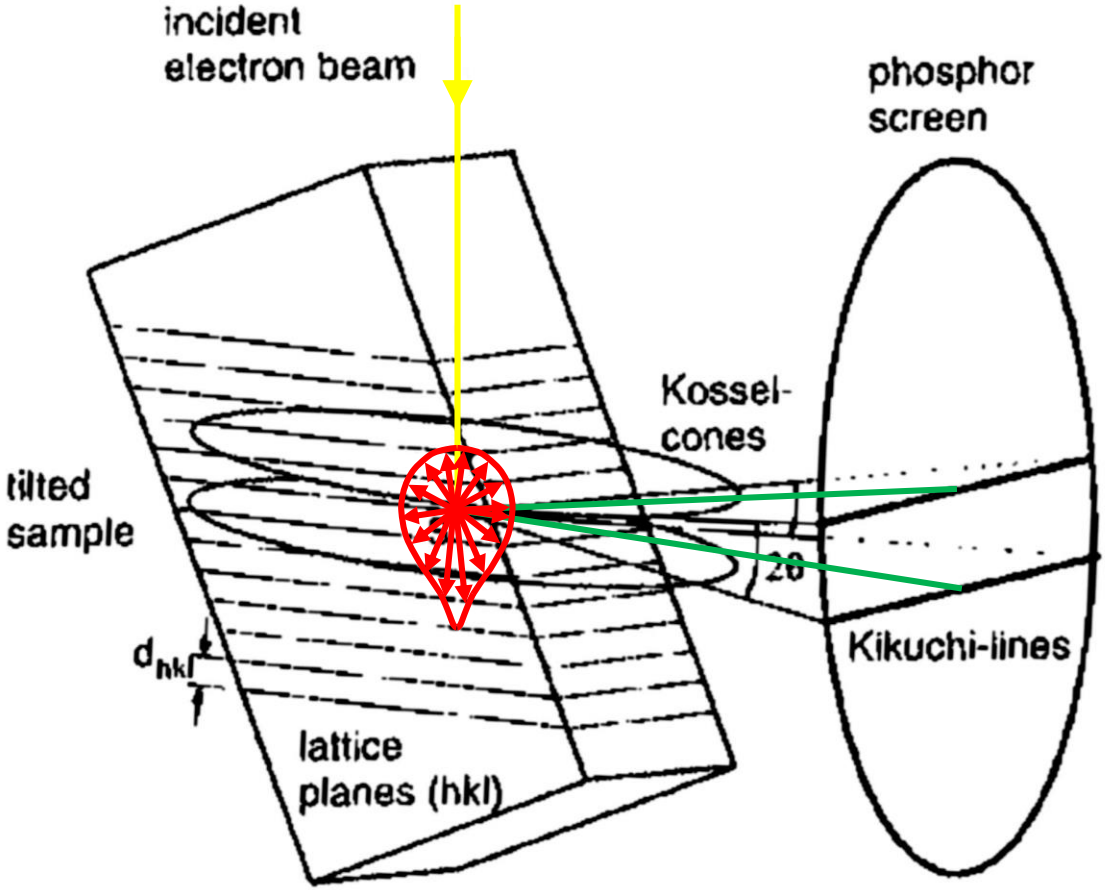

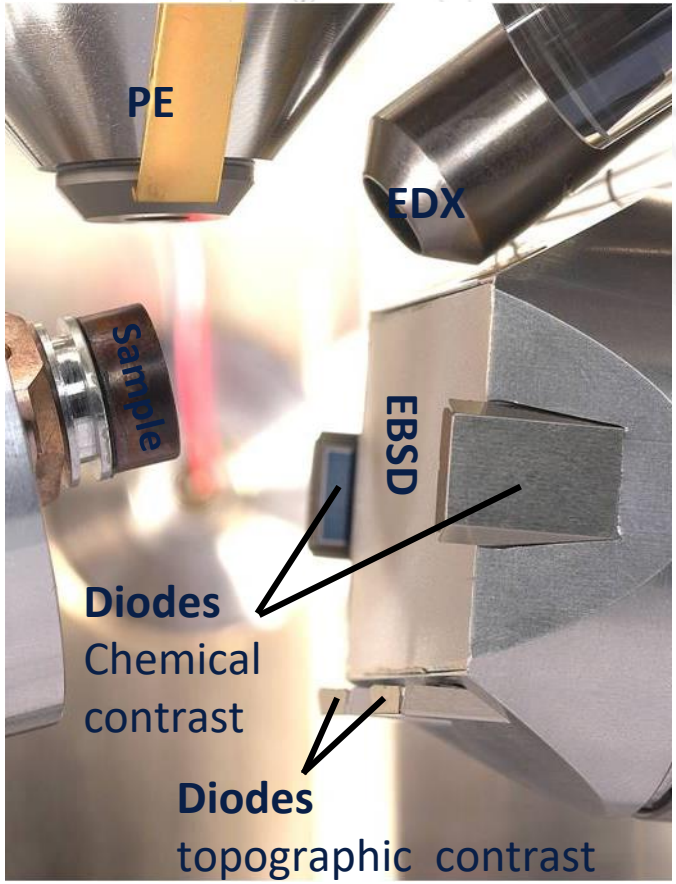

2d Mappings

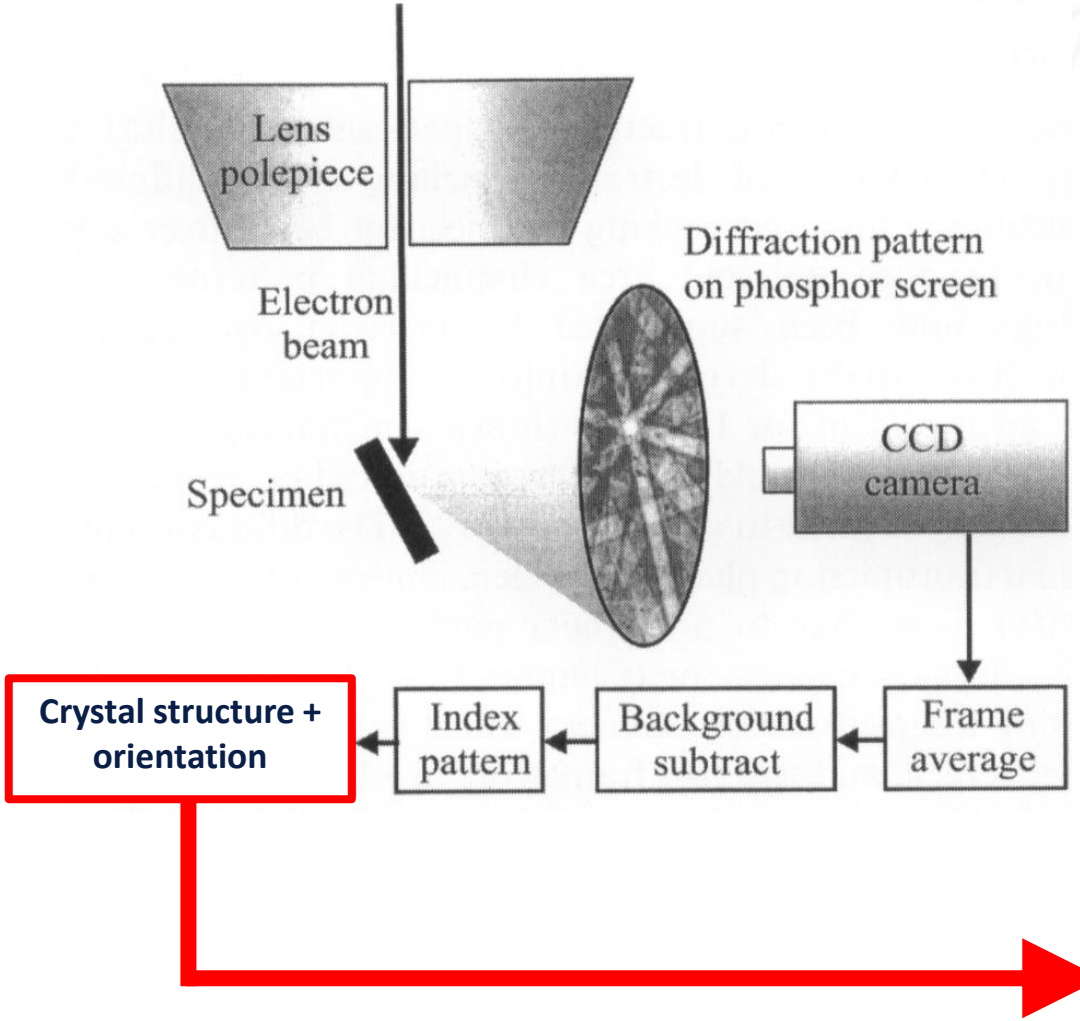

Goodhew, Humphreys, Beanland, *Electron Microscopy and Analysis*, p. 152

Applications

- **Grain size** analysis
- **Strain** analysis
- **Orientation determination** for
  - analysis of global/local texture
  - anisotropic growth
  - crystal rotation (deformation, recrystallization)
  - misorientation
- **Substructure analysis** (twinning)
- **Grain boundary characterization**
- **Phase identification** (in combination with analytical analysis)
- **Phase distribution**
- ***In situ* phase transformations**
- **Recrystallization**

Optimal surface quality essential

Electro-chemical polishing
Ion-beam preparation
Healing by thermal treatment

FIB-SEM for EBSD

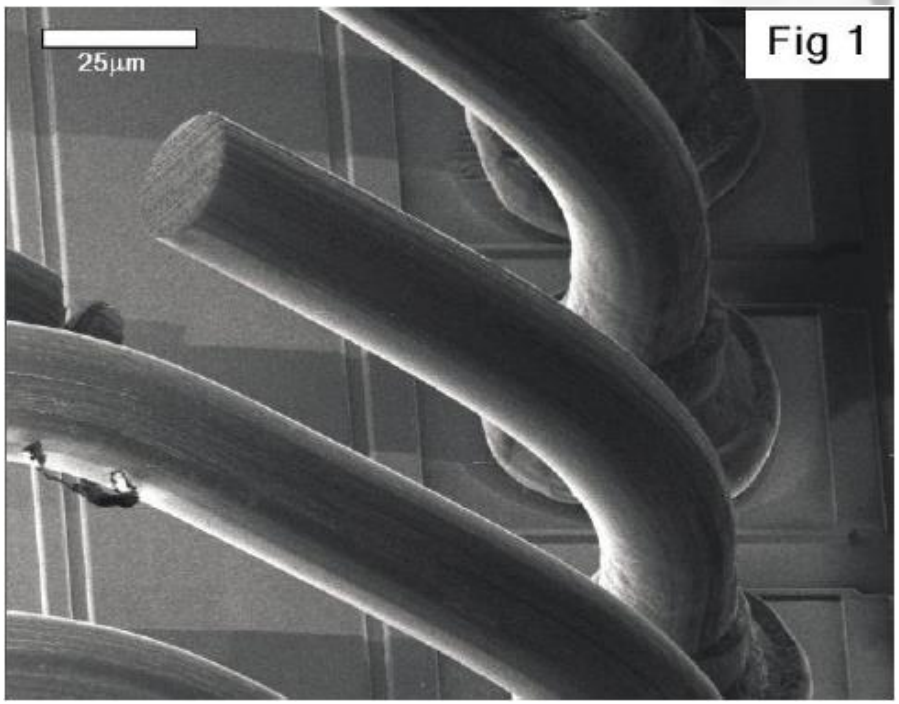

Au wires on circuit

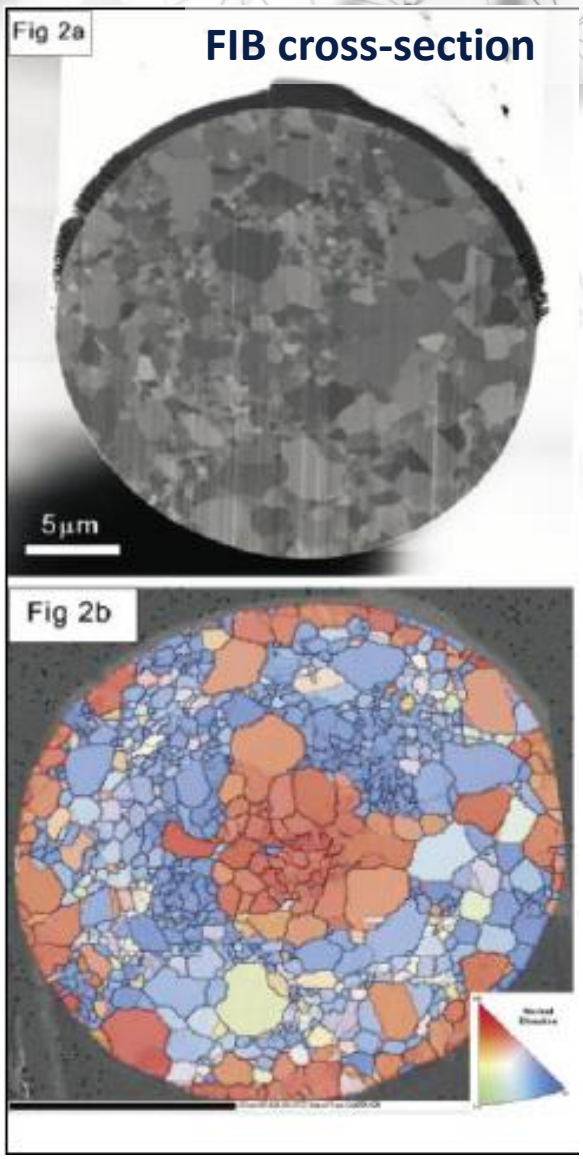

http://www.oxford-instruments.com/Campaigns/microanalysis/ebsd/ebsd-aplications/

EBSD — Lessons learned

- **Local crystal structure information**
- **EDSB resolution on the sub-100 nm level**
- Channeling contrast/EBSD only with **excellent sample-surface quality**
- **Sophisticated data analysis neede** (pattern recognition, phase identification/ strain anlysis, data analysis)

*Voltage Contrast Imaging

Integrated logic circuit

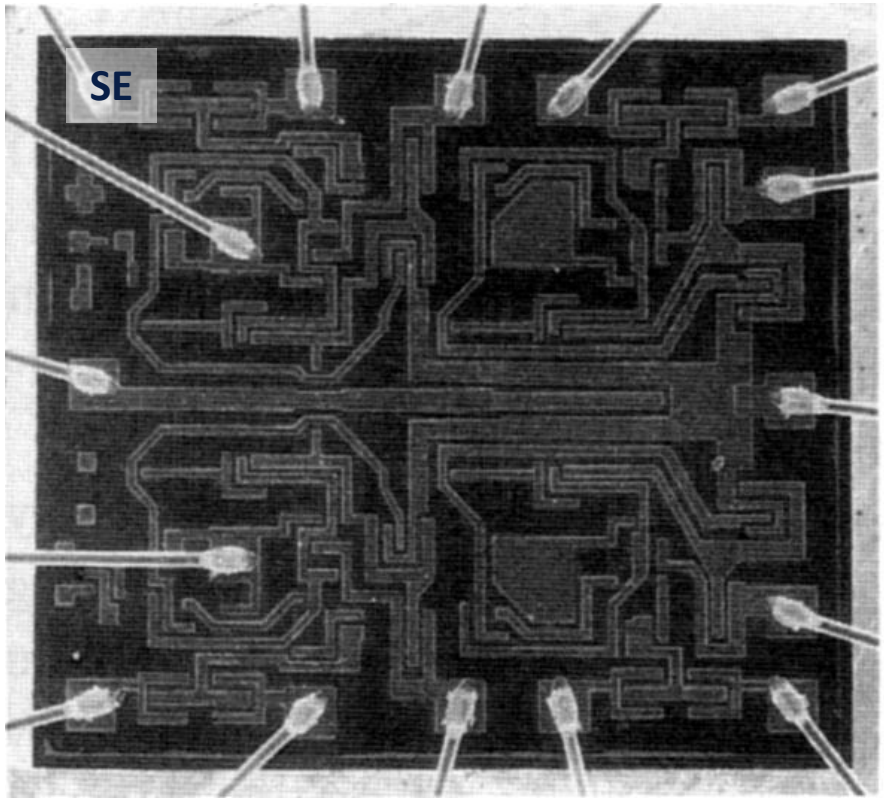

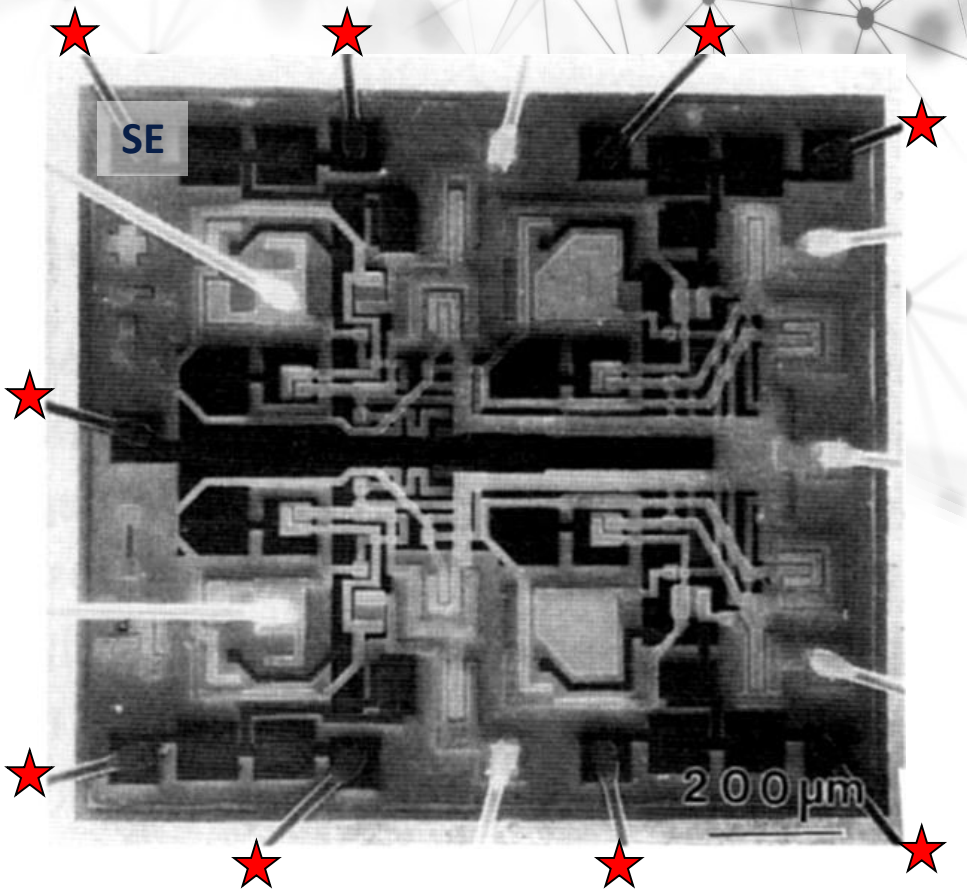

★**+12V** (reduced SE signal)

Passive voltage contrast for static testing of circuits

in Fuchs, Oppolzer, Rehme, *Particle Beam Microanalysis* (p. 364)

*Resistive Switching of Percolated NW network

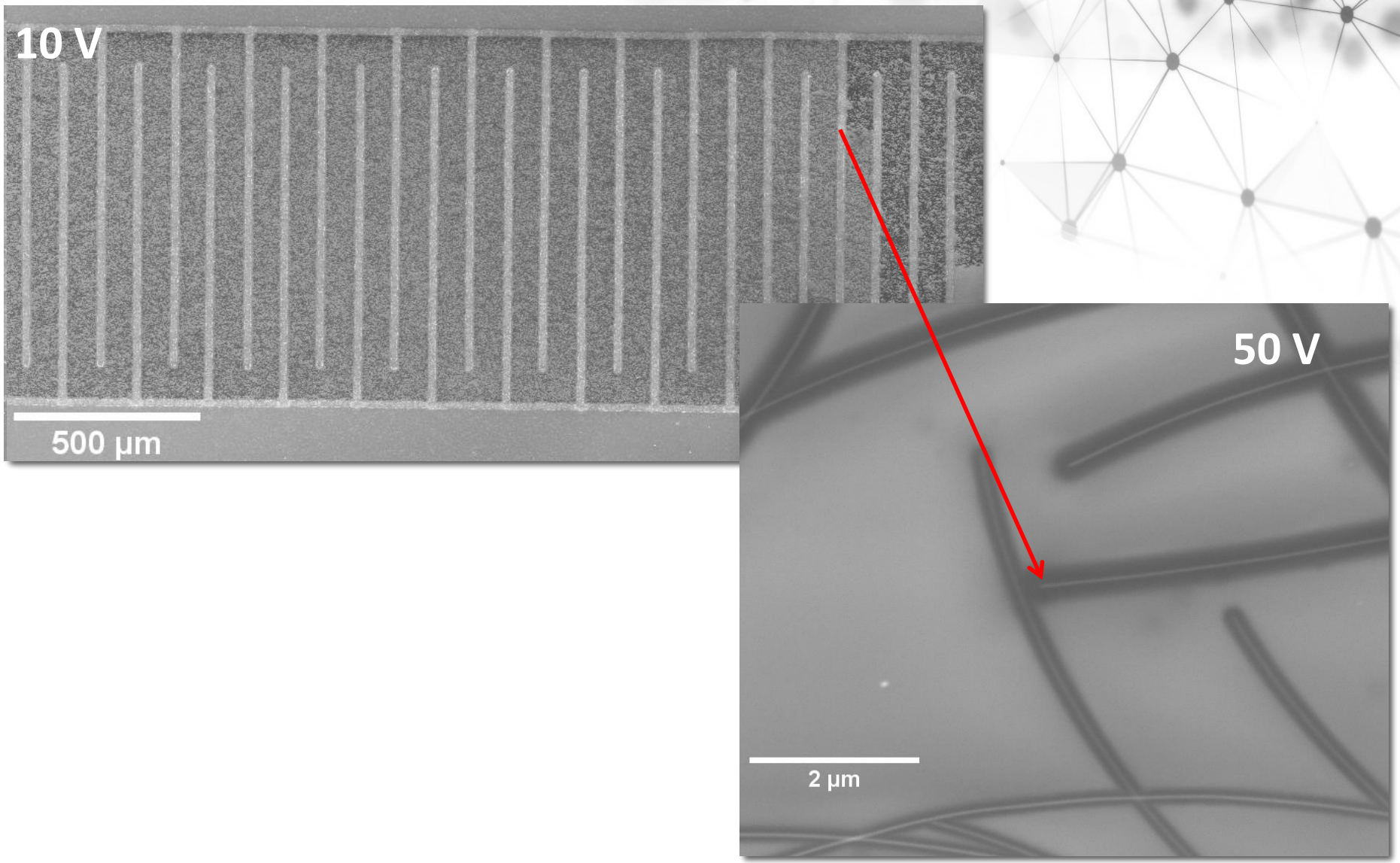

*Magnetic Contrast Imaging

Type-1 magnetic contast (SE)

- Deflection of SE by magnetic stray field $\vec{B}$
- E-T at low attractive potential

Contrast: varying fraction of SE towards E-T

$$\vec{F}_{Lorentz} = -e\vec{v} \times \vec{B}$$

$\vec{v}$ Velosity vector of SE
$\vec{B}$ Magnetic field

$BaFe_{12}O_9$ single crystal

in Fuchs, Oppolzer, Rehme, *Particle Beam Microanalysis* (p. 133)

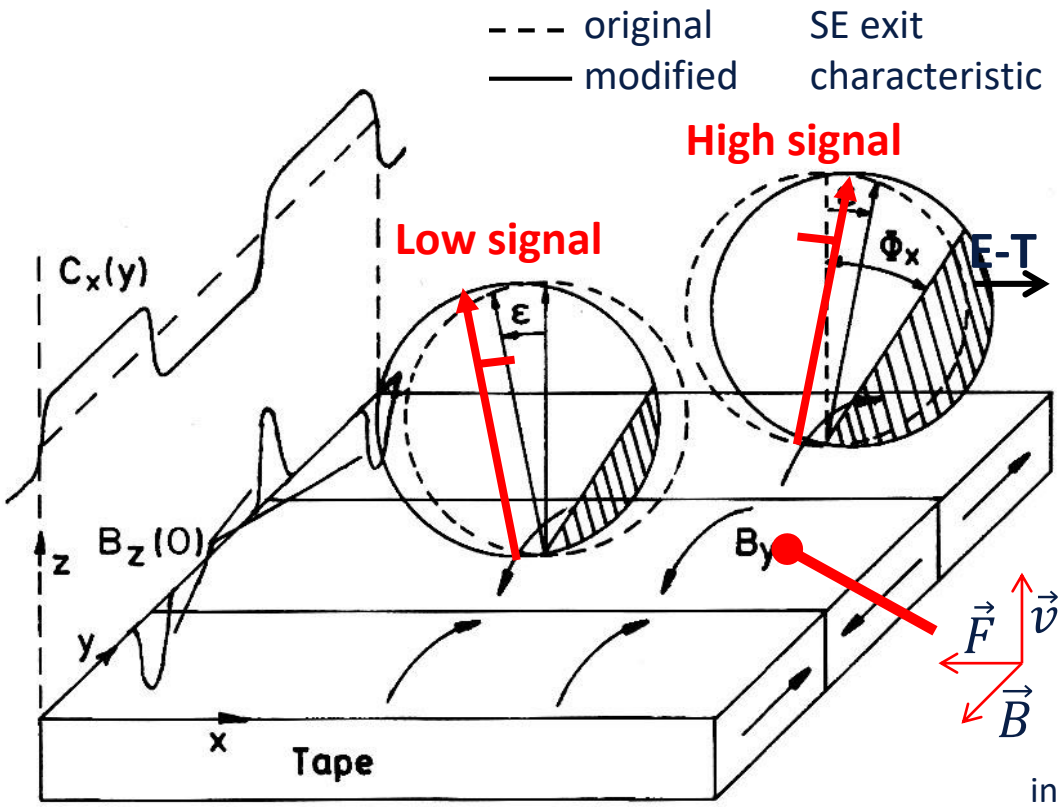

Magnetic tape

Contrast reversal by 180° sample rotation

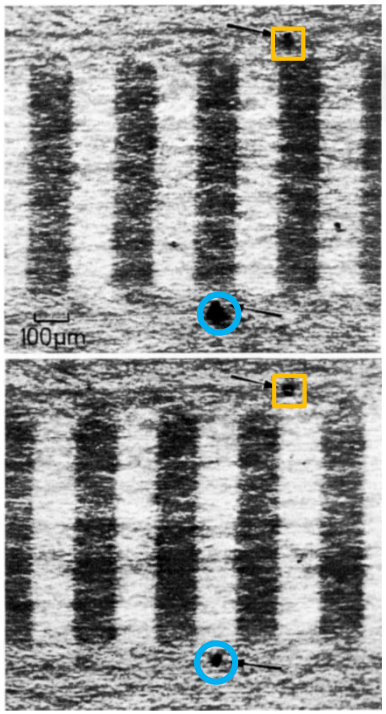

in L. Reimer, *Scanning Electron Microscopy* (pp. 291)

*Electron-Beam Induced Current

Electron beam induced current (EBIC)

- Generation of electron-hole pairs carriers by electron impact ($\bar{E}_i[\mathrm{eV}]$)
- Charge separation in internal field regions (e.g., pn-junctions, Schottky-barriers)

Local charge-collection current (I_{CC}) depends on charge generation and separation efficiency

Charge carrier generation

Charge carrier separation

→ **Current**

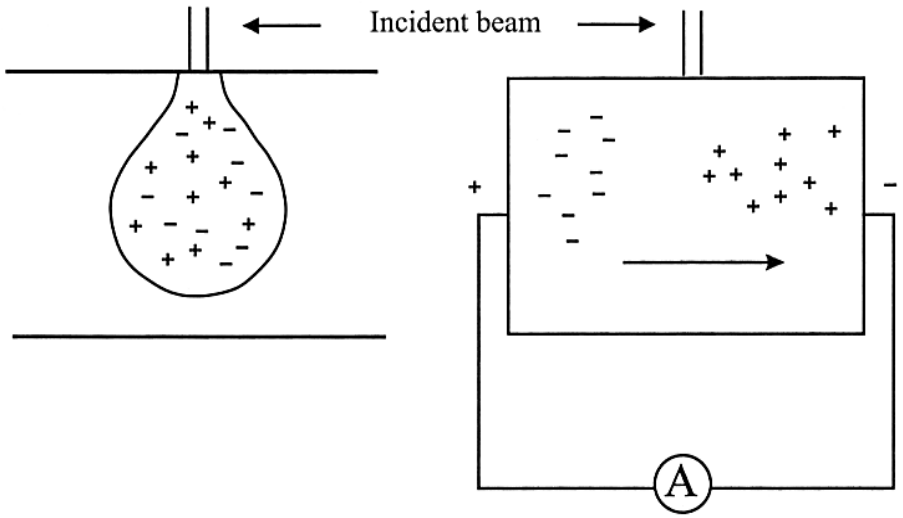

	$\bar{E}_i[\mathrm{eV}]$
Si	3.65
Ge	2.85
GaAs	4.6
InSb	0.42
CdS	7.3

In Goodhew, Humphreys, Beanland, *Electron Microscopy and Analysis*, p. 153

*Recombination at Defects

Plan-view of burried pn-junction (P in-diffusion): near-surface dislocations

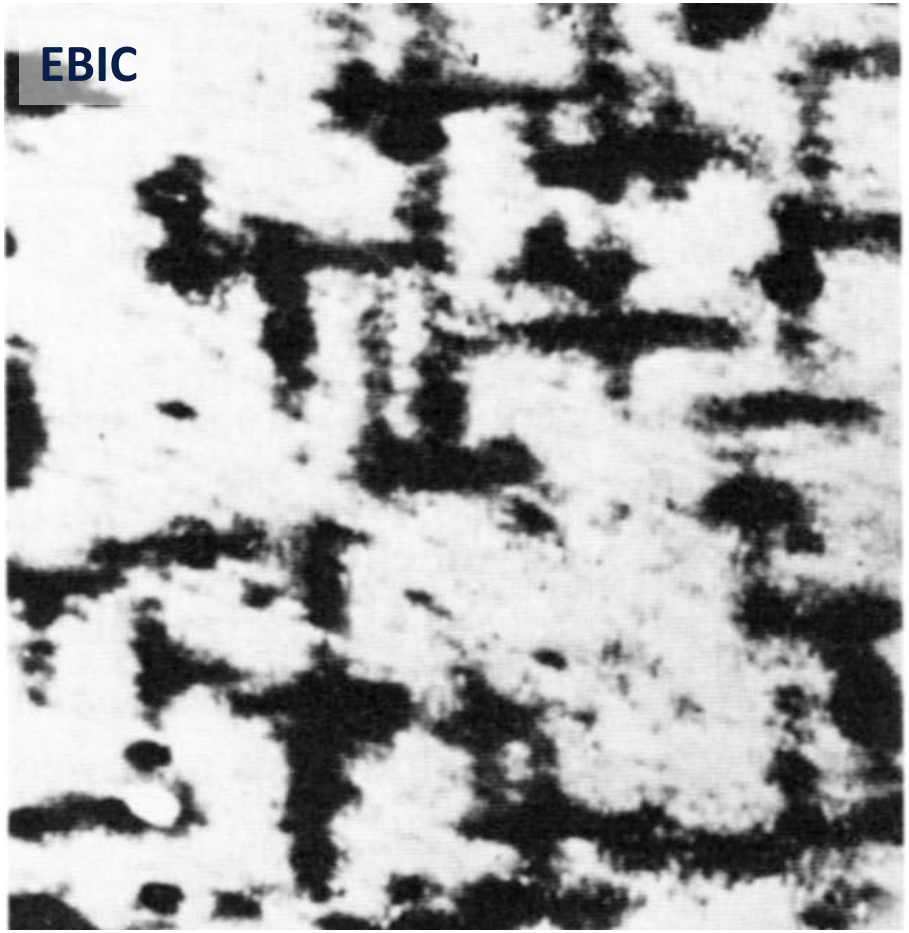

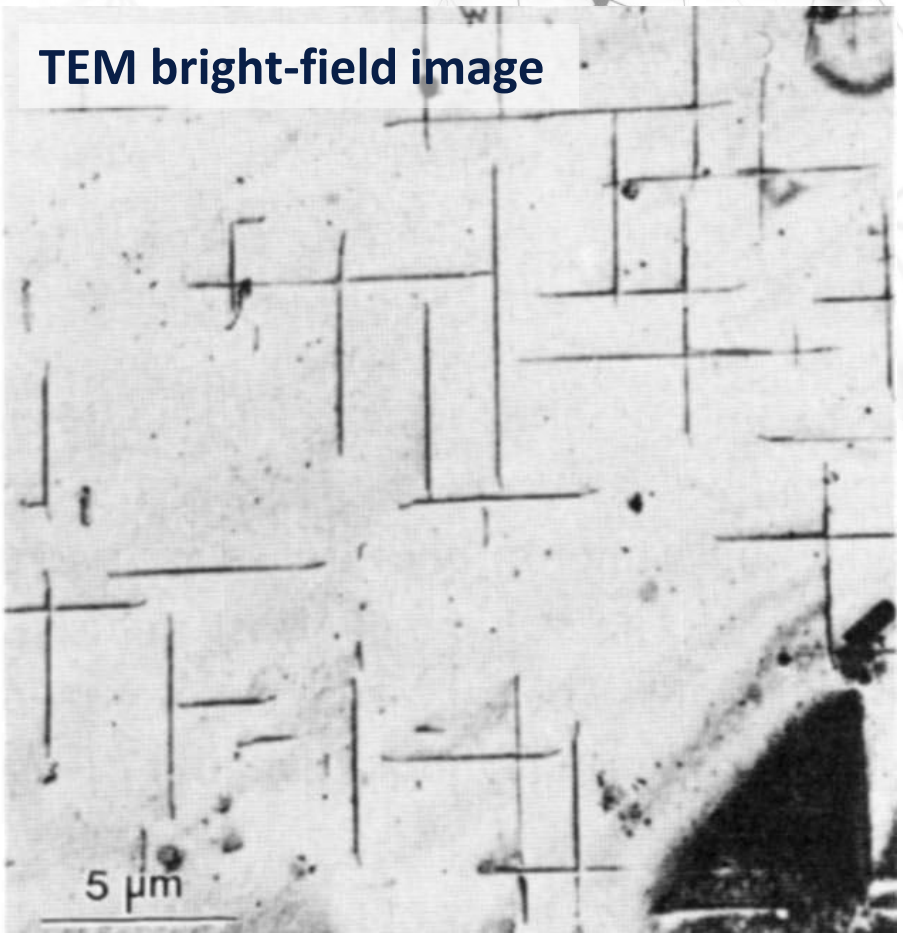

in Fuchs, Oppolzer, Rehme, *Particle Beam Microanalysis* (p. 131)

Energy Dispersive X-ray Spectroscopy (EDXS)

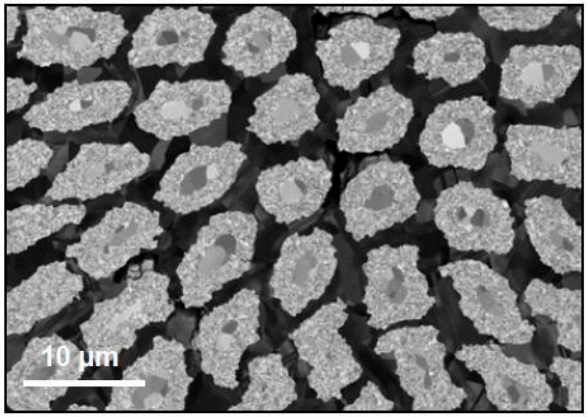

EDXS-tomo. of superconducting material

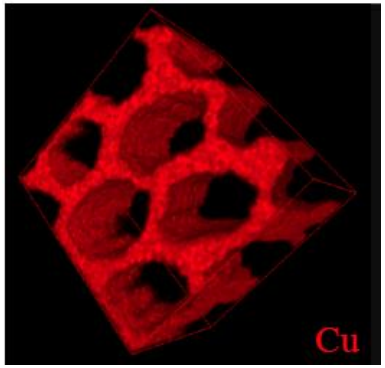

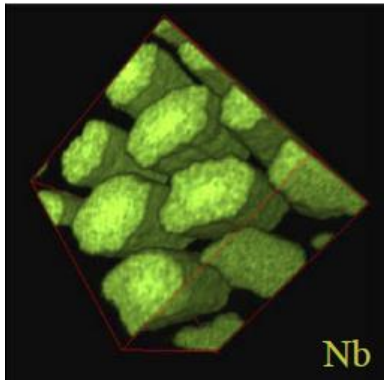

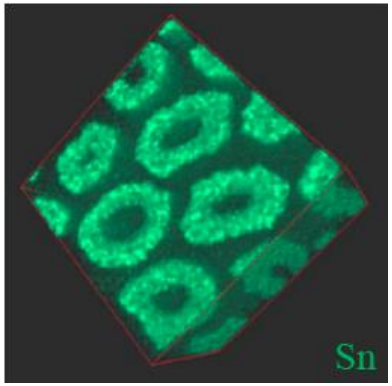

Pavia et al. – Microsc. Mircoanal. 21 (Suppl 3), 2015

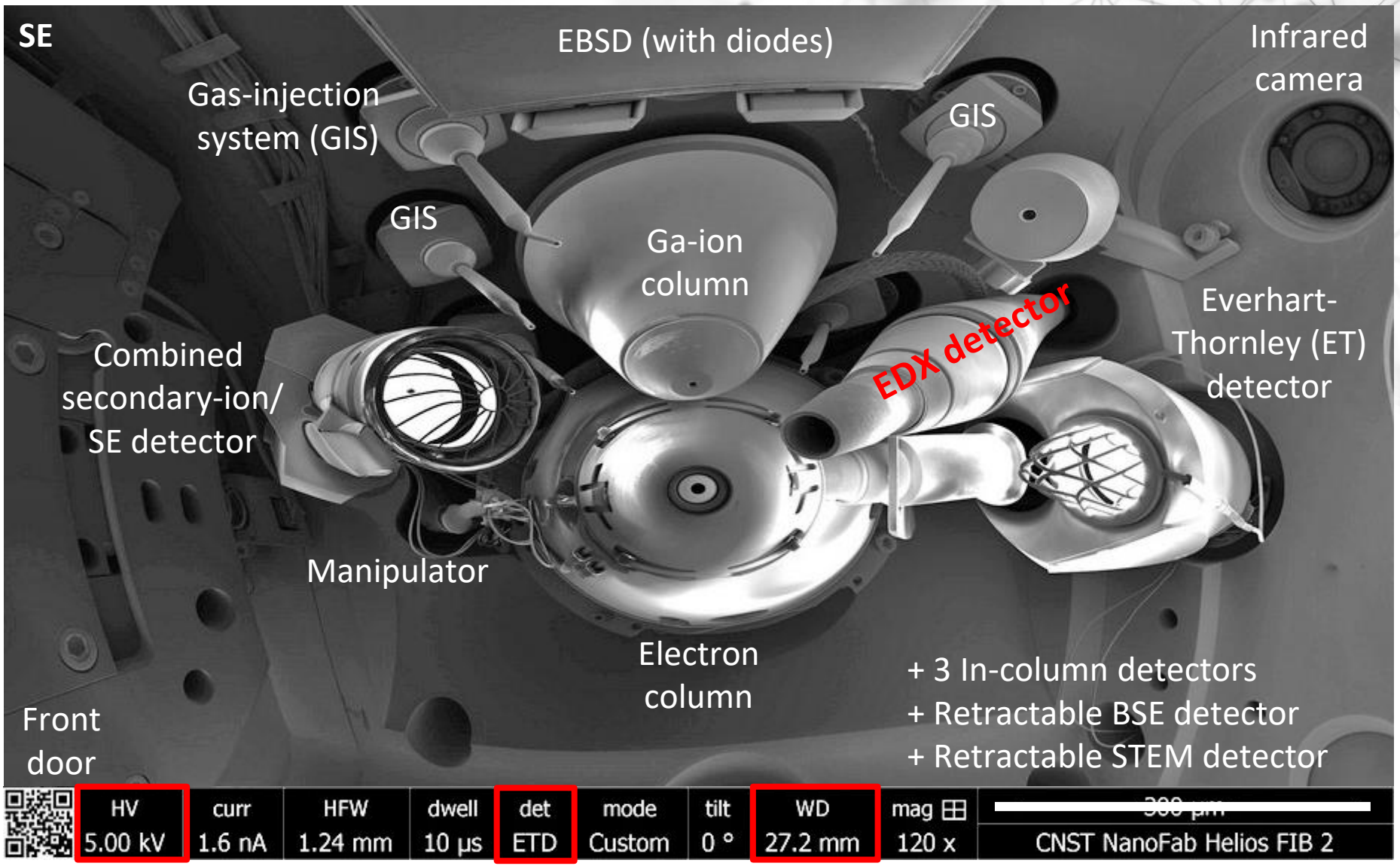
SE
EBSD (with diodes)
Infrared camera
Gas-injection system (GIS)
GIS
GIS
Ga-ion column
Everhart-Thornley (ET) detector
EDX detector
Combined secondary-ion/ SE detector
Manipulator
Electron column
+ 3 In-column detectors
+ Retractable BSE detector
+ Retractable STEM detector
Front door
HV 5.00 kV
curr 1.6 nA
HFW 1.24 mm
dwell 10 µs
det ETD
mode Custom
tilt 0 °
WD 27.2 mm
mag 120 x
CNST NanoFab Helios FIB 2

Analytical Techniques (OV)

Primary Process

Ionization by high-energetic PE

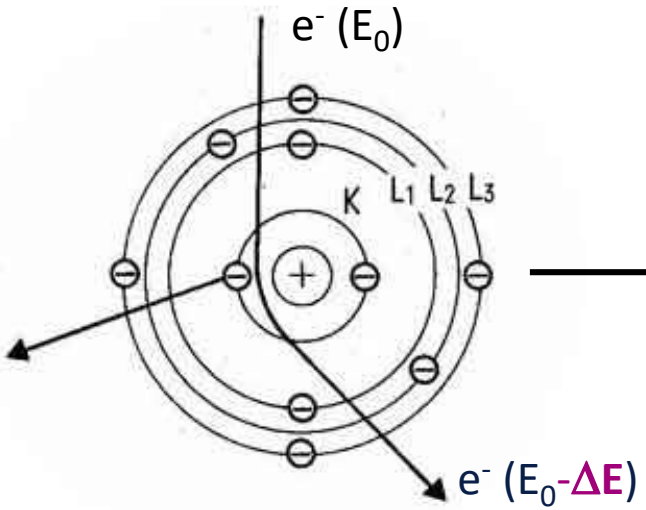

EELS (TEM)

Electron Energy-Loss Spectroscopy (**ΔE**)

Secondary Processes

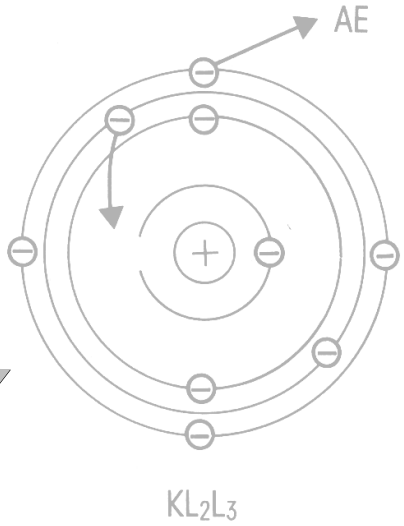

Auger-Electron Emission

X-Ray Emission

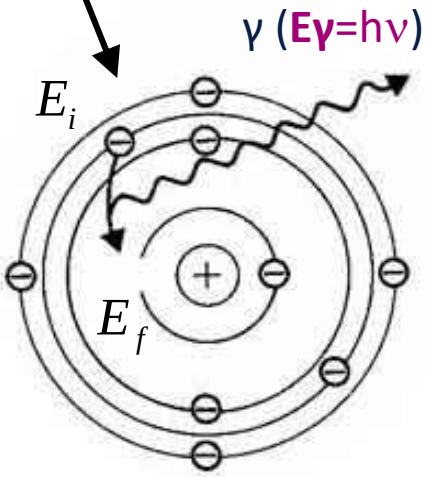

EDXS/WDXS

Energy-/wavelength-dispersive X-Ray Spectroscopy

$$h\nu = E_i - E_f$$

E. Fuchs, H. Oppolzer, H. Rehme, *Particle Beam Microanalysis*, Fig. 2.43

X-ray Energies — Moseley's Law

Fig. 10.6. Demonstration of the Moseley law – linear relation between $E_x^{1/2}$ and Z – by plotting the ionization (edge) energies E_I, (I = K, L_1, L_2, L_3) (o o o) and the quantum energies $E_x^{1/2}$ of the x-ray lines (• • •) against the atomic number Z (values for E_x in keV on the left-hand ordinate)

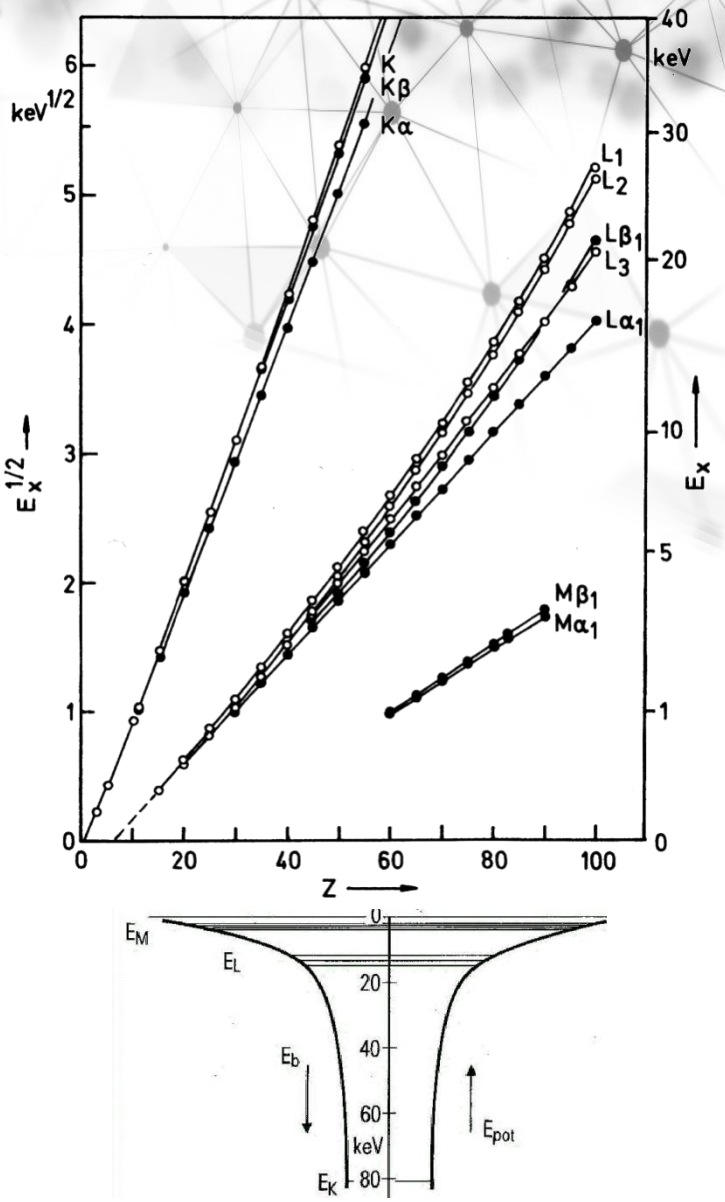

Z-dependency of X-ray energies

$$h\nu = E_i - E_f$$

Binding energy of hydrogen

K-series (Kα n=2, Kβ n=3)

$$E_{n,K} = E_n - E_1 = -13{,}6eV(Z-1)^2\left(\frac{1}{n^2} - 1\right)$$

L-series (n=3,4)

Screening constant

$$E_{n,L} = E_n - E_2 = -13{,}6eV(Z-7.4)^2\left(\frac{1}{n^2} - \frac{1}{4}\right)$$

Moseley's law

Screening constant

$$E_{n,K} \propto (Z-\sigma)^2$$

in L. Reimer, *Scanning Electron Microscopy* (p. 386)

Element-Specific X-Rays

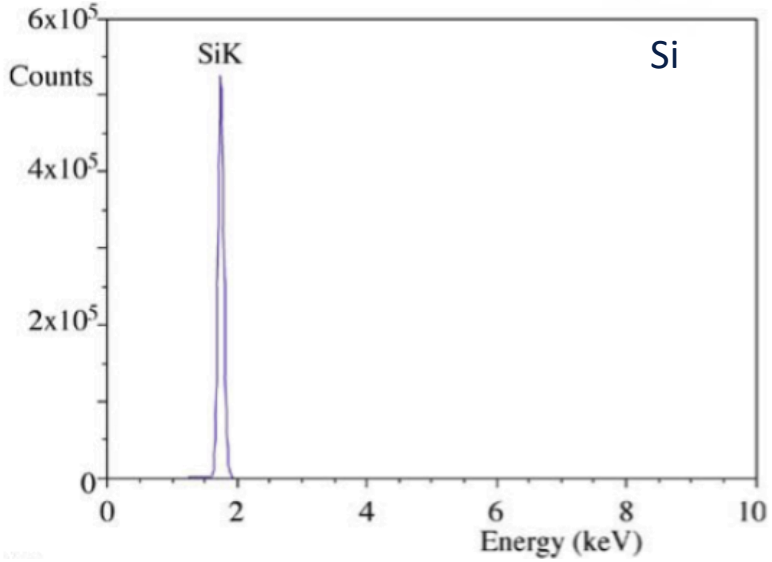

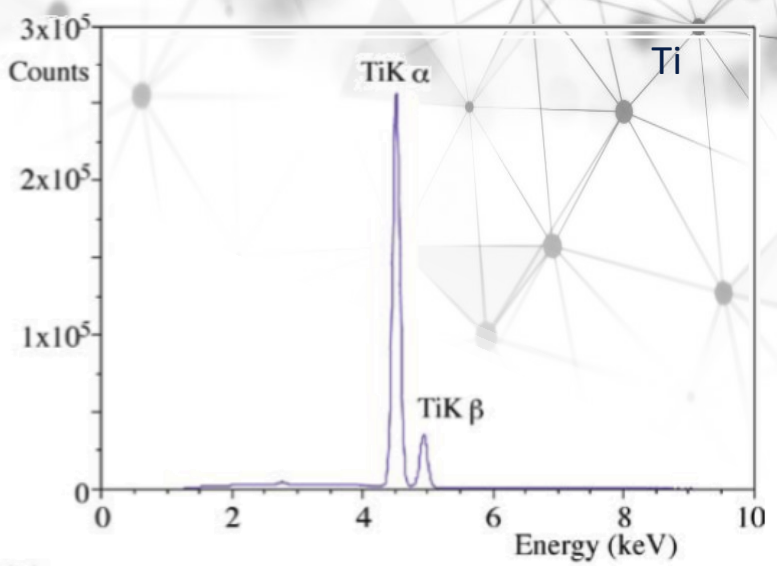

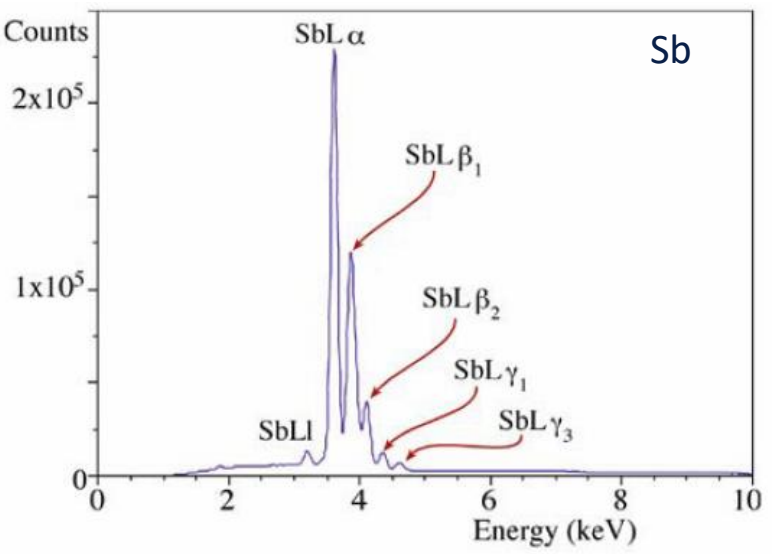

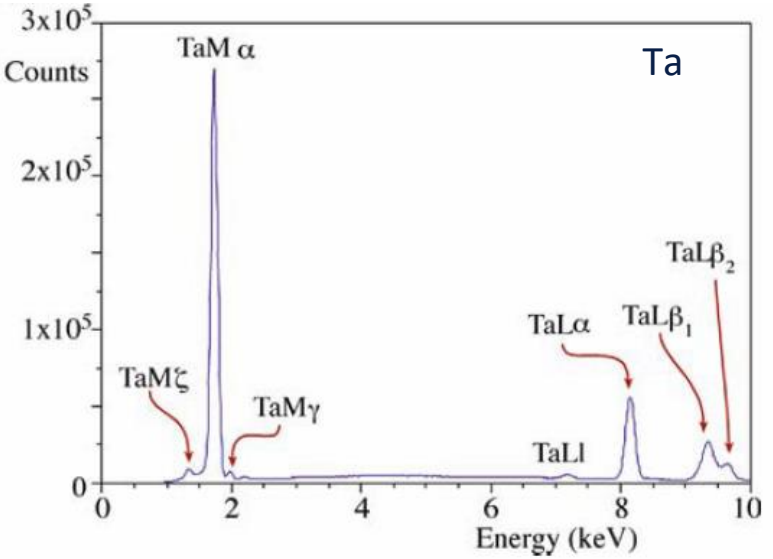

in D. Williams, B. Cater, , *transmission Electron Microscopy* (p. 629)

Deconvolution of Peaks

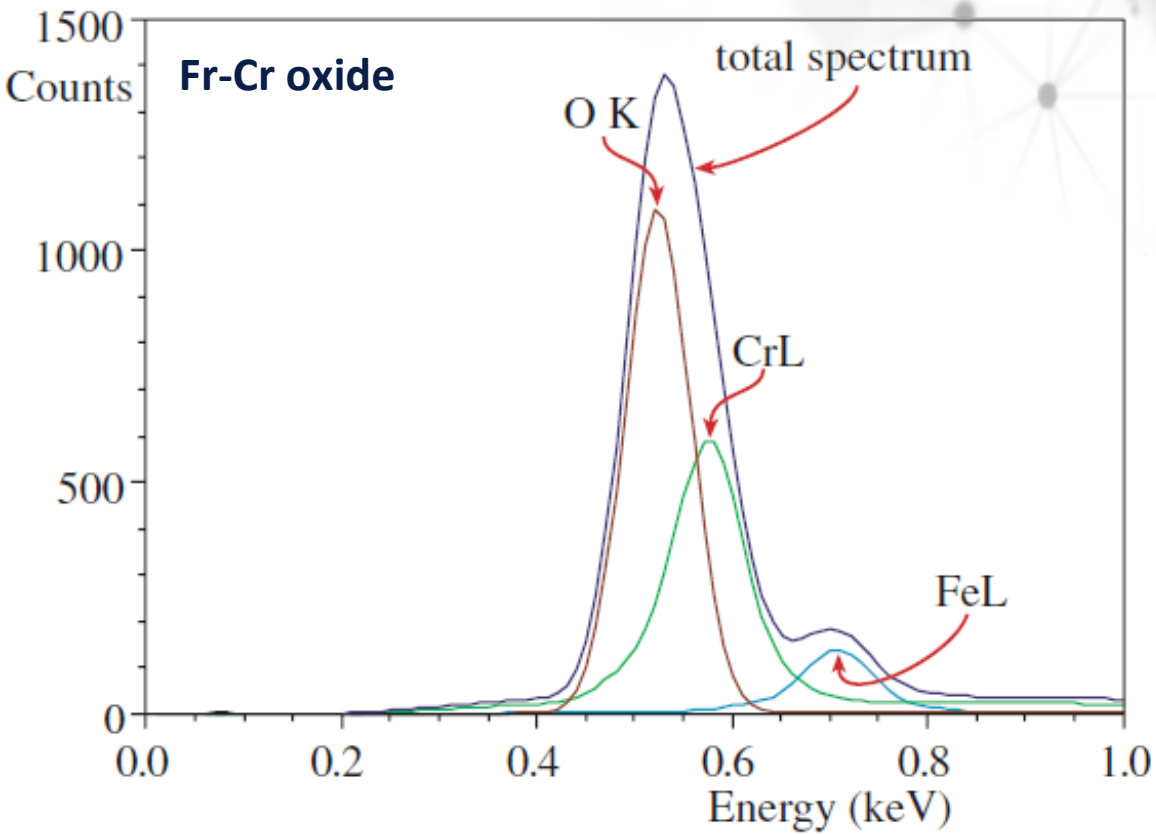

Due to the limited energy resolution of the semiconductor detectors (i.e. Si(Li) = 125 eV) peaks can often not be resolved.

→ **Deconvolution necessary**

Solution:
→ Wave-length dispersive spectroscopy (WDX, see later)
→ Digital deconvolution (implemented in commercial software)

in D. Williams, B. Cater, , *transmission Electron Microscopy* (p. 631)

Si(Li)-EDXS Detector

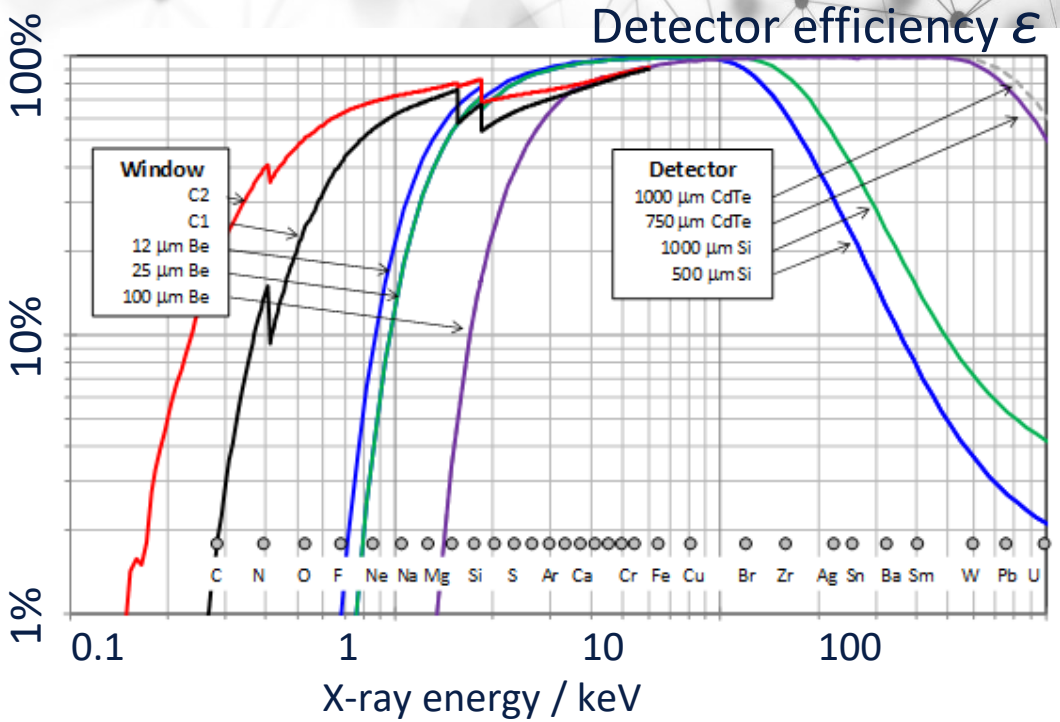

Efficiency depends on X-ray energy

- Low energy: absorption (window)
- High energy: penetration through sensor

Energy resolution ~125 eV (@Mn Ka 5,9 keV)

Thermo Fisher Scientifc

Amptec

Si(Li)-EDXS Detector

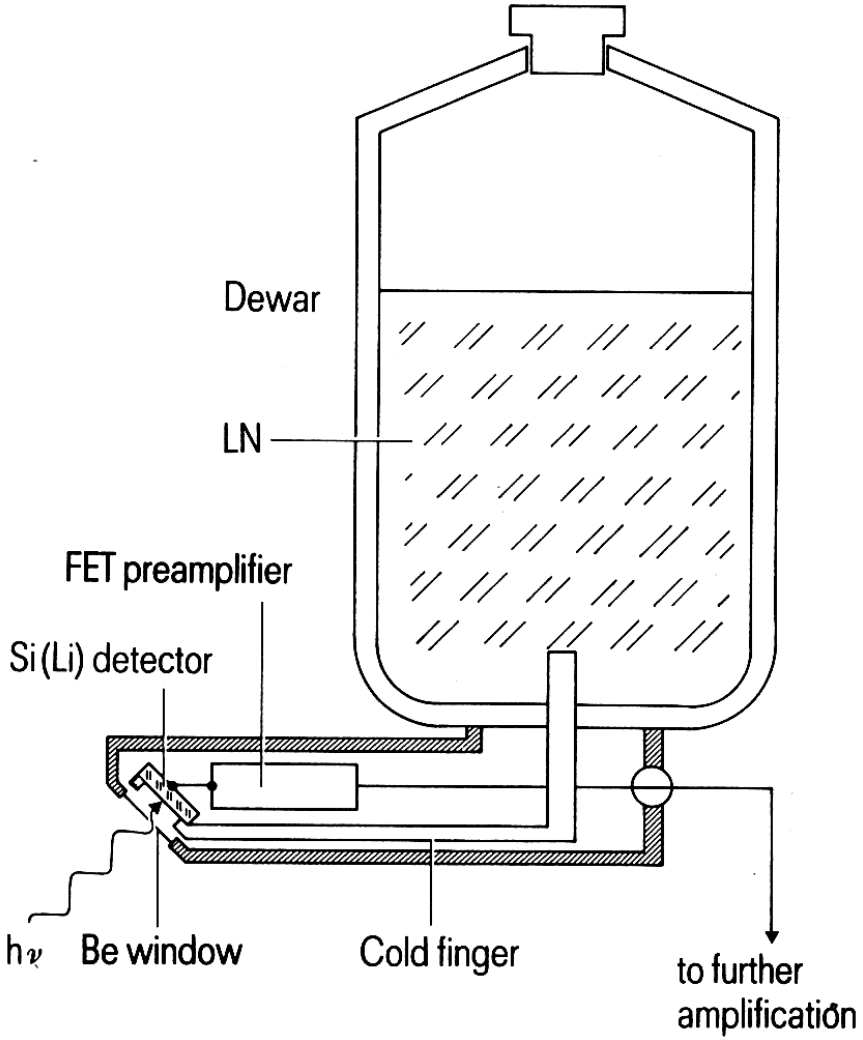

in Fuchs, Oppolzer, Rehme,
Particle Beam Microanalysis (p. 238)

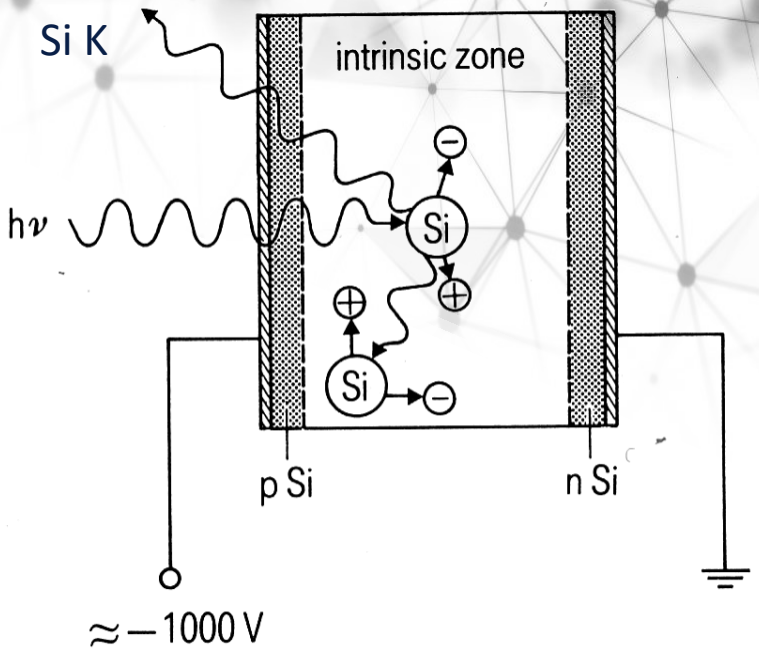

Li-doped Si-Crystal

- 3,8 eV per e^-/h^+-pair
- Charge separation by electrical field

➡ **Number of pairs proportional to energy of incoming X-ray**

Energy resolution ~125 eV (@ 5,9 KeV)

Silicon Drift Detector (SDD)

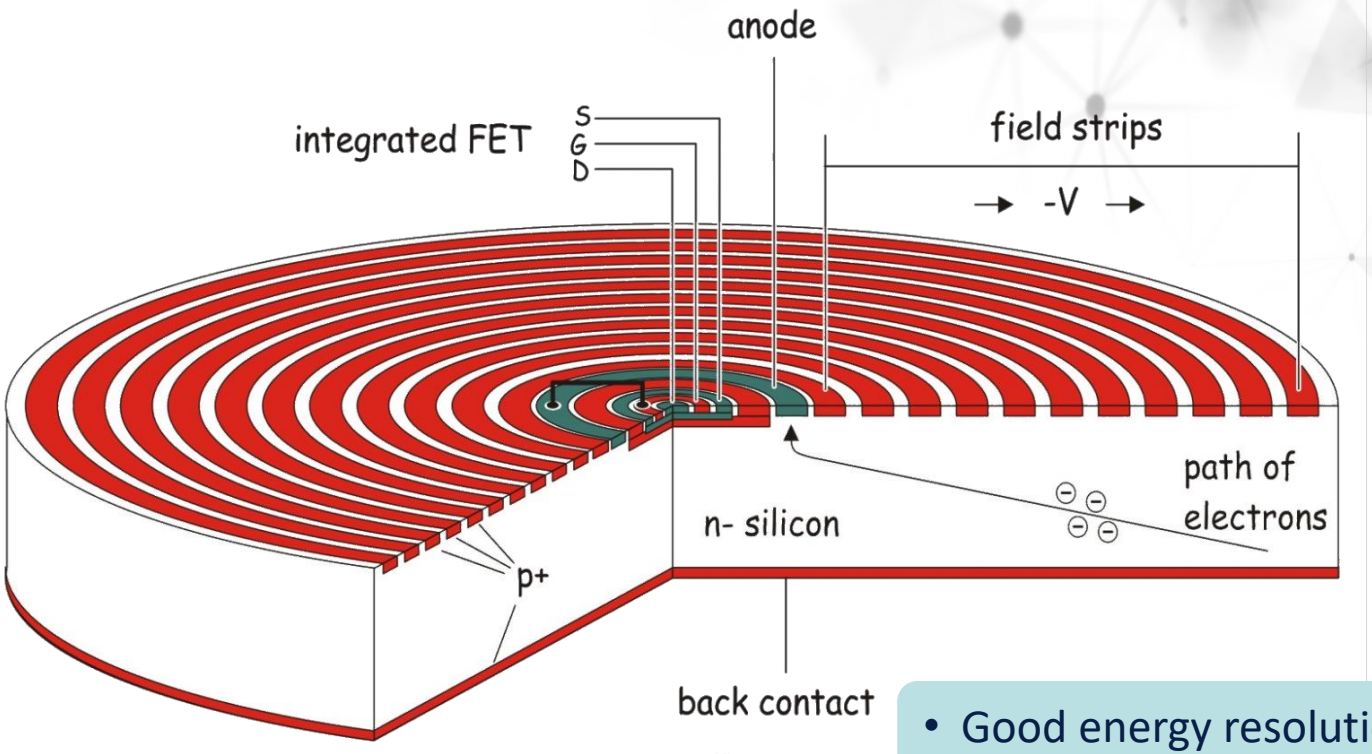

Thermo Fisher Scientific

- Good energy resolution down to 121 eV @ Mn Ka
- Peltier cooling (no LN_2)
- Maintains good energy resolution at high input count rates
- **Large sensors realizable (150 mm², 06/2013) without decrease of resolution**
- **High input count rates up to 10^6 cps**

Artifacts

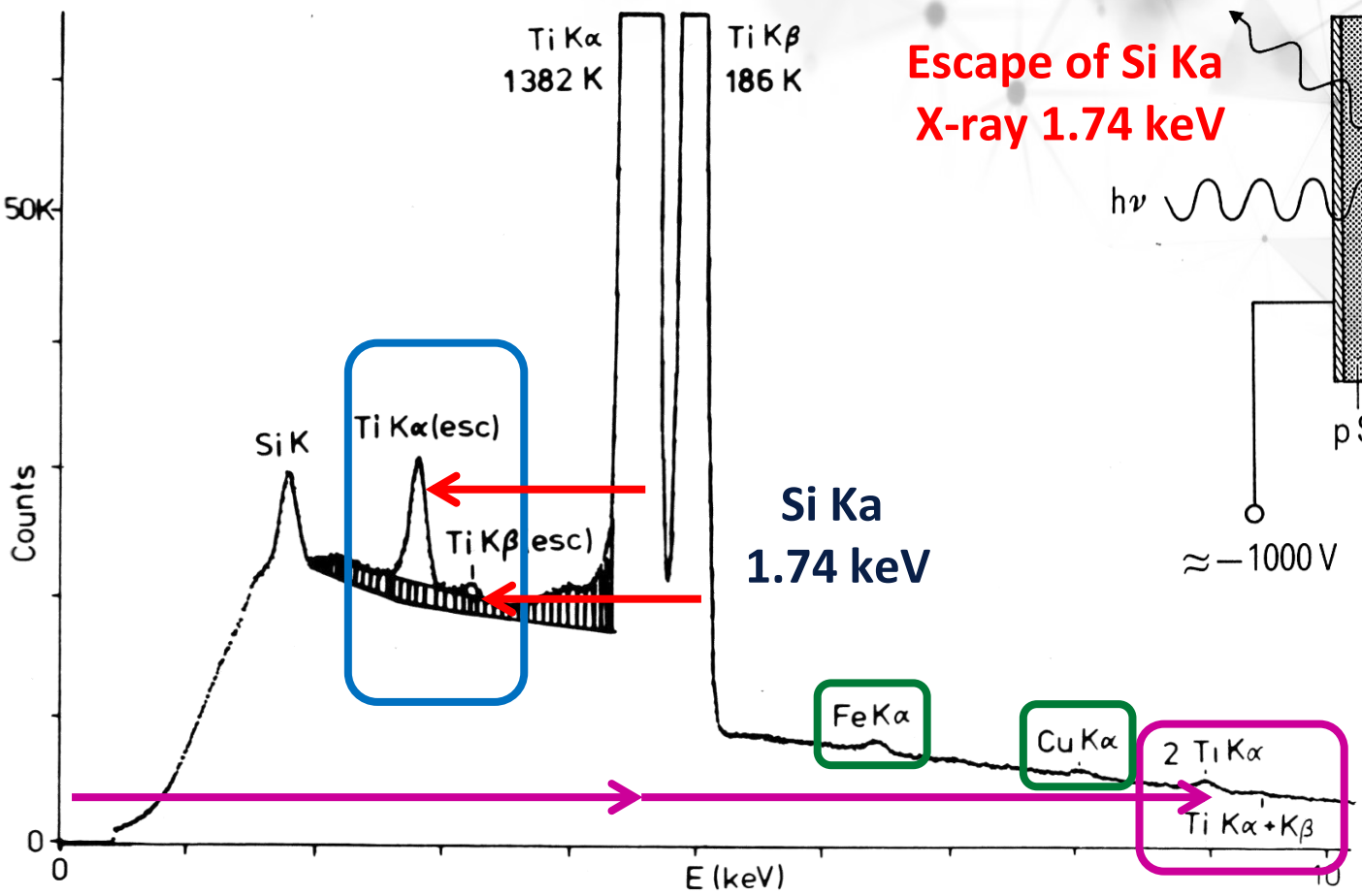

Escape of Si Ka X-ray 1.74 keV

Si Ka 1.74 keV

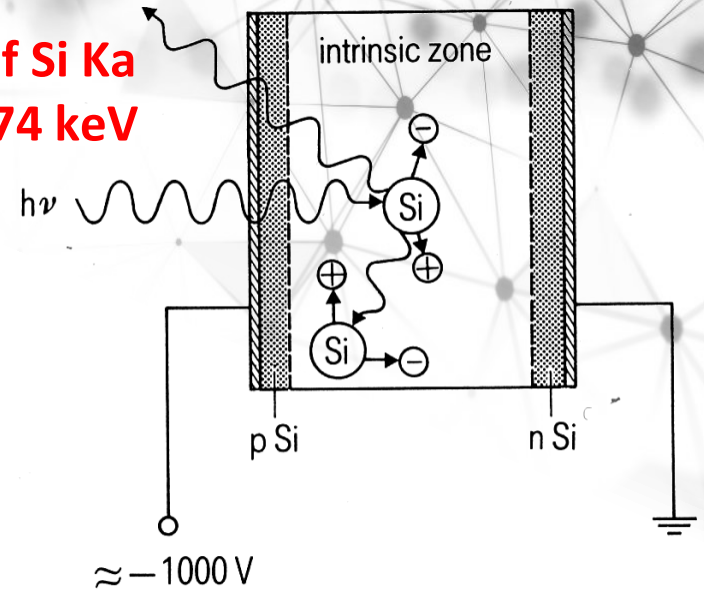

Escape peak: artificial peak at $E = E_g - 1.74$ keV
Sum peak (pile up): artificial peak at $E = E_{g1} + E_{g2}$
Additional peaks from stray electrons (BSE)

Reduction of count rate!

in Goldstein et al., *Scanning Electron Microscopy and X-Ray Microanalysis* (p. 231)

*X-ray Microprobe Instrument

Jeol JXA-8100 at WW2 (WTM) with five wave-length dispersive spectrometers (**X**)

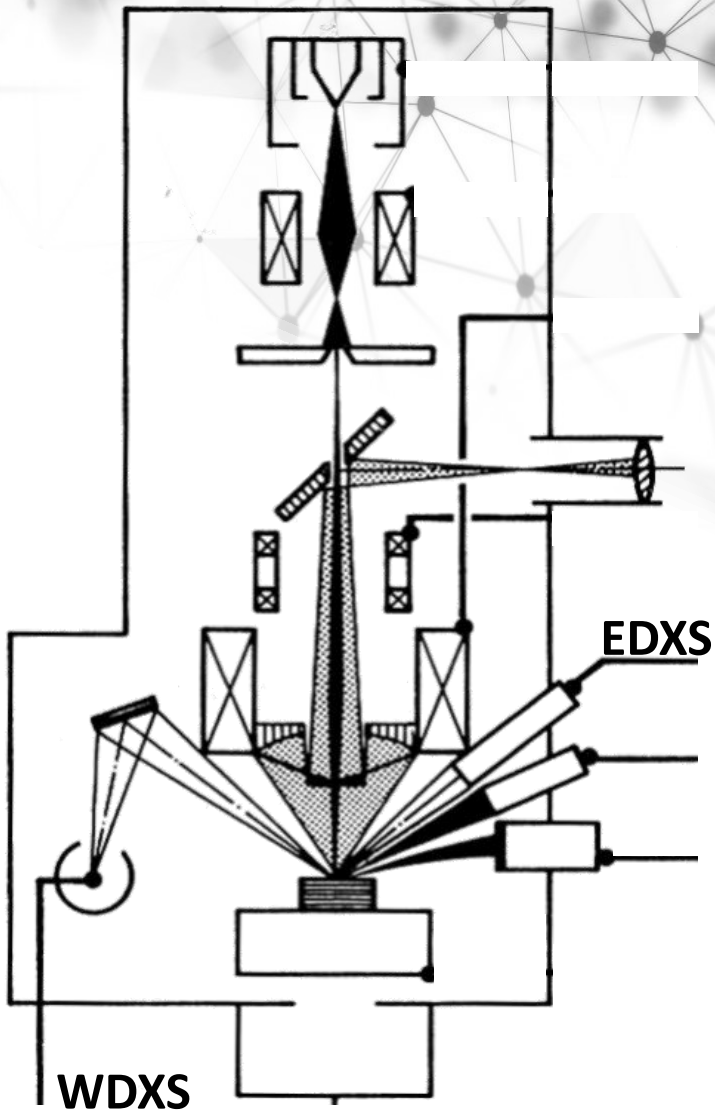

http://www.uni-stuttgart.de/imi/institut/ausstattung.html

*EDXS vs. WDXS: Energy Resolution

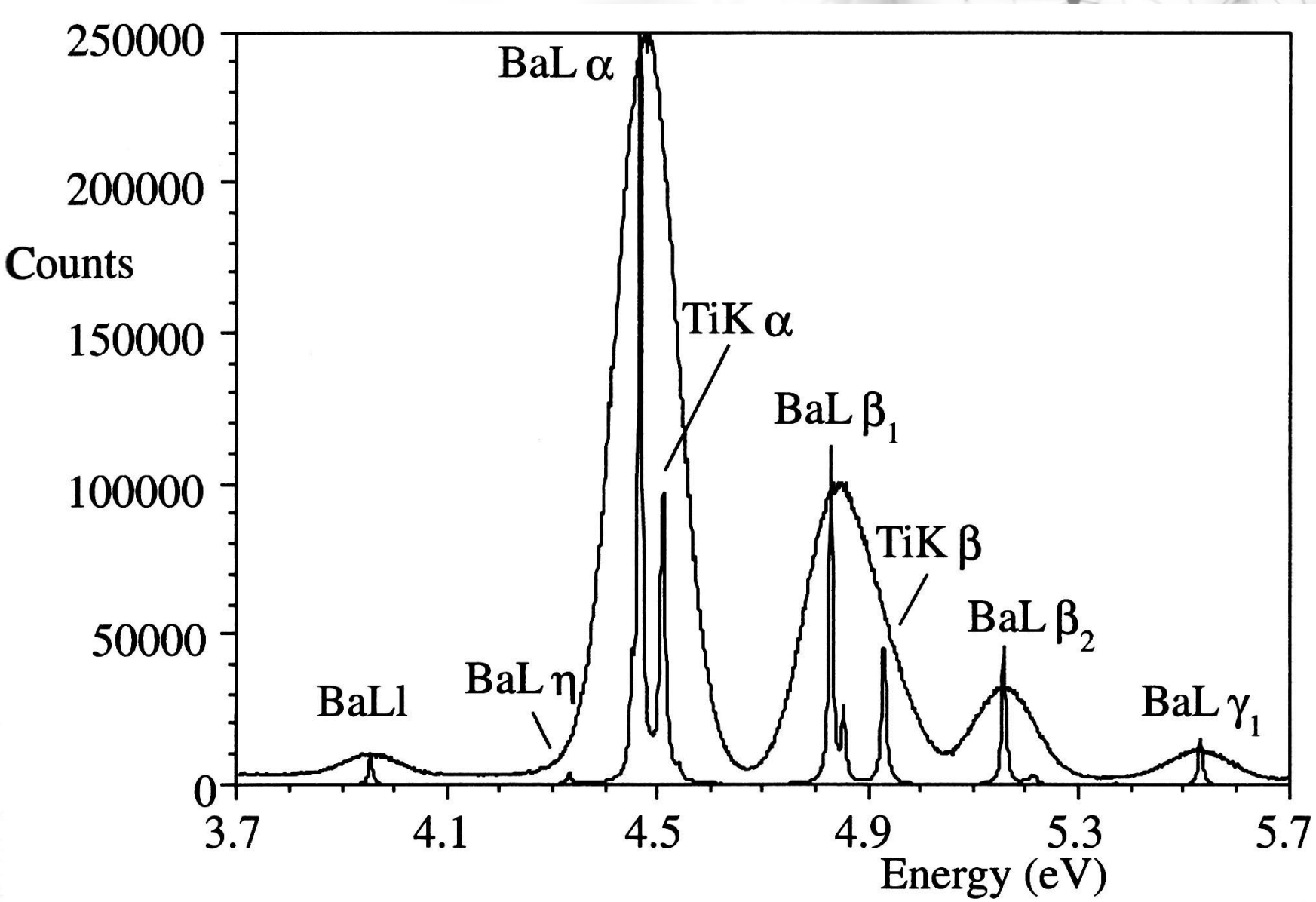

*EDXS vs. WDXS

	EDXS	WDXS
Energy resolution	~ **125 eV** @ Mn Ka (5.9 keV), <65 eV @ C Ka, depends on X-ray energy	**5 - 10 eV** (depends on crystal)
Collection efficiency Beam current	covered solid angle Si(Li) ~0.1 sr, up to >1 sr for large-area SDD + energy-dependent detector efficiency **minimal 10^{-10} A**	covered solid angle ~0.001 sr **minimal 10^{-8} A**
Spectral range	0-40 keV (Dispersion 20 eV/channel) **Spectral overview**	Limited by used crystals — Separate measurement of each interested emission line
Detection limitation	0,1 % (depends on elements, geometry, count rates)	**100 ppm** or even better
Data treatment	**Complicated evaluation** (Peak separation, background correction)	Often linear background correction
Spectral artifacts	Escape peaks, pulse pileup, scattering, peak overlap, window absorption (contamination)	Rare, second-order reflections
Samples	Topological (rough) surfaces as well (problematic quantification)	Polished surface for optimal focussing of X-rays

Essential Questions

- **Generation**
  - **Where do the X-rays come from?**
  - **How probable is the ionization of an atom by electron impact?**
    - **Ionization cross-sections**
  - **How probable is the emission of an element-specific X-ray?**
    - **Fluorescence yield**
- **Detection**
  - **How probable is the detection of such X-ray by the detector system?**
    - **Absorption, Fluorescence, Detector efficiency**

Interaction volume: X-Ray Generation

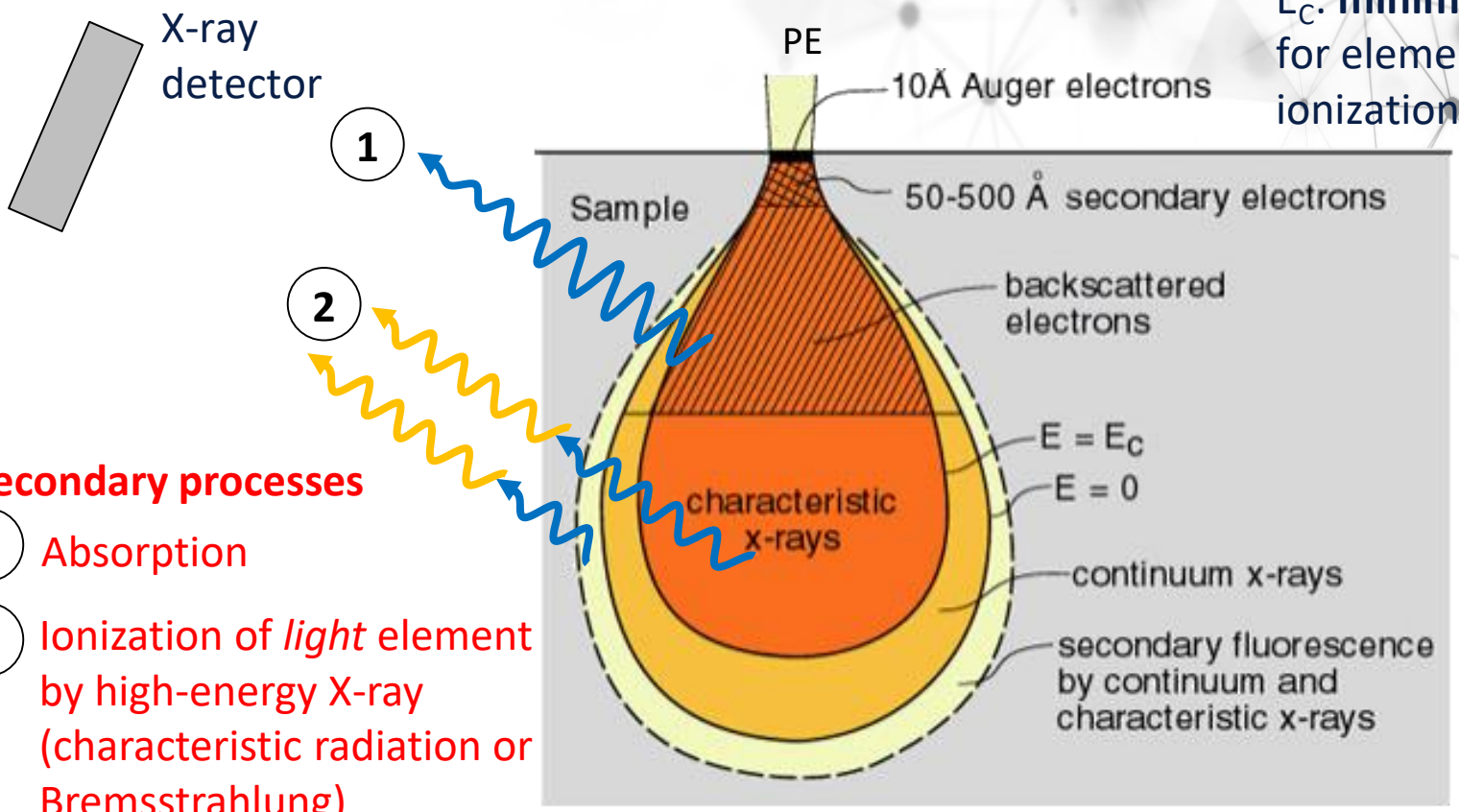

E_C: **minimum energy** for element-specific ionization (specific shell!)

Secondary processes

1. Absorption
2. Ionization of *light* element by high-energy X-ray (characteristic radiation or Bremsstrahlung)

Due to progressive energy loss along PE trajectories, the effective volume (part of the whole IV) for ionization (X-ray generation) of specific element (shell) depends on E_0 and E_c

- **Different elements A, B ($E_{C,A} \neq E_{C,B}$) → different volumina probed!**
- **Same element, but different X-ray emission lines → different volumina probed!**

Geometrical Effects

The larger U_{ac}, the larger the inter-action volume

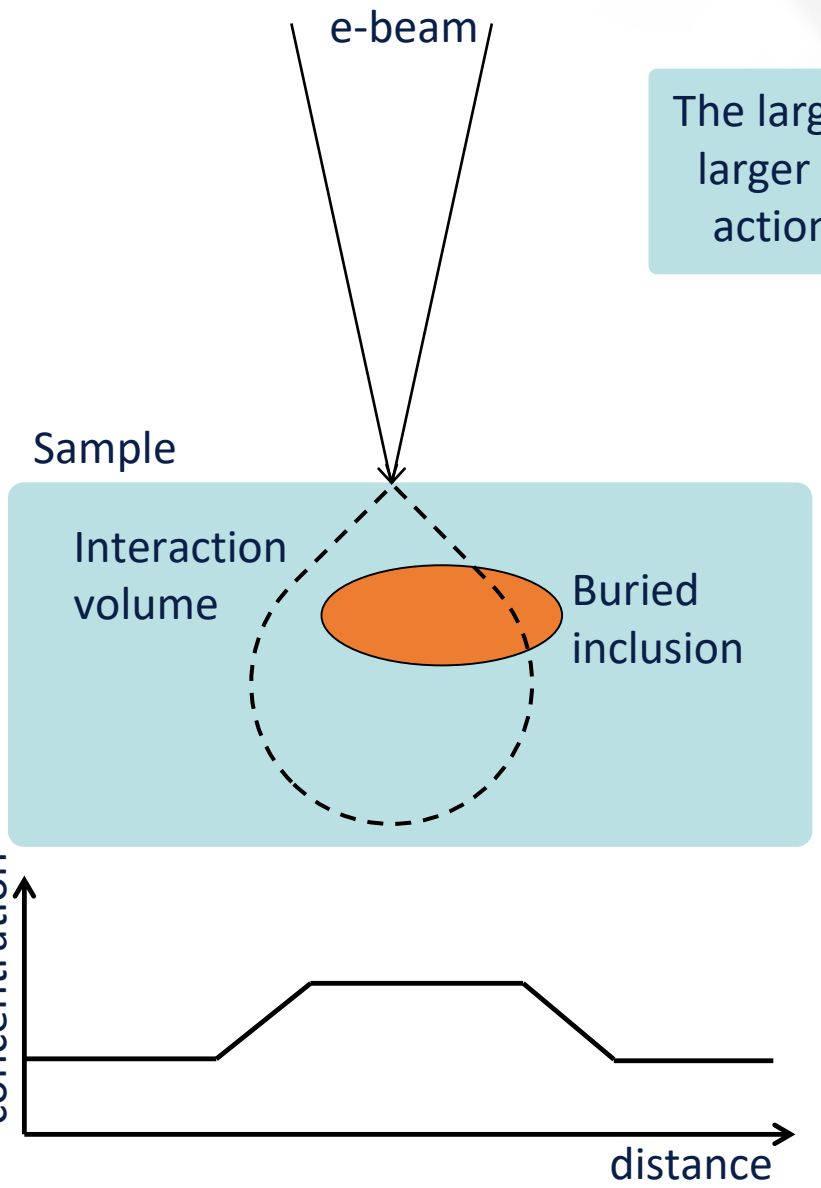

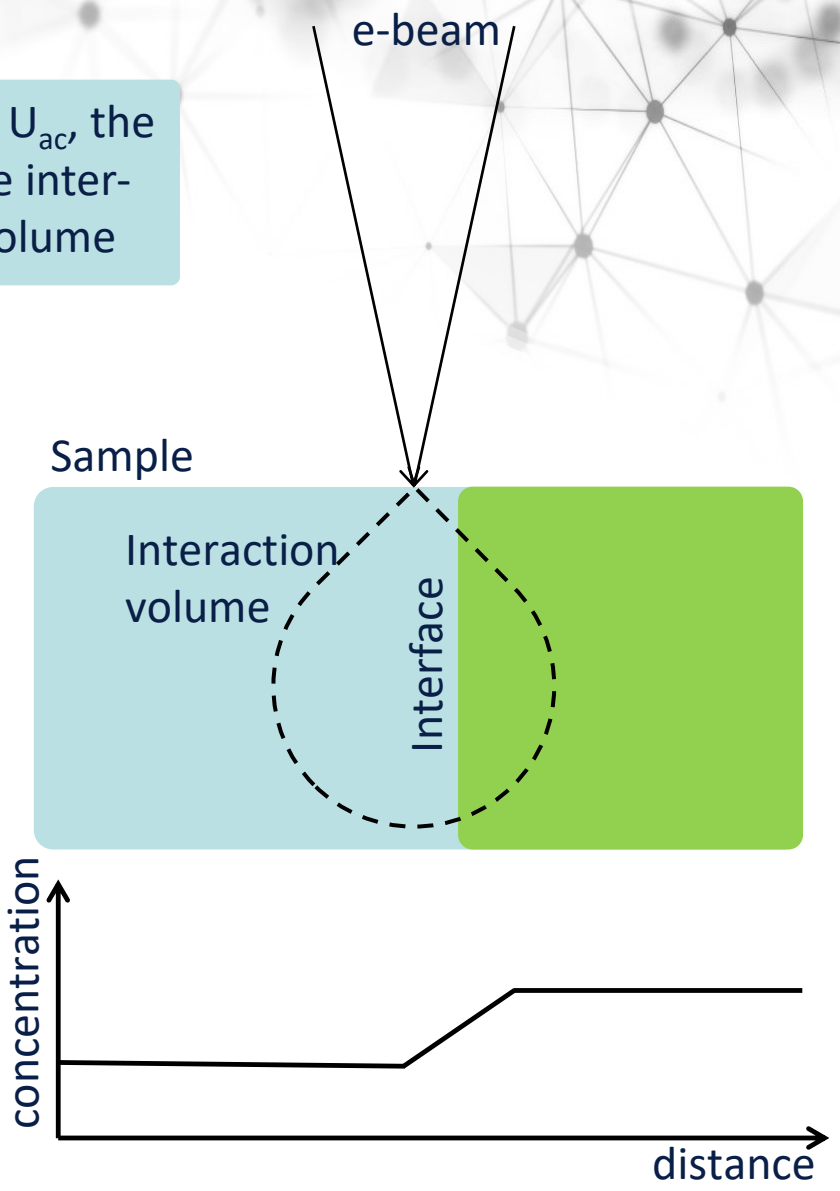

Resolution & Geometric Effects

Cu L 0.93 keV

Nb L 2.16 keV

30 kV

5 kV

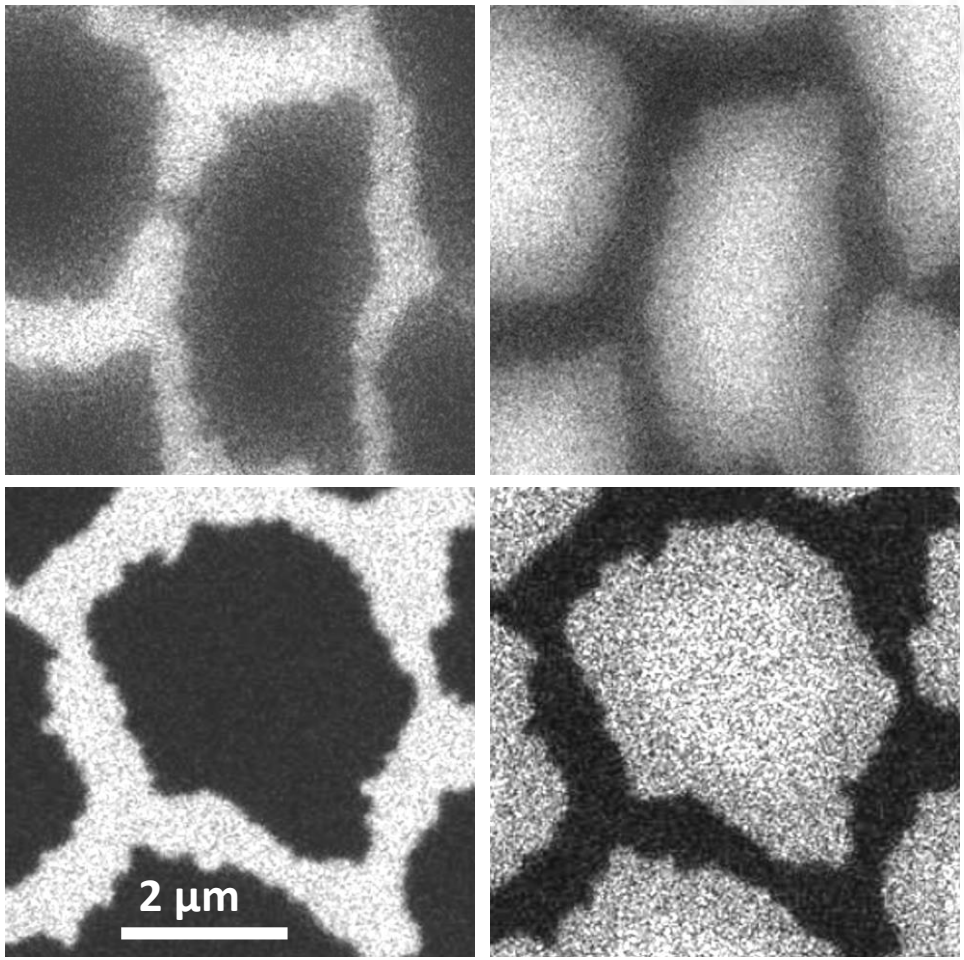

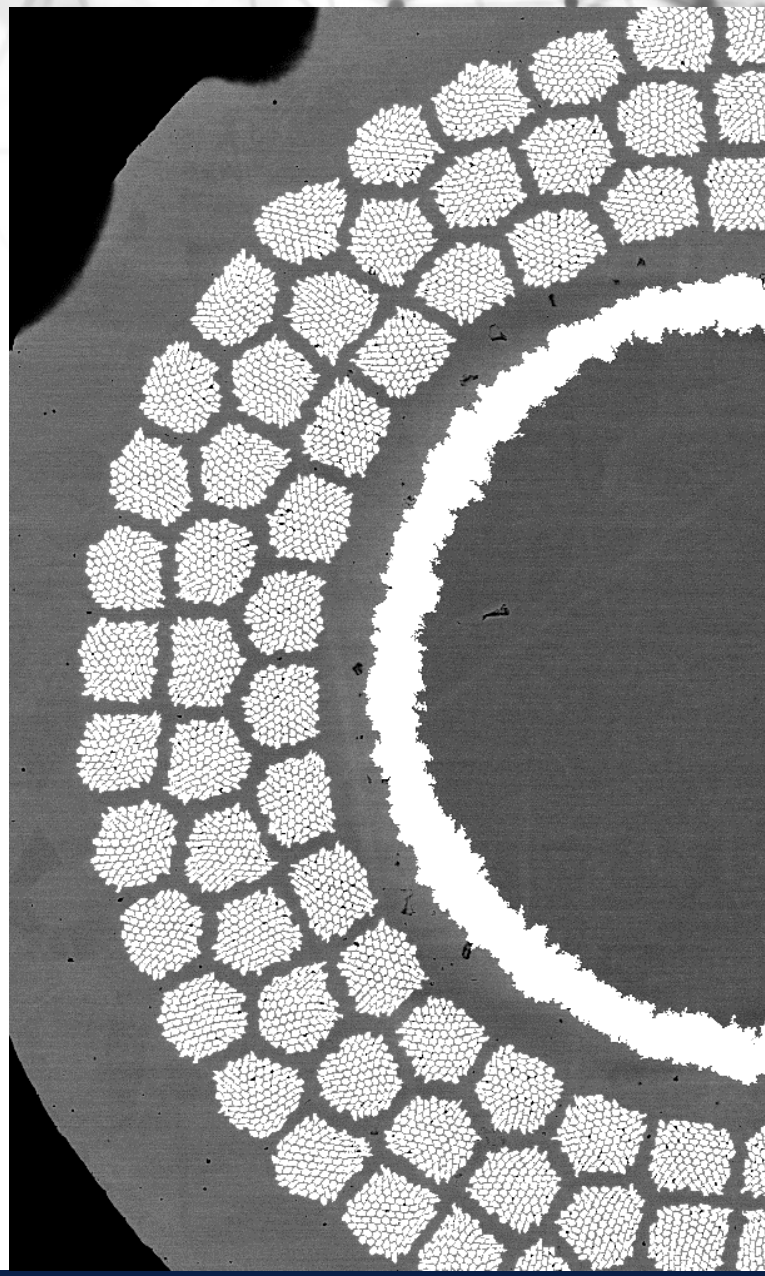

Much better EDXS resolution at lower primary energy → Adapt HT accordingly!

K-shell Ionization Cross-Section

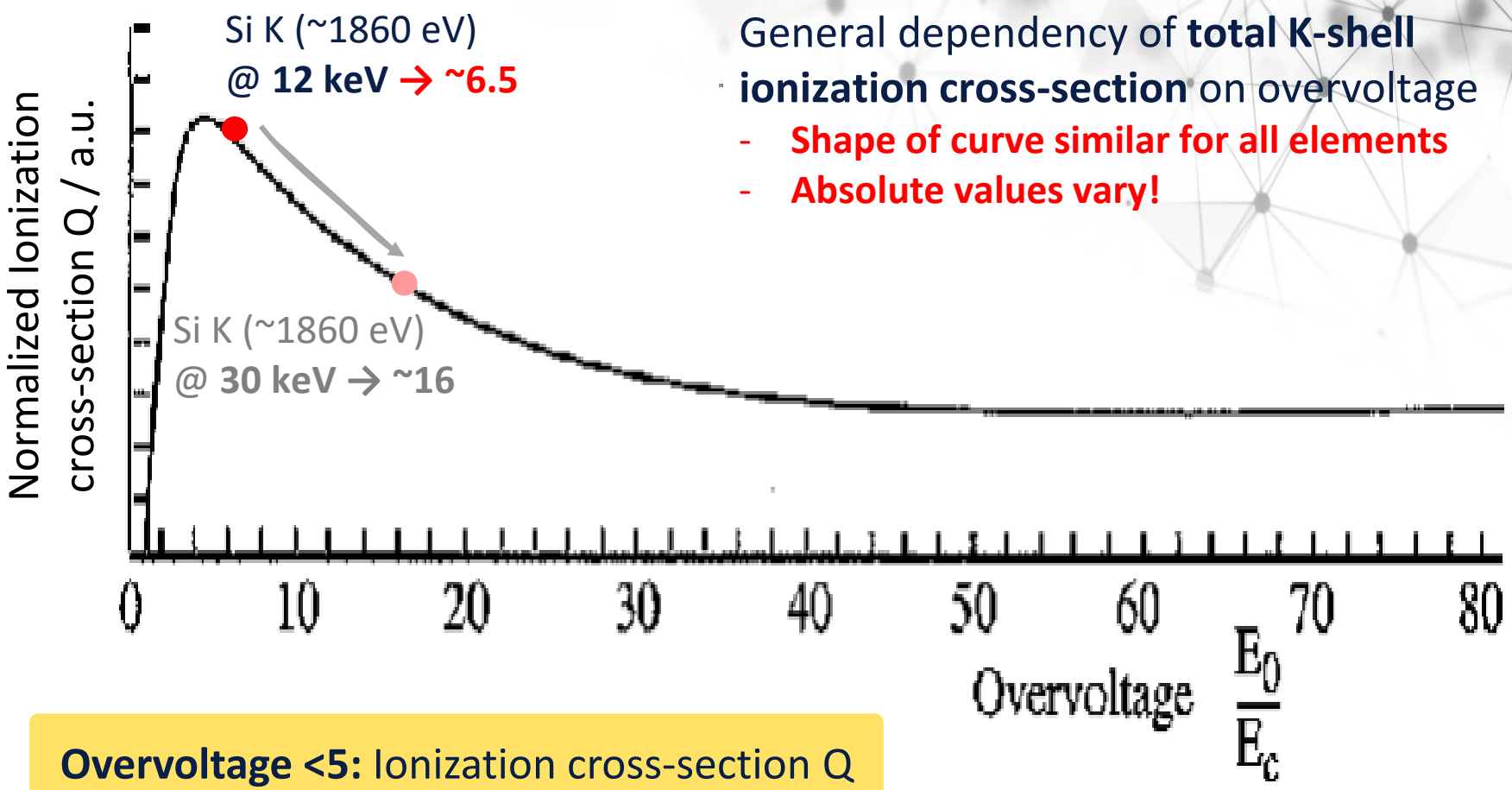

General dependency of **total K-shell ionization cross-section** on overvoltage

- **Shape of curve similar for all elements**
- **Absolute values vary!**

Overvoltage <5: Ionization cross-section Q increases with increasing overvoltage

EDXS in SEM: E_0/E_C min. 2.5, opt. 5

D.B. Williams, C.B. Carter, *Transmission Electron Microscopy* (Fig. 4.4)

K-shell Ionization Cross-Section

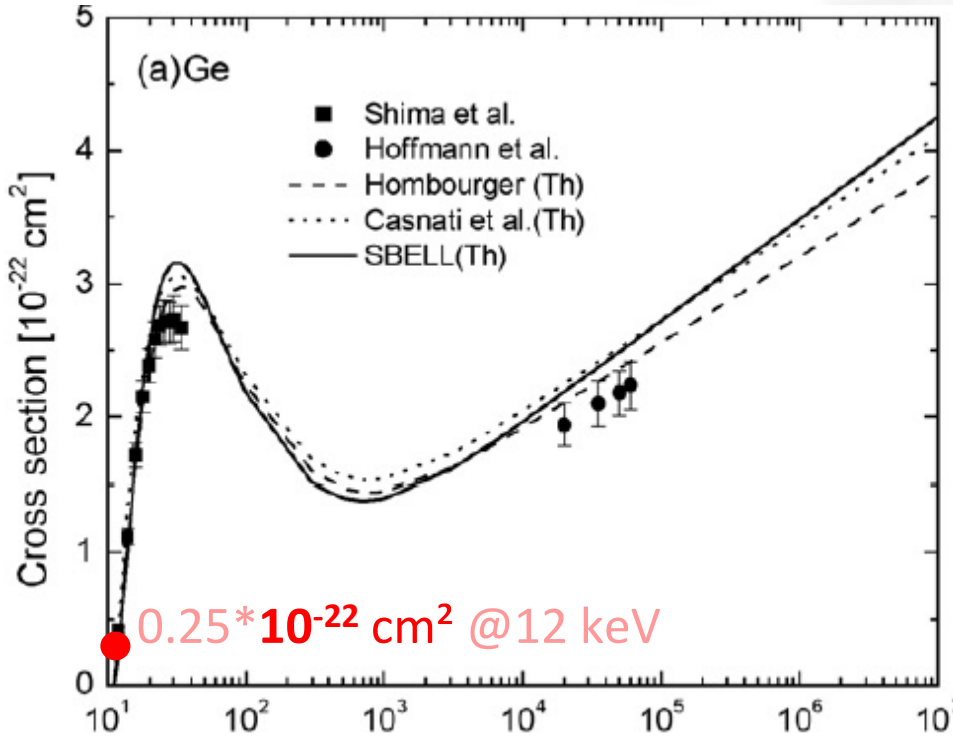

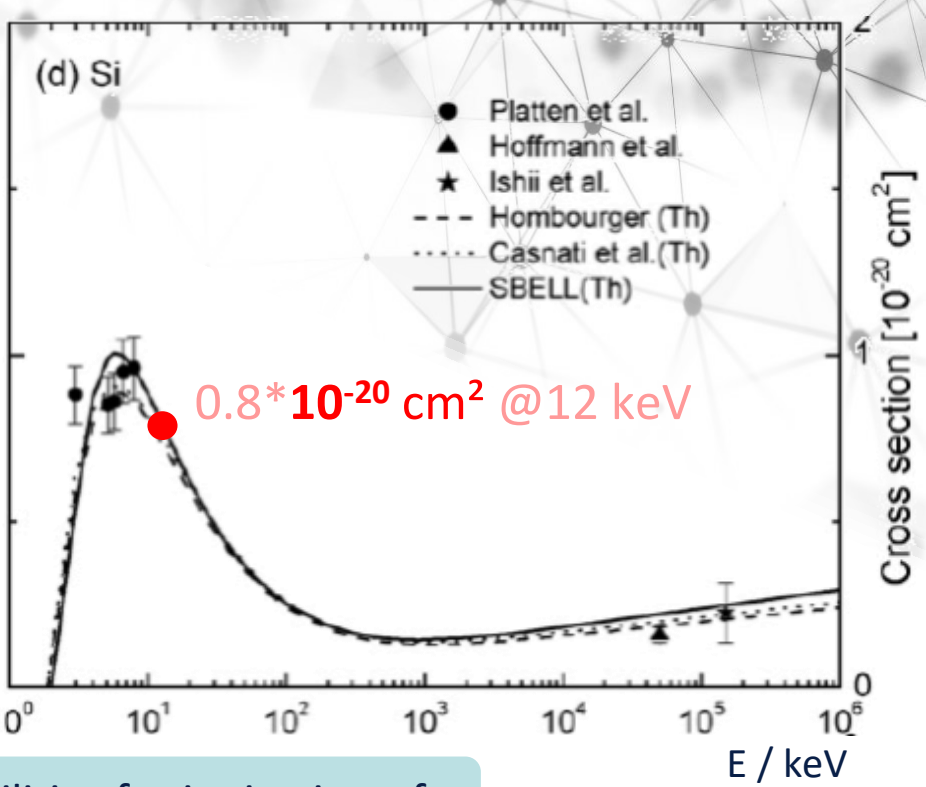

Strongly different probabilities for ionization of different elements in a multi-element sample

No intuitive interpretation of measured X-ray intensities

More aspects: X-ray emission + detection

M.R. Talukder, S. Bose, S. Takamura, Int. J. Mass Spectrom. 269 (2008) 118–130

Bulk — Matrix effects (ZAF)

Z Atomic number effect

PE loose energy the deeper they penetrate into the sample. The mean loss of energy depends on the average atomic number of the target material. **As a result the X-ray production depends on the depth below the surface (depth-distribution function Φ(z)).**

A X-Ray absorption

Some of the X-ray quanta produced in the sample are absorbed on their path toward the surface, depending on path length through sample

F Fluorescence

X-rays of higher energy can produce X-rays of lower energy by fluorescence

$$\frac{C_i}{C_{(i)}} = [ZAF]_i * \frac{I_i}{I_{(i)}} = [ZAF]_i * k_i$$

*Why Quantification?

Amorphous SiO_2 ($Si_{0.33}O_{0.66}$)

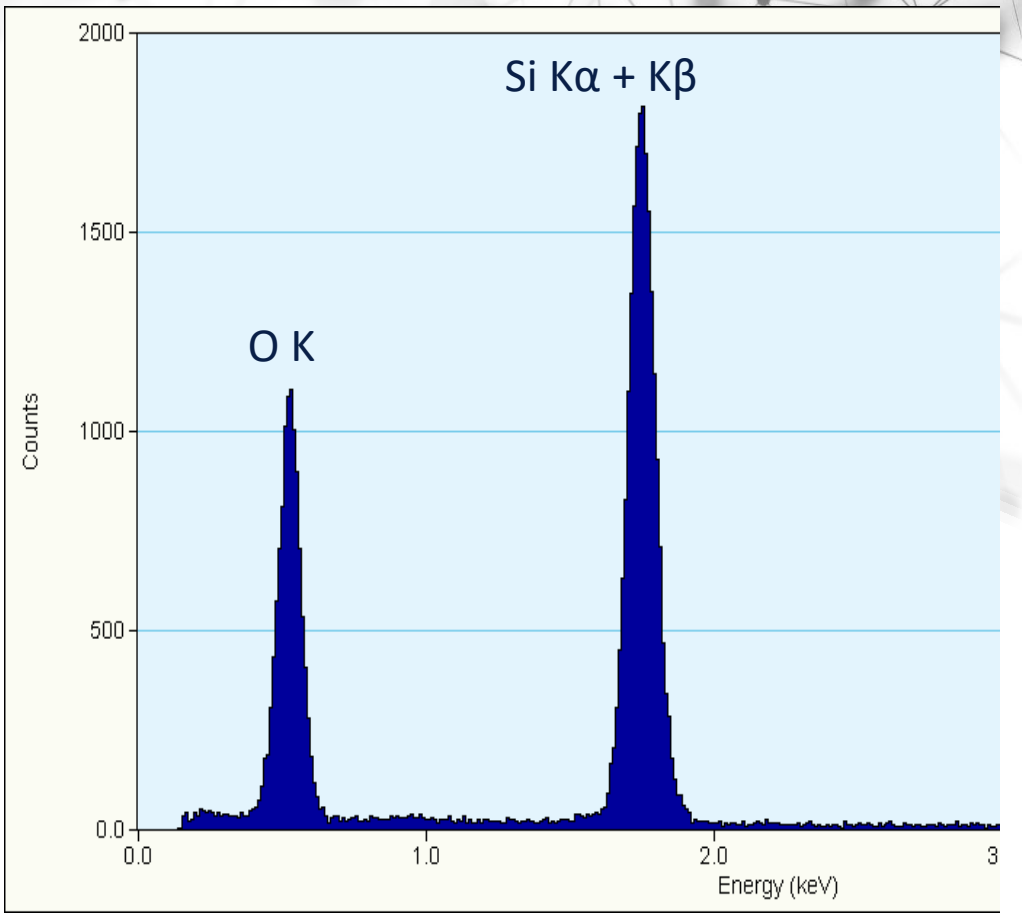

*Quantitative Analysis

- **Quantitative analysis:** What is the local concentration of the present elements?

- **Background correction** (empirical, linear, Top-Hat filtering)
- **Determination of net intensities** (multiple peak fitting, deconvolution)
- **Check residual spectrum!**
- **Selection of feasible emission lines**
- **Quantification** by theoretical approach (ionization cross-section, X-ray yield, detector efficiency, etc.) or reference material (k-factor)

*Why Quantification?

Amorphous SiO_2 ($Si_{0.33}O_{0.66}$)

Spectrum pre-processing:

- Peak identification
- Energy calibration
- Background correction
- Extraction of net intensities (fitting)

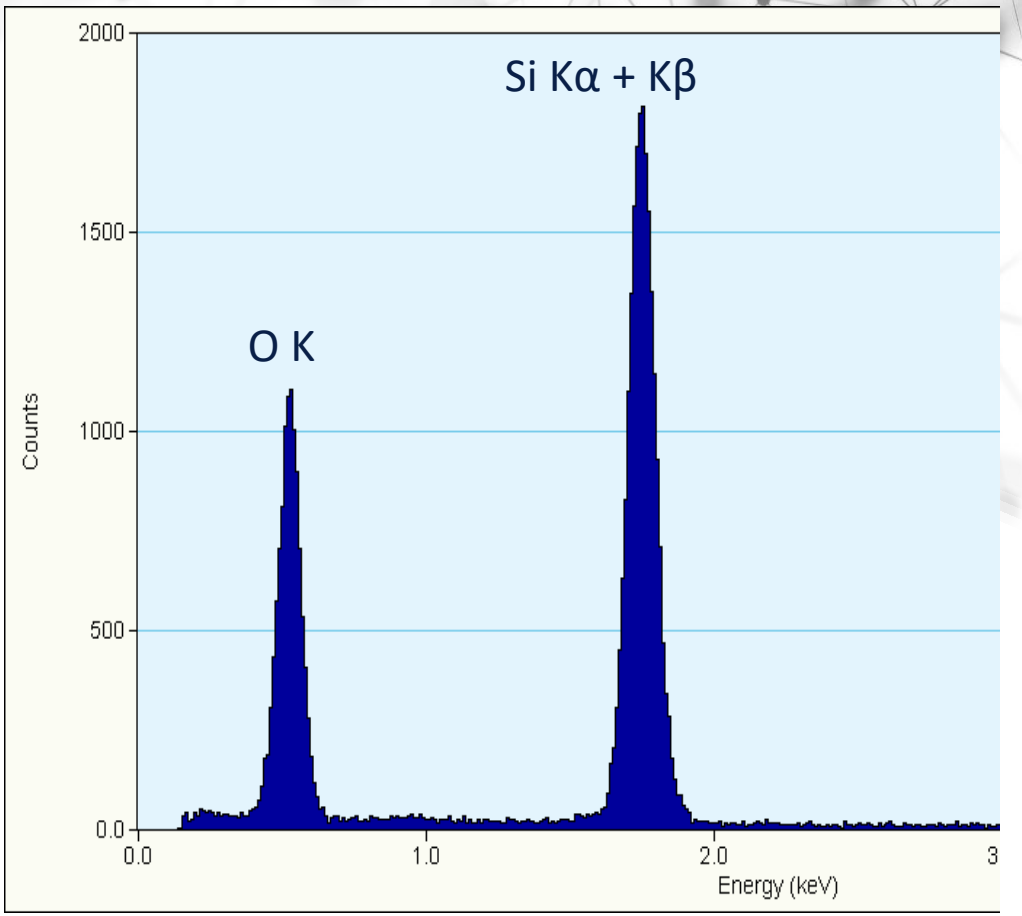

*Why Quantification?

Amorphous SiO_2 ($Si_{0.33}O_{0.66}$)

Spectrum pre-processing:

- Peak identification
- Energy calibration
- Background correction
- Extraction of net intensities (fitting)

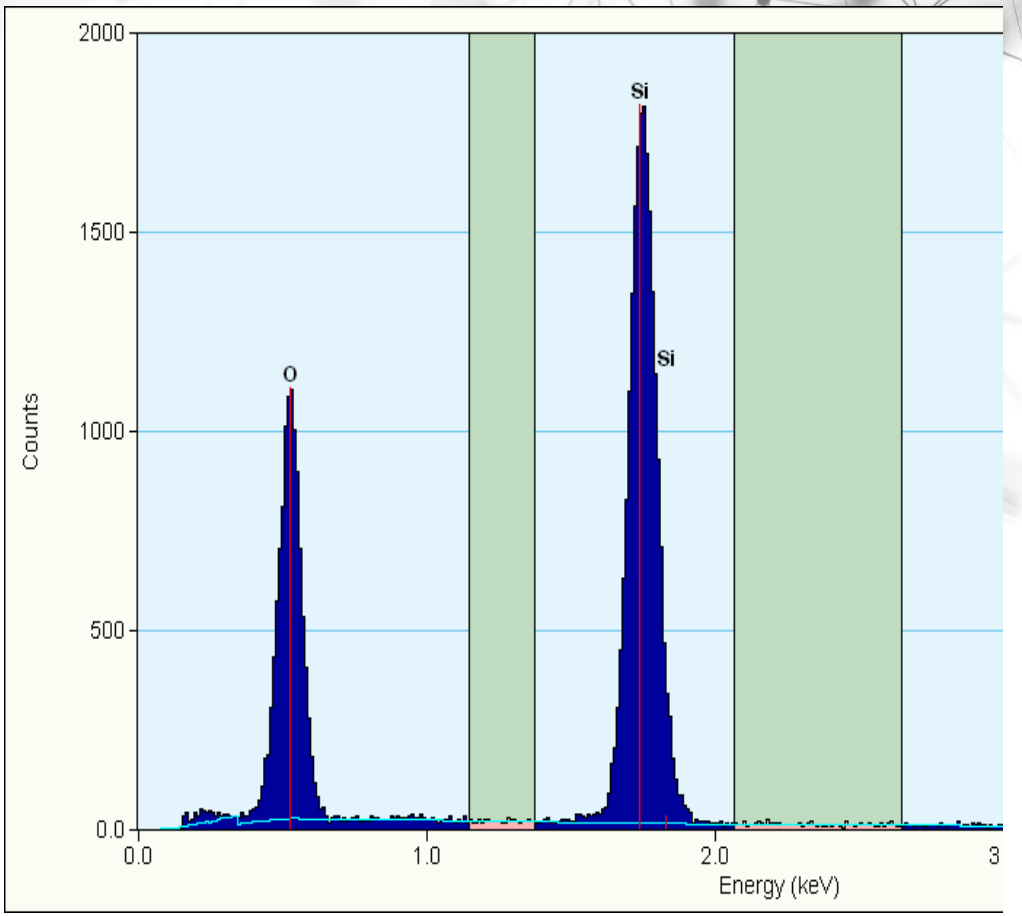

*Why Quantification?

Amorphous SiO_2 ($Si_{0.33}O_{0.66}$)

Spectrum pre-processing:

- Peak identification
- Energy calibration
- Background correction
- Extraction of net intensities (fitting)

  O-K 10380 counts

  Si-K 20320 counts

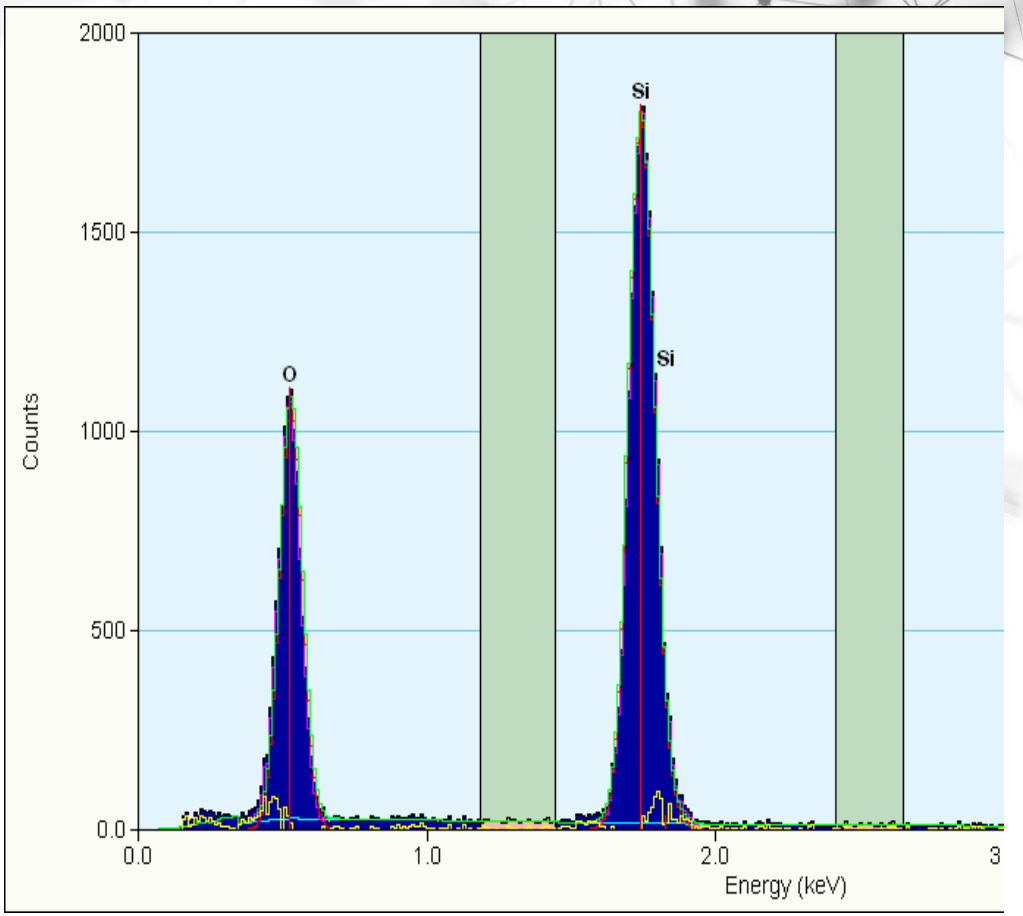

*Why Quantification?

Amorphous SiO_2 ($Si_{0.33}O_{0.66}$)

Spectrum pre-processing:

- Peak identification
- Energy calibration
- Background correction
- Extraction of net intensities (fitting):

O-K	10380 counts
Si-K	20320 counts

- **Quantification**

Element	Atomic %	Correction
O(K)	**63.90**	0.49
Si(K)	**36.09**	0.92

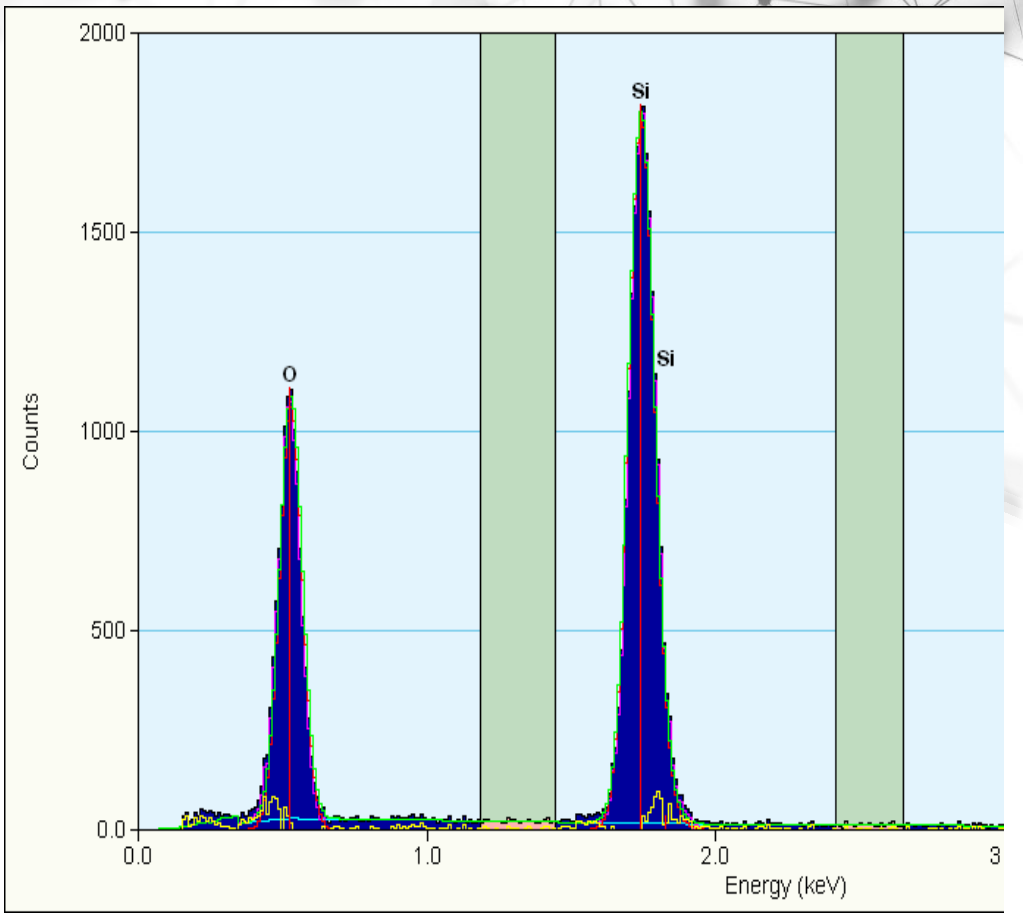

Focused Ion Beam (FIB)

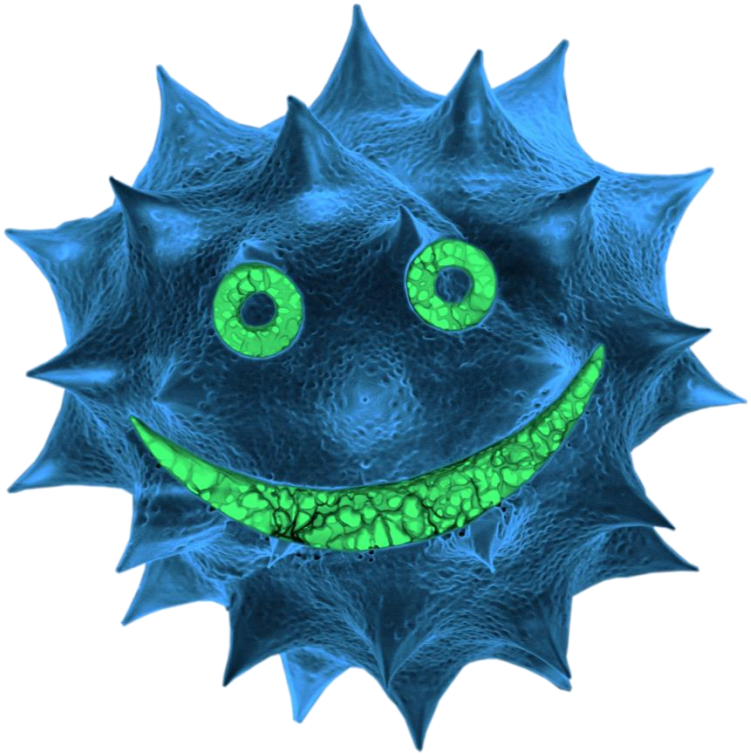

Focused Ion Beam (FIB)

Dual Beam set up

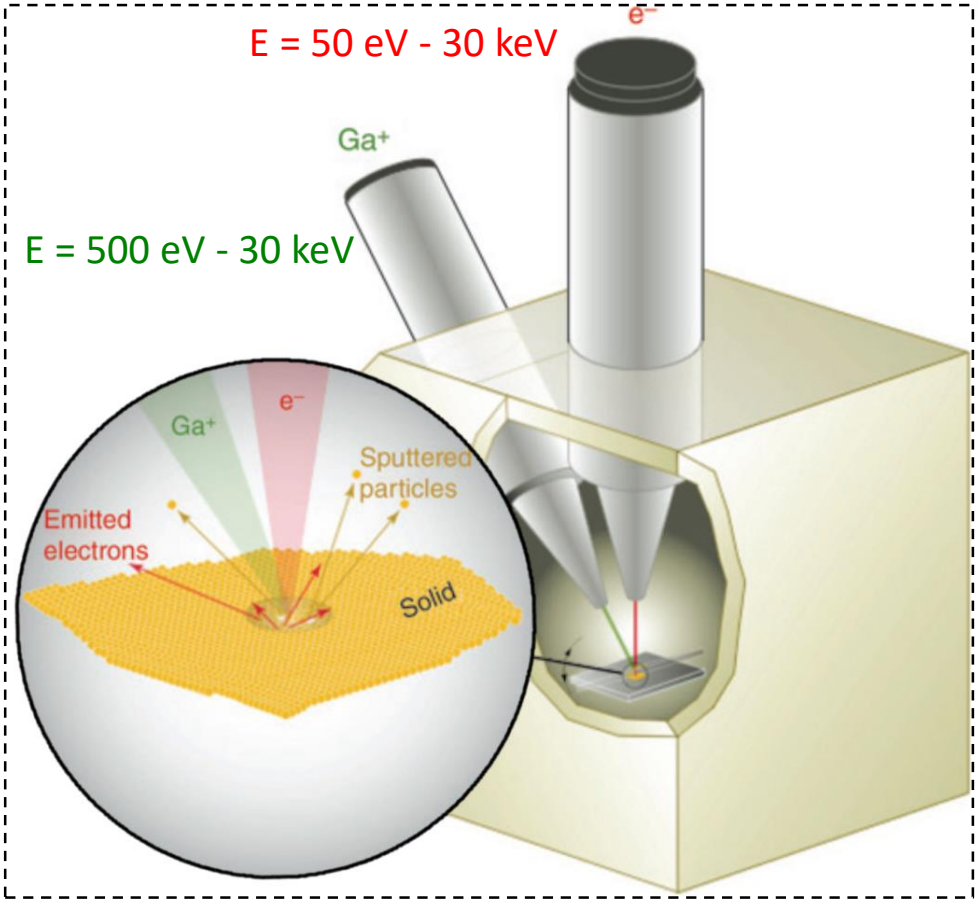

Volkert and Minor (2007)

FIB functionality

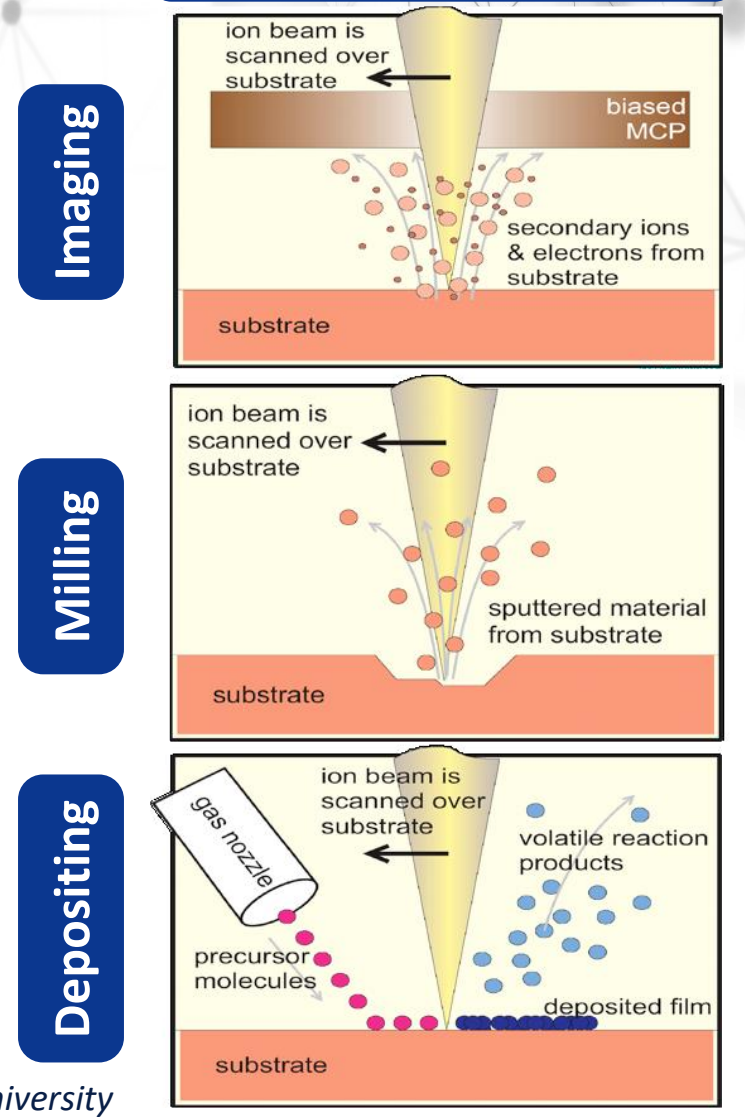

F. Ernst, Case Western University

Motivation - fields of application

Cross sectioning

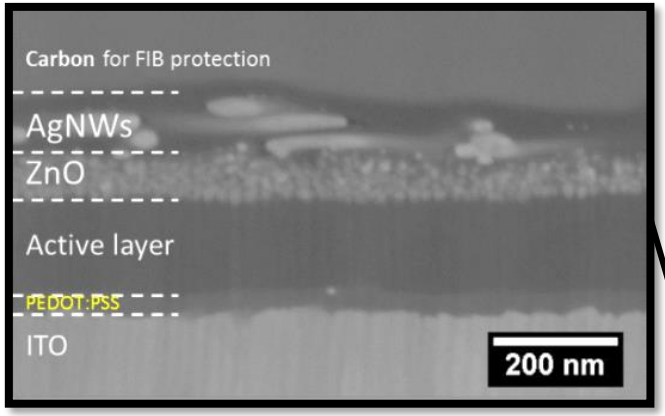

Organic solar cell device

TEM sample preparation

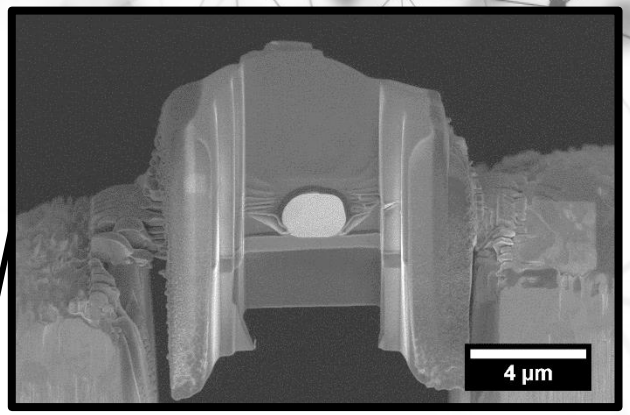

Compressed Au microparticle

FIB

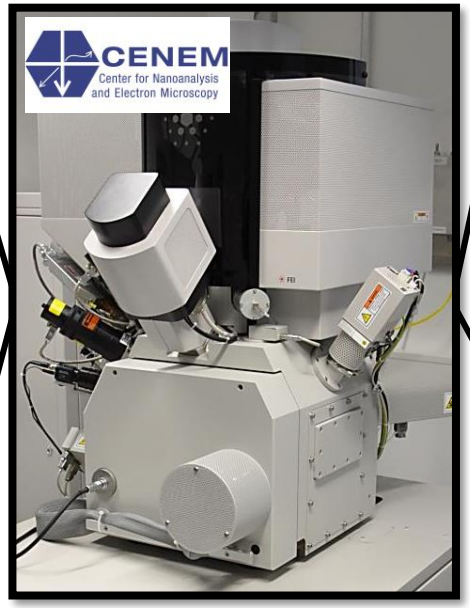

In situ testing (i.e. micromechanics)

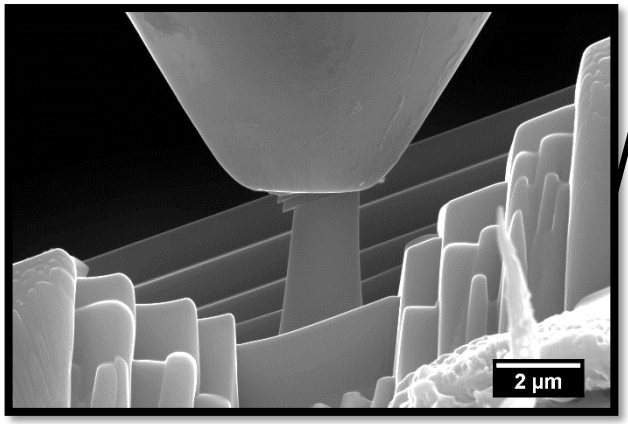

Layered crystal (VSe_2)

Further fields of application

(FIB tomography, prototyping & nanofabrication, micromanipulation, ...)

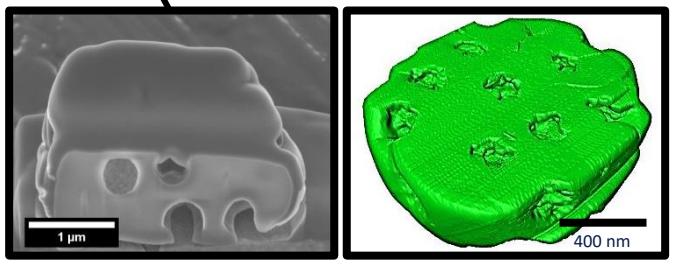

FIB tomography of zeolite particle

Instrumentation – FIB source

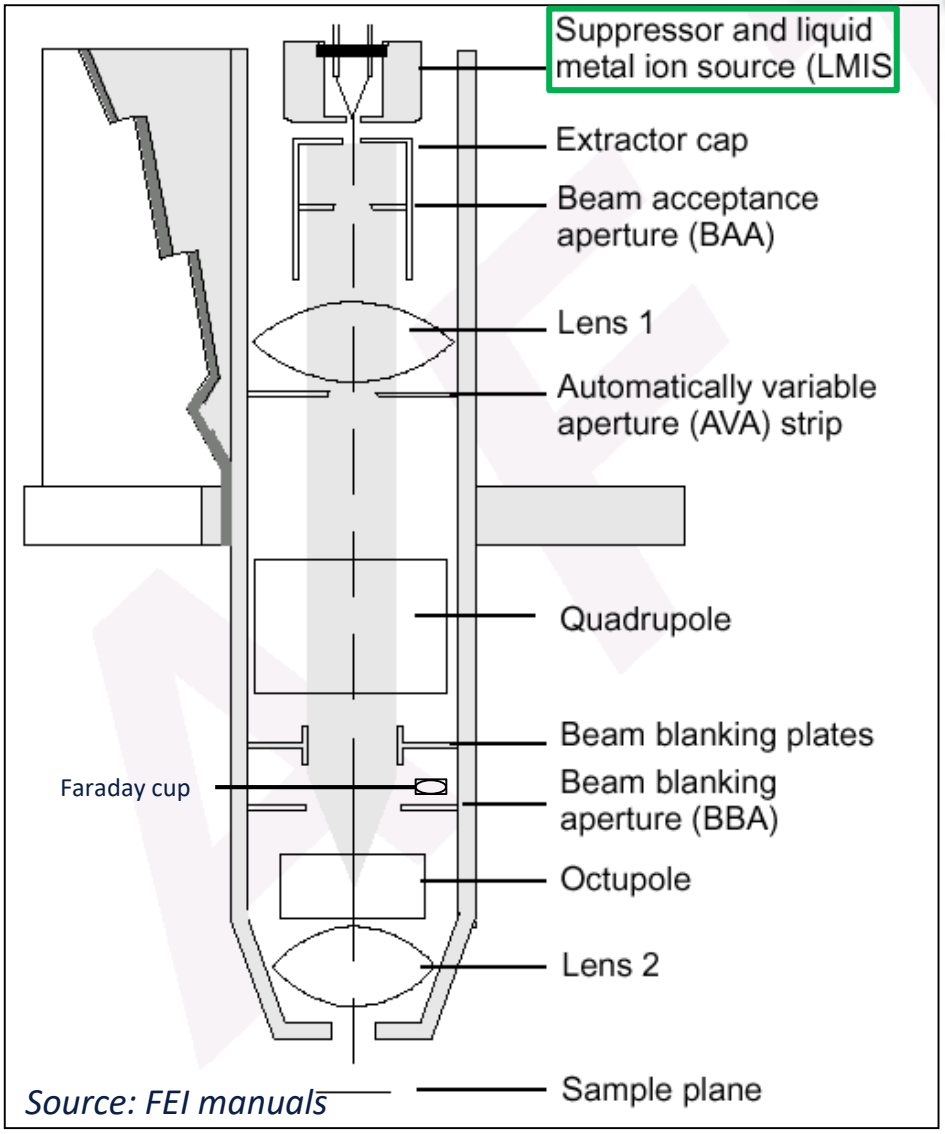

Source: FEI manuals

Liquid metal ion source (LMIS)

consumable (lifetime ~ 1000 – 4000 working hours)

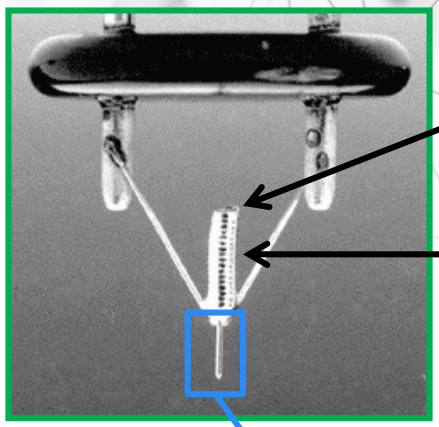

Source: FEI manuals

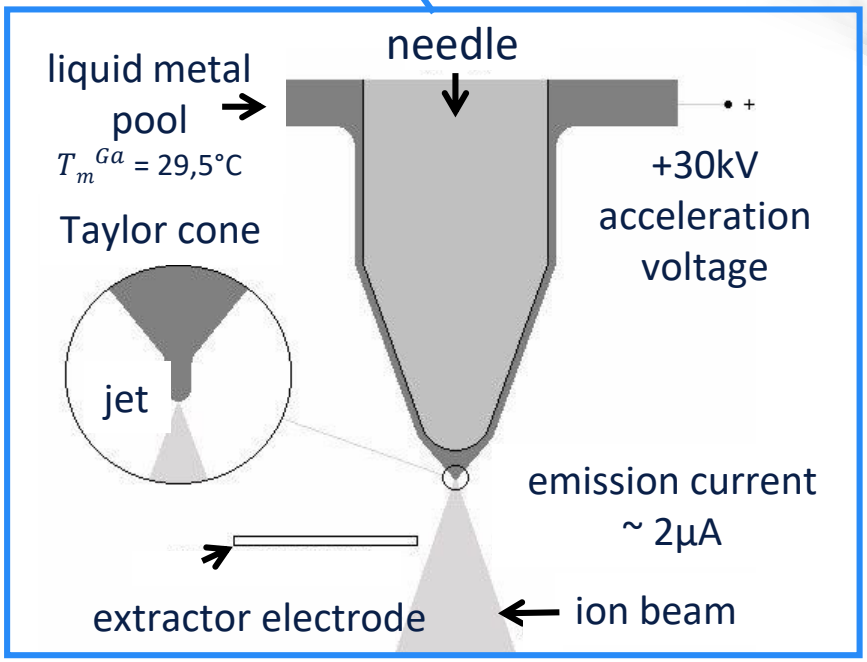

http://www.hindawi.com/journals/ijae/2011/361215.fig.002.jpg

Instrumentation - optics

V. A. G. Rivera, Plasmonic Principles and Applications, 2012

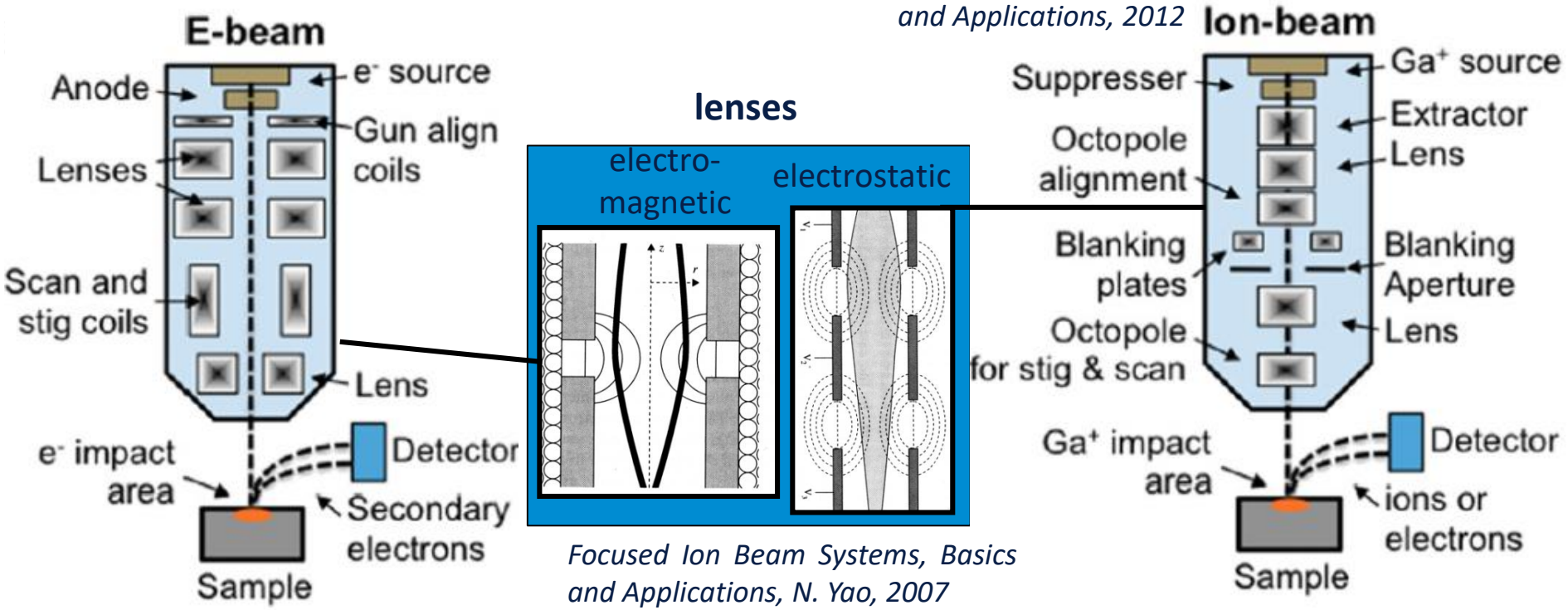

Focused Ion Beam Systems, Basics and Applications, N. Yao, 2007

E-beam column	Fundamental differences:	Ion-beam column
Field emission gun (FEG)	source	Liquid metal ion souce (LMIS)
electrons	probe	Ions (much heavier)
Electromagnetic lenses	beam deflection	Electrostatic lenses

Instrumentation – electro-magnetic vs. electrostatic lenses

electro-magnetic

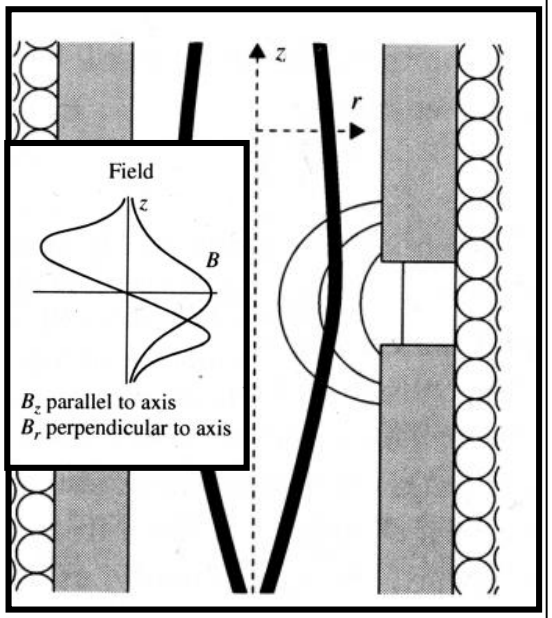

Focused Ion Beam Systems, Basics and Applications, N. Yao, 2007 (p. 17 & 19)

$$\vec{F} = q\vec{v} \times \vec{B}$$

deflection angle γ **dependent on mass**

$$\gamma \sim \sqrt{\frac{q}{m}}$$

Gallium ions vs electrons at 30 keV

$v(ion) = 0.28\% \cdot v(electron)$

while $p(ion) = 370 \cdot p(electron)$

Deflection of ions by electrostatic lenses

B: magnetic field strength	q: el. charge
V: voltage	v: velocity
E: electrical field strength	P: momentum
F: acting force	m: mass
γ: small deflection angle	

electrostatic

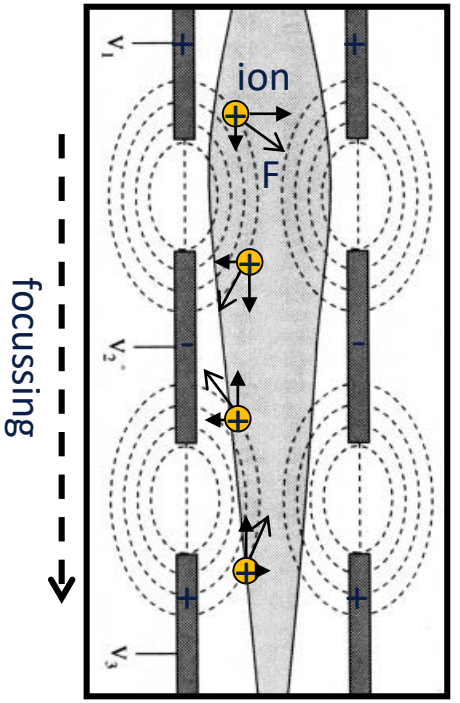

$$\vec{F} = q\vec{E}$$

deflection angle γ **independent of mass**

See lecture SEM-instrumentation I (p. 24-28)

Instrumentation – Ion Pathway

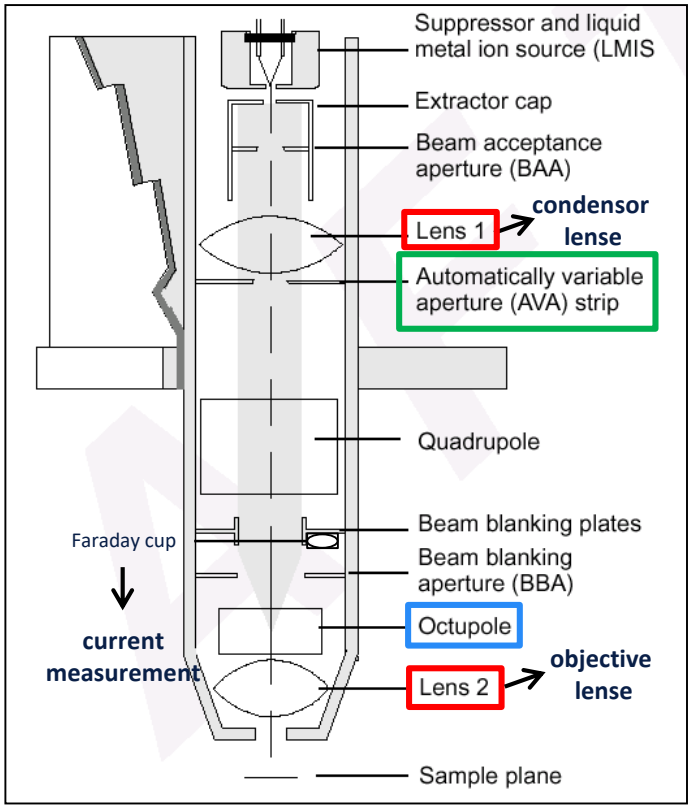

Source: FEI Manuals

APERTURE STRIPE (consumable)

→ limiting beam current/spot size

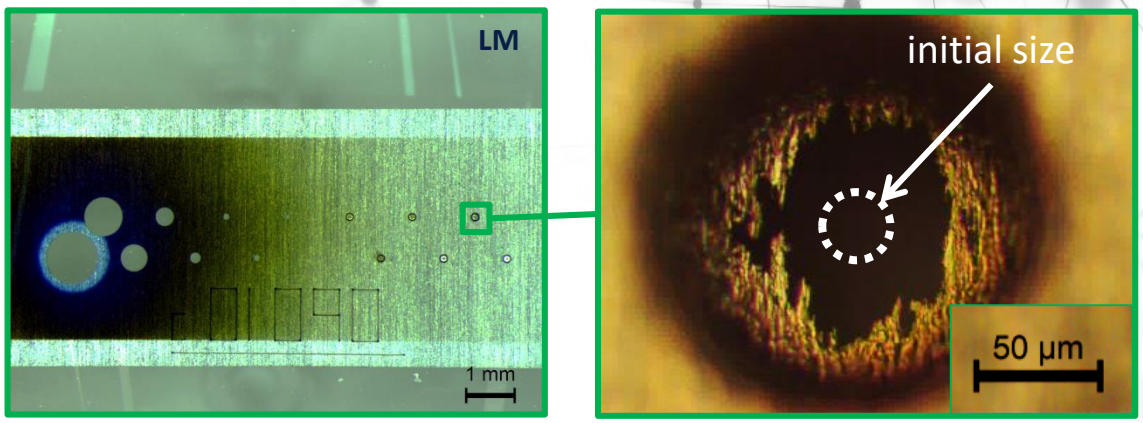

→ worn out aperture

Octupole

→ handling astigmatism, deflection

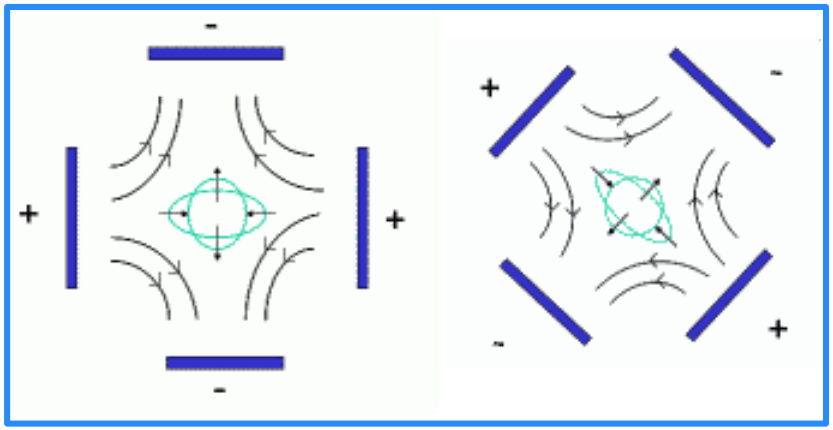

Detection of secondary ions (SI)

In chamber electron & ion (ICE) detector:

- Detector **based on ETD principle** (scintillator → light pipe → PMT)
- **Conversion electrode** between grid and scintillator **enables secondary electron (SE) or secondary ion (SI) detection**
- Signal chain: **secondary ions → converted to secondary electrons** → generate photons on the scintillator → generate electrons in the photomultiplier → preamplifier → video signal

SI mode

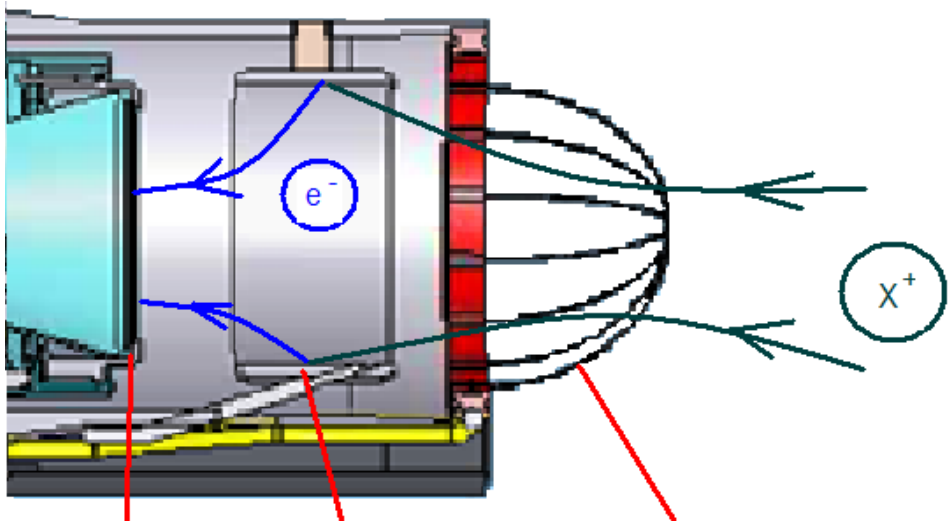

SE mode

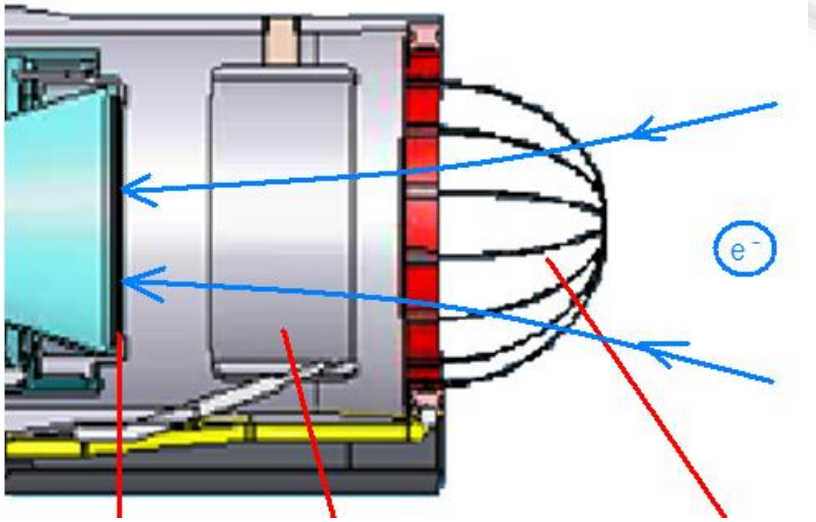

Source: FEI, ICE Detector Presentation

FIB imaging resolution

In principle not limited by diffraction, but by several other parameters:

- Lens aberrations
- Space Charge Effects
- Source Size
- Interaction volume

Gallium FIB resolution: ~4nm

Ultimate limit: signal to noise ratio before destroying the information in a sample

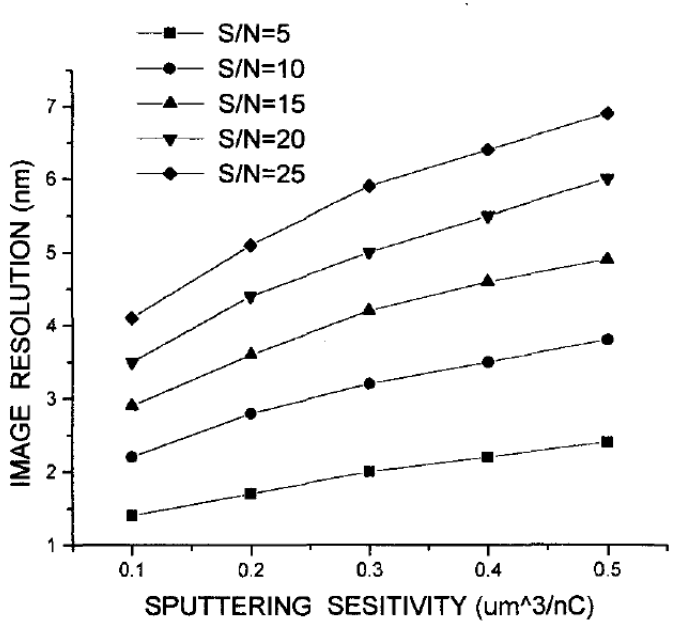

Orloff, Phys. Fac. Pub. And Pres., 1996

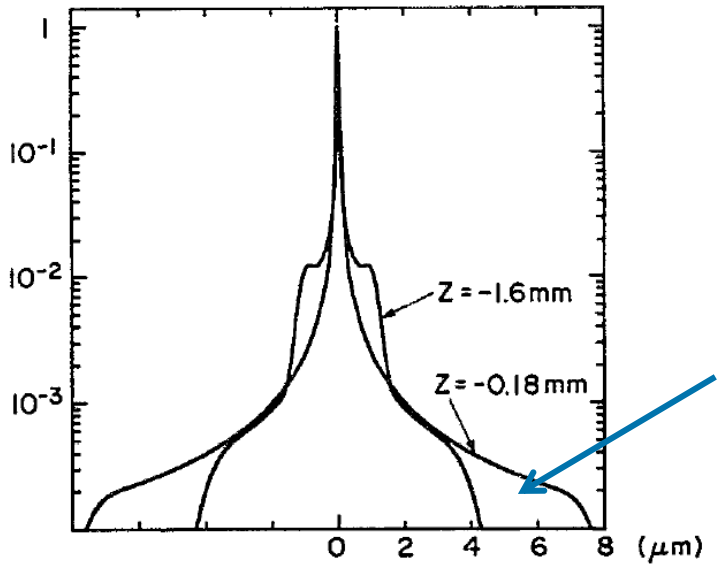

Beam tail

Current density at different focussing parameters

Coloumb interactions

In practice one of the biggest problems is **Energy spread** and **beam broadening** due to **Coloumb repulsion** between ions.

- High current densities near the source ~ 10^6 A/cm²
- Increased energy spread and virtual source size
- Increased contribution of the chromatic abberation

Resolution vs Beam current

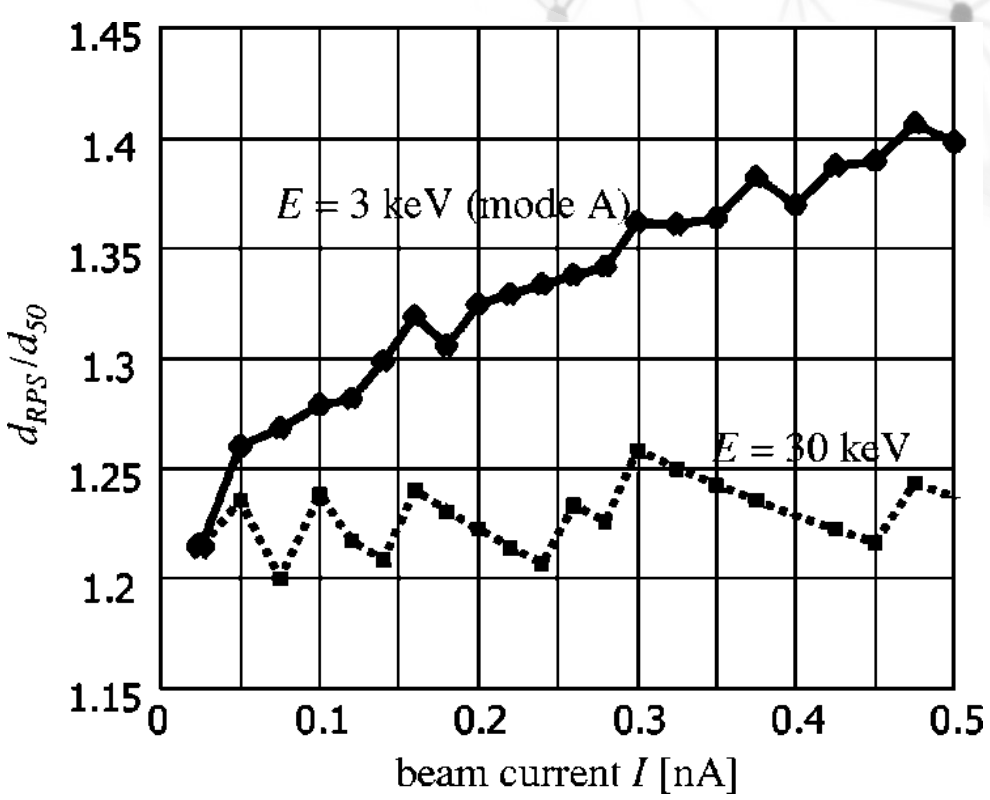

Ruscher, J. Appl. Phys, 2005

Gas injection systems (GIS)

Gas injection systems for material deposition (e.g. Pt, C)

- Local e^--beam or ion-beam induced material deposition by cracking of precursor gas
- Application examples:
  - **Protective layers** against ion beam damage (cross sectioning, preparation of TEM lamella, …)
  - **Attachment** of micro- and nanoobjects (e.g. transfer of TEM lamella)

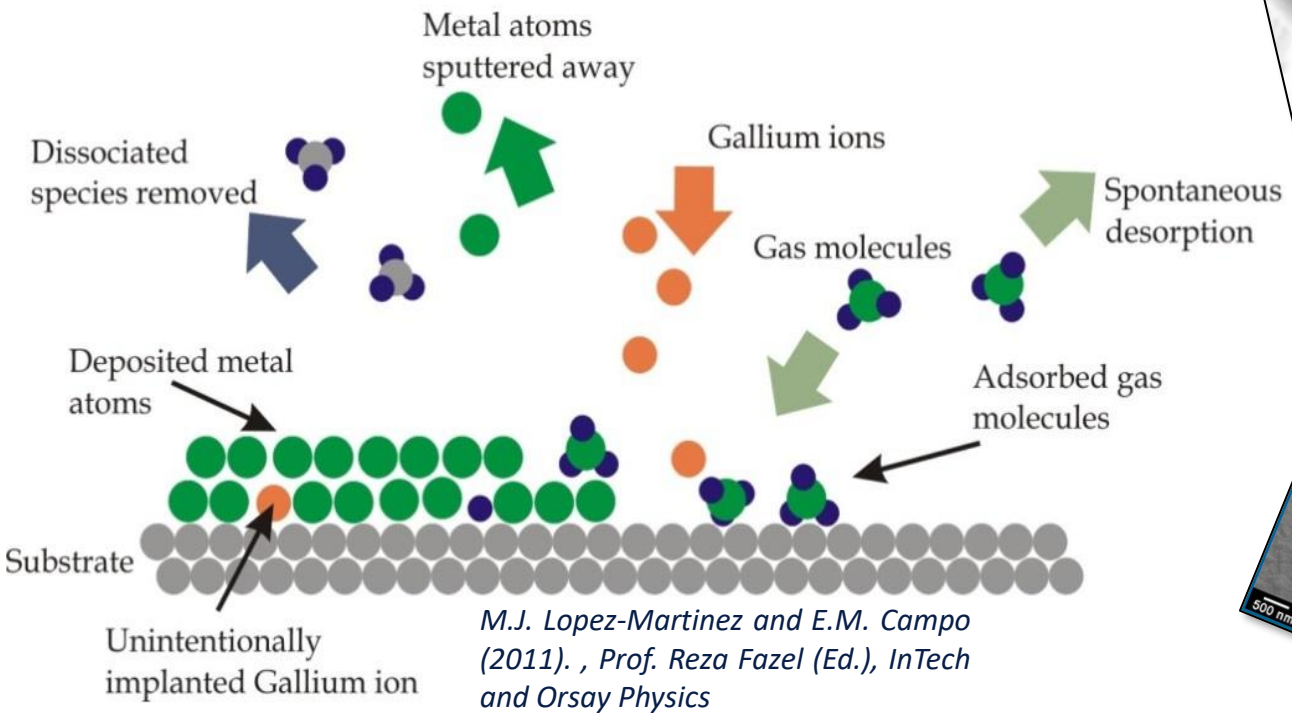

M.J. Lopez-Martinez and E.M. Campo (2011). , Prof. Reza Fazel (Ed.), InTech and Orsay Physics

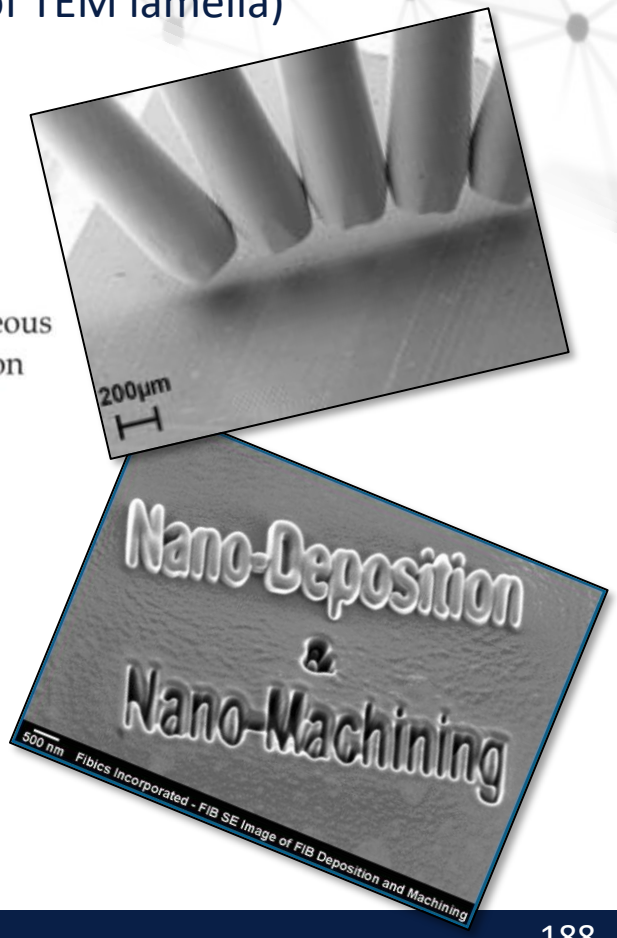

Platinum deposition with the electron/ion beam

Precursor for deposition: **Metallorganic complex**

HRTEM of deposition layers

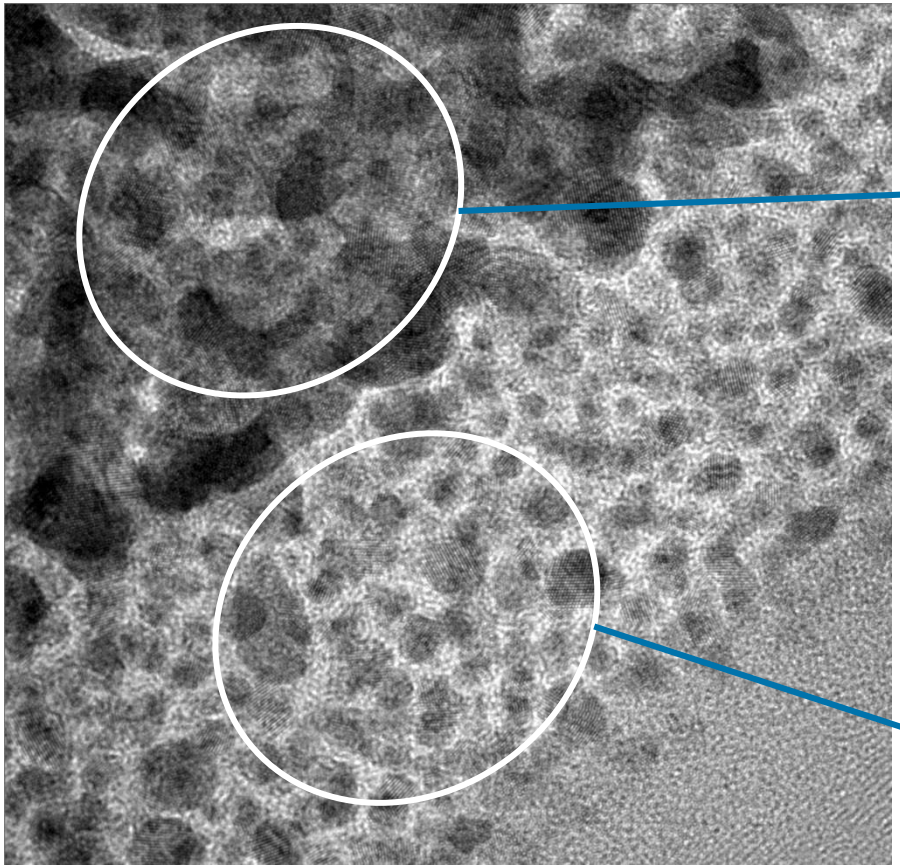

Ion beam induced deposition

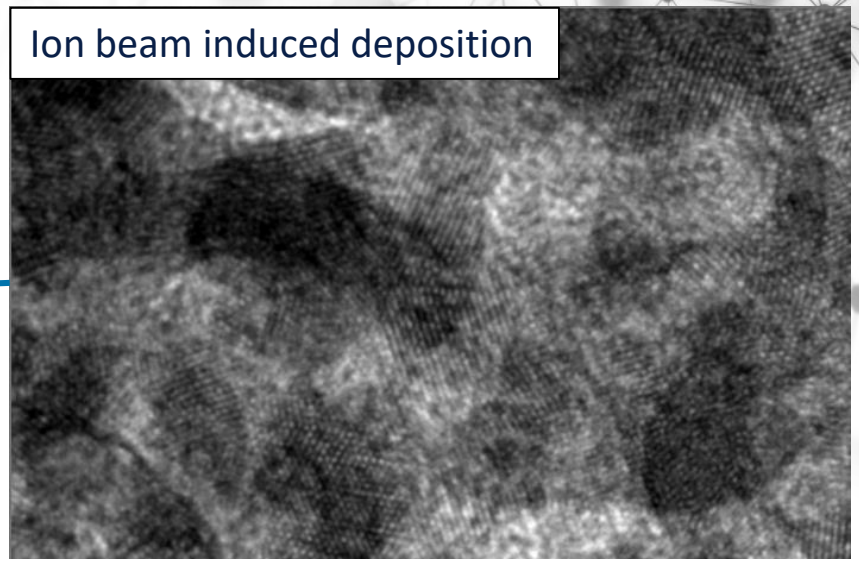

Electron beam induced deposition

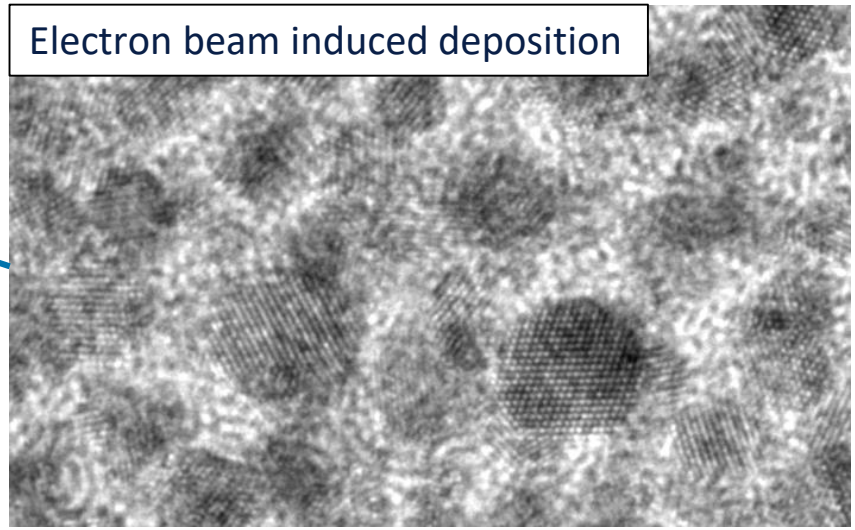

The Deposition is different from the real metal!

Schweizer, unpublished work, 2014

Comparison between ions and electrons

Electron

Gallium^{+} Ion

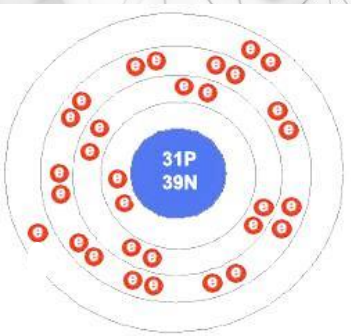

Mass:	5,49 x 10^{-4} u	69.72 u (factor of 125000x)
Charge:	-1	+1
Velocity at 30 keV:	1x10^{8} m/s	2.8x10^{5} m/s (factor of 0.0028)
Wavelength at 30 keV:	**7** pm	**0.02** pm
SE yield at 20 keV:	0.5-0.75	1-2

Both electrons and ions are **charged particles** but ions are much **heavier!**

⇨ **The detailed interactions of ions with matter have to be considered**

Ion Interactions with solids

Ion-solid interactions can be understood with a **collision cascade**

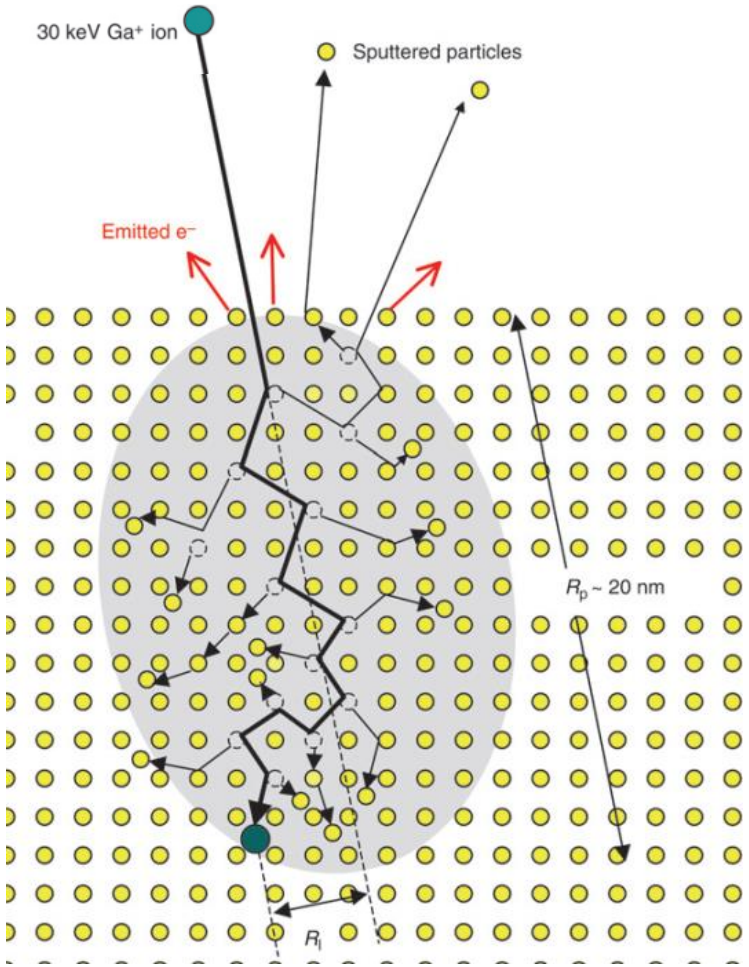

Volkert et al. MRS Bulletin ,Volume 32 , May 2007

Different Signals escape the solid upon ion interaction which can be collected for **imaging** and **spectroscopy**

Ions are **slowed down** in a cascade until they come to rest

Energy is transferred to the solid according to the **Stopping Power *S***

$$S(E) = -\frac{dE}{dx}$$

Signals and Imaging contrast

- **Emitted signals:**

- **Secondary electrons**
- **Secondary ions**
- **Backscattered ions**
- **Ionoluminescence**
- **X-ray**
- **Auge**

Commonly used Signals for Imaging

Image contrast influences similar to SEM:
Topography, Atomic weight, Crystal orientation – But not diffraction

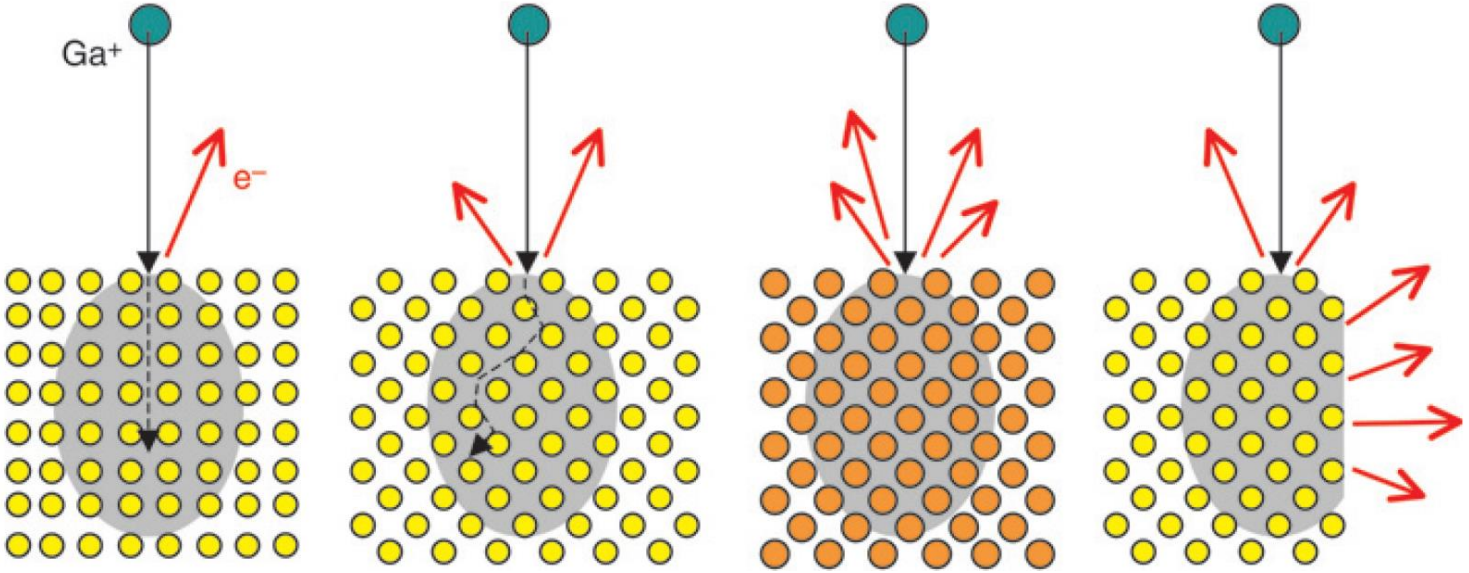

Volkert et al., MRS BULLETIN, VOLUME 32, 2007

Simulation of many ion paths

Monte Carlo simulations can give good **statistical values** for **ion ranges**, **implantation depth** and **sputtering yield**

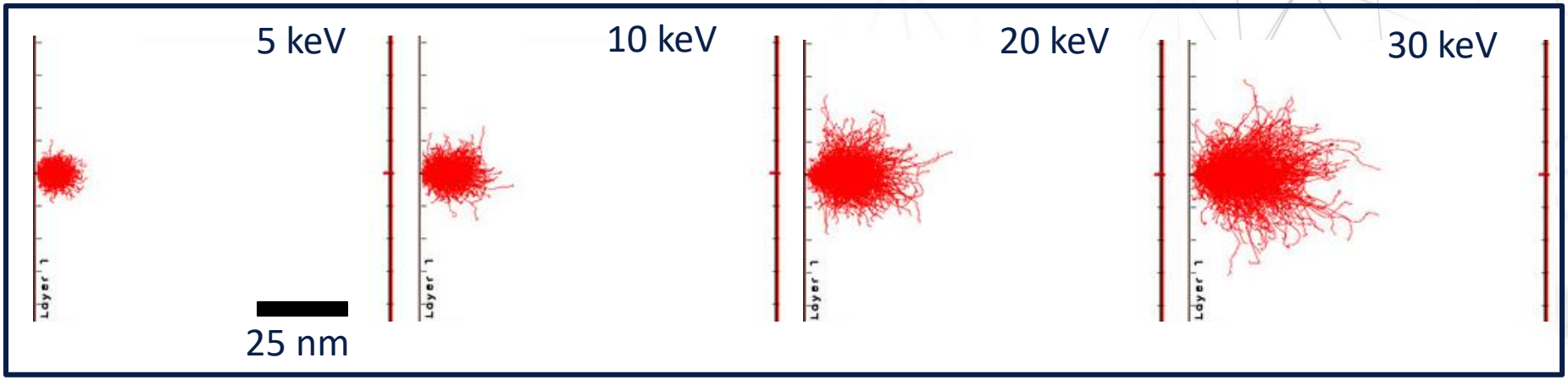

Ion implantation profiles generated by calculations with **100000** ions

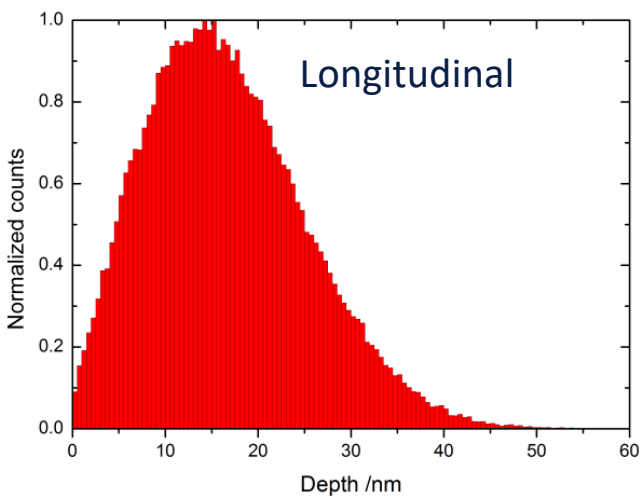

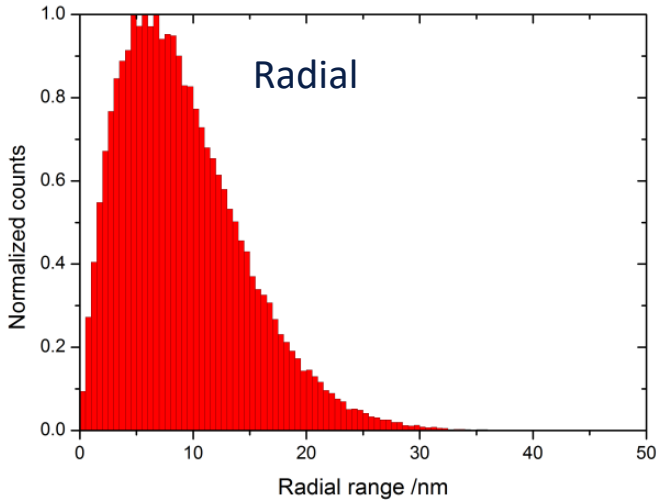

Simulations performed with **SRIM (**http://www.srim.org)

Comparison of cascades for different projectiles

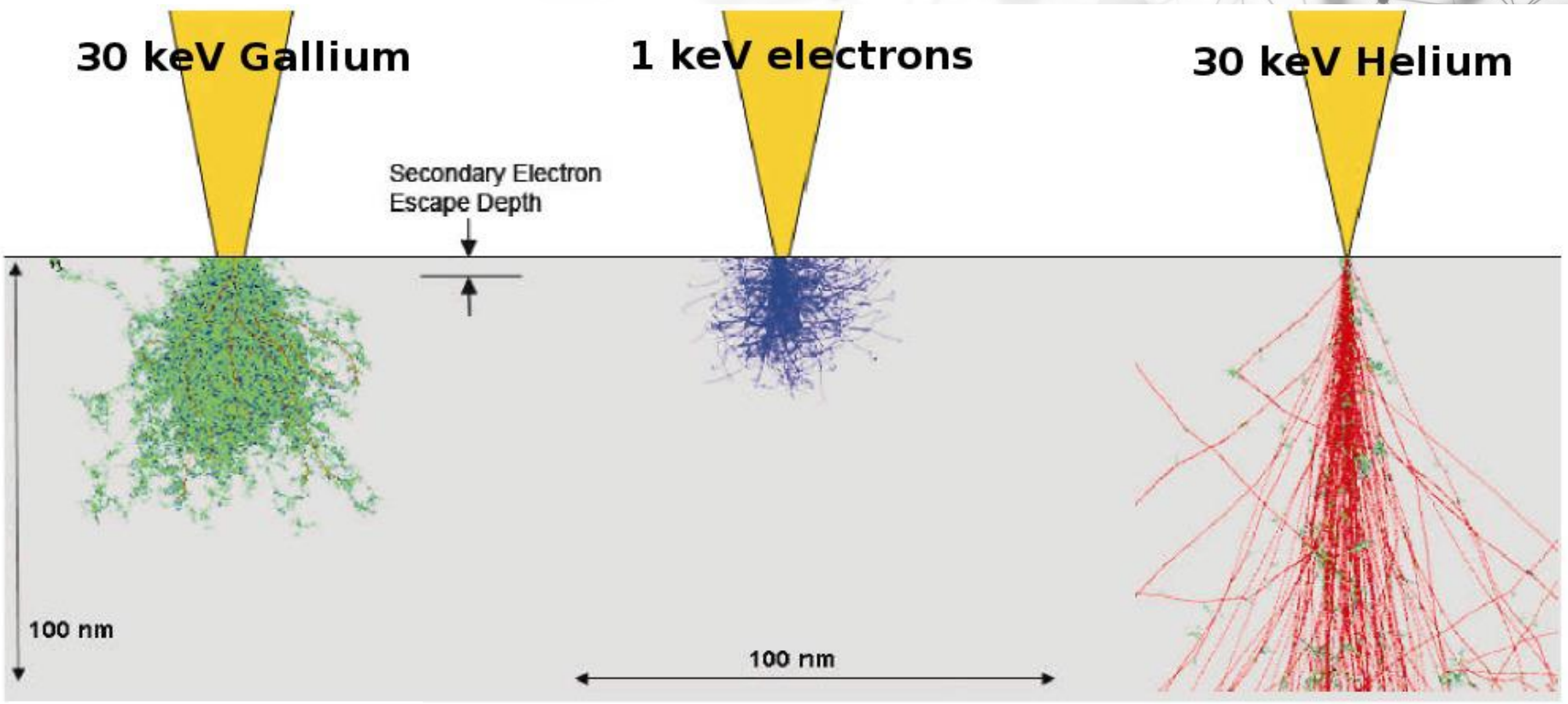

Hlawacek, J. Vac. Sci. Technol. 2014

Target: silicon

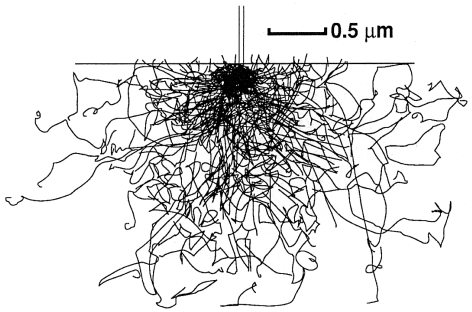

30keV electrons: **off the chart**

Collision cascade simulated with MD

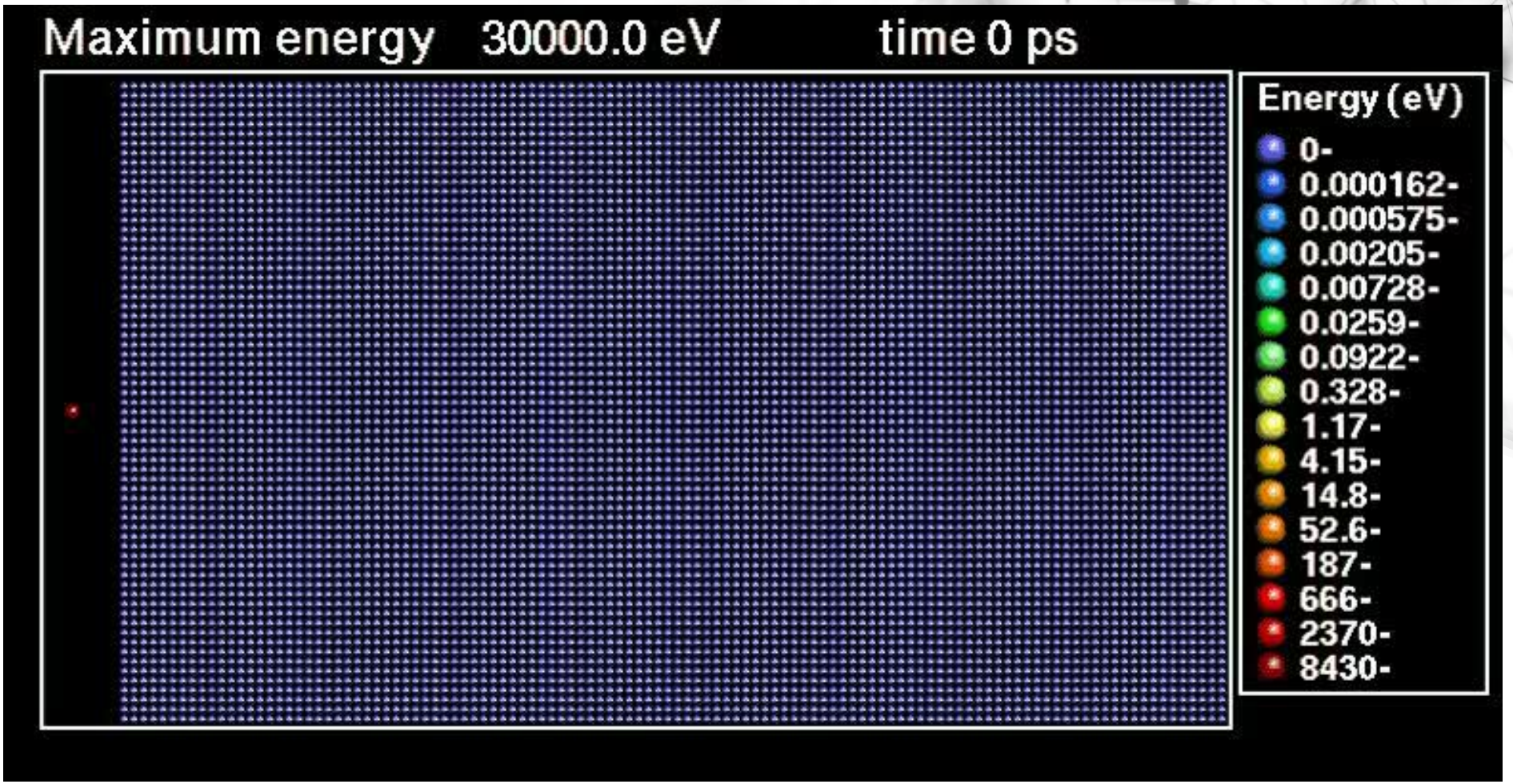

30 keV Xe ion irradiation of Au

K. Nordlund, 2008

Zone of **plastic flow** generated in the center of the collision cascade!
FIB induced **damage!**

Damage in real scenarios

The FIB damage depends on:

- Milling parameters
- Sample chemistry

Rule of Thumb: 1 nm damage / kV

Metals:

- Dislocation loops
- Point defects
- Implanted ions

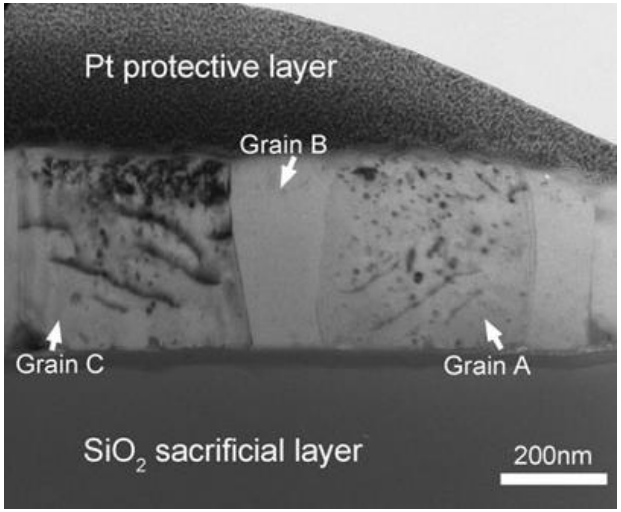

Idrissi, Microsc. Microanal, 2011

Semiconductors:

- Amorphization
- Implanted ions
- Point defects

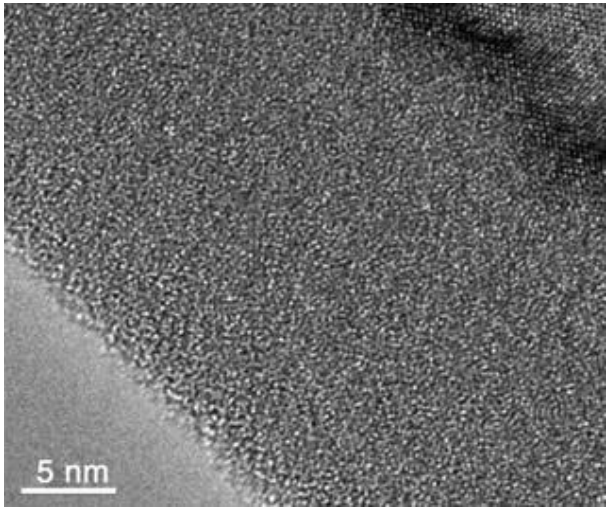

Mayer, MRS Bulletin, 2007

Polymers:

- Distorted morphology
- Ion implantation
- Damage due to heating

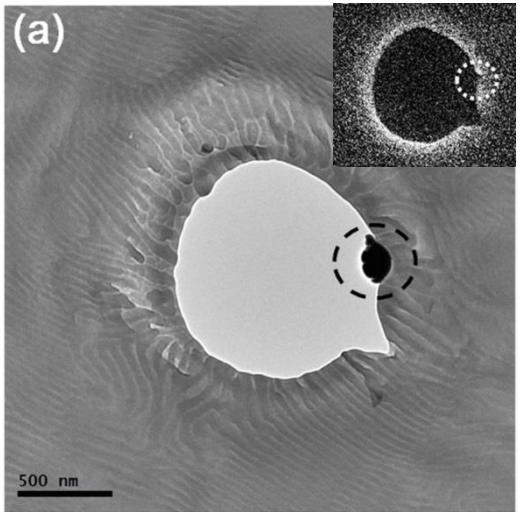

Kim, Ultramicroscopy, 2011

Effects of ion induced damage

Example: Change of the mechanical Properties of Molybdenum

Sample preparation with the FIB

Uchich, Science, 2004

Stress-strain curves for Mo Pillars

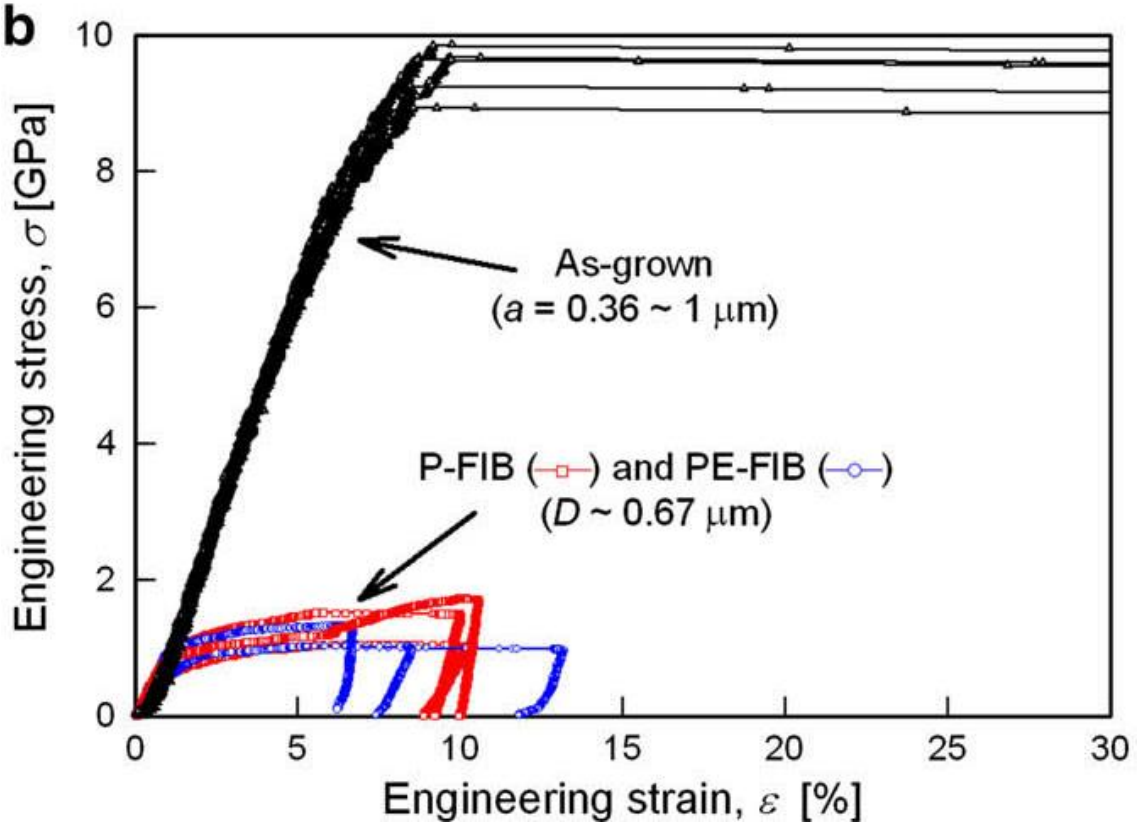

FIB induced damage has to always be considered!

Shim, Acta Materialia, 2008

Reducing FIB damage

Influence factors:

- Decreasing accelerating voltage
- Post process with light/low-energy ions
- Chemical etching
- Thermal annealing

Accelerating voltage vs amorphization

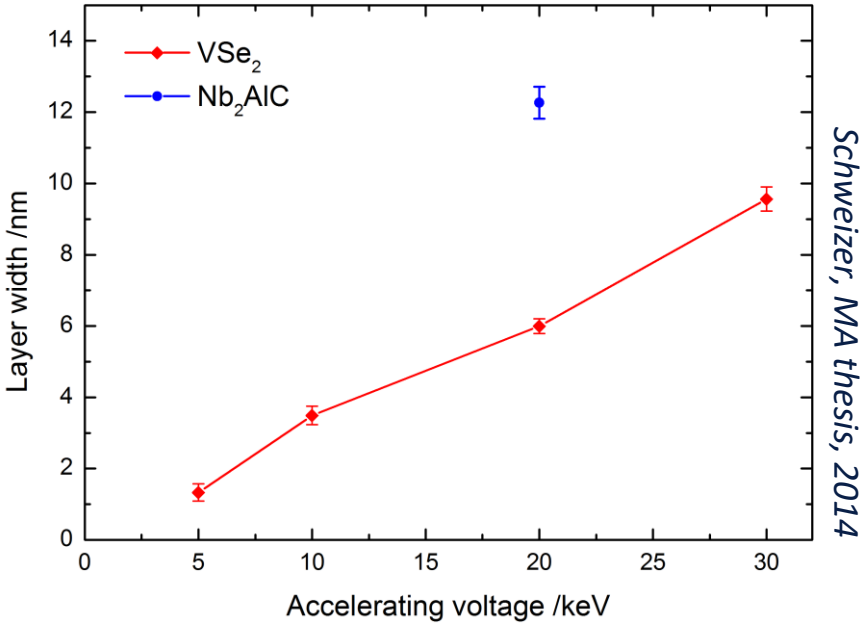

Schweizer, MA thesis, 2014

Only certain methods work.
FIB damage remains a challenge!

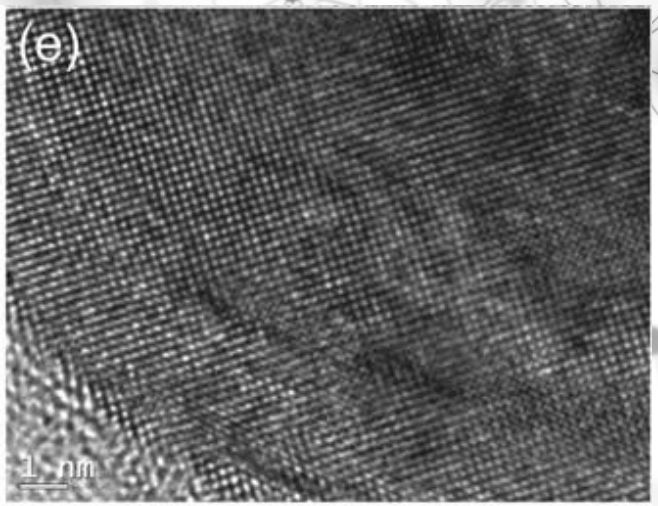

Annealing step

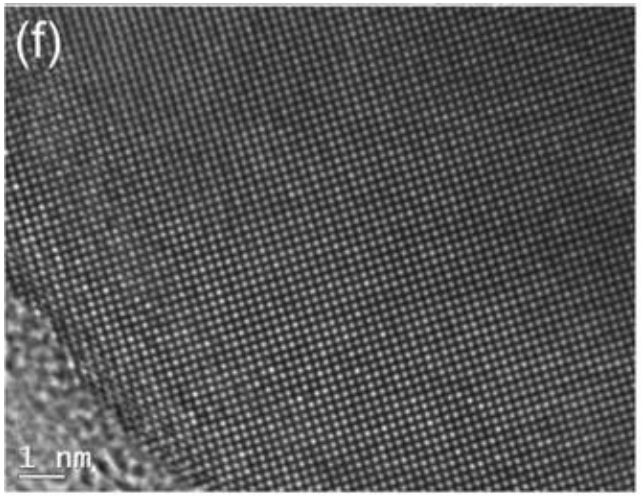

Kiener, Phil. Mag., 2012

FIB milling in practice

There are many parameters for milling:

- Ion current
- Acceleration voltage
- Pattern shape
- Pattern size
- Dwell time/ Number of scanning passes
- Overlap/Pitch
- Total dose
- Defocus
- Scan direction

Every parameter influences the final result significantly!

The sample properties are equally as important as beam properties!

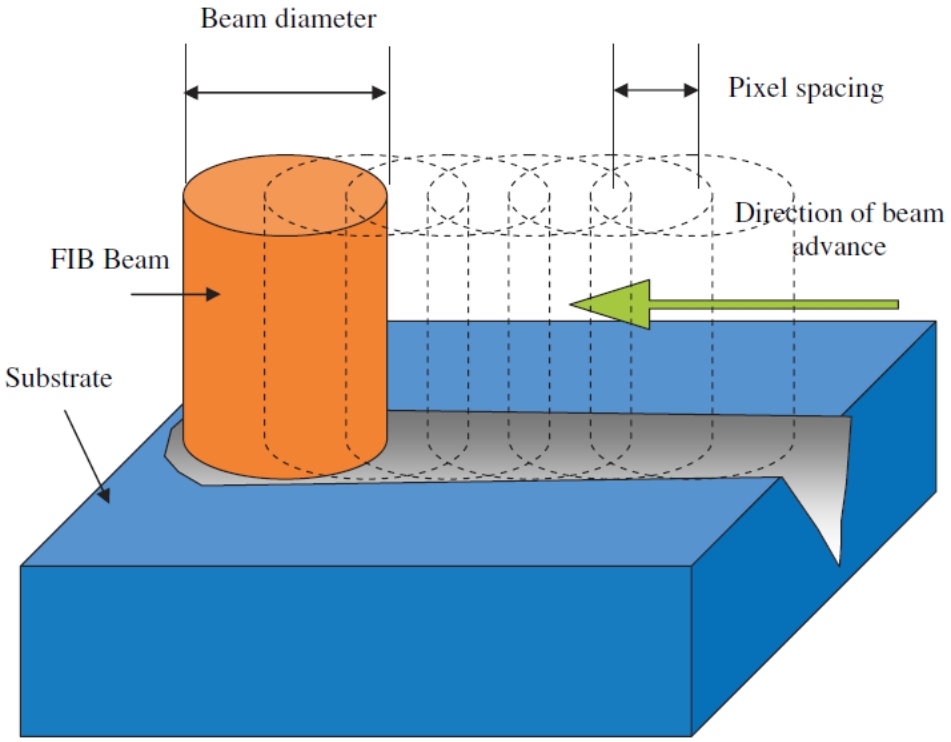

Tseng, J. Micromech. Microeng. 14, 2015

Influence of the acceleration voltage

20 keV

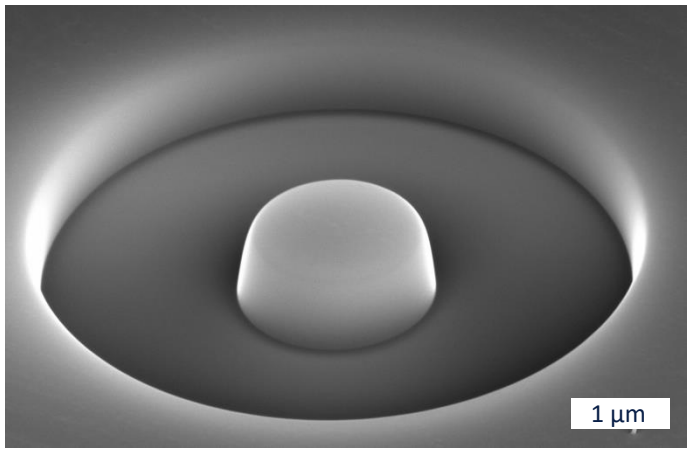

10 keV

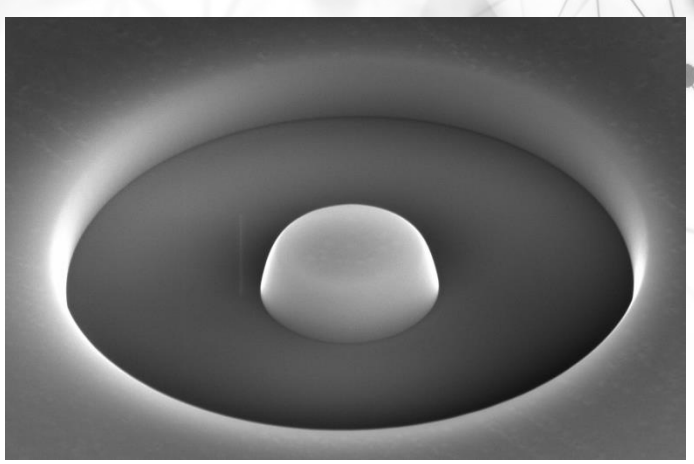

5 keV

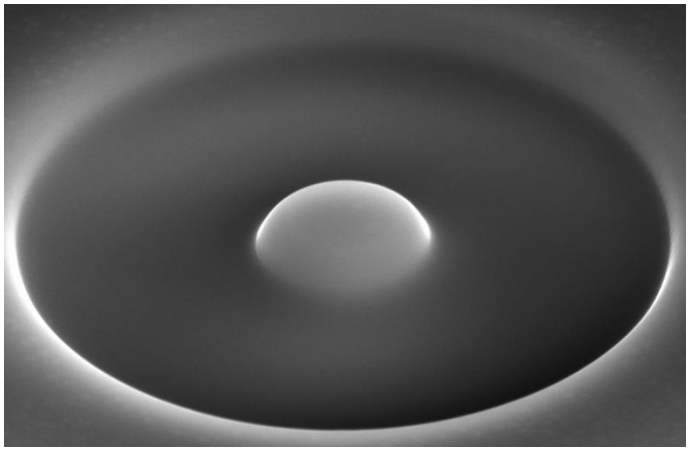

2 keV

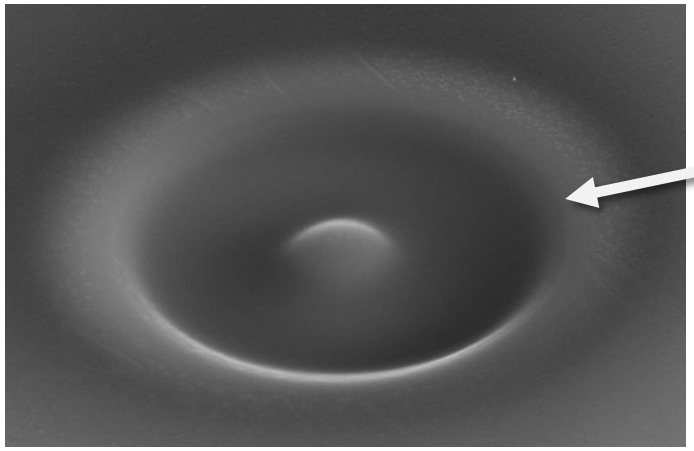

Beam „Tail“ becomes more pronounced

Sputter yield goes down. Pattern quality suffers! But: less beam damage!

Influence of the beam overlap

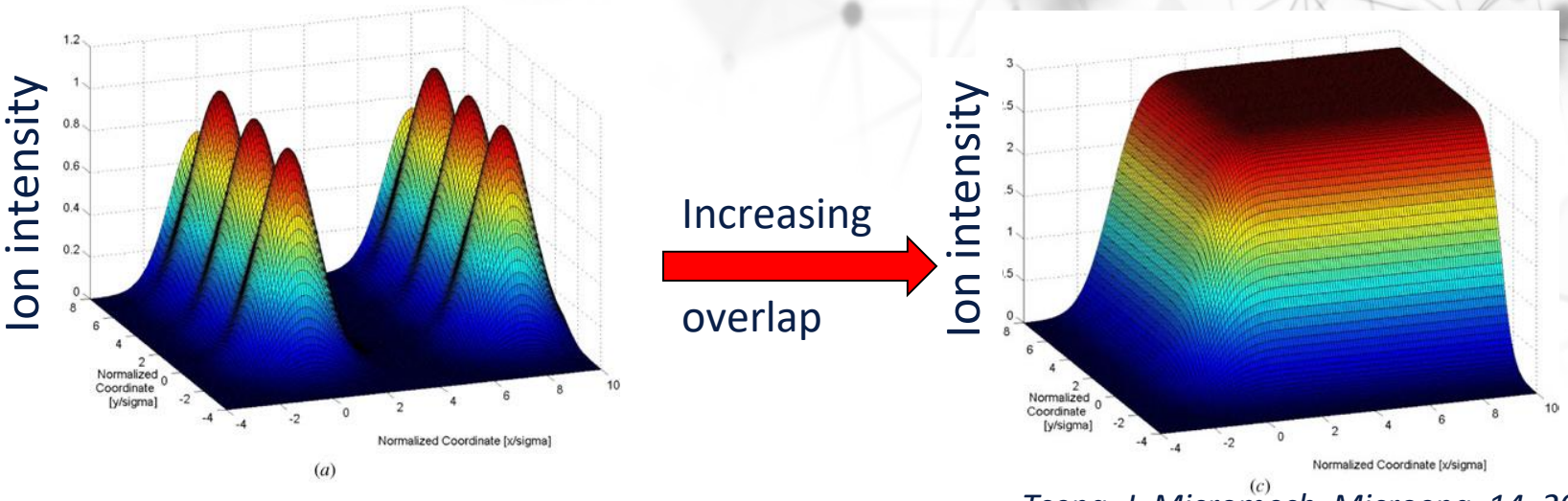

Tseng, J. Micromech. Microeng. 14, 2015

Example: Striations in nanoporous gold caused by insufficient beam overlap

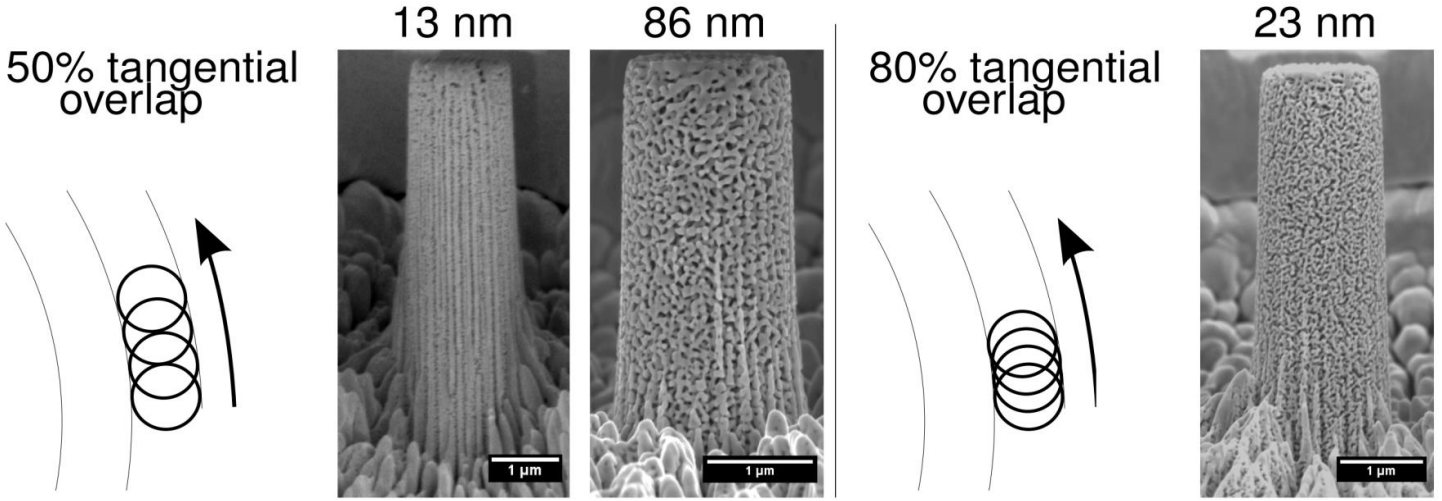

Influence of Milling passes

Sputtered Material is partially **redeposited!**

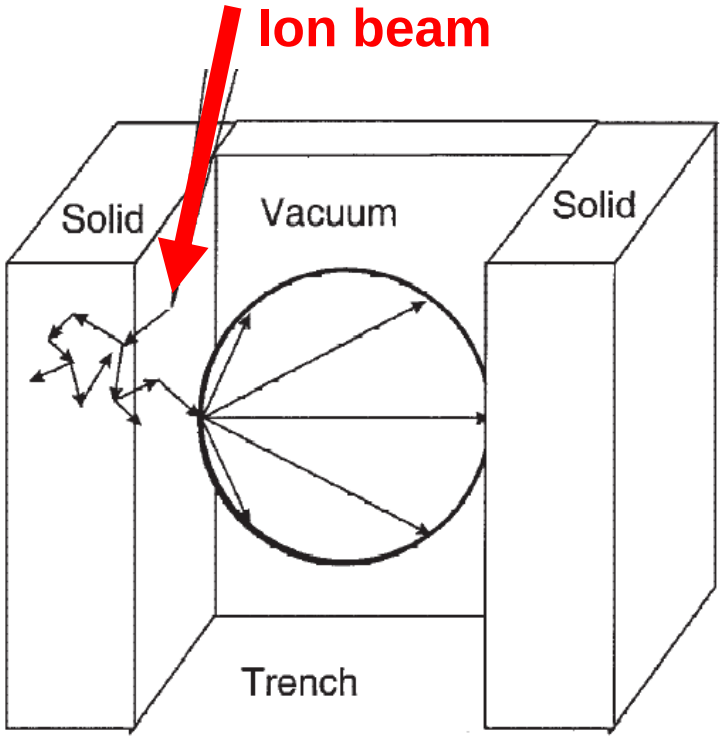

Prenitzer, Microsc. Microanal. 9, 2003

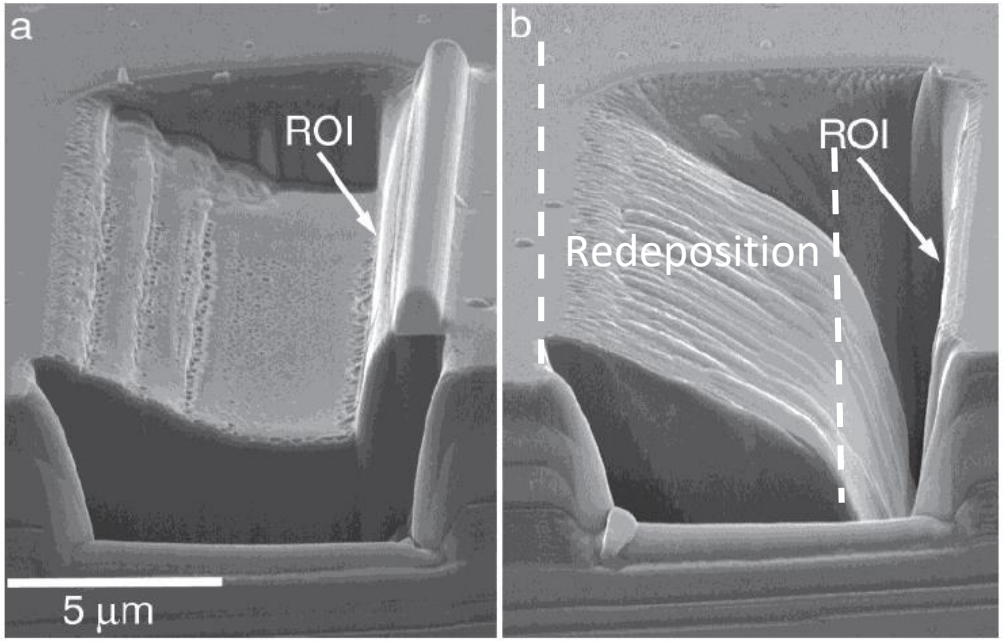

Multi pass (equal Ion Dose) **Single pass**

Multiple passes of the ion beam leads to averaging of the redeposition

Influence of the sample material

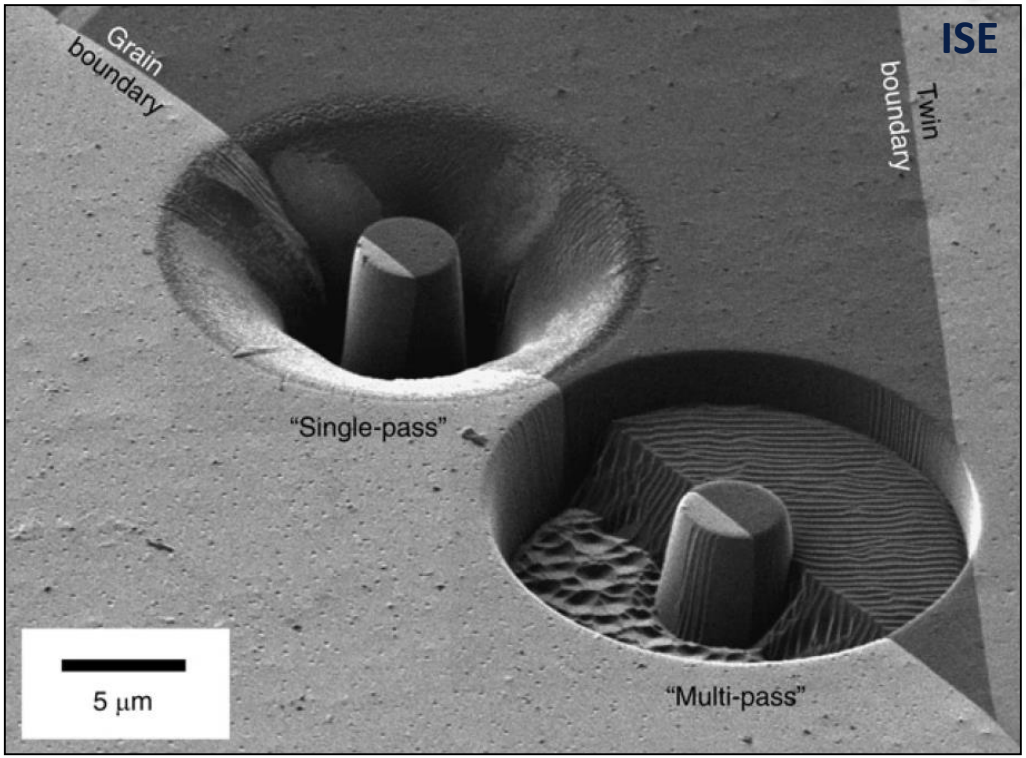

Volkert et al., MRS BULLETIN, VOLUME 32, 2007

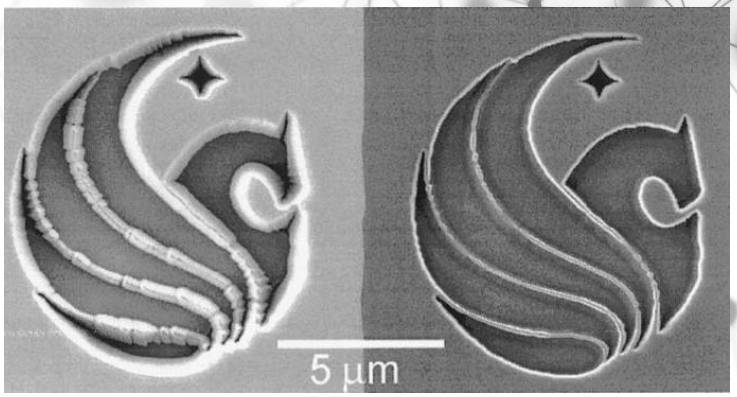

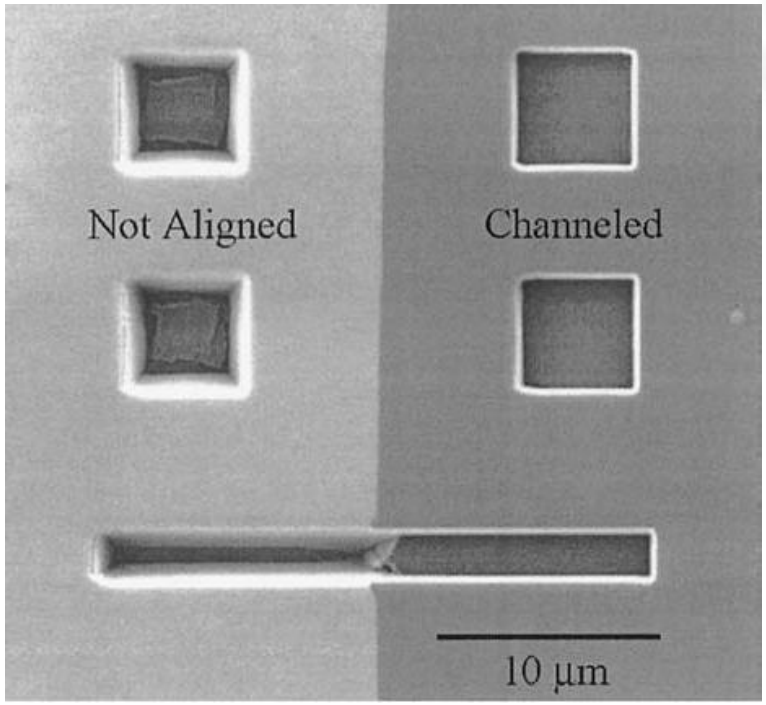

Gianuzzi, Introduction to Focused Ion Beams, 2005

Patterning is strongly influenced by the **microstructure** and **orientation** of the sample.

Curtaining

Severe case of curtaining

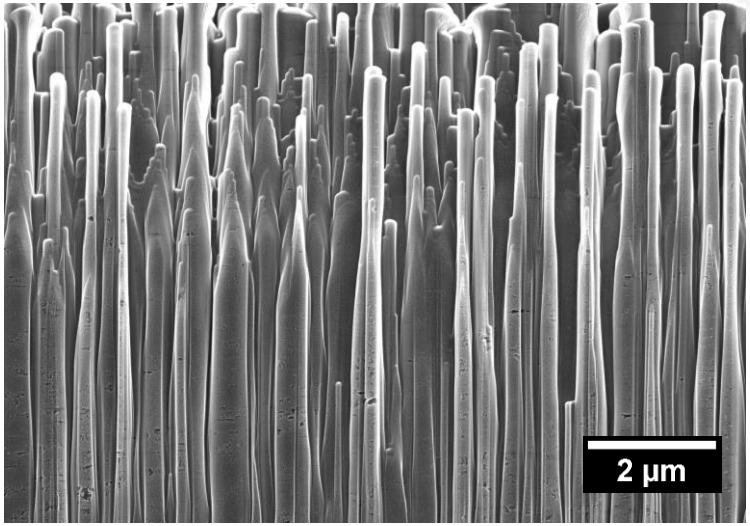

Typical curtaining in a cross-section

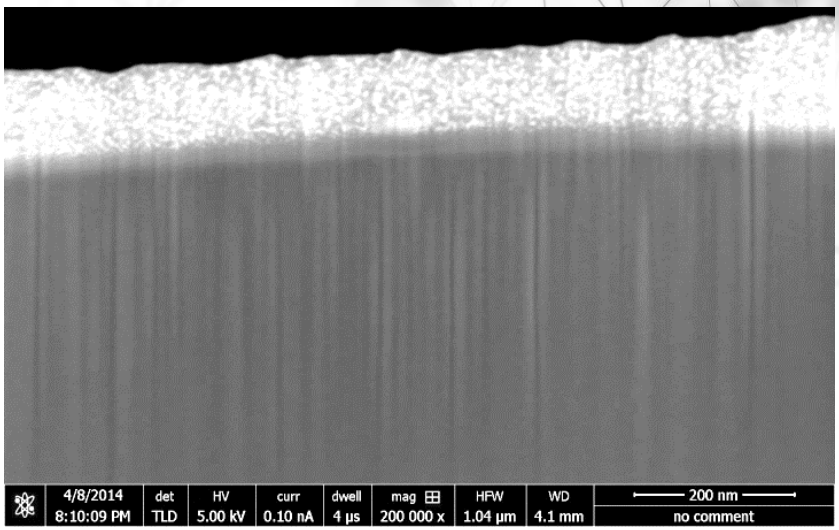

Bryce Canyon, Jean-Christophe Benoist, CC

Curtaining depends on:

- Surface-curvature
- Local density
- Heterogeneous sputter yield
- Beam parameters

Similar process in erosion: Cheminée de fée or Hoodoo

TEM sample preparation - Overview

TEM sample preparation

Conventional

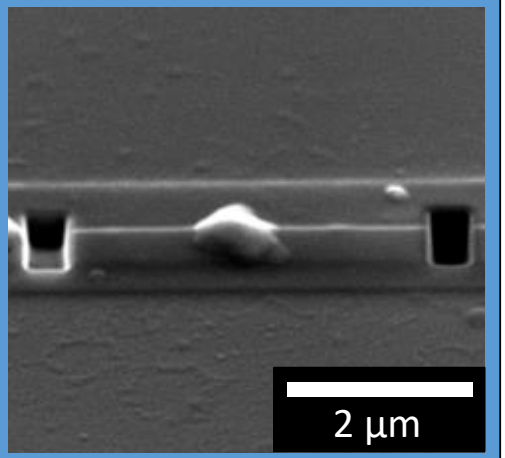

J. Schornbaum et al., Adv. Funct. Mater. (2014)

Double lift-out

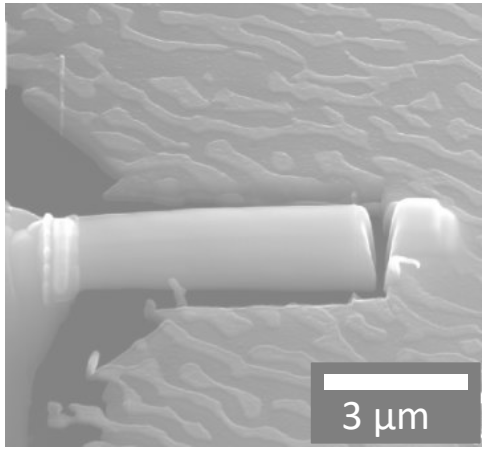

J. Müller, E. Spiecker, in preparation 2015

Shadow FIB (backside milling)

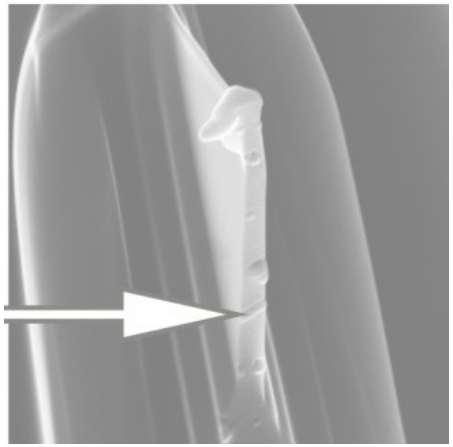

B. Vieweg et al., Ultramicroscopy, 2012

360° TEM tomography

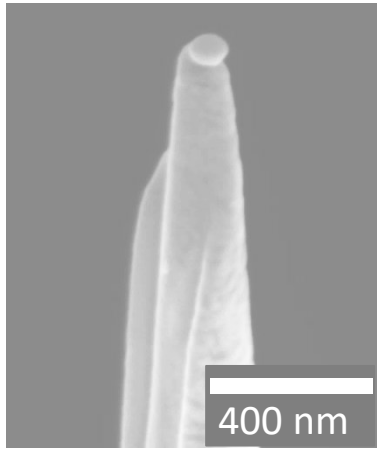

T. Przybilla, B. Winter et al., in preparation 2015

TEM sample preparation: lift-out movie

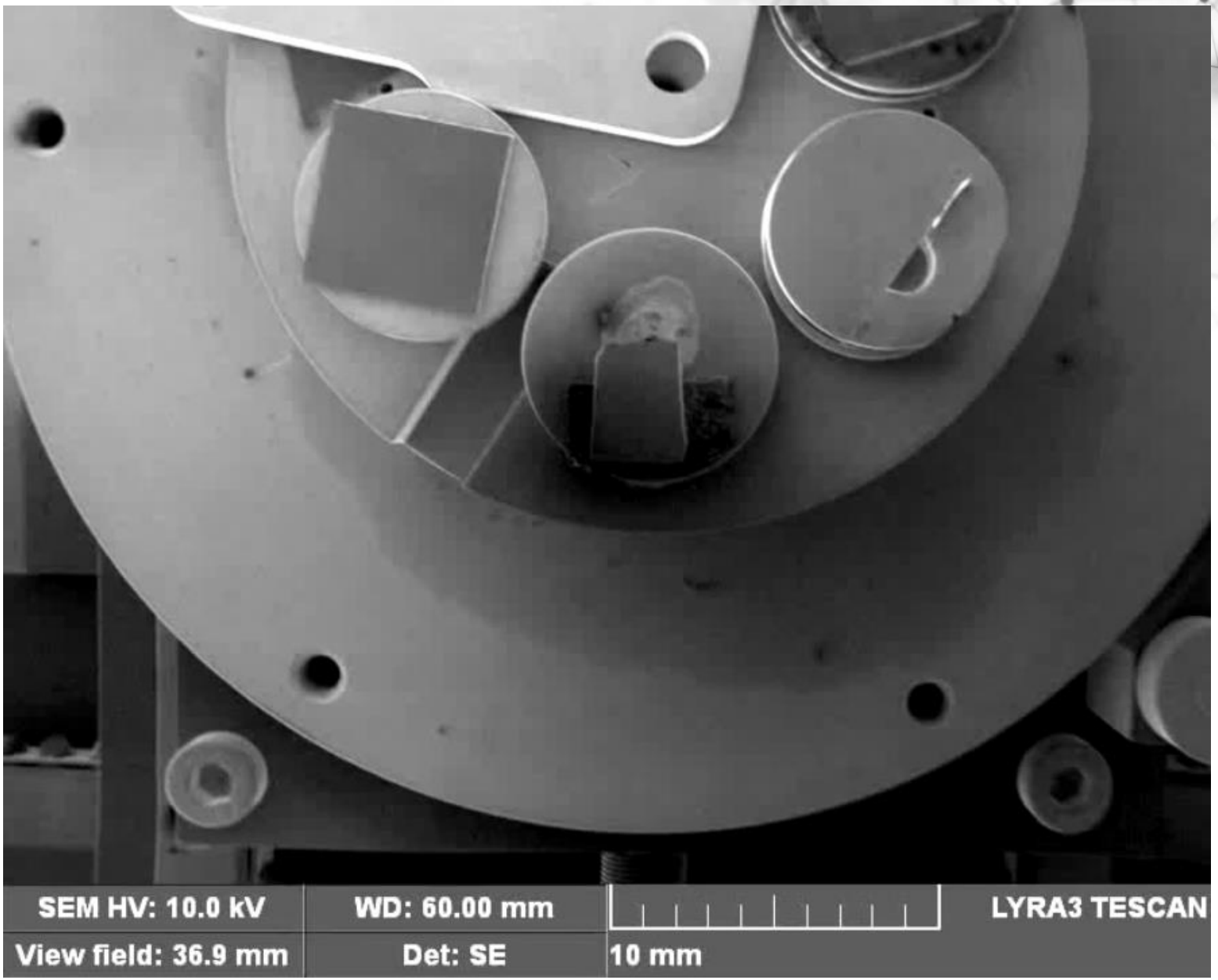

Video from Tescan

TEM sample preparation

Epitaxial growth of PbSe quantum dots on MoS_2 nanosheets

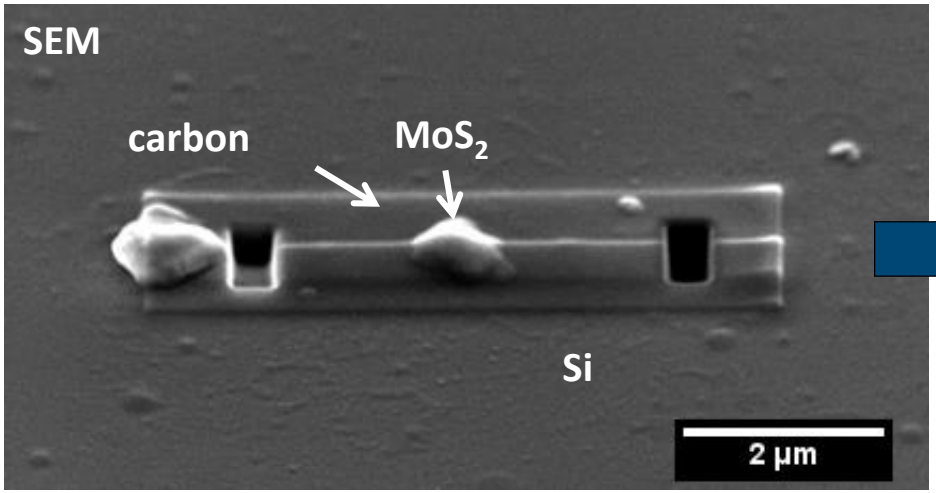

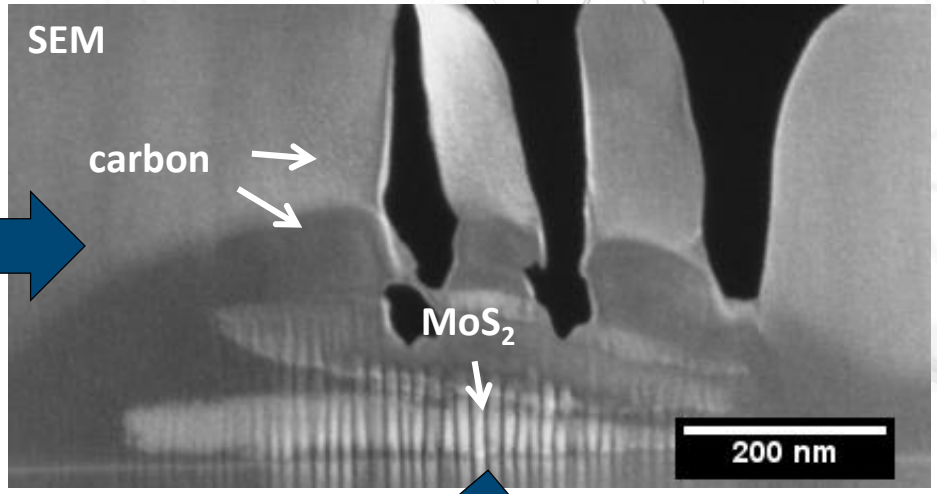

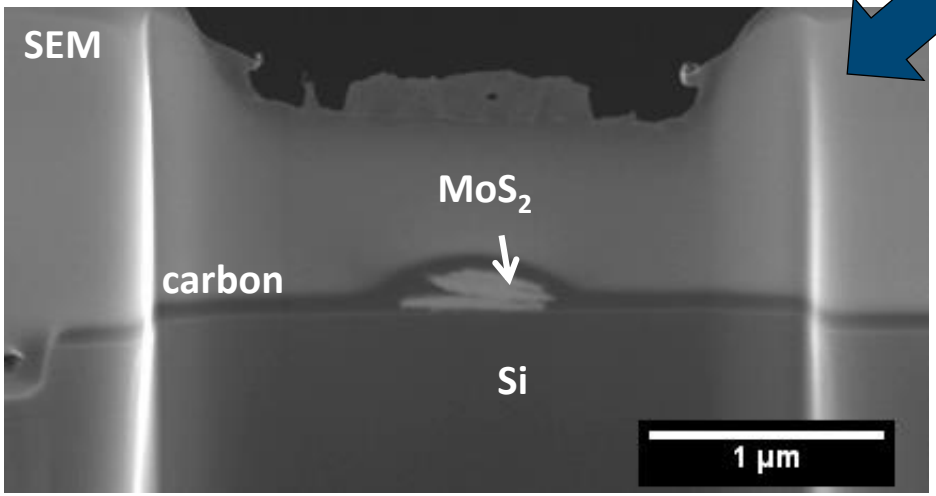

NANOMATERIALS FOR OPTOELECTRONICS

J. Schornbaum et al., Adv. Funct. Mater. (2014)

TEM characherization

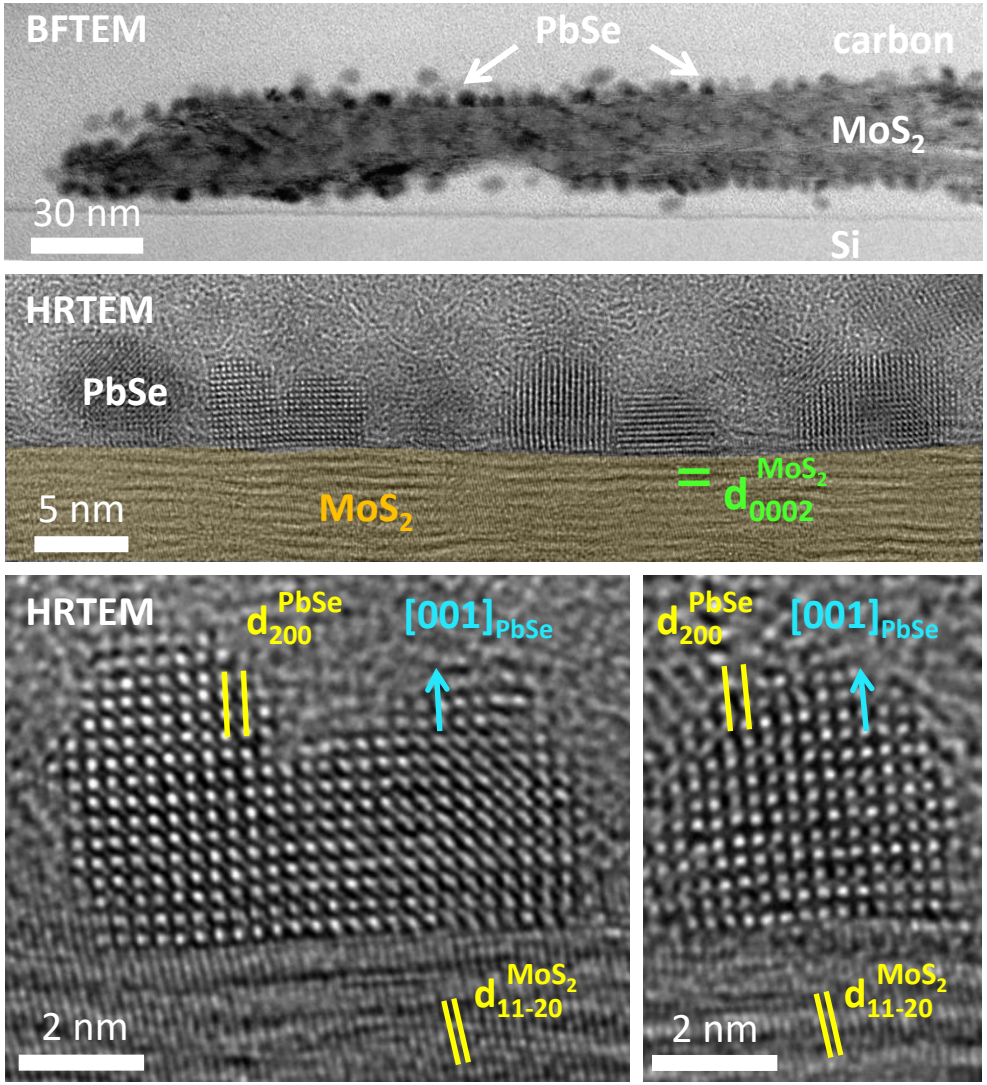

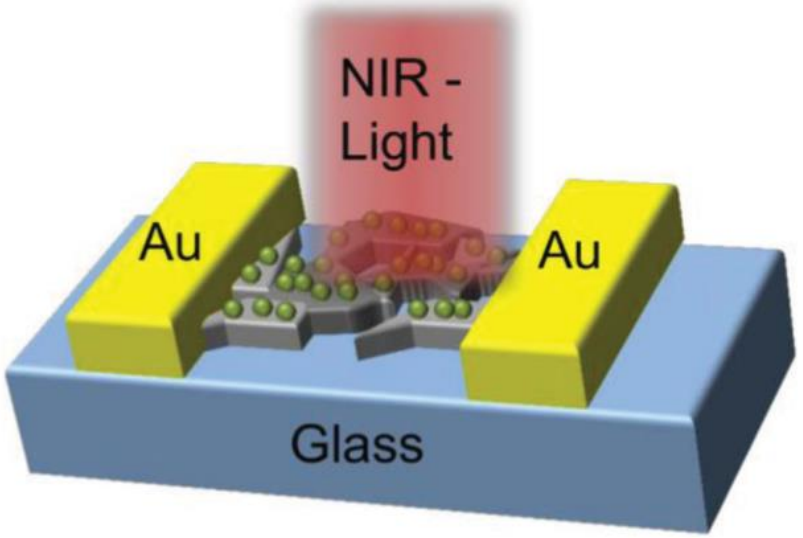

J. Schornbaum et al., Adv. Funct. Mater. (2014)

Nanomechanics

Micropillars

Uchich, Science, 2004

Micro-cantilevers

T. Przybilla, diploma thesis

Tensile Specimen

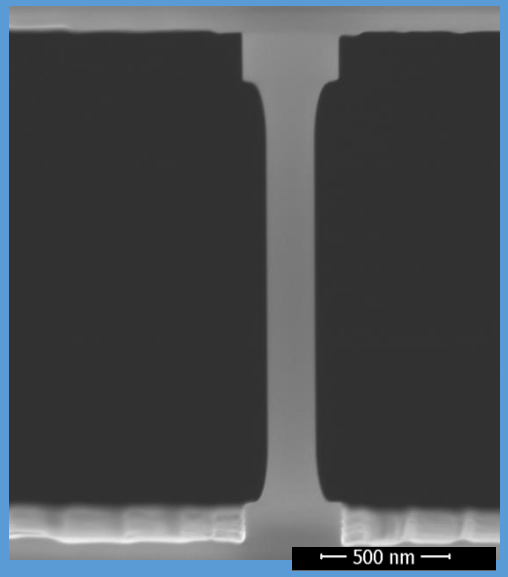

T. Przybilla, unpublished work, 2015

→ Analysis of the mechanical properties at the nano scale

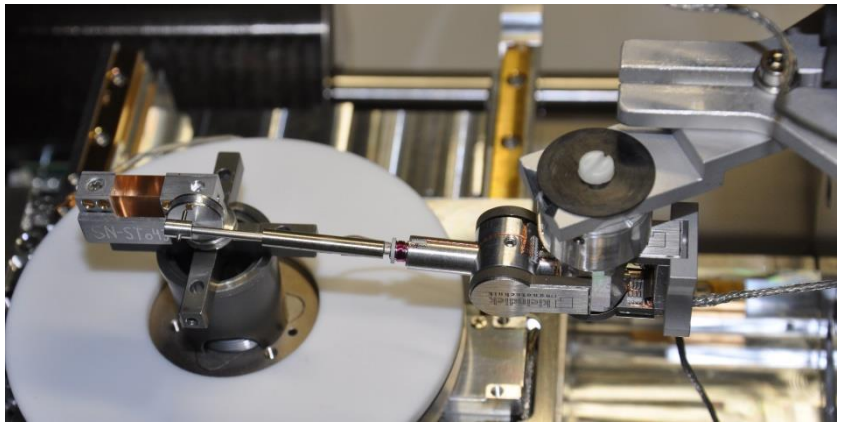

Micropillar compression tests with local strain mapping

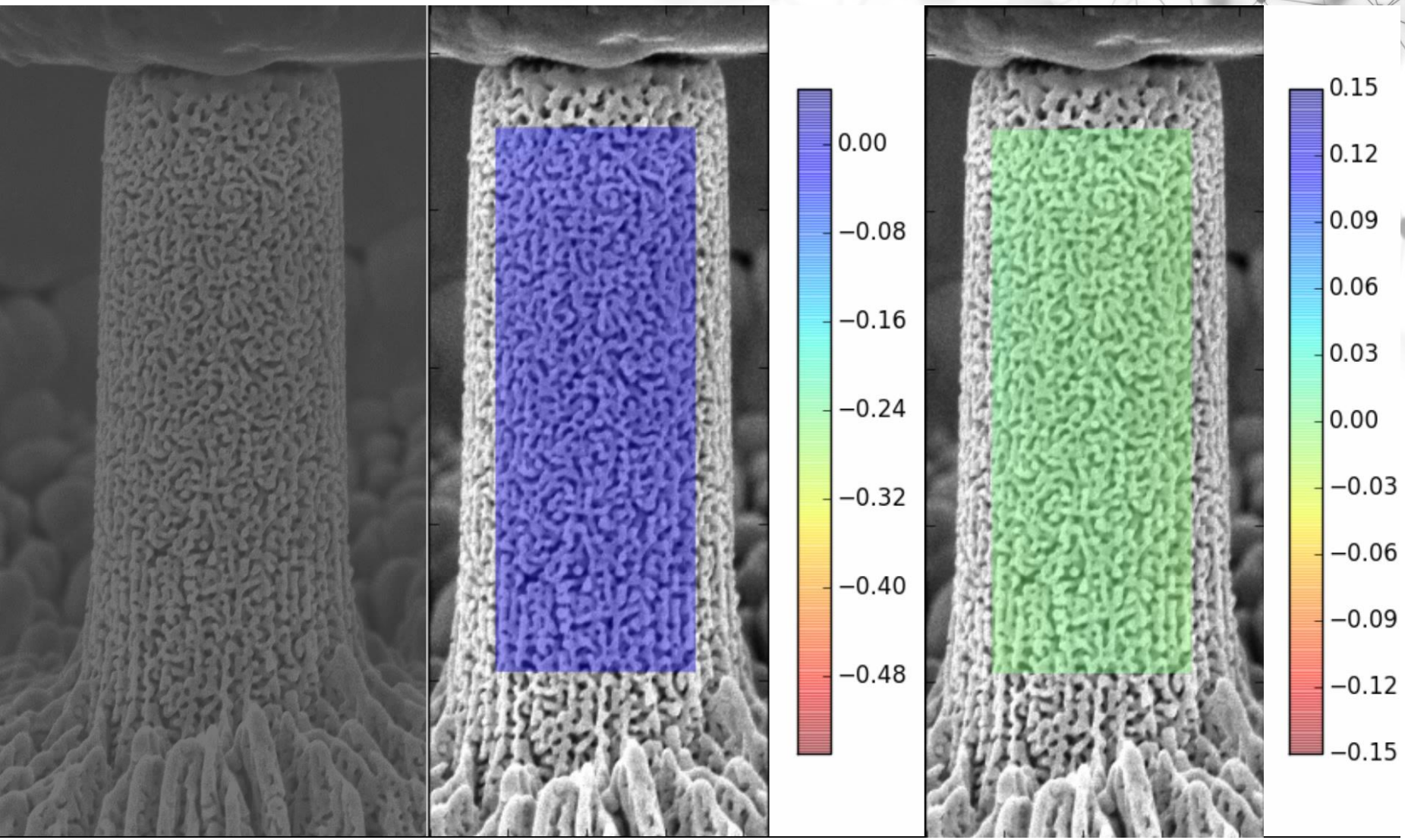

Nanoporous gold

Compression of layered crystals

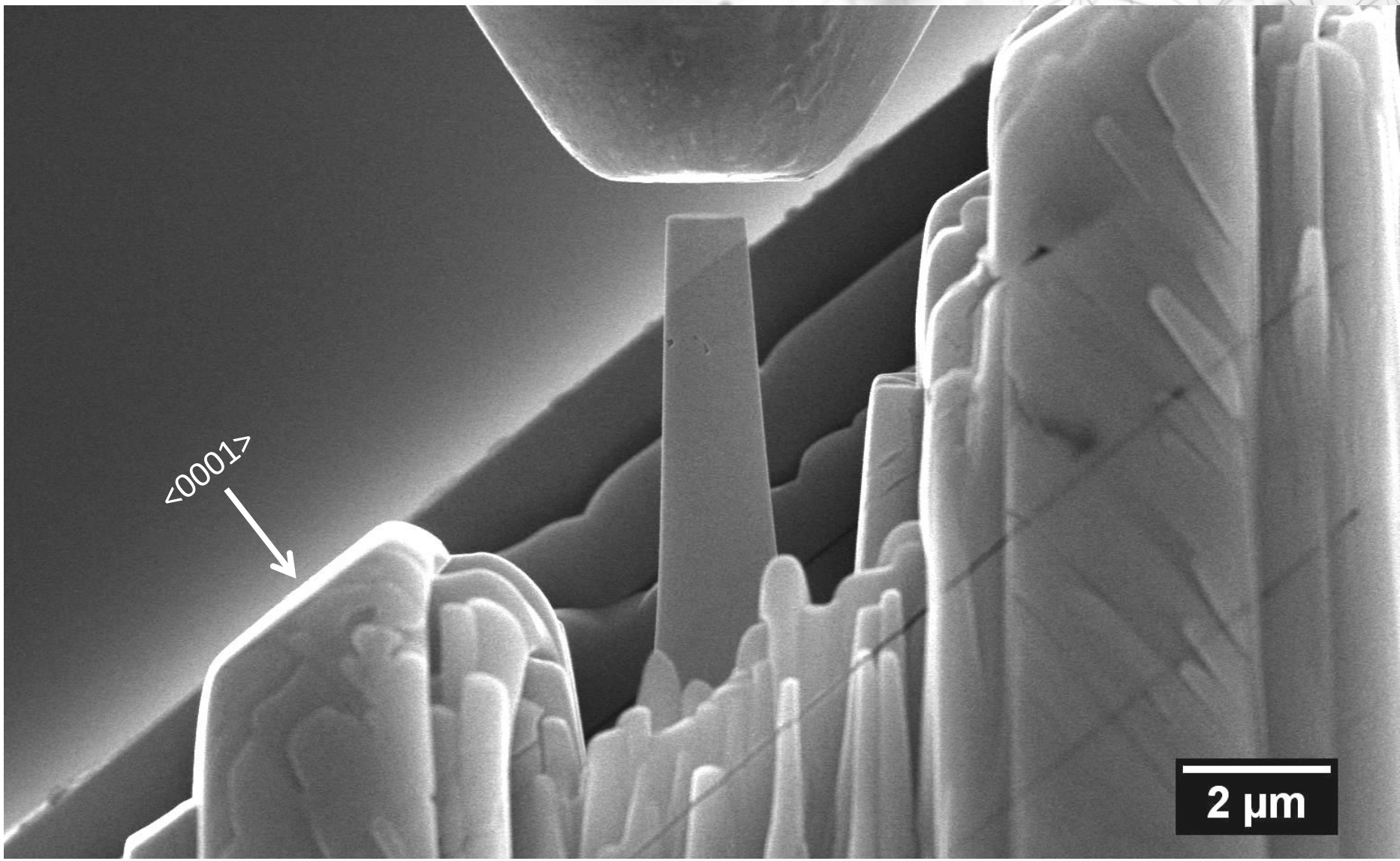

3D EBSD/EDX

Polycrystalline sample for which the 3D-grain structure and -orientation has to be studied

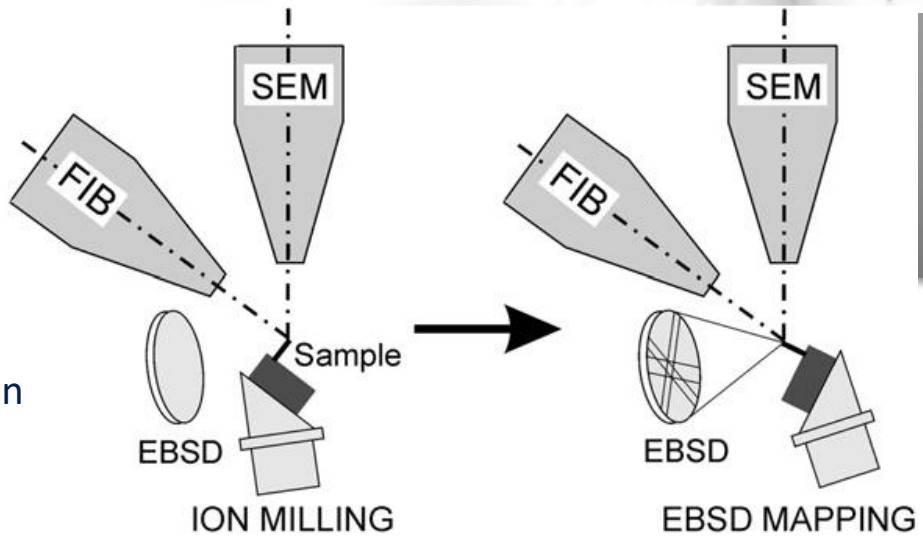

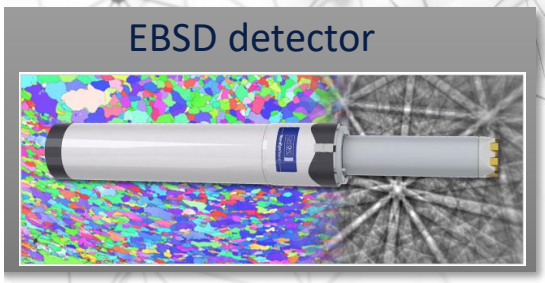

Oxford instruments Analytical – technical briefing brochure, 2014

Xu et al., Mater. Char. (2007)

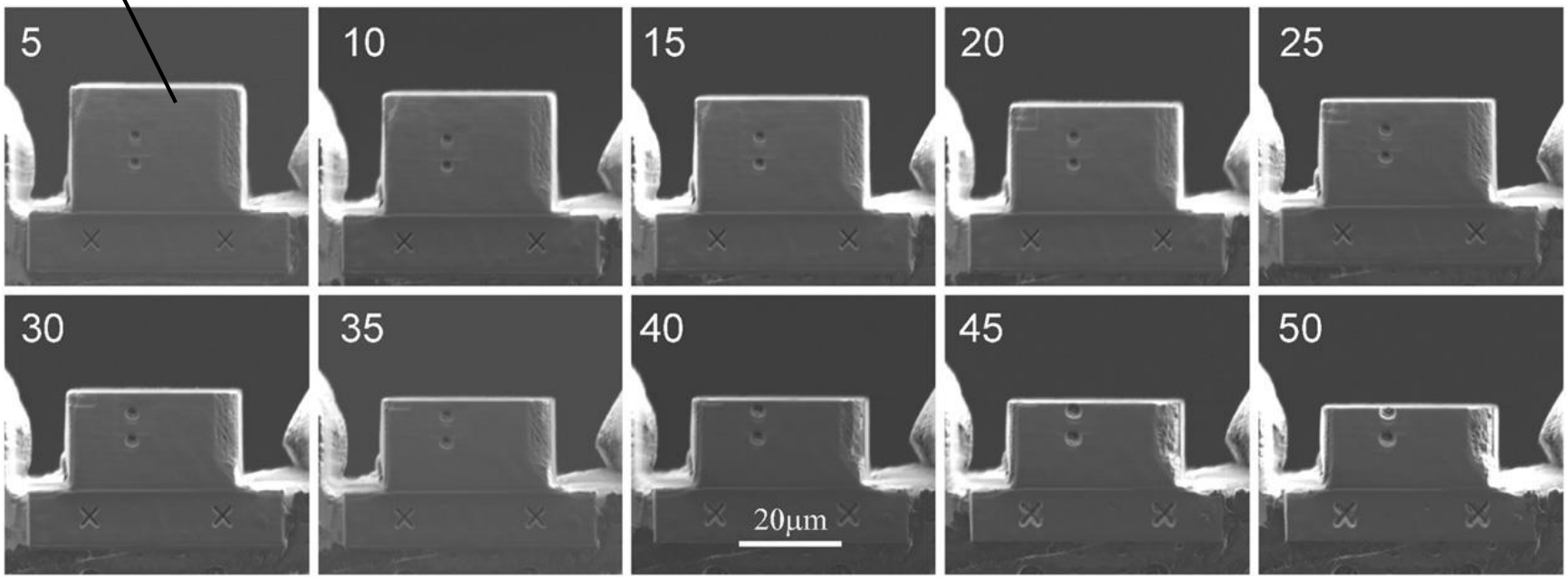

3D EBSD/EDX

EBSD-derived images at two different depths

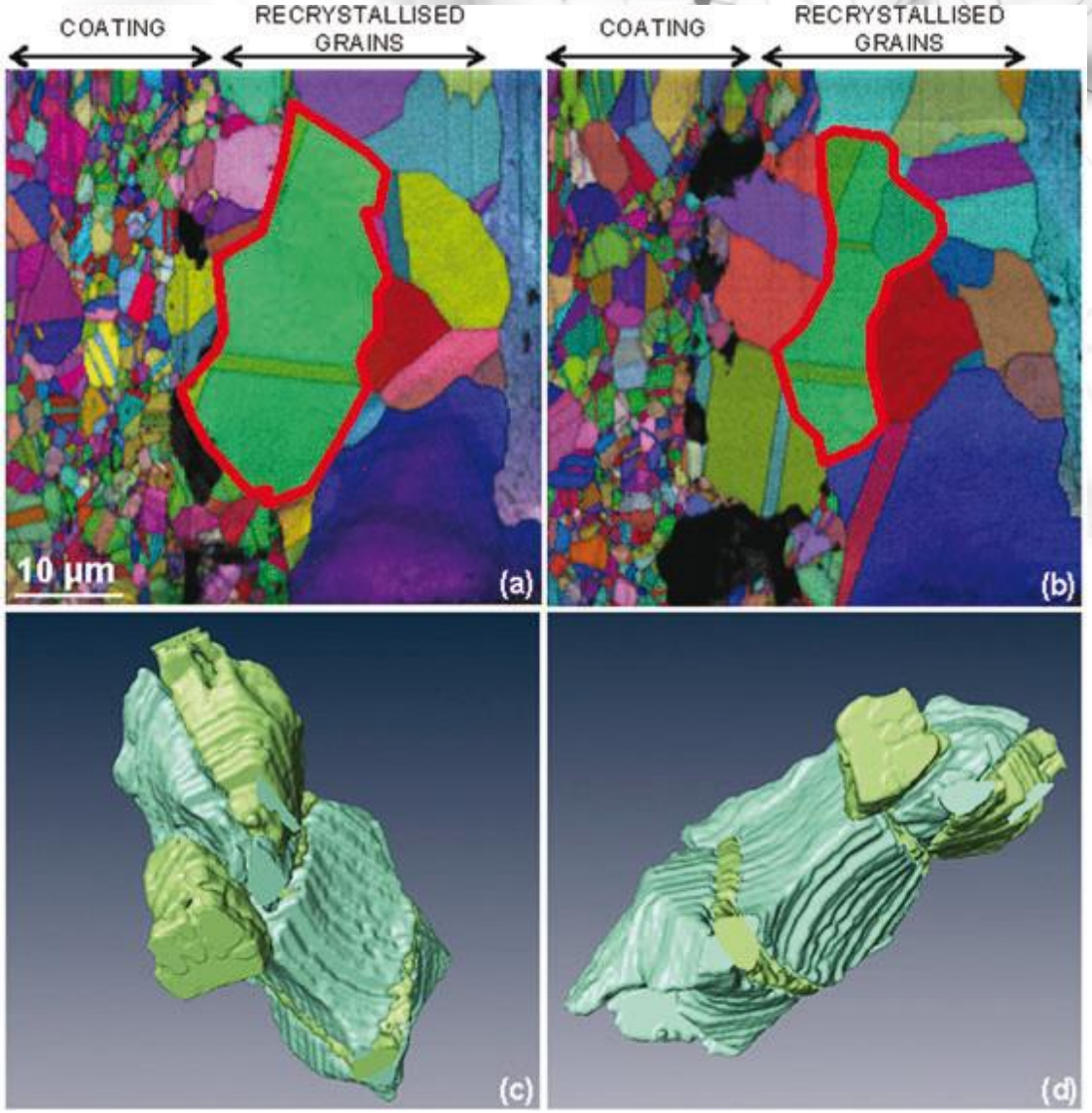

50 mm x 50 mm
40 slices à 1.7 mm

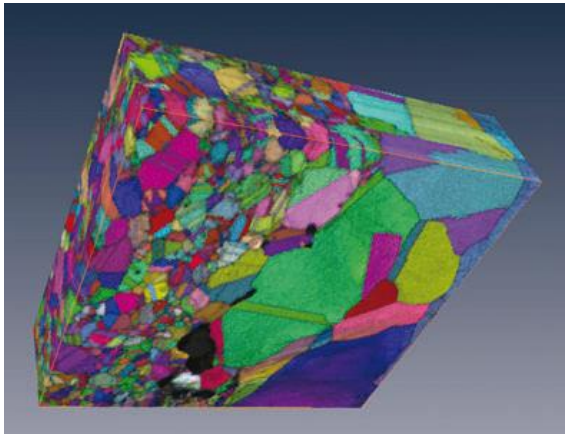

3d-reconstruction of individual grains

West and Thomson (2009)

Questions?

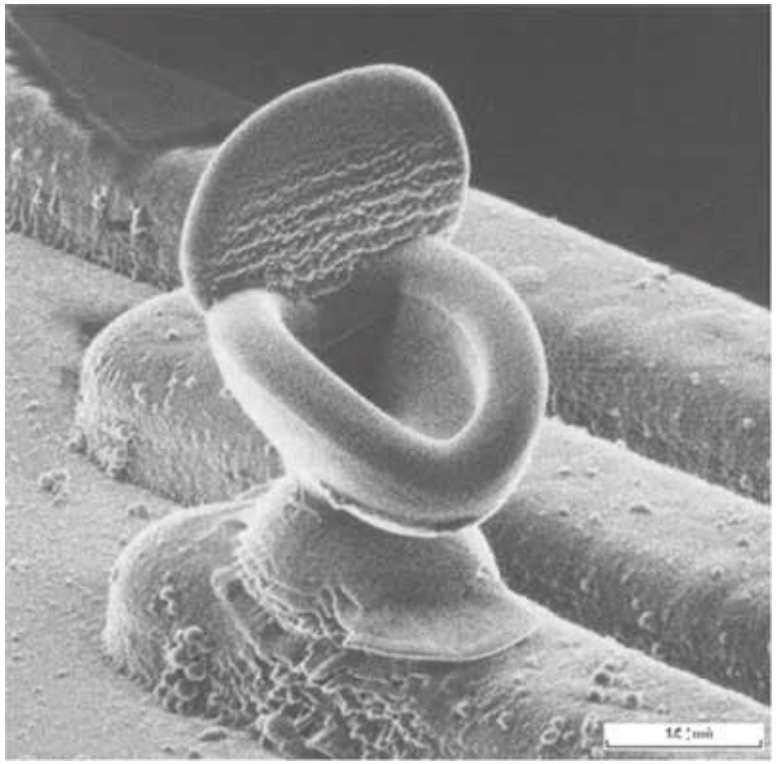

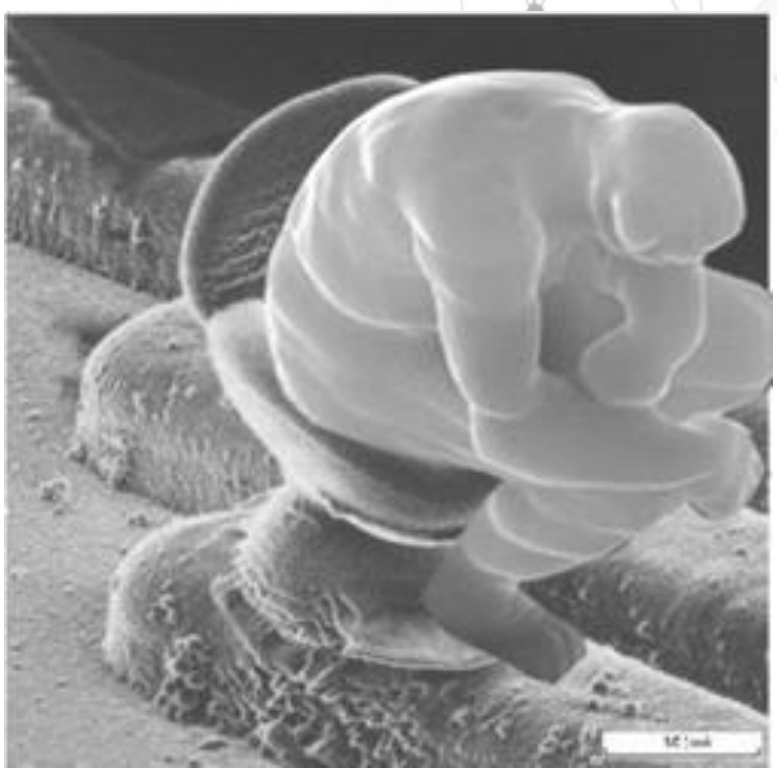

Takahashi Kaito, 2005